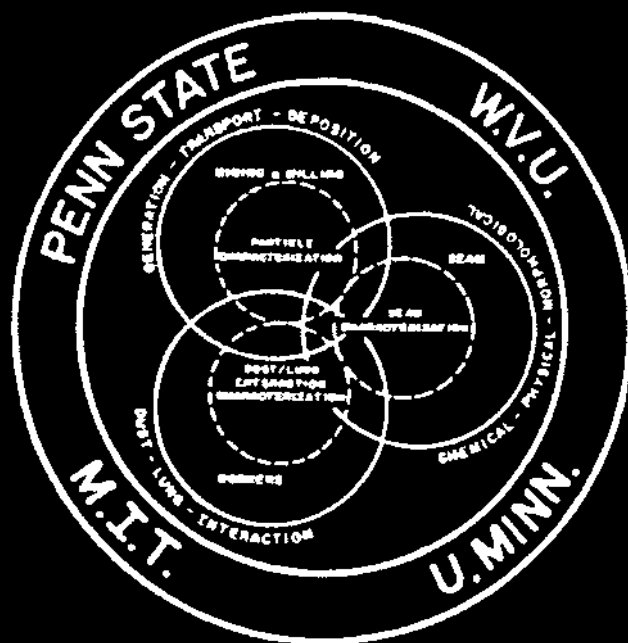


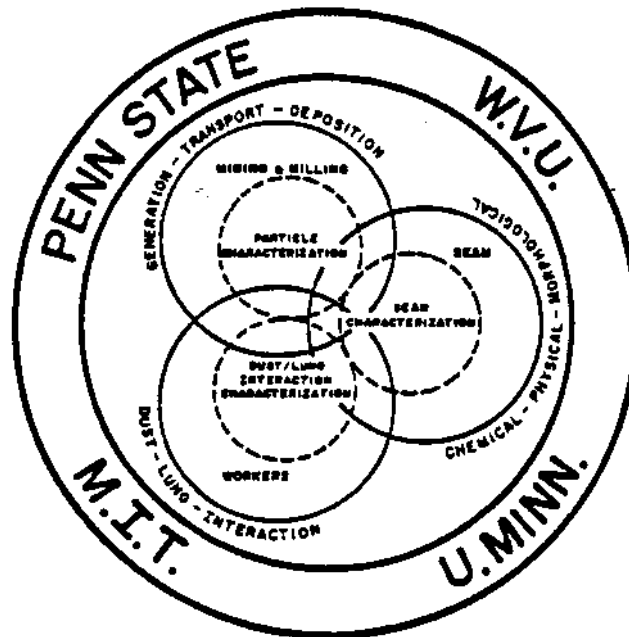
PUBLICATIONS 1987

Edited by
ROBERT L. FRANTZ
and
RAJA V. RAMANI



**GENERIC MINERAL
TECHNOLOGY CENTER
FOR RESPIRABLE DUST**

PUBLICATIONS 1987



GENERIC MINERAL TECHNOLOGY CENTER FOR RESPIRABLE DUST

The Pennsylvania State University
West Virginia University
University of Minnesota
Massachusetts Institute of Technology
Michigan Technological University

Submitted To
Office of Mineral Institutes
U.S. Bureau of Mines
Washington, D.C.

May 31, 1989

The views and conclusions contained in this document are those of the authors and should not be interpreted as necessarily representing the official policies or recommendations of the Interior Department's Bureau of Mines, the U.S. Government or of the Generic Mineral Technology Center for Respirable Dust. Reference to specific brands, equipment or trade names in this report is made to facilitate understanding and does not imply endorsement by the Bureau of Mines or the Dust Center.

PUBLICATIONS

PRODUCED IN

THE GENERIC MINERAL TECHNOLOGY CENTER FOR RESPIRABLE DUST

IN THE YEAR

1987

Edited by
Robert L. Frantz
Raja V. Ramani

PENNSTATE



WEST VIRGINIA UNIVERSITY



Volumes of the Respirable Dust Center

VOLUME 1	Status Report, 1984-1988
VOLUME 2	Report to the Committee on Mining and Mineral Resources Research, 1987
VOLUME 3	Publications, 1984
VOLUME 4	Publications, 1985
VOLUME 5	Publications, 1986
VOLUME 6	Publications, 1987
VOLUME 7	Respirable Dust Center Research Program Review
CONFERENCE PROCEEDINGS	Coal Mine Dust Conference West Virginia University Morgantown, West Virginia October 1984
CONFERENCE PROCEEDINGS	Respirable Dust in the Mineral Industries: Health Effects, Characterization and Control The Pennsylvania State University University Park, Pennsylvania October 1986

CONTENTS

	Page
Foreword	xi
National Plan	xii
Advisory Council Members	xiii
I. Control of Dust and Particulate Matter Generation	1
1. Development of a Mixed Mode Testing System for Geological Materials	3
<i>R. Karl Zipf and Z. T. Bieniawski, Department of Mineral Engineering, The Pennsylvania State University, University Park, PA 16802. Published in the Proceedings of the International Conference on Fracture of Concrete and Rock, eds., S. P. Shaw and S. E. Swartz, SEM, Houston, TX, July 17-19, 1987, pp. 338-352. (PS-1)</i>	
2. Identification of Fracture in Coal by AE in Dynamic Test	18
<i>A. Wahab Khair and S. Jung, Department of Mining Engineering, West Virginia University, Morgantown, WV 26506. Presented at the 4th Conference on Acoustic Emission, The Pennsylvania State University, University Park, PA, October 22, 1987, pp. 1-15. (WV-1)</i>	
II. Dilution, Dispersion and Collection of Dust	33
3. Applications of Knowledge Based Systems in Mining Engineering	35
<i>R. V. Ramani and K. V. K. Prasad, Department of Mineral Engineering, The Pennsylvania State University, University Park, PA 16802. Published in the Proceedings of the 20th APCOM, Volume 1, Mining, SAIMM, Johannesburg, South Africa, October 1987, pp. 167-180. (PS-13)</i>	
4. A Comparison of the Performance of Impactors and Gravimetric Samplers in Mine Airflow Conditions	50
<i>R. Bhaskar and R. V. Ramani, Department of Mineral Engineering, The Pennsylvania State University, University Park, PA 16802. Published in the Proceedings of the 3rd Annual Ventilation Symposium, The Pennsylvania State University, University Park, PA 16802. October 12-14, 1987. pp. 1-6. (PS-13)</i>	
III. Characterization of Dust Particles	57
5. Particle Size Distribution of Airborne Dust in Coal Mines	59
<i>T. Dumm and R. Hogg, Department of Mineral Engineering, Mineral Processing Section, The Pennsylvania State University, University Park, PA 16802. Published in the Proceedings of the 3rd Mine Ventilation Symposium, ed. by J. Mutmanský, University Park, PA, October 12-14, 1987, pp. 510-516. (PS-3)</i>	

	Page
<p>6. Distribution of Sulfur and Ash in Ultrafine Coal <i>T. Durnm and R. Hogg</i>, Department of Mineral Engineering, Mineral Processing Section, The Pennsylvania State University, University Park, PA 16802. Published in the Proceedings of the 2nd International Conference on Processing and Utilization of High Sulfur Coals II, eds. Y. P. Chugh and R. D. Caudle, Carbondale, IL, September 1987, pp. 23-32. (PS-3)</p>	66
<p>7. Surface Characterization of Coal Processing <i>R. Hogg and S. Chander</i>, Department of Mineral Engineering, Mineral Processing Section, The Pennsylvania State University, University Park, PA 16802. Published in Fine Coal Processing, eds. S. K. Mishra and R. R. Klimpel, Noyes Publications, 1987. (PS-3)</p>	76
<p>8. Wetting Behavior of Coal in the Presence of Some Nonionic Surfactants <i>S. Chander, B. R. Mohal and F. F. Aplan</i>, Department of Mineral Engineering, Mineral Processing Section, University Park, PA 16802. Published in Colloids and Surfaces. 26 (1987), pp. 205-216, Elsevier Science Publishers, B. V., Amsterdam. (PS-8)</p>	94
<p>9. Surfactant Adsorption and Wetting Behavior of Freshly Ground and Aged Coal <i>B. R. Mohal and S. Chander</i>, Department of Mineral Engineering, Mineral Processing Section, The Pennsylvania State University, University Park, PA 16802. Published in Interfacial Phenomena in Biotechnology and Materials Processing, eds. Y. A. Attia, B. M. Moudgil and S. Chander. Presented at the Fine Particle Society Symposium on Interfacial Phenomena in Materials Processing, Boston, MA, August 3-7, 1987. (PS-8)</p>	106
<p>10. Photoacoustic Spectroscopy of Quartz: Chopping Frequency Dependence, Saturation Phenomena and Quantative Analysis <i>M. Seehra, P. S. Raghootama and L. Cheng</i>, Physics Department, West Virginia University, Morgantown, WV 26506. Published in Applied Spectroscopy, 1987. (WV-13)</p>	123
<p>11. Oxygen Effects on Free Radicals and Cytotoxicity of Freshly Crushed Coals <i>N. S. Dalal, B. Jafari, M. M. Suryan and V. Vallyathan</i>, Department of Chemistry, West Virginia University, Morgantown, WV and Pathology Section, National Institute of Occupational Safety and Health, Morgantown, WV 26506. Presented at the 4th International Congress on Oxygen Radicals, June 27 - July 3, 1987, organized by the National Bureau of Standards, held at the University of California at San Diego, La Jolla, California. pp. 91-94. (Abstract only) (WV-10)</p>	134
<p>12. Role of Reactive Oxygen Radicals in Silica Cytotoxicity <i>V. Vallyathan, X. Shi, N. S. Dalal and W. Irr</i>, National Institute of Occupational Safety and Health and Chemistry Department, West Virginia University, Morgantown, WV 26505. Presented at the 4th International Symposium on Oxygen Radicals, San Diego, California, July 1987. Extended abstract published in the Proceedings, pp. 98-99. (WV-10)</p>	138

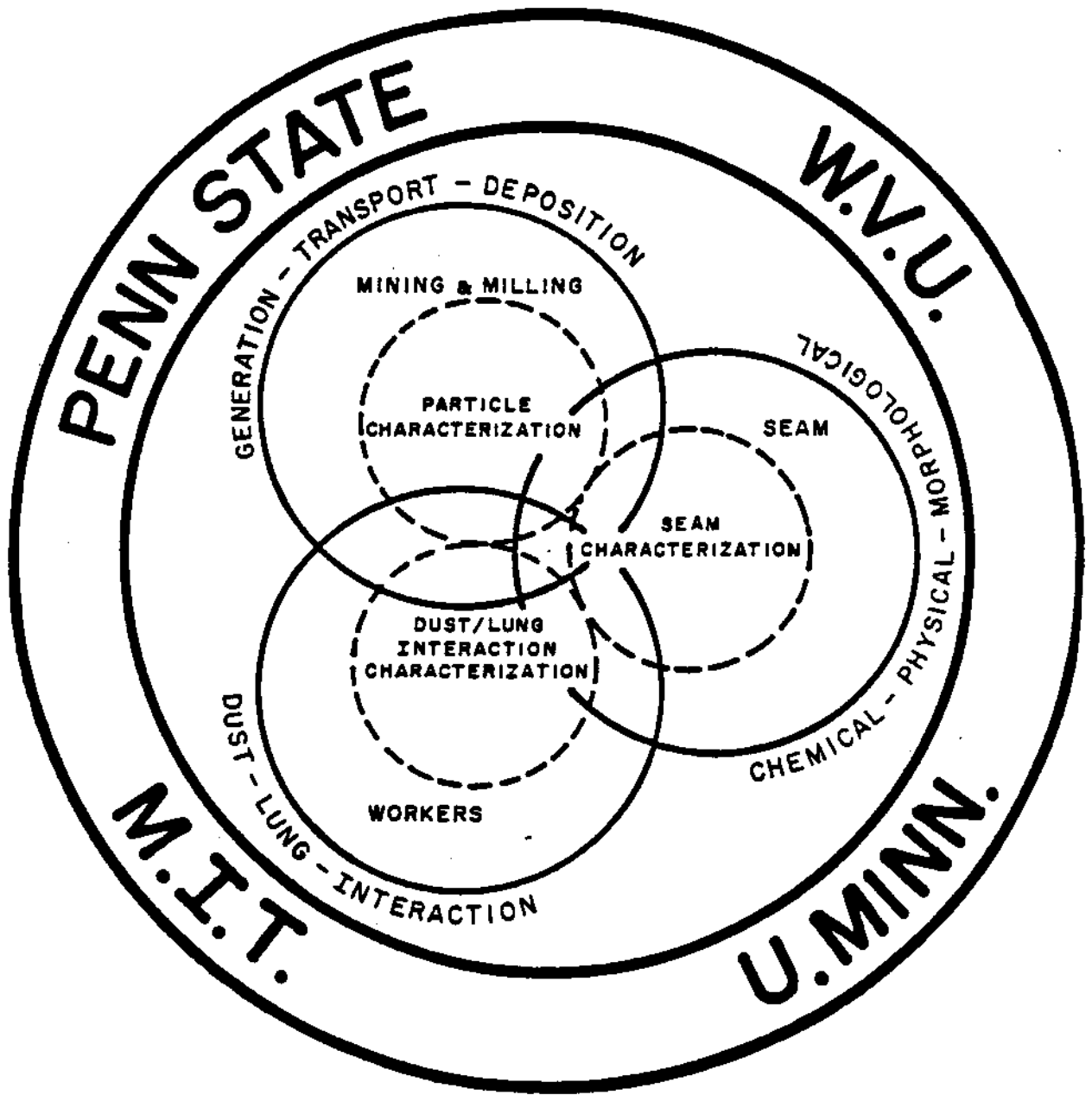
TABLE OF CONTENTS

	Page
<p>13. Mutagenicity of Diesel Exhaust Particles and Oil Shale Particles Dispersed in Lecithin Surfactant</p> <p><i>W. E. Wallace, M. J. Keene, C.A. Hill, et al.,</i> , Appalachian Laboratory for Occupational Safety and Health, Division of Respirable Disease Studies, National Institute of Occupational Safety and Health. Published in the Journal of Toxicology and Environmental Health, 21, pp. 167-171, 1987. (WV-12)</p>	141
<p>14. A Method for Resuspending Particles Deposited on Filters</p> <p><i>K. L. Rubow and V. A. Marple,</i> Mechanical Engineering Department, University of Minnesota, Minneapolis, MN. Presented at the American Industrial Hygiene Conference, Montreal, Canada (1987). Abstract published in the Proceedings. (Abstract only) (MN-1)</p>	149
<p>15. An Impactor with Respirable Penetration Characteristics and Size Distribution Capabilities</p> <p><i>V. A. Marple and K. L. Rubow,</i> Mechanical Engineering Department, University of Minnesota, Minneapolis, MN. Presented at the American Industrial Hygiene Conference, Montreal, Canada (1987). Abstract published in the Proceedings. (Abstract only) (MN-1)</p>	150
<p>16. Crossflow Influence on Collection Characteristics of Multinozzle Micro-orifice Impactor</p> <p><i>C. P. Fang and V. A. Marple,</i> Mechanical Engineering Department, University of Minnesota, Minneapolis, MN. Presented at the Annual Meeting of the American Association for Aerosol Research, Seattle, WV (1987). Abstract published in the Proceedings. (Abstract only) (MN-1)</p>	151
<p>17. Fragment Size Distribution from Simple Fracture of Coal and Rock</p> <p><i>C. J. Tsai, D. Y. H. Pui, R. Caldow, K. Olson and B. Cantrell</i> Mechanical Engineering Department, University of Minnesota, Minneapolis, MN. Presented at the Annual Meeting of the American Association for Aerosol Research, Seattle, WA (1987). Abstract published in the Proceedings. (Abstract only) (MN-1)</p>	152
<p>18. Measuring the Size Distribution of Diesel Exhaust and Mine Dust Aerosol Mixtures with the Micro-orifice Uniform Deposit Impactor</p> <p><i>K. L. Rubow, V. A. Marple, D. B. Kittleson and C. P. Fang,</i> Mechanical Engineering Department, University of Minnesota, Minneapolis, MN. Presented at the Annual Meeting of the American Association for Aerosol Research, Seattle, WA (1987). Abstract published in the Proceedings. (Abstract only) (MN-1)</p>	153
<p>IV. Interaction of Dust and Lungs</p>	
<p>19. Detection of Receptor and Synthesis Antagonists of Platelet Activating Factor in Human Whole Blood and Neutrophils Using Luminol-Dependent Chemiluminescence</p> <p><i>K. Van Dyke and V. Castranova,</i> Department of Pharmacology and Toxicology, West Virginia University, Morgantown, WV and Division of Respirable Disease Studies, National Institute for Occupational Safety and Health. Published in New Horizons in Platelet Activating Factor Research, edited by C. M. Winslow and M. L. Lee, 1987, John Wiley & Sons Ltd., pp. 181-187. (WV-17)</p>	157

	Page
20. Measurement of Superoxide Release from Single Pulmonary Alveolar Macrophages	163
<i>E. V. Cilento, R. C. Lantz and K. A. DiGregorio, Department of Chemical Engineering, West Virginia University, Morgantown, WV 26506. Published in the Journal of Physiology, 252 (21): C677-C683, 1987. (WV-9)</i>	
21. Mucins Secreted by Rat Tracheal Explants in Culture, Characterization and Influence of Coal Dust	170
<i>V. P. Bhavanandan and S. B. Dubbs, The Milton S. Hershey Medical Center, The Pennsylvania State University, Hershey, PA 17033. Presented at the Annual Meeting of the American Society for Complex Carbohydrates, November 1987, Bethesda, MD. (Abstract only) (PS-11)</i>	
V. Relationship of Mine Environment, Geology and Seam Characteristics to Dust Generation and Mobility	171
22. Application of the Size and Elemental Characteristics of Airborne Coal Dust for Source Identification	173
<i>C. Lee and J. M. Mutnansky, Department of Mineral Engineering, The Pennsylvania State University, University Park, PA 16802. Published in Coal Mining and Safety, pp. 321-330, Korean Institute of Mineral Engineering, Seoul, Korea (1987). Presented at the International Symposium on Coal Mining and Safety, Seoul, Korea, April 22-24, 1987. (Abstract only) (PS-5)</i>	
23. World Wide Coal Mine Dust Research—Where Are We Going?	183
<i>J. M. Mutnansky, Department of Mineral Engineering, The Pennsylvania State University, University Park, PA 16802. Presented at the International Symposium on Coal Mining and Safety, Seoul, Korea, April 22-24, 1987. (PS-5)</i>	

INDEX

Cumulative Author Index	195
Cumulative Subject Index	198



The Respirable Dust Center

FOREWORD

This volume contains publications resulting from respirable dust research performed in the Generic Mineral Technology Center for Respirable Dust by faculty, staff and graduate students at The Pennsylvania State University, West Virginia University, University of Minnesota, Michigan Technological University, and Massachusetts Institute of Technology. These publications have appeared in scientific journals, the proceedings of national and international symposiums and at professional meetings in 1987. Complete citations of the publications can be found in the text. The Generic Mineral Technology Center for Respirable Dust is funded by the U.S. Bureau of Mines through the Mining and Mineral Resources Research Institute Program. The opinions and conclusions expressed in the papers are those of the authors alone and do not represent the opinions of the Generic Mineral Technology Center for Respirable Dust, the Mining and Mineral Resources Research Institute program or the U.S. Bureau of Mines. Citation of manufacturers' names in the papers was made for general information purposes and does not imply endorsement of the products by the authors.

All of the publications in this volume are on research that has been supported by the Department of the Interior's Mineral Institute program and administered by the Bureau of Mines through the Generic Mineral Technology Center for Respirable Dust under allotment grant number G1135142 or G1175142.

In addition to publishing these papers, the Center has organized a dust conference and an international symposium. In October 1984, a dust conference was held at West Virginia University. Co-sponsored by the Generic Mineral Technology Center for Respirable Dust, ACGIH, MSHA, NIOSH and USBM, the proceedings are available in the publication 1984 Coal Mine Dust Conference, edited by Syd S. Peng, Morgantown, WV (Publication #PB86-169380). This publication is available from NTIS. An international symposium, Respirable Dust in the Mineral Industries: Health Effects, Characterization and Control, was held at The Pennsylvania State University in October 1986. Co-sponsored by the Generic Mineral Technology Center for Respirable Dust, ACGIH, MSHA, NIOSH and USBM, the proceedings are available in the publication Respirable Dust in the Mineral Industries, edited by Robert L. Frantz and Raja V. Ramani, University Park, PA. This publication is available from ACGIH, ISBN: 0-936712-76-7 (Publication #3010).

The Generic Center maintains a reference center that serves as a clearinghouse for technical information for the generic area and supplies reports on generic center accomplishments.

The support for the Generic Mineral Technology Center for Respirable Dust from the United States Congress is gratefully acknowledged. We also acknowledge and appreciate the support and input from USBM, NIOSH, MSHA, the Research Advisory Council and the Committee on Mining and Mineral Resources Research which have significantly contributed to the activities of the Generic Mineral Technology Center for Respirable Dust.

Respectfully submitted,

Robert L. Frantz
Co-Director, Generic Mineral Technology
Center for Respirable Dust
Co-Editor

R. V. Ramani
Co-Director, Generic Mineral Technology
Center for Respirable Dust
Co-Editor

Excerpted From The
1988 UPDATE TO THE NATIONAL PLAN
FOR
RESEARCH IN MINING AND MINERAL RESEARCH

Report to:

December 15, 1987

The Secretary of the Interior
The President of the United States
The President of the Senate
The Speaker of the House of Representatives


Section 9(e) of Public Law 98-409 of August 29, 1984, (98 Stat. 1536 et seq.) mandates that the Committee on Mining and Mineral Resources Research submit an annual update to the National Plan for Research in Mining and Mineral Resources: "Improving Research and Education in Mineral Science and Technology through Government-(Federal, State and Local), Industry, and University Cooperation."


Respirable Dust (centered at Pennsylvania State U. and West Virginia U., with affiliates at U. of Minnesota and Massachusetts Institute of Technology): brings together experts concerned with particles causing potentially disabling or fatal diseases, including pneumoconiosis ("black lung"), silicosis, and asbestosis, the latter of deep concern not just to workers in the mineral sector of the economy but also to the general populace.


SIGNED:



Carl K. Randolph
Mining Industry

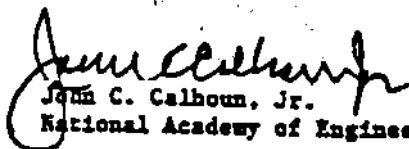

Win Aung
National Science
Foundation

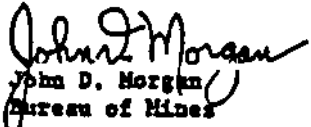

Don L. Warner
University Administrator


Walter R. Hibbard, Jr.
National Academy of
Sciences



John H. DeYoung, Jr.
U.S. Geological
Survey

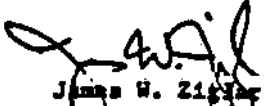

Joseph N. Crowley
University Administrator


John C. Calhoun, Jr.
National Academy of Engineering


John D. Morgan
Bureau of Mines


Edward S. Franklin
Mining Industry


Orme Lewis, Jr.
Conservation Community
COCHAIR


James W. Ziff
Asst. Secretary
Water & Science
U.S. Department of
the Interior
COCHAIR

Excerpted From The
1988 UPDATE TO THE NATIONAL PLAN
FOR
RESEARCH IN MINING AND MINERAL RESEARCH

Report to:

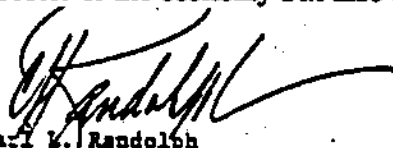
December 15, 1987

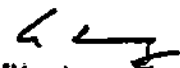
The Secretary of the Interior
The President of the United States
The President of the Senate
The Speaker of the House of Representatives

Section 9(e) of Public Law 98-409 of August 29, 1984, (98 Stat. 1536 et seq.) mandates that the Committee on Mining and Mineral Resources Research submit an annual update to the National Plan for Research in Mining and Mineral Resources: "Improving Research and Education in Mineral Science and Technology through Government-(Federal, State and Local), Industry, and University Cooperation."

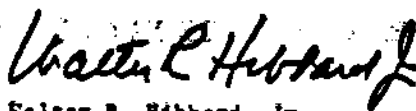
Respirable Dust (centered at Pennsylvania State U. and West Virginia U., with affiliates at U. of Minnesota and Massachusetts Institute of Technology): brings together experts concerned with particles causing potentially disabling or fatal diseases, including pneumoconiosis ("black lung"), silicosis, and asbestosis, the latter of deep concern not just to workers in the mineral sector of the economy but also to the general populace.


SIGNED:


Carl K. Randolph
Mining Industry

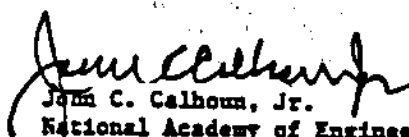

Win Aung
National Science
Foundation

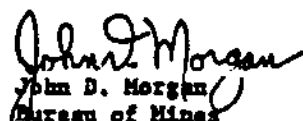

Don L. Warner
University Administrator

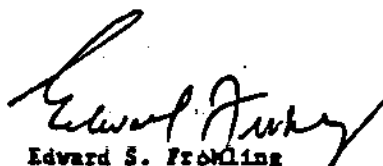

Walter R. Hibbard, Jr.
National Academy of
Sciences

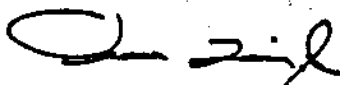

John H. DeFoung, Jr.
U.S. Geological
Survey



Joseph N. Crowley
University Administrator


John C. Calhoun, Jr.
National Academy of Engineering


John D. Morgan
Bureau of Mines


Edward S. Frowling
Mining Industry


Orme Lewis, Jr.
Conservation Community
COCHAIR


James H. Ziffer
Asst. Secretary-
Water & Science
U.S. Department of
the Interior
COCHAIR

THE RESPIRABLE DUST CENTER

Generic Mineral Technology Center For Respirable Dust

RESEARCH ADVISORY COUNCIL MEMBERS

Dr. John A. Breslin
Senior Staff Physical Scientist
U.S. Bureau of Mines
2401 E Street, N.W.
Columbia Plaza
Washington, D.C. 20241
(202) 634-1220

Dr. Ronald Munson
Director, Office of Mineral
Institutes - MS 1020
U.S. Department of the Interior
2401 E Street, N.W.
Washington, D.C. 20241
(202) 634-1328

Dr. Lewis Wade
Research Director
Twin Cities Research Center
U.S. Bureau of Mines
5629 Minnehaha Avenue, S.
Minneapolis, MN 55417
(612-725-4610)

Dr. John A. Campbell
Director, Engineering and
Technology Support
Kerr-McGee Corporation
P.O. Box 25861
Oklahoma City, OK 73125
(405) 270-3778

Mr. John Murphy
Research Director
Pittsburgh Research Center
U.S. Bureau of Mines
P.O. Box 18070
Pittsburgh, PA 15238
(412-675-6601)

Dr. James L. Weeks, C.I.H.
Deputy Administrator for
Occupational Health
United Mine Workers of
America
900 15th Street, N.W.
Washington, D.C. 20005
(202) 842-7300

Mr. Robert E. Glenn
Director, Division of Respiratory
Disease Studies - NIOSH
944 Chestnut Ridge Road
Morgantown, WV 26505
(304) 459-5978

Dr. Kandiah Sivarajah
State Toxicologist
Room 825--Health and Welfare
Building
Harrisburg, PA 17108
(717) 787-1708

Dr. Jerome Kleinerman
Department of Pathology
Cleveland Met. General Hospital
3395 Scranton Road
Cleveland, OH 44109
(216) 459-5978

Dr. Pramod Thakur
Research Group Leader
CONOCO, Inc.
R & D Division
Route #1, Box 119
Morgantown, WV 26505
(304) 963-2251

PAST RESEARCH ADVISORY COUNCIL MEMBERS

Mr. Darrel Auch
Senior Vice President
Northern West Virginia Region
Consolidation Coal Company
P.O. Box 1314
Morgantown, WV 26507
(304) 296-3461

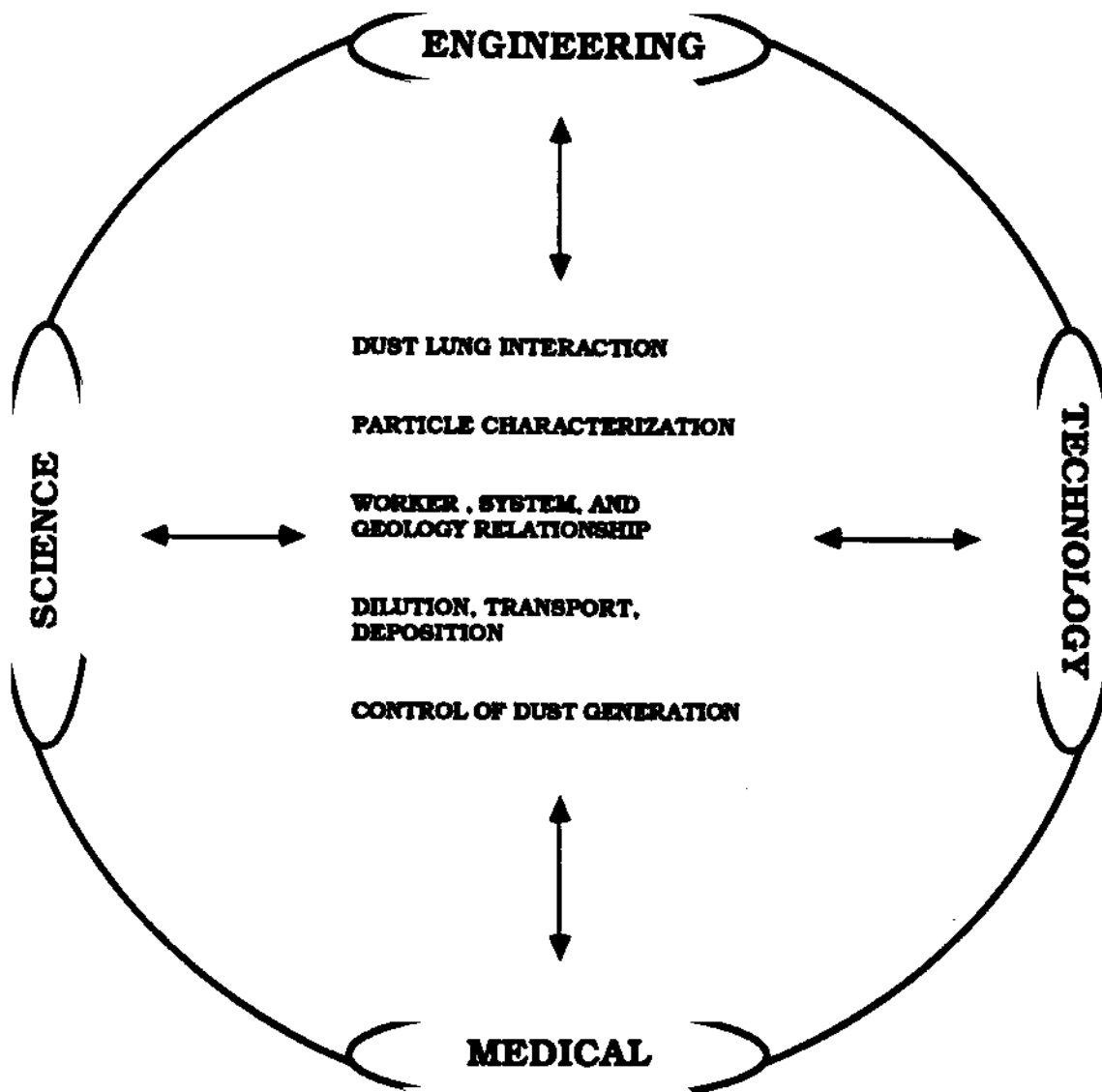
Dr. Thomas Falkie
President
Berwind Natural Resources
Company
Centre Square West
1500 Market Street
Philadelphia, PA 19102
(215) 563-2800

Mr. C. Wealey McDonald
Senior Vice President
(Mining)
Northern West Virginia
Region
Consolidation Coal Company
P.O. Box 1314
Morgantown, WV 26505
(304) 296-3461

Dr. J. Harrison Daniel
Program Manager, Mining
Research
Health and Safety
2401 E Street, N.W.
Washington, D.C. 20241
(202) 634-1253

Dr. Fred Kissell
Research Supervisor
Pittsburgh Safety Research Center
U.S. Bureau of Mines
4800 Forbes Avenue
Pittsburgh, PA 15213
(412) 675-6679

Dr. Donald Reid
Deputy Secretary for Public
Health Programs
Department of Health
Health and Welfare Building
P.O. Box 90
Harrisburg, PA 17108
(717) 783-8804



Standardized protocols for Respirable Dust Research in scientific, engineering, and medical areas.

RESEARCH



CONTROL OF GENERATION

- Amount
- Fracture

**DILUTION,
TRANSPORT
AND
DEPOSITION**

- Concentration
- Size Consist
- Modeling

**MINE WORKER,
MINING SYSTEM,
SEAM GEOLOGY**

- Seam Sections
- Silica
- Trace Elements
- System Configuration
- Worker Location



- Coal Data Bank
- Mine Samples

**SUITE OF
GENERATED
RESPIRABLE
DUSTS**

- Anthracite
- Medium Volatile Bituminous
- High Volatile Bituminous
- Silica
- Fireclay
- Rock Dust



CHARACTERIZATION

- Size/Shape/Composition
- Surface/Functional Groups
- Particle Interaction

**DUST LUNG
INTERACTION**

- Medical/Cellular
- Medical/Animal
- Medical/Human
- Medical/Engineering



TRAINING

Train engineers, scientists, medical personnel, graduate students and undergraduate students in the interdisciplinary aspects of respirable dust.

THE RESPIRABLE DUST CENTER

The Generic Mineral Technology Center for Respirable Dust

SUITE OF CHARACTERIZED DUST SAMPLES	SAMPLING AND DUST GENERATION METHODS	SUITE OF MEDICAL TESTS
1. Anthracite (Low Volatile)	Dust/Lung Interaction	1. Rats
2. Bituminous (Medium Volatile)	Particle Characterization	2. Guinea Pigs
3. Bituminous (High Volatile)	Mine Workers, Mining System Seam Geology Dust Relationships	3. Dogs
4. Fireclay	Respirable Dust Dilution, Transport and Deposition	4. Non-Human Primates
5. Silica	Control of Dust Generation	5. Black Lung Patients
6. Rockdust		6. Healthy People

**SIZE, CHEMICAL AND
MINEROLOGICAL ANALYSIS**

STATEMENT OF GOAL

The primary goal of the Generic Mineral Technology Center for Respirable Dust is to reduce the incidence and severity of respirable dust disease through advancing the fundamental understanding of all aspects of respirable dust associated with mining and milling and the interaction of dust and lungs.

The holistic approach to standardized protocols and procedures.

I
CONTROL OF DUST AND
PARTICULATE MATTER
GENERATION

Development of a Mixed Mode Testing System for Geological Materials

R. Karl Zipf and Z.T. Bieniawski
Department of Mineral Engineering, The
Pennsylvania State University

ABSTRACT

Fracture mechanics plays an important role in studies of geologic materials such as rock and coal. Yet, fracture data are scarce for rock and most limited or unreliable for coal. A testing system was developed which can apply mixed mode loads to a crack tip in many rocks and geologic materials. It is possible to subject the test specimen to pure mode I, various mixed modes and a nearly pure mode II fracture load. The system is currently used to study the mechanics of fine fragment formation in various coals. Experimental measurements include K_I and K_{II} , fracture velocity and acoustic emission.

INTRODUCTION

A major research program at The Pennsylvania State University is directed to understanding the fundamental mechanics of fine fragment formation in various coals. The program represents an effort to reduce the incidence of coal workers pneumoconiosis (black lung) in coal miners. The principal source of the respirable coal fragments is the cutting operation which forms and liberates the particles by a fracture process. Present understanding of the mechanics of the events which form and liberate these particles is meager (Cook, 1982).

Current knowledge of the fundamental mechanisms of coal dust generation and entrainment in terms of the underlying fracture mechanics is critically needed to improve and possibly control the processes involved. Whether the cutting operation is done with a 'continuous miner' cutting machine, a plow or a longwall shearer, it is fundamentally a problem of mixed-mode crack propagation. When a cutting tool interacts with coal, it causes numerous cracks to propagate through the intact material. Numerous larger fragments are broken free, but another quantity of undesirable fine fragments is also created. The formation of these respirable fragments may be a direct result of the crack propagation process; hence, a thorough understanding of the fracture mechanics of coal is required to minimize production of the unwanted fine fragments.

In most rock engineering applications, the rock material properties are of secondary importance to the rock mass properties; however, for rock fragmentation and rock cutting problems, it is rock material properties such as fracture toughness which are of prime interest (Bieniawski, 1980). Several rock cutting and rock failure theories have been proposed, but it is only very recently that fracture mechanics concepts have been successfully applied to the study of rock cutting mechanics. All cutting models seek to predict the cutting forces and the cutter geometry necessary to cause rock breakage and chip formation given some fundamental mechanical properties of the rock. Such models have wide applications in drilling, tunnel boring and mining problems. Nelson et al., (1985, 1986) has provided a very useful correlation between the laboratory measured fracture mechanics properties of rock and the performance of the disk cutters on tunnel boring machines.

Only one model successfully analyzes rock cutting using fracture mechanics concepts. Saouma and Ingraffes (1981) designed an interactive finite element program called FEFAP that simulates mixed mode crack propagation based on linear elastic fracture mechanics. The program can predict the failure loads and the radial pattern of cracking under a TBM roller cutter (Ingraffes, 1985). Saouma and Kleinosky (1984) use a similar program called SICRAP to effectively model the action of a drag bit cutter. The finite element mesh and the calculated crack path for chip formation are shown in Figure 1. The analyses are qualitatively highly realistic but the predicted failure loads are somewhat lower than the experimentally determined values.

R. Karl Zipf is a Doctoral Student and Z. T. Bieniawski is Professor of Mineral Engineering, Department of Mineral Engineering, Pennsylvania State University, University Park, PA. 16802.

THE RESPIRABLE DUST CENTER

The research reported in this paper seeks to provide accurate measurements of the fracture toughness of coal subjected to realistic mixed mode loading conditions. In conjunction with the mixed mode fracture toughness measurements are fracture velocity measurements during unstable crack propagation in coal. This novel experimental concept is based on the observation that crack bifurcation occurs above some critical fracture velocity. The hypothesis is that in part, fine fragments are formed as a result of crack bifurcation; hence, knowledge of the fracture velocity and the factors controlling it may lead to further understanding of the mechanics of respirable dust formation.

The same models used to predict cutting forces and chip formation are very similar to those used to understand the fundamental mechanisms of airborne respirable dust (ARD) formation. The model proposed by Roepke (1984) served as a basis for several postulates by researchers at the Southwest Research Institute (Stecklein et. al. 1982) regarding the mechanics of ARD production. These postulates have been modified and extended at The Pennsylvania State University to include the following:

- 1) Crushing, grinding and scraping by the tool tip
- 2) Energy dissipation during fracture within the fracture process zone
- 3) Crack bifurcation during unstable crack propagation
- 4) Explosive disintegration during chip formation caused by violent release of elastic strain energy
- 5) Preferential detachment of impurity particles during fracture due to differing elastic moduli.

The relative importance of these mechanisms and the factors which influence their relative importance are not well understood. Most regard the crushing mechanism as most important; although, experimental evidence for this contention is sparse (Zipf and Bieniawski, 1986 b). The present research focuses on the energy dissipation and the crack bifurcation mechanisms and their influence on fine fragment formation. Two experimental approaches have been advanced to understand and quantify the fracture process as it relates to fine fragment formation according to the mechanisms discussed above (Zipf and Bieniawski, 1986 a).

In the first approach, theoretical models which describe the size of the fracture process zone in a brittle material are related to the amount of material damage on a new fracture surface which may characterize the propensity of a coal to generate undesirable fine fragments. The second approach is based on relationships between crack tip stress intensity and the measured fracture velocity and their effect on new fracture surface appearance. Higher stress intensities and higher fracture velocities are shown to have a significant effect on fracture surface appearance and therefore the potential for increased respirable dust formation. Figure 2 shows a typical SEM micrograph obtained during the course of this study. Damage to and fragments on the newly created fracture surfaces appear as lighter areas in these images. A detailed discussion and interpretation of these images is beyond the scope of this paper which intends to focus more on our mixed mode testing methodology.

NATURE OF COAL

As a test material, coal is probably one of the more difficult substances. It can be very friable, heavily flawed and frequently moisture and oxygen sensitive. Extreme care in collecting, preserving, and preparing test specimens is a pre-requisite to obtaining quality test results.

Coal is a sedimentary rock composed of the decayed, altered remains of ancient plant life. Just as a rock is composed of minerals, coal is composed of a variety of macerals that are readily distinguishable under a microscope. Of great importance to fracture mechanics testing of coal is the complex flow structure that exists within coal. Typically, coal is dissected by an orthogonal set of discontinuities called the bedding planes, the face cleat and the butt cleat. Their spacing may range from less than a millimeter to tens of centimeters. Many other randomly oriented discontinuities may be present as well.

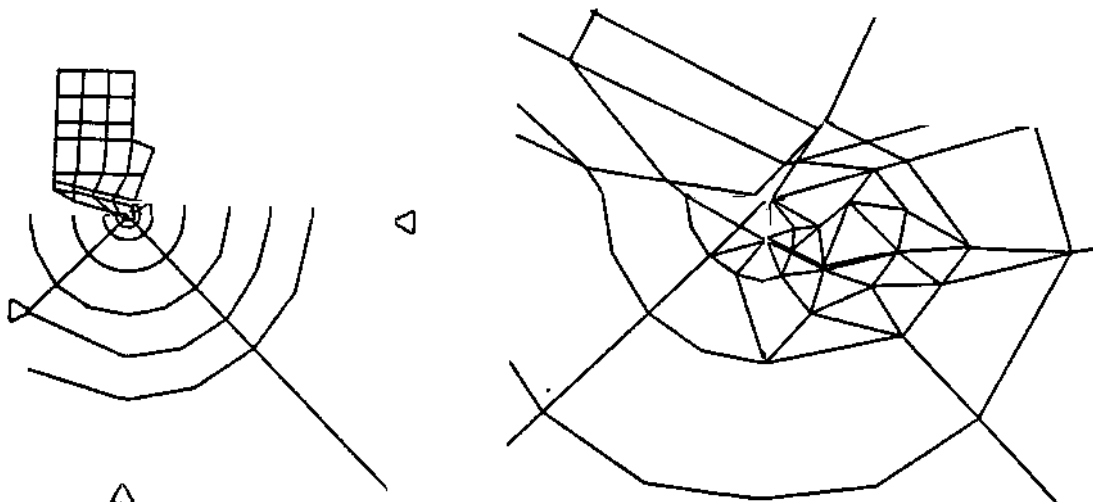


Figure 1 - Finite Element Mesh And Crack Path For Drag Cutter (Saouma and Kleinovsky, 1984)

MIXED MODE TESTING SYSTEM

On the smallest scale of these flaws are those discontinuities arising from differences in molecular structure and composition within individual macerals. At a higher scale which is of particular interest to this research, there are microcracks, voids, etc. At the next higher scale which is about the size of most fracture toughness test specimens there are cracks, small joints and the coal cleats. Finally, at the highest scale are major joints and faults.

In fracture toughness testing, it is critical to remember the key underlying assumption that the starter notch is by far the most dominant "flaw" in the material. In practice, this assumption may be difficult to meet because flaws exist at all scales within coal and in most rocks. Thus, for practical testing, it is difficult to get a test specimen that is say one order of magnitude larger than some flaw size of interest without introducing effects from the next highest scale of flaw.

Many factors complicate the brittle fracture of rock materials (Bieniawski, 1980). They are: anisotropy, confining pressure, moisture content, loading rate, specimen size and shape, temperature and humidity. While all these factors are important, the size effect is of greatest practical importance. This effect is related to the scale of flaws within the test specimen. As shown in Figure 3, the compressive strength of a cube of rock decreases as the test cube size increases. For coal, above a critical size of about 1 meter, the strength remains constant. This size effect is intimately related to the scale of flaws one can expect in a material. Flaws on a scale greater than about 1 meter are much less frequent in coal so the strength remains constant. A similar size effect exists for ceramics (Batdorf, 1978 and Mecholsky et al. 1979). The upper bound on the inherent flaw size in ceramics is on the order of one millimeter; therefore,

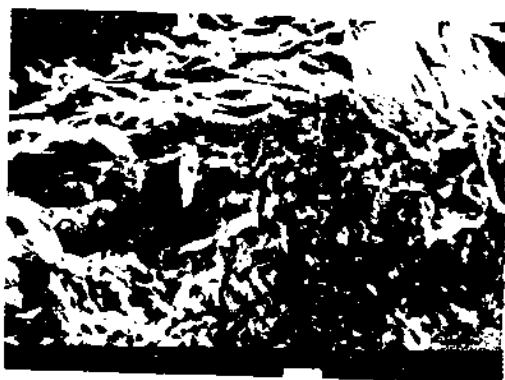


Figure 2 - SEM Micrograph Of Pittsburgh Coal

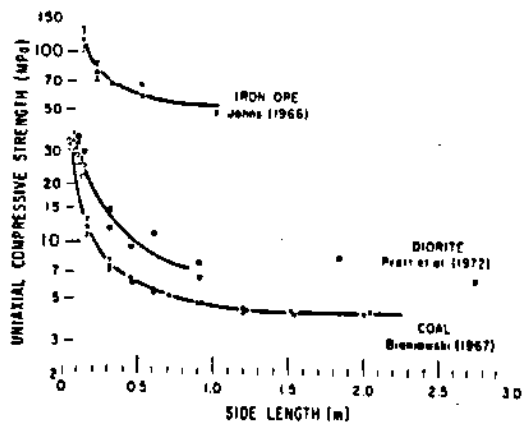


Figure 3 - Size Effect On The Compressive Strength Of Coal And Rock (Bieniawski, 1980)

THE RESPIRABLE DUST CENTER

Calculated loads from these equations serve as input to the finite element program ANSYS used for stress and displacement analysis of the test specimen geometry. ANSYS* uses a crack tip element with an inverse square-root singularity in the displacement field at the crack front. The final mesh used in these analyses is shown in the Figure 10. Forces A, B and C and zero displacements at A', B' and C' are applied as shown in this figure. Model dimensions are 100 by 100 millimeters. Material properties are E= 3.45 GPa (500,000 psi) v = 0.25 for the coal. Elements along the top and bottom rows of elements are modeled as aluminum with E= 70 GPa (10,000,000 psi) and v = 0.33. Convergence studies demonstrated that a final mesh with 588 elements provided sufficiently accurate numerical results for estimates of K_I and K_{II} as a function of loading conditions.

Stress intensity factors are then computed from these stresses with the following relations.

$$K_I = \sqrt{2\pi r} \begin{matrix} \sigma_1 a_{22} - \sigma_2 a_{12} \\ a_{11}a_{22} - a_{21}a_{12} \end{matrix} \qquad K_{II} = \sqrt{2\pi r} \begin{matrix} \sigma_2 a_{11} - \sigma_1 a_{21} \\ a_{11}a_{22} - a_{21}a_{12} \end{matrix}$$

$$a_{11} = \cos \frac{\theta}{2} (1 + \sin \frac{\theta}{2}) \qquad a_{21} = \cos \frac{\theta}{2} (1 - \sin \frac{\theta}{2})$$

$$a_{12} = -\sin \frac{\theta}{2} + \frac{1}{2} \sqrt{4 - 3\sin^2 \theta} \qquad a_{22} = -\sin \frac{\theta}{2} - \frac{1}{2} \sqrt{4 - 3\sin^2 \theta}$$

The computed K factors are given by the following relation:

$$K_{I,II} = \frac{P}{t} f_{I,II}(\theta)$$

where K = stress intensity factor (Pa \sqrt{m})
 P = specimen load (N)
 t = specimen thickness (m)

Values of f(θ) for the different testing rig position are tabularized as follows:

θ	0° (mode I)	15°	30°	45°	60°	75°	90° (mode II)
$f_I(\theta)$	10.58	8.78	6.40	4.22	2.51	1.14	0.00
$f_{II}(\theta)$	0.00	0.40	0.86	1.31	2.51	4.11	5.71

Richard (1984) derived the following more general stress intensity factor equations for the original compact tension shear test rig valid in the range $0.5 \leq a/w \leq 0.7$

$$K_I = \frac{P}{wt} \sqrt{\pi a} \frac{\cos \theta}{1 - \frac{a}{w}} \sqrt{0.26 + 2.65 \left(\frac{a}{w-a} \right) - 0.08 \left(\frac{a}{w-a} \right)^2}$$

$$K_{II} = \frac{P}{wt} \sqrt{\pi a} \frac{\sin \theta}{1 - \frac{a}{w}} \sqrt{-0.23 + 1.40 \left(\frac{a}{w-a} \right) + 2.08 \left(\frac{a}{w-a} \right)^2}$$

where w = specimen width (m)
 a = crack length (m)

In addition, fresh coal is stored in a chamber at 100% humidity at all times to prevent drying and shrinkage cracking. In order to obtain more meaningful cross correlations between tests, specimens for a mixed mode test, compressive strength test, tensile strength test and all the other tests are all cut from the same lump of raw coal. With these procedures, sample preparation has been extremely reliable, since it is possible to prepare fracture toughness test specimens from over 75% of the coal lumps collected in the field. Such practice certainly leads to better quality fracture toughness data more representative of the in situ coal.

*ANSYS is developed by Swanson Analysis Systems, Inc., Houston, Pa.

MIXED MODE TESTING SYSTEM

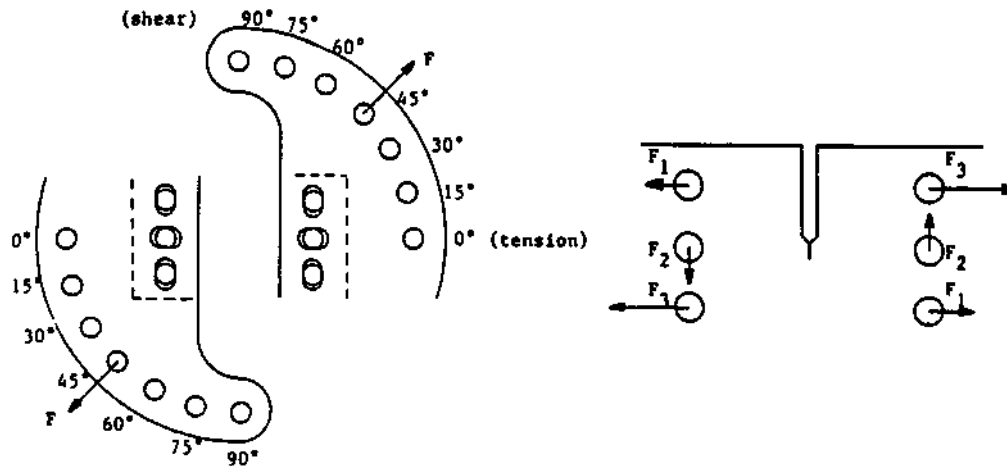


Figure 4 - Schematic Of Richard's Compact Tension Shear Specimen And Loading Rig (Richard, 1984)

MIXED MODE TEST SYSTEM DESIGN

To realistically study the mechanics of fine fragment formation in coal requires a mixed mode test procedure since the actual crack propagation in the vicinity of a coal cutting tool is also a mixed mode process. From a general review of the rock mechanics literature, relatively little test work has been completed under mixed mode loading conditions (Ouchterlony, 1982). Only recently has such testing become important in other materials such as metals and ceramics. Ingraffea (1977, 1981) completed the most recent studies on rock under mixed mode loading conditions using Indiana Limestone and Westerly Granite. He used a variant of a single edge notch beam in four point bending to generate a spectrum of mode I through mode II loading conditions on the starter notch. More recently, Laqueche et.al., (1986), studied mode I and mode II crack propagation in a highly orthotropic slate schist.

For practical reasons, a specimen width of 100 mm with a crack length of 50 mm was selected even though this specimen is theoretically subsize (Zipf and Bieniawski, 1986 a). Such a specimen size does match the scale of fracture occurring in the vicinity of a coal cutting tool. Beam type fracture specimens were considered for mixed mode testing; however, for the large sizes that were desired, such specimens became quite impractical. For this reason, we elected to modify and develop a mixed mode testing concept initially presented by Richard (1984). Figure 4 shows a schematic of the compact tension shear specimen and loading rig used by Richard on metals and plastics. A tensile load is applied to the appropriate pair of outer holes in the loading rig. This load in turn generates tensile and bending loads on the specimen through the six pins placed in holes near the outer boundary of the specimen. With this concept, it is possible to subject the test specimen to pure mode I, various mixed modes and a nearly pure mode II load. Using a compact specimen has the advantage that effectively larger test specimens of difficult materials like coal become more feasible to test.

The system as designed and in use at Penn State is shown in Figure 5. Very basically, the system contains the following major components:

- 1) a test specimen equipped with a pair of glue-on specimen grips.
- 2) two pairs of loading plates that apply tensile and bending loads to the specimen.
- 3) an assortment of hardware for attaching the loading fixture in an Instron testing machine.

The test specimens are square or nearly square in cross section with the length and width ranging from 80 to 110 mm and a thickness ranging from 40 to 60 mm. A 0.6 mm starter notch is cut to the specimen midpoint with the small diamond bandsaw. Instead of applying load to the test specimen through holes drilled in the specimen, sets of gripping fixtures which contain the appropriate loading holes were fabricated from aluminum channel. These fixtures are then firmly attached to the test specimen with epoxy adhesives (3M brand 1838) using a special gluing jig. Figure 6 shows a typical test specimen in this gluing jig. Tensile and bending loads are applied to the test specimen through the gripping fixtures via two pairs of lobe shaped aluminum plates. It is possible to change the main load application point on these plates and thereby subject the specimen to a range of fracture mode loadings. Other hardware in the fixture is a section of chain to eliminate any applied torsion on the specimen and a turnbuckle to take up play in the system prior to starting the testing machine.

Test methodology and monitoring are straightforward. A 2500 N (500 lb) load cell above the test fixture records load and an LVDT placed across the specimen grips monitors the crack opening. Resolution of these instruments is less than 2.5 N (0.5 lb) and less than 10^{-3} mm (25 micro-inch). Total acoustic emission counts are monitored with a transducer placed ahead of the starter notch tip. Signals from these devices are recorded on a strip chart recorder. Fracture velocities are measured with a crack propagation gage (Micro-Measurements Division). One of these gages is shown in Figure 7. These gages are bonded to the specimen much like a strain gage ahead of the area of expected crack growth. A known voltage is applied across the gage and as the crack propagates, the gage strands break which causes the voltage to change in

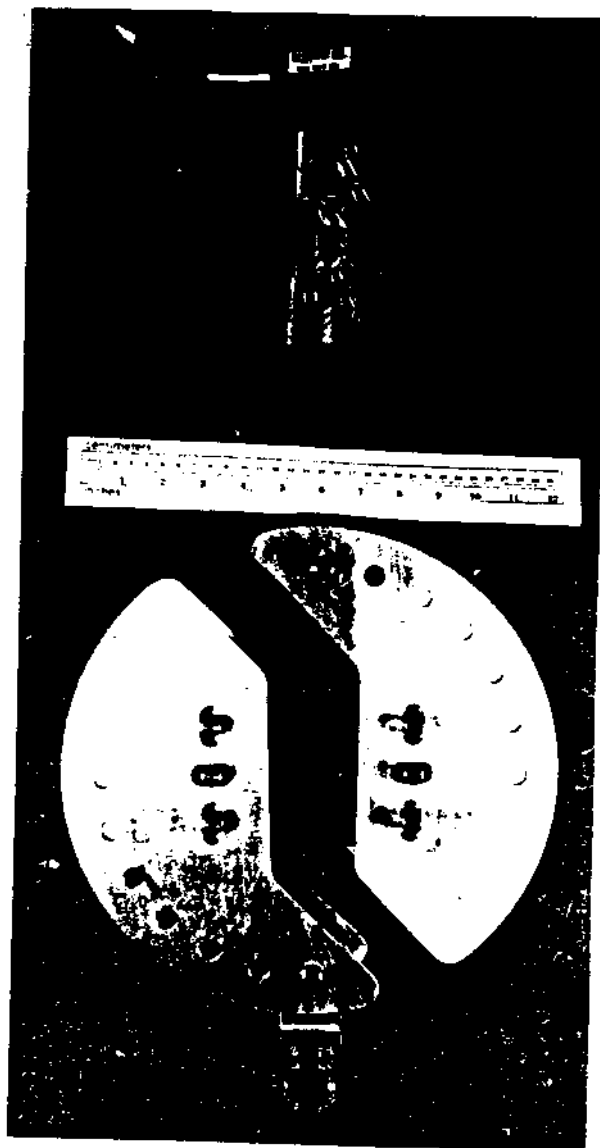


Figure 5 - Photograph Of The PSU
Mixed Mode Test Fixture

steps. The changing voltage versus time is recorded with a NICOLET 4094 digital storage oscilloscope. From the voltage versus time recording, it is straightforward to extract distance versus time and hence fracture velocity. The oscilloscope provides time measurements as small as 0.5 micro second which is enough resolution to calculate high speed crack velocities. A photograph of the NICOLET displaying a typical voltage versus time recording from a crack gage is shown in Figure 8.

ANALYSIS OF MIXED MODE TEST SYSTEM

K_I and K_{II} factors for this particular specimen and loading geometry were derived. Static equilibrium analysis gave equations relating the rig load P to the applied forces on the specimen. Free body diagrams for the specimen and rig are shown in Figure 9. The resulting load equations are

$$A = \frac{P}{2} \left(\frac{bb'}{ac} \sin \theta - \cos \theta \right) \quad B = P \sin \theta \quad C = \frac{P}{2} \left(\frac{bb'}{ac} \sin \theta + \cos \theta \right)$$

the strength or fracture toughness remains fairly constant above test specimen sizes greater than a few centimeters.

TEST PROGRAM

The present experimental work aims to provide the necessary mechanical properties data to quantify the energy dissipation and crack bifurcation mechanisms postulated for dust production. The most important

MIXED MODE TESTING SYSTEM

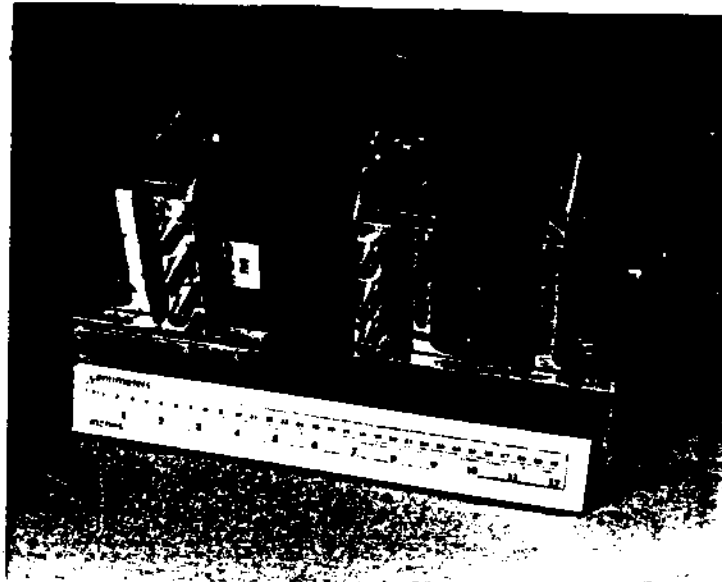


Figure 6 - Photograph Of Typical Test Specimen In Gluing Jig

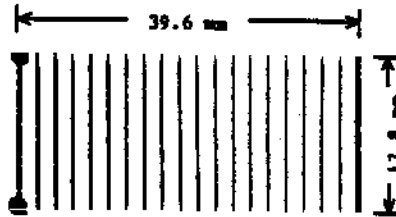


Figure 7 - Drawing Of A Crack Propagation Cage



Figure 8 - Photograph Of Nicolet 4094 Displaying A Fracture Velocity Record

measurements are mixed mode fracture toughness measurements many with associated fracture velocity determinations. In designing this test program for coal, the following factors were considered essential to address:

- 1) fracture loading mode
- 2) fracture orientation
- 3) loading rate

Table 1 shows the basic structure of the test program that is presently well underway. It features seven mixed mode fracture toughness tests for each of three fracture orientations and three loading rates. In the testing rig that is utilized, there are seven positions ranging from mode I at 0° to mode II at 90° by 15°

THE RESPIRABLE DUST CENTER

increments for mixed modes. The initial starter notch is cut parallel to either the bedding planes, the face cleat or the butt cleat. Last, the different loading rates are achieved by changing the cross-head speed on the testing frame to 0.05 mm/min (slow load rate), 0.5 mm/min (medium load rate) or 5 mm/min (fast load rate).

Table 1
Mechanical Properties Tests For Each Coal Seam

Test Type	Perpendicular to Bedding Planes	Perpendicular to Face Cleat	Perpendicular to Butt Cleat	Total
Mixed Mode Fracture Toughness Tests				
- slow load rate	7	7	7	21
- medium load rate	7	7	7	21
- fast load rate	7	7	7	21
Tensile Strength Tests	5	5	5	15
Unconfined Compressive Strength Tests	5	5	5	15
Dynamic Moduli Tests	21	21	21	63
Point Load Index Tests	10	10	10	30
Schmidt Hardness Tests	10	10	10	30
NCB Indenter Tests	10	10	10	30

In conjunction with the fracture toughness testing, determination of related coal material properties is essential. These properties include the direct tensile strength, the unconfined compressive strength, sonic velocity tests for the dynamic moduli, the point load index, Schmidt hardness number and NCB indenter tests. Determination of these related coal material properties enables more complete characterization of the various coals and also provides useful cross checks and possible correlations with the fracture mechanics properties. In addition, fracture velocity determinations are attempted on all mode I tests (at the 0° rig position), mode II tests (at the 90° rig position) and mixed mode tests (at the 45° rig position).

In essence, the test program is designed to supply input data for two approaches that may quantify the energy dissipation and crack bifurcation mechanisms for dust production. These approaches use models of the size of the fracture process zone and relationships between crack tip stress intensity, fracture velocity and surface appearance as viewed under a scanning electron microscope (Zipf and Bieniawski, 1986 a). The program addresses the mixed mode fracture processes and different loading rates that occur in a real cutting operation as well as the highly anisotropic nature of the coal material.

Sample preparation is a crucial aspect of this test program. Because of the friable, moisture sensitive nature of coal, only the strongest, most durable samples ever survive the preparation efforts. Inferior sample collection, preservation and preparation practices tend to produce very suspect fracture toughness test data. Accordingly, the laboratory at Penn State has acquired a suite of delicate, 'low energy', dry preparation equipment. The major pieces are:

- 1) a horizontal bandsaw with a tungsten carbide abrasion blade for major cutting and trimming
- 2) a belt/disc sander for minor shaping and finishing
- 3) a small diamond bandsaw for cutting a 0.6 mm wide starter notch.

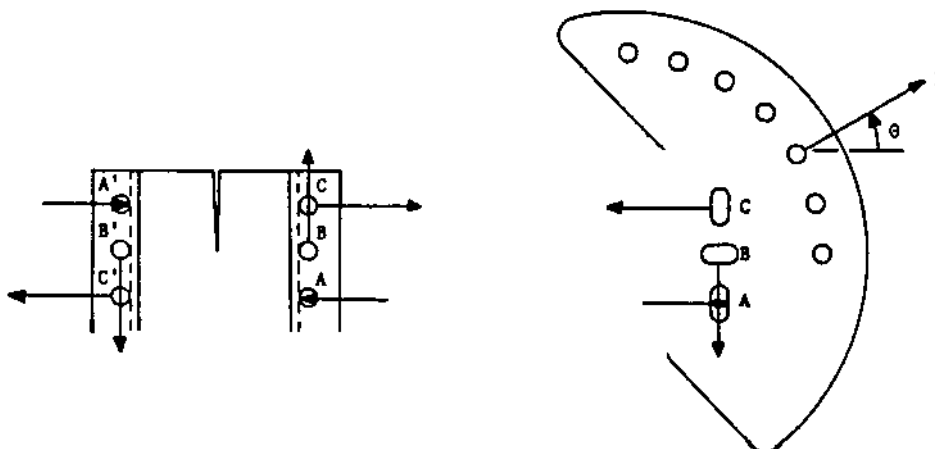


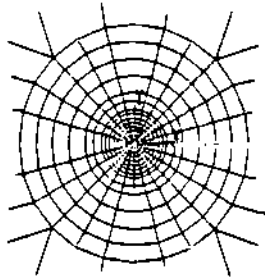
Figure 9 - Free Body Diagrams Of Test Specimen And Loading Plate

MIXED MODE TESTING SYSTEM

V → A

ANSYS 4.2
 JAN 6 1986
 11:26:06
 PLOT NO. 1
 POST1 ELEMENTS

ORIG SCALING
 ZV=1
 DIST=2.31
 ZF=.5



588 ELEMENTS WITH CRACK TIP

Figure 10 - Finite Element Mesh For Stress And Displacement Analyses At Crack Tip

For $a = 0.05$ m and $w = 0.10$ m, these equations become

$$K_I = \frac{P}{t} 11.15 \cos \theta \quad K_{II} = \frac{P}{t} 5.52 \sin \theta$$

There is good agreement between these equations and our equations at the endpoints, but there is considerable discrepancy in mixed mode conditions. One possible reason for the discrepancy is our method for computing K factors. While the stress and displacement fields calculated by ANSYS are evidently quite good, it is better to use the displacement field to determine K as opposed to the stress field (Ingraffea, 1979). Another source of the discrepancy may be related to non singular stresses in the vicinity of the crack tip. The general solution for stresses around a crack tip is a power series with terms containing $r^{-1/2}$, r^0 , $r^{1/2}$, r , $r^{3/2}$, r^2 ... In our computation for K_I and K_{II} , only the first term with $r^{-1/2}$ is included in the solution. Dally et.al. (1985) discusses studies showing the necessity of including higher order terms to reduce errors in determining K. Aside from trying to resolve these problems of accurate K factor computation, we must also generalize our K factor relations to include a wider range of specimen geometries.

MIXED MODE TEST RESULTS

Prior to embarking on the mixed mode program as outlined in Table 1, several test specimens prepared from Plaster of Paris were fractured in the test rig. It was found that the initial fracture angle increases as the proportion of mode II load increases. Qualitatively, this observation agrees with expectations; however, no quantitative analyses were conducted.

Twenty five mixed mode tests were then conducted on the Pittsburgh Coal according to the test plan for various fracture modes, different fracture orientations and increasing loading rates. The fracture toughness test results are shown in Tables 2, 3 and 4. Each test provided K_I and K_{II} data at failure from which K_{IC} and S_{IC} are calculated based on Sih's strain energy density theory. (Sih, 1973 and Gdoutos, 1984). The calculated K_{IC} and S_{IC} values are based on an average Young's Modulus and Poisson's Ratio of 3.01 GPa and 0.37 as reported by K6 and Gerstle (1976) for the Pittsburgh Coal. Average values for K_{IC} and S_{IC} for three orientations in Pittsburgh Coal are presented in Table 5. The K_{IC} values are considerably higher than earlier results for this coal. Advani (1978) obtained 0.0281 MPa \sqrt{m} based on 2 tests and Powell et.al. (1981) reported 0.0629 MPa \sqrt{m} based on 15 tests and 0.0472 MPa \sqrt{m} based on 25 tests. The measured K_I and K_{II} values are also plotted in Figure 11. Though testing and analysis are still in progress, the bedding plane,

THE RESPIRABLE DUST CENTER

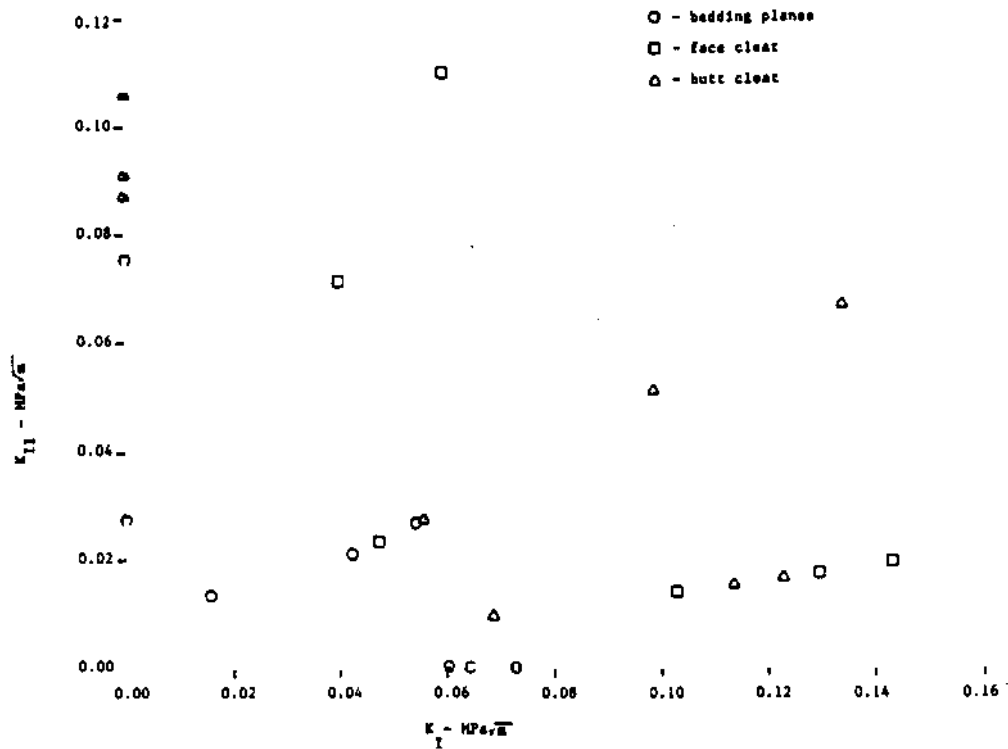


Figure 11 - K_I Versus K_{II} Values For Pittsburgh Coal

the face cleat and the butt cleat orientations have significant differences, but it is still too early for conclusive statements.

FRACTURE VELOCITY MEASUREMENTS

Measurements of the fracture velocities with the crack propagation gages have provided interesting results. Three good measurements and a fourth partial measurement are now available. The crack length versus time data for these tests are shown in Figure 12. Two tests labeled "S" are at test machine cross head displacement rates of 0.05 mm/min, one test labeled "M" is at 0.5 mm/min and the last test labeled "F" is at 5mm/min. In the slow loading rate tests, the crack appears to grow at velocities of about 6 and 22 m/s. In the higher loading rate test, the crack initially grows at about 500 m/sec then slows to 22 m/s. Finally, in the highest loading rate test, the crack appears to initially grow at speeds in excess of 1000m/s before slowing to again about 22 m/s.

Figure 13 is a semi-logarithmic sketch of instantaneous crack propagation velocity versus crack length as suggested by this data. It appears that higher loading rates induce higher initial crack velocities which then decrease to some indeterminate lower velocity. Wide variations exist in the determinations of instantaneous crack velocity as shown in Figure 14. Many possible causes exist for the variation, which unfortunately may be inherent to the gage.

DISCUSSION

The fracture toughness data reported in this study are the first ever mixed mode test results for coal, to the best of our knowledge. As is expected in most rock testing and especially in coal, considerable variations exist in the data. Preliminary observations and comments are as follows.

1) As shown in Table 5, the critical fracture toughness and the critical strain energy density factor are significantly lower for the test orientation with the starter notch parallel to bedding planes. K_{IC} and S_{CT} values for the face cleat and butt cleat orientations do not appear to differ significantly from one another. Several possible reasons exist for this observed difference which relate to the stress analysis about the crack tip, the subsequent K factor determinations and finally the data analysis. A linear, isotropic constitutive model is used throughout our analyses with E and ν values reported by Ko and Gerstle (1976). Using a more complex model may significantly change the reported K_{IC} and S_{CT} values or decrease the variance in the data. Sonic velocity measurements in three orthogonal directions have been completed on each specimen from which values of dynamic E and ν were calculated. Using these values may also contribute to

MIXED MODE TESTING SYSTEM

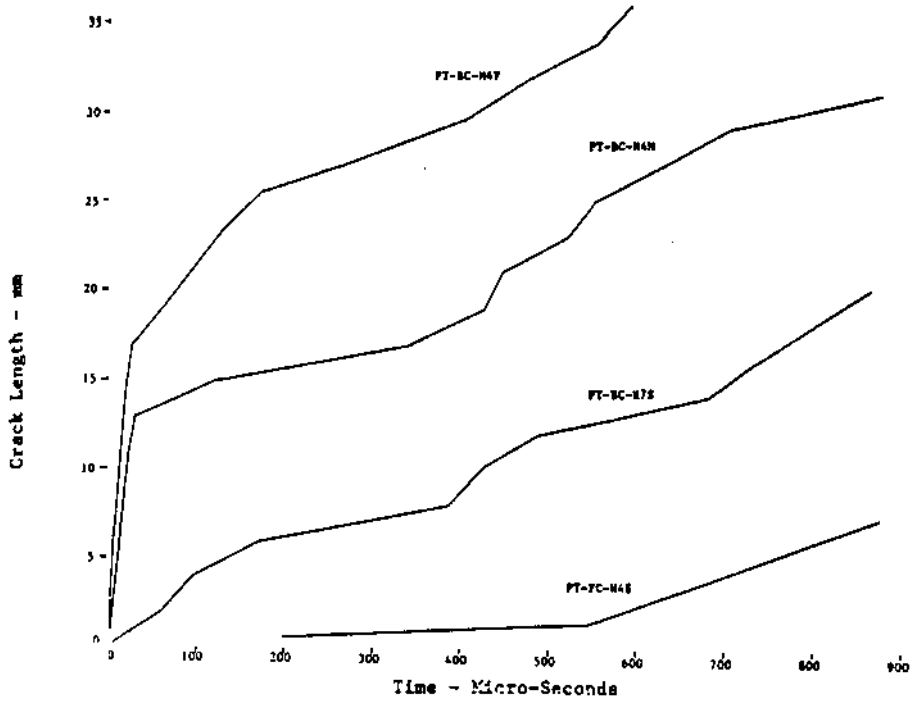


Figure 12 - Crack Length Versus Time

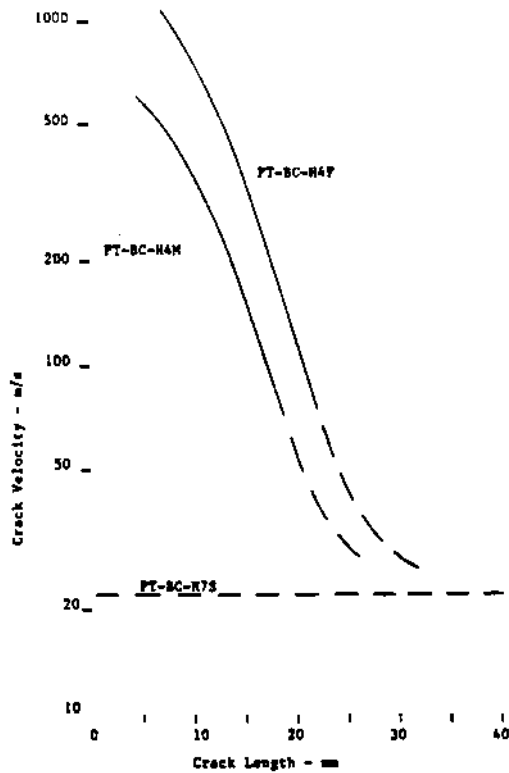


Figure 13 - Crack Velocity Versus Crack Length For Three Coal Specimens

THE RESPIRABLE DUST CENTER

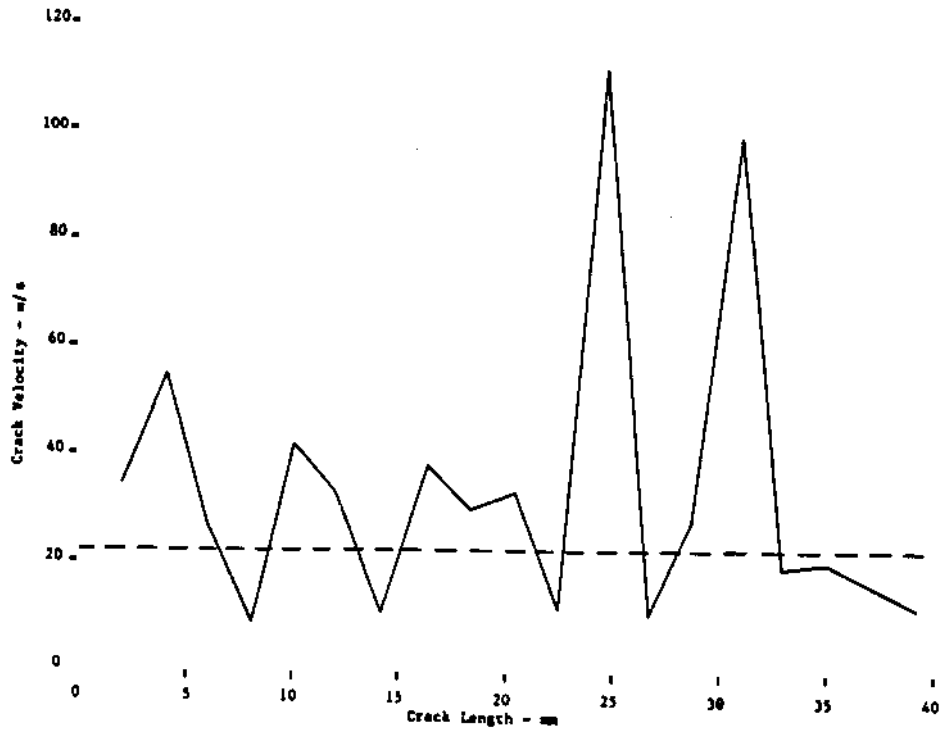


Figure 14 - Instantaneous Crack Velocity Versus Crack Length For Specimen PT-BC-H7S

Table 2 - Coal Fracture Toughness Data - Along Bedding Planes

Specimen Number	Load Angle	Cross-head Speed mm/min	K_{II} $\frac{K_{II}}{MPa\sqrt{m}}$	K_{IG} $\frac{K_{IG}}{MPa\sqrt{m}}$	Scr N/m	Fracture Angle	Total AE Counts	Comments
PT-BP-H1S	0° (mode I)	.05	.0601 .0000	.0601	.214	0°	87,000	broke along bedding
PT-BP-H4S	45° (mixed mode)	.05	.0420 .0208	.0585	.203	0°	75,000	broke along bedding
PT-BP-H7S	90° (mode II)	.05	---	---	---	---	---	failed test
PT-BP-H1M	0° (mode I)	.5	.0725 .0000	.0725	.311	0°	100,000	broke along bedding
PT-BP-H4M	45° (mixed mode)	.5	.0535 .0265	.0746	.329	0°	85,000	broke along bedding
PT-BP-H7M	90° (mode II)	.5	.0000 .0757	.1485	1.304	0°	335,000	broke along bedding
PT-BP-H1F	0° (mode I)	5	.0637 .0000	.0637	.240	0°	100,000	broke along bedding
PT-BP-H4F	45° (mixed mode)	5	---	---	---	---	---	failed test
PT-BP-H5F	60° (mixed mode)	5	.0151 .0129	.0295	.051	0°	33,000	broke along bedding
PT-BP-H7F	90° (mode II)	5	.0000 .0274	.0350	.072	70°	70,000	later turned and broke along bedding

MIXED MODE TESTING SYSTEM

Table 3 Coal Fracture Toughness Data - Along Face Cleats

Specimen Number	Load Angle	Cross-head Speed mm/min	K_{IC} $\frac{K_I}{MPa\sqrt{m}}$	K_{IC} $\frac{K_{IC}}{MPa\sqrt{m}}$	Scr N/m	Fracture Angle	Total AE Counts	Comments
PT-FC-H2S	15° (mixed mode)	.05	.1288 .0171	.1408	1.172	14°	44,000	- - - -
PT-FC-H4S	45° (mixed mode)	.05	.0469 .0232	.0540	.172	90°	19,000	turned and broke along bedding. partial velocity recording.
PT-FC-H7M	15° (mixed mode)	.5	.1028 .0136	.1128	.753	15°	92,000	- - - -
PT-FC-H6M	75° (mixed mode)	.5	.0387 .0714	.1157	.793	63°	185,000	- - - -
PT-FC-H2F	15° (mixed mode)	5	.1429 .0190	.1555	1.430	13°	64,000	- - - -
PT-FC-H6F	75° (mixed mode)	5	.0596 .1101	.1279	.967	90°	125,000	broke along bedding

Table 4 - Coal Fracture Toughness Data - Along Butt Cleats

Specimen Number	Load Angle	Cross-head Speed mm/min	K_{IC} $\frac{K_I}{MPa\sqrt{m}}$	K_{IC} $\frac{K_{IC}}{MPa\sqrt{m}}$	Scr N/m	Fracture Angle	Total AE Counts	Comments
PT-BC-H2S	15° (mixed mode)	.05	.0679 .0090	.0745	.329	15°	25,000	- - - -
PT-BC-H4S	45° (mixed mode)	.05	.0549 .0272	.0880	.458	35°	15,000	- - - -
PT-BC-H7S	90° (mode II)	.05	.0000 .0877	.1186	.832	63°	75,000	good velocity recording
PT-BC-H2M	15° (mixed mode)	.5	.1225 .0162	.1288	.981	5°	48,000	- - - -
PT-BC-H4M	45° (mixed mode)	.5	.0984 .0487	.1555	1.432	27°	102,000	good velocity recording
PT-BC-H7M	90° (mode II)	.5	.0000 .0916	.1107	.726	90°	600,000	broke along bedding
PT-BC-H2F	15° (mixed mode)	5	.1129 .0150	.1212	.869	10°	22,000	- - - -
PT-BC-H4F	45° (mixed mode)	5	.1337 .0662	.2090	2.584	23°	91,000	good velocity recording
PT-BC-H7F	90° (mode II)	5	.0000 .1066	.1360	1.095	70°	94,000	- - - -

significant changes in K_{IC} and S_{IC} values and the variance. Thus, the observed directional dependence of K_{IC} and S_{IC} may change with subsequent re-analysis. If it does remain though, the directionality of K_{IC} and S_{IC} might be exploited in a fragmentation process to decrease energy consumption and unwanted fine fragment formation during mining.

2) The observed fracture angle deviates substantially from the expected crack propagation path for test orientations parallel to bedding planes. From theoretical considerations, the fracture angle should increase as the mode II loading component increases. For starter notch orientations parallel to the face cleat or the butt cleat, this increase is observed and at least qualitatively agrees with theoretical expectations. With

THE RESPIRABLE DUST CENTER

Table 5 - Summary of Critical Fracture Toughness Values and Strain Energy Density Factors for Pittsburgh Coal

Direction	K_{IC} mean	$MPa\sqrt{m}$ standard deviation	Scr - mean	N/m standard deviation
along bedding planes	.0678	±54%	.341	±118%
along face cleats	.1178	±30%	.881	±49%
along butt cleats	.1269	±31%	1.034	±65%

the bedding plane orientation, the growing crack always remains in plane and does not change direction or increase as expected. Again, the theoretical direction of crack growth will certainly change if a more complex, anisotropic material model is used in calculations; however, the difference is likely to remain due to the directionality of K_{IC} and S_{cr} for coal.

3) The acoustic emission counts seem to increase as the amount of mode II loading increases. Part of the increase may be due to greater energy dissipation associated with mode II loading. Another part may be due to the different frequencies of elastic waves generated by mode II (shear) loadings.

4) The fracture velocity measurements conducted as part of this study show that increasing the loading rate on the test specimen appears to increase the velocity of initial crack growth. The velocity then decreases when the crack length increases as was shown in Figure 13. Measured dilatational and distortional velocities for Pittsburgh Coal are on the order of 2400 m/s and 1000 m/s. On specimen PT-BC-H4F, the initial crack velocity may have exceeded 2000 m/s and it decreased from speeds of 1000 m/s to 600 m/s over 10 mm of crack growth. These observations of high, almost supersonic crack velocities are identical to those reported by Huang and Vikar, 1985, in their tests on glass using a very similar velocity gage technique. Data is quite sparse at this time and significant experimental problems exist with these velocity gages. In many tests, especially those with the starter notch parallel to bedding planes, the crack did not grow in the expected direction, missed the gage completely, and rendered it useless. In other tests, the crack evidently began growing at a very slow rate perhaps less than 1 m/s. The slow growth period then filled the available time window in the storage oscilloscope which caused us to miss the later periods of crack growth. Also, there is some evidence that the fracturing strands of the velocity gage may lead or lag the actual crack tip as reported by Swan, 1975.

CONCLUSION

The test system developed in the course of this project to study the mechanics of fine coal fragment formation has provided the first mixed mode studies of the critical fracture toughness and strain energy density factor for coal. The testing system may have other applications in other geologic materials and possibly concrete. The fracture velocity measurement system has significant experimental difficulties and uncertainties, but does appear to provide some consistent measurements of the unstable fracture velocity.

ACKNOWLEDGMENT

This research has been supported by the Department of the Interior's Mineral Institutes program administered by the Bureau of Mines under allotment grant number G1135142, #4201-PS1.

REFERENCES

- Advani, S. H., Lin, Y.T., Gwindl, F. D. and Powell, W. R., "Coupled Roof Fracture Response and Surface Subsidence Evaluations Related to Underground Coal Gasification," Proc. 4th Underground Coal Conversion Conf., pp. 507-514 (1978)
- Batdorf, S. B., "Fundamentals of the Statistical Theory of Fracture," Fracture Mechanics of Ceramics, ed. R. C. Brandt, D.P.H. Hasselman and F. F. Lange, Plenum Press, New York, Vol. 3, pp. 1-30 (1978)
- Bieniaski, Z. T., "Rock Materials Under Mixed Mode Fracture," Proc. U.S. - Greece Symp. on Fracture, Athens, Greece, Sijthoff and Noordhoff, Rockville, MD., pp. 333-347 (1981)
- Cook, N. G. W., et.al., Measurement and Control of Respirable Dust in Mines, National Academy of Sciences, Washington, D.C., 405 pp (1980)
- Dally, J. W., Fourney, W. L. and Irvin, G. R., "On the Uniqueness of the Stress Intensity - Crack Velocity Relationship," Int. J. of Fracture, Vol. 27, pp. 159-168 (1985)
- Gdoutos, E. E., Engineering Application of Fracture Mechanics, VII, Problems of Mixed Mode Crack Propagation, Martinus Nijhoff Publishers, Boston, 204 pp. (1984)

MIXED MODE TESTING SYSTEM

- Huang, J. L. and Virkar, A. V., "High Speed Fracture in Brittle Materials: Supersonic Crack Propagation," Engng. Fracture Mechanics, Vol. 21, No. 1, pp. 103-113. (1985)
- Ingraffea, A. R., Heuze, F. E., Ko, H. Y., and Gerstle, K., "An Analysis of Discrete Fracture Propagation in Rock Loaded in Compression," Proc. 18th U.S. Symp. on Rock Mechanics, CSM Press, Golden, CO., pp. 2A4-1 to 2 A4-7 (1977)
- Ingraffea, A. R. and Manu, C., "Stress-Intensity Factor Computation in Three Dimensions with Quarter-Point Elements," Int. J. for Numerical Methods in Engineering, Vol. 15, pp. 1427-1445 (1980)
- Ingraffea, A. R., "Mixed-Mode Fracture Initiation in Indiana Limestone and Westerly Granite," Proc. 22nd U.S. Symp. on Rock Mechanics, MIT Press, Cambridge, MA, pp. 199-204 (1981)
- Ingraffea, A. R., "Fracture Propagation in Rock," Mechanics of Geomaterials, ed. Z. P. Bazart, Wiley-Interscience, New York, pp. 219-258, (1985)
- Ko, H. Y. and Gerstle, K. H., "Elastic Properties of Two Coals," Int. J. of Rock Mech. Min. Sci. and Geomech. Abstr., Vol. 13, pp. 81-90 (1976)
- Laqueche, H., Rousseau, A. and Valentin, G., "Crack Propagation Under Mode I and II Loading in Slate Schist," Int. J. of Rock Mech. Min. Sci. and Geomech. Abstr., Vol. 23, No. 5, pp. 347-354 (1986)
- Mecholsky, J. J. and Fraiman, S. W., "Determination of Fracture Mechanics Parameters Through Fractographic Analysis of Ceramics," Fracture Mechanics Applied to Brittle Materials, ASTM STP 678, S. W. Fraiman, Ed., pp. 136-150 (1979)
- Nelson, P. P. and Fong, F.L. C., "Characterization of Rock for Boreability Evaluation Using Fracture Material Properties," Proc. 27 US Symp. on Rock Mechanics, AIME, New York, pp. 846-851, (1986)
- Nelson, P. P., Ingraffea, A. R. and O'Rourke, T., "TBM Performance Prediction Using Rock Fracture Properties," Int. J. of Rock Mech. Min. Sci. and Geomech Abstracts, Vol. 22, No. 3, pp. 189-192, (1985)
- Ouchterlony, F., "Review of Fracture Toughness Testing of Rock," Solid Mechanics Archives, Vol. 7, pp. 131-211, (1982)
- Povell, W. R., Khan, S., Ramsey, D. G. and Gweindl, F. D., "Fracture Mechanics Model for Pittsburgh Coal," Paper 81-Pet-16, American Society of Mechanical Engineers, Petroleum Division (1981)
- Richard, H. A., "Some Theoretical and Experimental Aspects of Mixed Mode Fractures," Proc. 6th Int. Conf. on Fracture (ICF6), ed. Valluri, S. R., Taplin, D.M.R., Rao, P. R., Knott, I. F. and Dubey, R., Pergamon Press, New York, pp. 3337-3344 (1984)
- Roepke, W. W., "General Methods of Primary Dust Control During Cutting," Mining Engineering, Vol. 26, No. 6, pp. 636-644 (1984)
- Saouma, V. E. and Ingraffea, A. R., "Fracture Mechanics Analysis of Discrete Cracking," Proc. IABSE Colloquium on Advanced Mechanics of Reinforced Concrete, Delft, p. 393 (1981)
- Saouma, V. E. and Kleinovsky, M. I., "Finite Element Simulation of Rock Cutting, a Fracture Mechanics Approach," Proc. 25th Symp. on Rock Mechanics, Evanston, IL, pp. 792-800 (1984)
- Sih, G. C. Mechanics of Fracture 1, Methods of Analysis and Solutions of Crack Problems, Noordhoff International Publishing, Leyden, pp. XXI-XLV, (1973)
- Stecklein, G., Branstetter, R., Arrowood, R., Davidson, D., Laskford, I., Lyle, R., and Nulte, C., Basic Research on Coal Fragmentation and Dust Entrainment, USBM Contract No. I0215009, South West Research Institute, 121 pp. (1982)
- Svan, C., "The Observation of Cracks Propagating in Rock Plates," Int. J. Rock Mech. Min. Sci. and Geomech. Abstr., Vol. 12, pp. 329-334 (1975)
- Zipf, R. K. and Bieniawski, Z. T., "Mixed Mode Testing for Fracture Toughness of Coal Based on Critical-Energy-Density," Proc. 27th U.S. Symp. on Rock Mechanics, AIME, New York, pp. 16-23, (1986a)
- Zipf, R. K. and Bieniawski, Z. T., "Fracture Mode and Loading Rate Influences on the Formation of Respirable Size Fragments on New Fracture Surfaces," Proc. Int. Symp. on Respirable Dust in the Mineral Industries, Pennsylvania State University (1986b)

Identification of Fracture in Coal by AE in Dynamic Test

A. Wahab Khair and S. Jung

Department of Mineral Engineering, West Virginia University

ABSTRACT

This paper deals with the fracturing process of laterally confined blocks of coal subjected to impact indentation. During the test, blocks of coal with approximate dimensions of 10 in. x 10 in. x 6 in. were laterally confined to predetermined equivalent in-situ stresses and then subjected to an impact indentation by dropping coal cutting bits (various shapes) attached to a known weight from a known height. During the test a number of parameters, namely surface strains (using strain gages), penetration depth (using L.V.D.T.) and acoustic emission characteristics were measured. After the test, the fractured surfaces were photographed with the aid of a camera attached to a microscope. The fracture, its intensity and extended zone within the coal blocks were mapped using sonic techniques. By correlating measured parameters, fractured zones under a given set of test parameters were identified and characterized.

INTRODUCTION

To improve the understanding of basic failure mechanisms in coal cutting, a better knowledge of fracture and crack regions caused by the indentation in coal is needed. This study reports the detailed experimental procedure used in fracture analysis of indentation experiments on coal specimens using the Acoustic Emission (A.E. hereafter) and sonic techniques.

The relationship between microcracking and the inelastic deformation of rock was confirmed by a series of experiments in which the A.E. generated by the cracking in the rock specimen were recorded and the number of events were compared to the strain measurement (Scholz, 1967).

According to fracture mechanism theory, crack initiation in brittle materials such as rocks begins from "flaws" either pre-existing or induced by the indentation process itself. Rocks are pervaded by

FRACTURE IN COAL BY AE

natural cracks and pores, from which numerous possibilities for crack initiation arise (Lindquist, Lai and Alm, 1984).

Microseismic/A.E. techniques are based on the fact that many materials including coal, emit transient noises or vibration. These vibrations are called microseismic activity, rock noise, seismo-acoustical or A.E. The fact that these microseismic activities are generated from regions of instability probably due to local failure, makes it possible to monitor failure of geologic materials (Khair, 1981).

The main objective of this study was to understand the fracture mechanism in coal using impact indentation technique with five different types of bits at various predetermined confining pressures simulating equivalent in-situ stresses.

Hence, development of cracks due to impact indentation was recorded by A.E. and was mapped with the help of photographs taken by microscope (Zoom .66) with an attached camera. Also L.V.D.T. and SR-4 strain gages were used to measure the penetration depth and surface strain on the coal block respectively. Sonic technique was used to determine the dynamic Young's modulus, and depth and intensity of fracture during the impact indentation tests.

SPECIMEN PREPARATION

Coal specimens used in this study were part of the Waynesburg coal seam. Large blocks of coal were obtained from a surface mine. These blocks were then cut in the laboratory to an approximate dimension of 7 in. x 7 in. x 5.5 in. A typical specimen with cutting face, perpendicular to face cleat direction, was placed in a wooden box of 10 in. x 10 in. x 6 in. in dimension. Two pieces of wood 1.25 in. x 1.5 in. x 5 in. were wedged between the coal sample and the wooden box to make room for housing the sonic transducers. Then plaster of paris was poured in the box to fill all the remaining space other than that occupied by the coal block. After a week, the molded coal sample was removed from the box and the wooden blocks that were wedged before pouring the mold were dislodged from the sample carefully, thus creating room to house the sonic transducers. Finally, a sander was used to grind the sample surface by hand. This process gave a perfect dimension of 10 in. x 10 in. x 6 in. which was very essential to avoid stress concentration in the specimen when confining pressure was applied. After this process, the strain gages were mounted in a rosette form to provide strain distribution on the surface of the coal block; one was attached parallel to bedding plane direction, another was attached at an angle of 45 degrees from the bedding plane direction and the other was attached perpendicular to the bedding plane direction. Each of the three strain gages were set 2 in. away from the impact point.

THE RESPIRABLE DUST CENTER

EXPERIMENTAL PROCEDURE

The molded specimen was placed in the confining chamber, the test conditions were set, and in-situ and operating parameters were marked on the top mold layer of the specimen. A sonic test was done by which the stress wave travel time through the coal sample and the amplitudes of the signals were measured and recorded (Fig. 1-A) before and after applying confining pressure. Predetermined equivalent in-situ stresses were then applied to the specimen using two sets of hydraulic jacks (one set for horizontal and the other set for vertical). A 1 in. thick steel plate was positioned between the specimen and hydraulic jacks in order to distribute the pressure uniformly over the whole surface of the specimen. Each set of hydraulic jacks were connected in parallel to a hand pump. Total impact weight was 90 lbs including weight of guide frame, bit holder and bit. The impact weight was raised by a hand driven winch, which allows the weight to drop freely when unlocked. In order to give better free drop effect, grease was put on the guiding pipe line.

Throughout these experiments, a 10 channel signal conditioner (Fig. 1-B) and a 6 channel recorder (Fig. 1-C) were used to monitor the output of strain gages, L.V.D.T. and A.E. activity (Fig. 1-D). After the impact, data were recorded for a short period of time corresponding to the diminishing A.E. activity. A sonic test was made and the corresponding stress wave travel time and amplitude were measured. Deep fracture formation in the coal block results in reduction of the stress wave amplitude and increases its travel time. After completion of the experiment, the weight was raised and the microscope was placed on the specimen. Then photographs were taken in order to trace the crack propagation with zoom .66 (Fig. 1-E). This process was repeated three times for each sample.

RESULTS AND DISCUSSION

The mechanical properties of coal which is part of the Waynesburg coal seam was determined in the laboratory and are tabulated in Table 1.

Table. 1. Mechanical Properties of Waynesburg Coal

Cleat/Bedding Plane Orientation	Compressive Strength psi(KPa)	Young's Modulus psi (KPa)	Poisson's Ratio	Indirect Tensile Strength psi (KPa)	Direct Shear Strength psi (KPa)
Face Cleat	3289 (473.9)	5.1×10^5 (7.3×10^4)	0.25	154 (22.2)	104 (29.4)
Butt Cleat	3459 (490.1)	4.7×10^5 (6.8×10^4)	0.31	205 (29.5)	180 (25.9)
Bedding Plane	4912 (707.4)	4.6×10^5 (6.6×10^4)	0.32	146 (21.0)	80 (11.5)

FRACTURE IN COAL BY AE

The five different types of bits used in this study are shown in Fig. 2. Tests were done under different drop heights and confining pressures. To simulate the general cutting condition in the mine, specimens were tested parallel to bedding plane along the face cleat direction. The specimens were tested with two different drop heights (1' and 2') and five different types of bit.

Duration of tests were very short due to the nature of the experiment. The data obtained during the test was characterized by the fracture-deformation behavior of coal within this period. For example, the magnitude of strain was the highest at the instant of impact imposed upon the coal block. Due to chipping and fracture propagation, strain redistribution occurred in the coal block. This strain redistribution and relaxation can be observed on the strain gages. After this relaxation period, changes in strains were diminished as shown on each experimental data. This relaxation period was also identified by the A.E. activity.

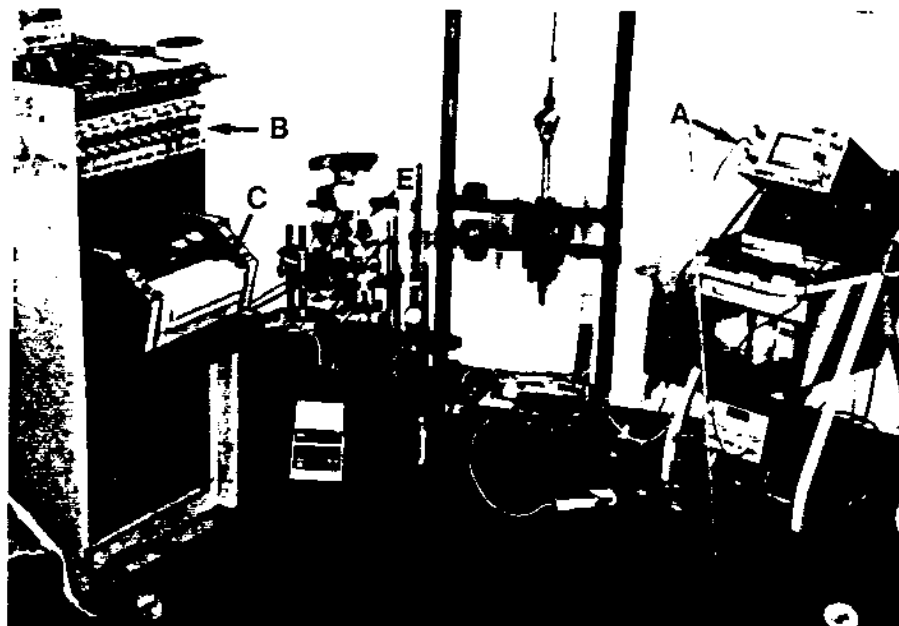
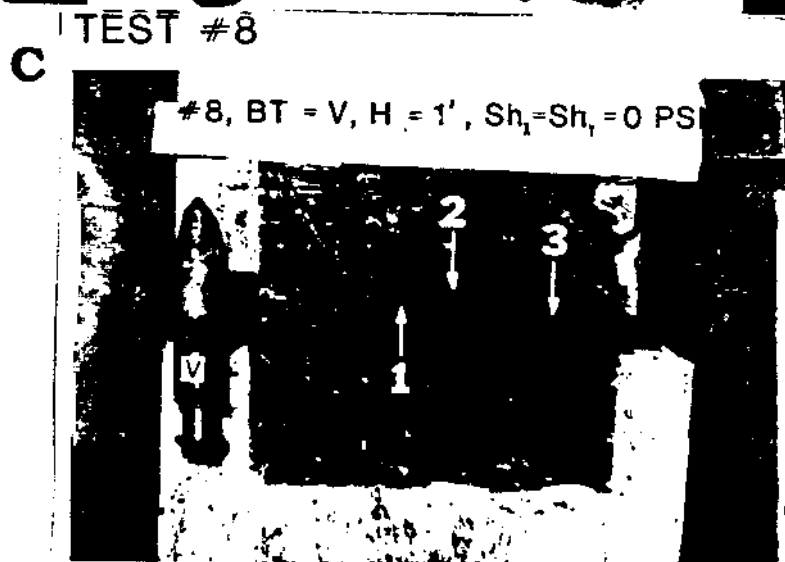
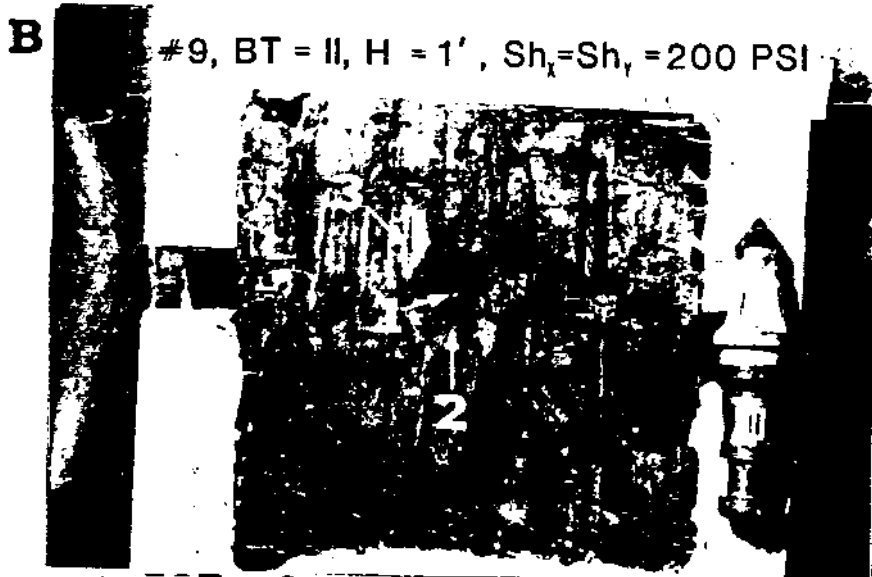
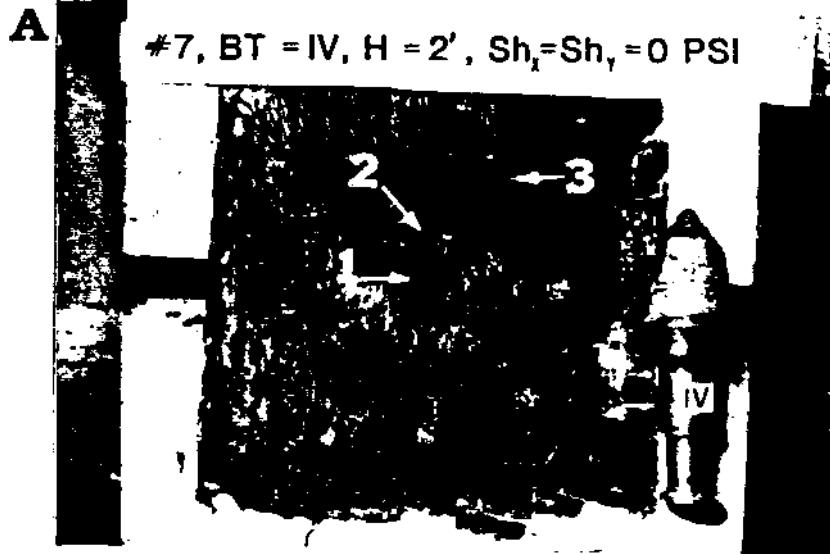


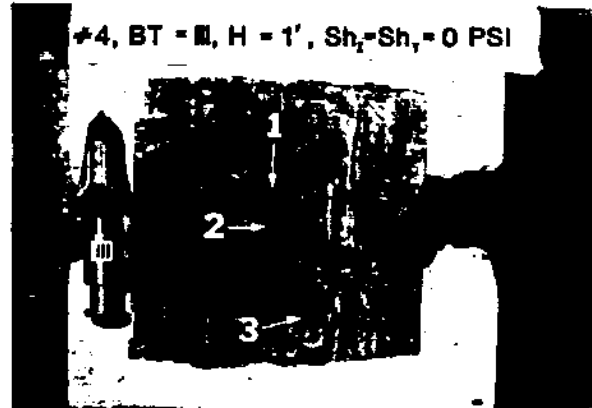
Fig. 1. Experimental set-up A) sonic test unit, B) 10 channel signal conditioner, C) 6 channel recorder, D) acoustic emission unit, E) microscopic photographic unit.

A.E. rate (Fig. 3, line 5) showed peak value at the impact time, then fractures were further developed for a short period of time as shown by both A.E. rate and total count (Fig. 3, line 6). Therefore further A.E. activity indicated fracture propagation. Generally, deeper penetration produces higher rate of A.E. activity. The impact load created numerous cracks. The major cracks generally developed parallel to the bedding plane while chipping and minor cracks developed in the radial direction from impact point. Strain gages located perpendicular to the bedding plane generally showed tensile strain



D

TEST #4



E TEST #3

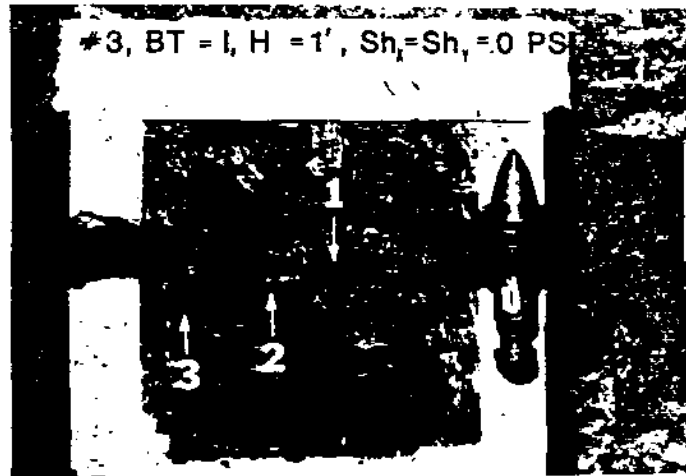


Fig. 2. Five types of bits and specimen after the test with the corresponding bit shown in the figures.

(indicating bending deformation of the coal block) while those at the other direction showed compressive strain. However, magnitude of the tensile strain was much less than that of the compressive strain.

Drop tests in which the weight was dropped from 2 ft. high were conducted with the same test conditions described in the case of 1 ft. high drop test. The magnitude of A.E. activity indicated higher rate and total counts. Also the magnitude of strain was higher (Fig. 4). During these experiments, the impact energy was so high that, some of the strain gages failed at impact moment. By observation and sonic technique, it was determined that damage zone was deeper and wider than

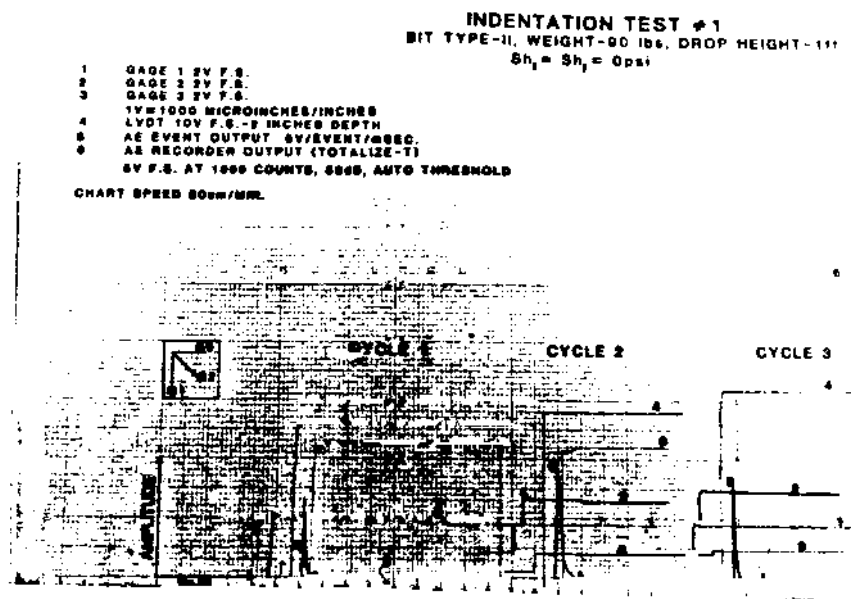
THE RESPIRABLE DUST CENTER

the 1 ft. high experiment. Furthermore, most of the cracks developed were major when the drop height was 2 ft. Bit penetration was deeper in unconfined specimens than in those subjected to confining pressure.

Under the confining condition, A.E. activity rate and counts were higher after the impact than in the unconfined condition. This increase in A.E. activity after the impact is probably due to the effect of confining pressure causing oscillation/vibration, stress redistribution in order to create new equilibrium state in the coal block. Under these conditions only small fractures were developed in the radial direction without the formation of deep fracture in the coal block. The lack of this deep fracture was substantial by sonic technique. Furthermore, only small crushed area developed. The magnitude of strain and depth of penetration in tested specimen under confining pressure was less than in the unconfined case. As the confining pressure increased, the magnitude of strain, penetration depth and A.E. activity were decreased. The rate and total count of A.E. decreased further in subsequent cycles (Fig. 5). This decrease in A.E. activity is indicative of less penetration and damage (less fracture formation) in the coal block, resulting in localized crushing of the coal under the bit.

The microscopic photographs were taken with zoom .66. Generally, pictures were taken at the impact point where the bit made contact with the coal specimen. Major cracks around the impact point are characterized by glitter which was caused by the high dynamic force. The width of major crack increased as the cycle number increased. Major cracks developed parallel to the bedding plane direction. Near the impact point, coal chipped out, thus creating a crater. The size of the crater developed decreased as the confining pressure increased. No major cracks developed in specimens tested under confined conditions. Only minor cracks were developed in the radial direction. However, size of cracks were getting smaller as the confining pressure increased (Fig. 6).

A



A. Drop test for bit Type II.

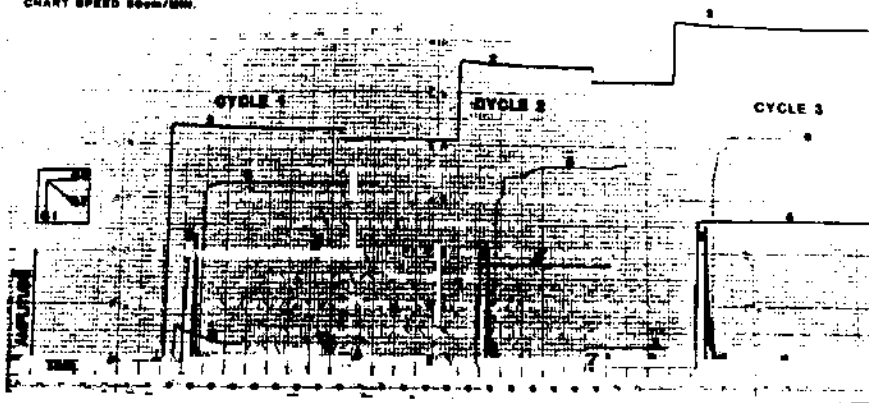
FRACTURE IN COAL BY AE

B

- 1 GAGE 1 BY F.S.
- 2 GAGE 2 BY F.S.
- 3 GAGE 3 BY F.S.
- 4 LVDT 10V F.S. - 2 INCHES DEPTH
- 5 AE EVENT OUTPUT SV/EVENT/SEC.
- 6 AE RECORDER OUTPUT (TOTALIZED-T)
- SV F.S. AT 1000 COUNTS, 5000. AUTO THRESHOLD

INDENTATION TEST #4
BIT TYPE-III, WEIGHT-90 LBS, DROP HEIGHT-1 FT
Sh = Sh = 0psi

CHART SPEED 5000/INCH



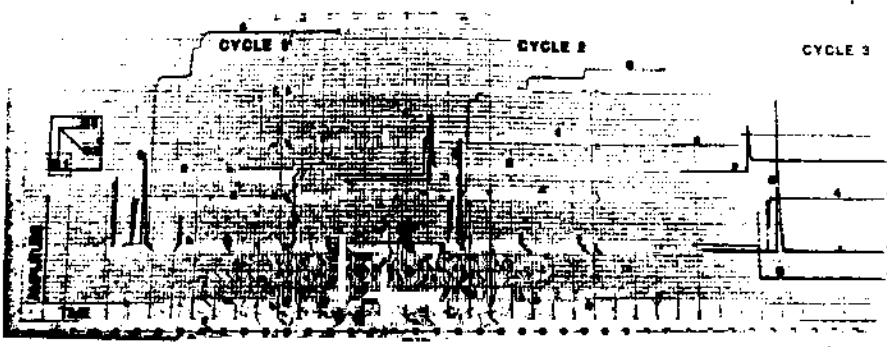
B. Drop test for bit type III.

C

- 1 GAGE 1 BY F.S.
- 2 GAGE 2 BY F.S.
- 3 GAGE 3 BY F.S.
- 4 LVDT 10V F.S. - 2 INCHES DEPTH
- 5 AE EVENT OUTPUT SV/EVENT/SEC.
- 6 AE RECORDER OUTPUT (TOTALIZED-T)
- SV F.S. AT 1000 COUNTS, 5000. AUTO THRESHOLD

INDENTATION TEST #5
BIT TYPE-IV, WEIGHT-90 LBS, DROP HEIGHT-1 FT
Sh = Sh = 0psi

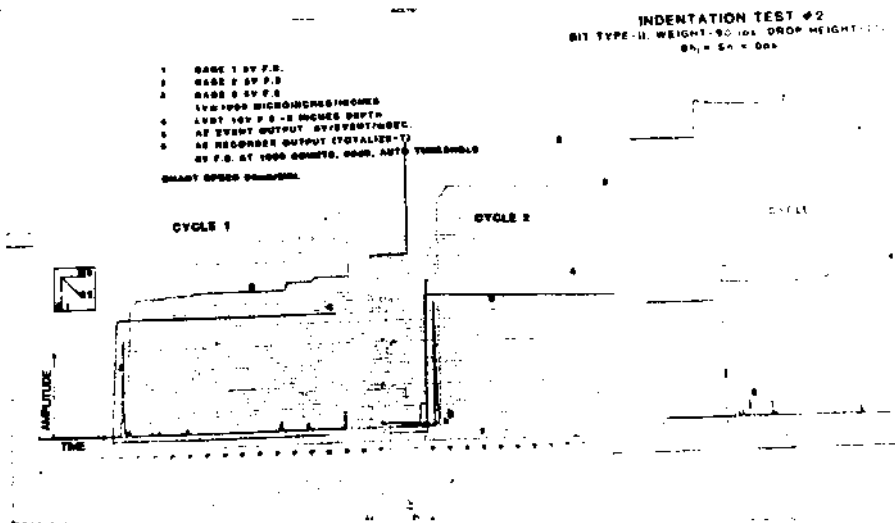
CHART SPEED 5000/INCH



C. Drop test for bit type IV.

Fig. 3. Typical data from drop test showing surface strain, bit penetration, A.E. rate and total count at the impact moment and shortly after for three repeated tests (drop height is 1 ft.; A) bit type II, B) bit type III, C) bit type IV).

A



B

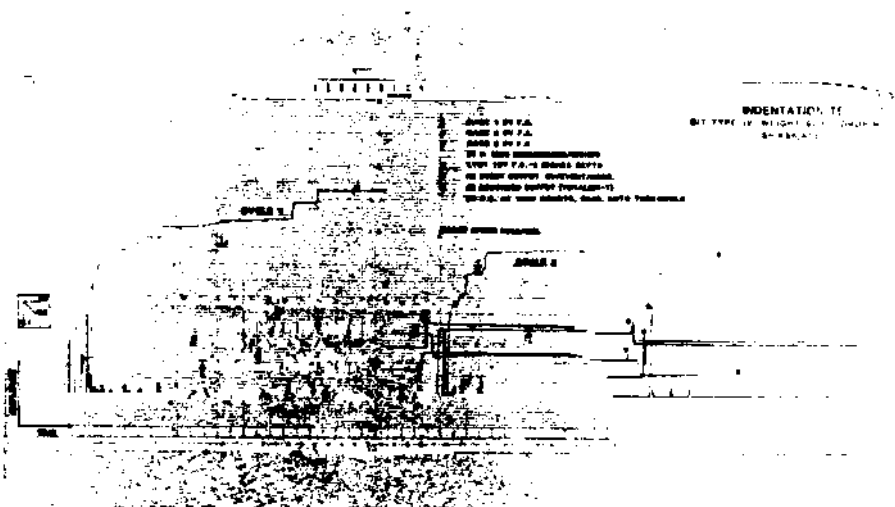
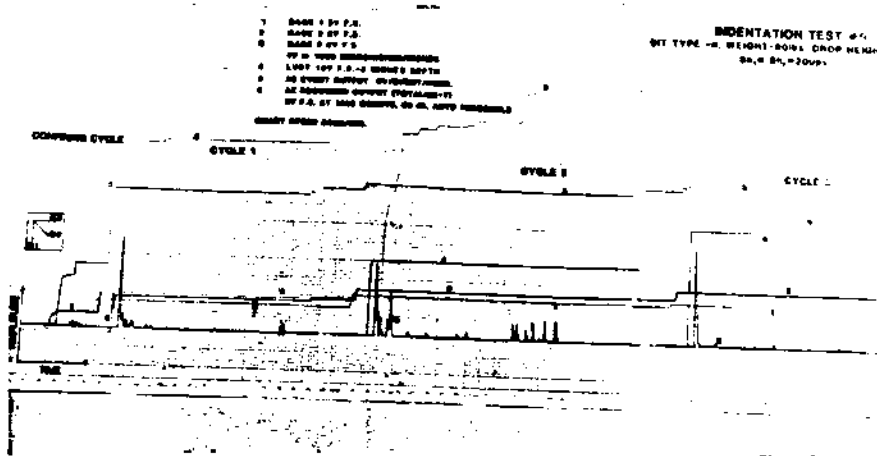


Fig. 4. Typical data from drop test showing surface strain, bit penetration, A.E. rate and total count at the impact moment and shortly after for three repeated tests (drop height is 2 ft.; A) bit type II, B) bit type IV).

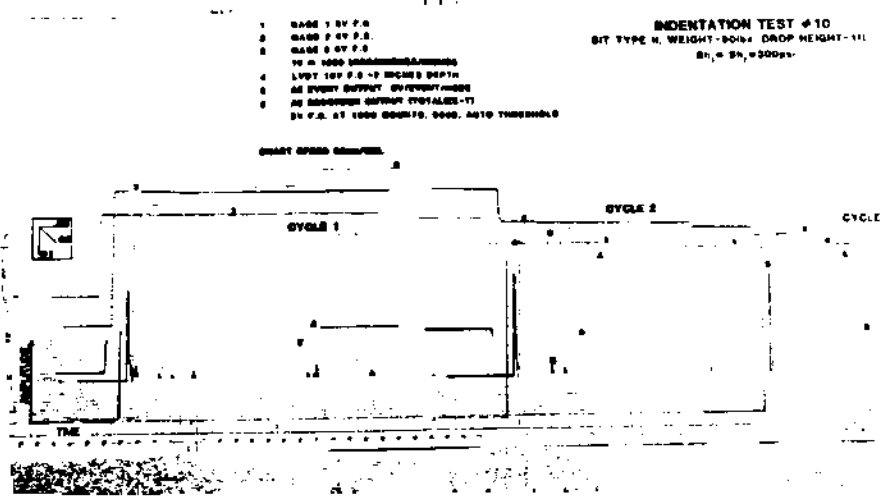
FRACTURE IN COAL BY AE

A



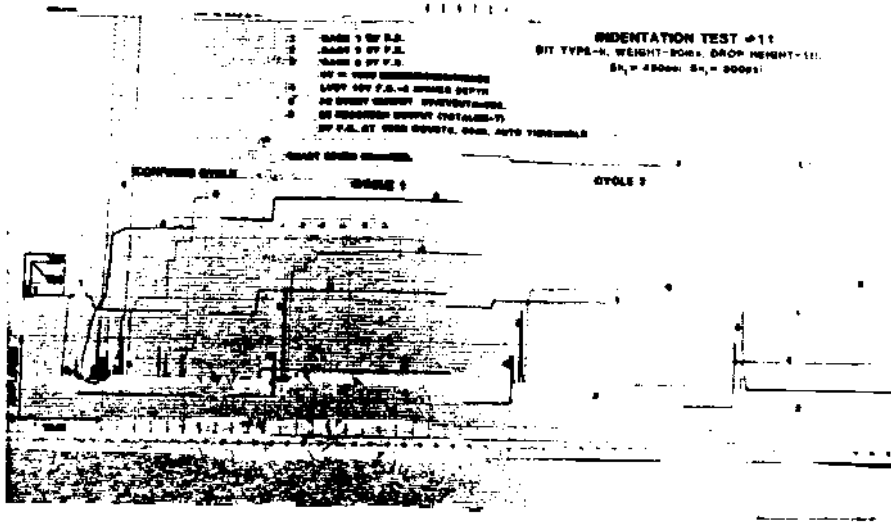
A. $Sh_x = Sh_y = 200 \text{ psi}$

B



B. $Sh_x = Sh_y = 300 \text{ psi}$

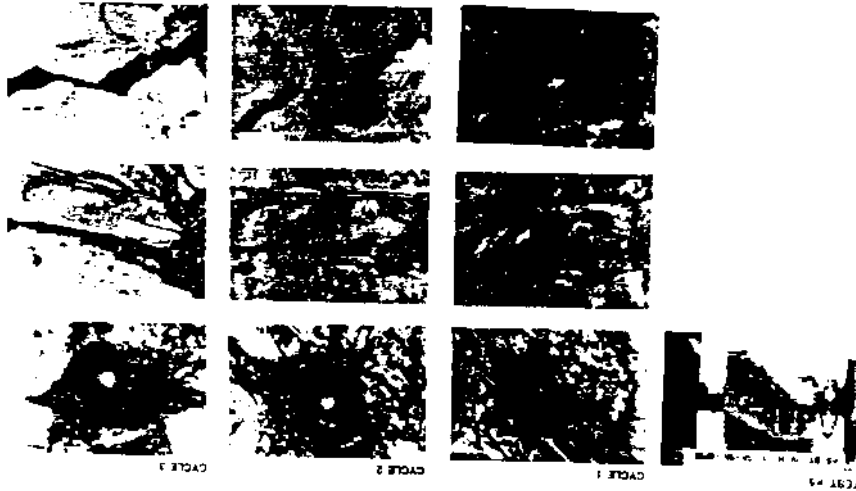
C



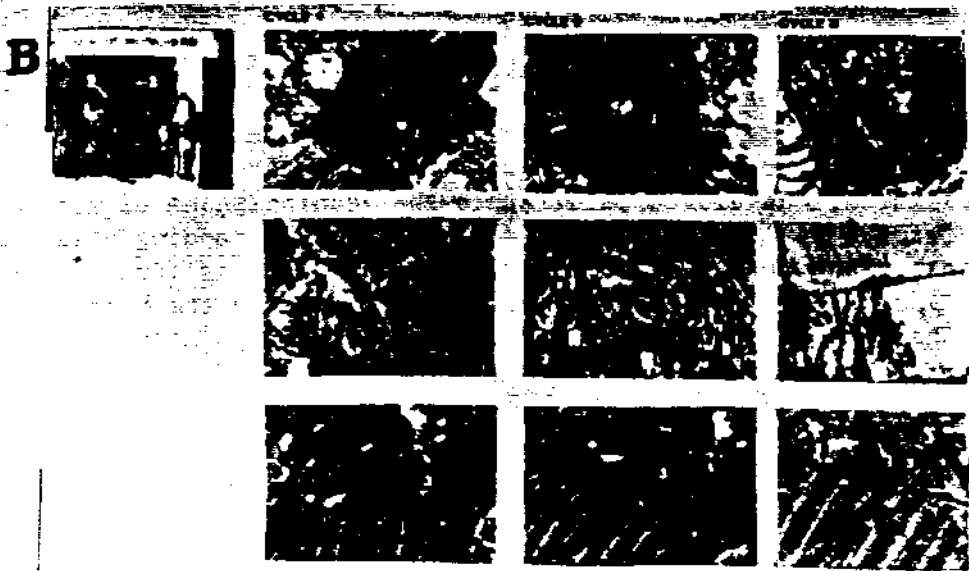
C. $Sh_x = 450 \text{ psi}, Sh_y = 300 \text{ psi}$

Fig. 5. Typical data from drop test showing surface strain, bit penetration, A.E. rate and total count at the impact moment and shortly after for three repeated tests (drop height is 1 ft. and bit type II confining pressures are: A) $Sh_x = Sh_y = 200 \text{ psi}$, B) $Sh_x = Sh_y = 300 \text{ psi}$, C) $Sh_x = 450 \text{ psi}, Sh_y = 300 \text{ psi}$).

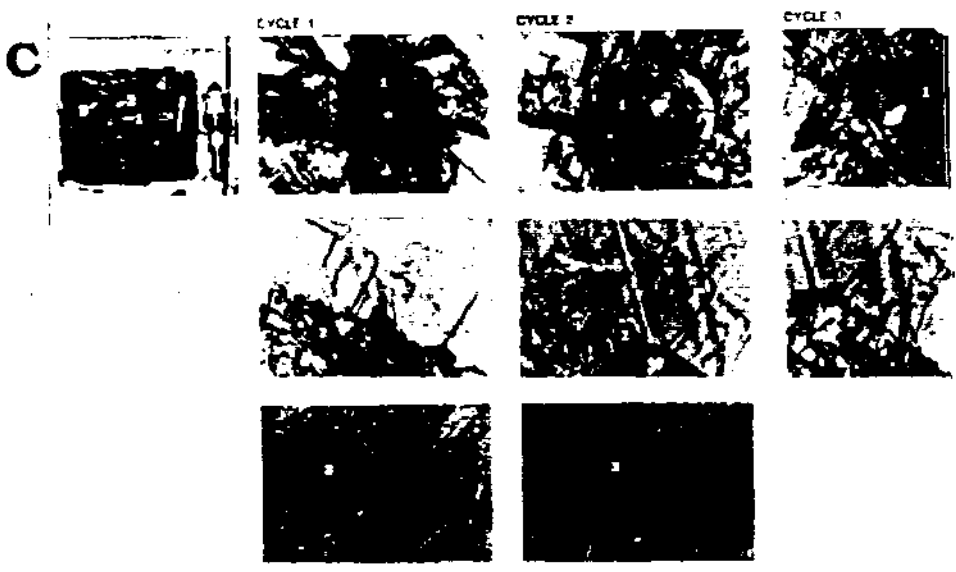
A



A. $Sh_x = Sh_y = 0 \text{ psi}$



B. $Sh_x = Sh_y = 0$ psi



$Sh_x = Sh_y = 200$ psi

Fig. 6. Microscopic photographs for tests under different confining pressure. Photographs were taken after each cycle
 A) $Sh_x = Sh_y = 0$ psi; B) $Sh_x = Sh_y = 0$ psi; C) $Sh_x = Sh_y = 200$ psi.

CONCLUSION

The failure mode developed in the coal block was a combination of tensile and shear failure. Generally, in the unconfined case, major cracks were developed parallel to the bedding plane direction and the failure was in tensile mode. In this case, bedding plane was the weakest plane, having the least tensile strength as indicated in Table 1. Major crack obviously developed parallel to the bedding plane. The formation of the crater near the impact point was in shear failure mode.

The results of the tests and observation could be summarized as follows:

1. Major cracks were developed when the specimen was impacted under the unconfined condition. Only minor cracks were developed under the confined condition.
2. A.E. technique could be very useful to detect the fracture propagation, its intensity and length if combined with sonic technique.
3. Microscopic photography proved to be very useful in observing crack propagation and the cracking pattern on the surface of coal block.
4. Sharper and thinner bits create more damage and thus create a larger crater with deep fractures in the specimen.

ACKNOWLEDGEMENTS

The authors acknowledge the assistance of N. P. Reddy and G. Begley, graduate students in the Mining Engineering Department, in preparing this paper. This project was funded by the Generic Center for Respirable Dust Research sponsored by the United States Bureau of Mines under Grant Number G1135142.

REFERENCES

- Khair, A. W., 1981, "Acoustic Emission Pattern: An Indicator of Mode of Failure in Geologic Materials as Affected by Their Natural Imperfections," Third Conference on Acoustic Emission/Microseismic Activity in Geologic Structures and Materials, Hardy, H. R., Jr. and Leighton, F. W., eds., Trans. Tech. Publ., October, 22 pp.
- Khair, A. W., 1982, "Study of Fracture Mechanisms in Coal Subjected to Various Types of Surface Fractures Using Holographic Interferometry," Proc., 25th U. S. Rock Mechanic Symposium, Northwestern University, June, Society of Mining Engineers, AIME, 12 pp.

FRACTURE IN COAL BY AE

Lindquist, P. A., Lai, H. H. and Alm, O., 1984, "Indentation Fracture Development in Rock Continuously Observed with a Scanning Electron Microscope," Int'l J. Rock Mech. Min. Sci. & Geomech., Vol. 21, No. 4, pp. 165-182.

Scholz, C. H., 1967, "Microfracturing of Rock in Compression," Ph.D. Dissertation, Massachusetts Institute of Technology.

II

**DILUTION, DISPERSION AND
COLLECTION IN MINE AIRWAYS**

Applications of Knowledge Based Systems in Mining Engineering

R.V. Ramani and K.V.K. Prasad
Department of Mineral Engineering, The
Pennsylvania State University

This paper was the subject of a cross-disciplinary presentation under the chairmanship of Dr A.M. Edwards

Managers need quality information for effective decision making. This demand, at the present time, is being fulfilled by the increased use of computers via information systems, decision support systems and management information systems. The idea of incorporating intelligence into computers to aid decision-makers has been evolving for over two decades. In recent years, significant progress is reported on applications to business and sciences. In engineering functions, the Artificial Intelligence approach that seems to have great potential is the application of Knowledge Based Systems.

The primary objective of this paper is to identify domains in mining engineering where application of knowledge based systems could be beneficial. Incorporation of the expertise required during the analysis and interpretation stages of an engineering design problem through knowledge based systems is recognized as an area of significant benefit. To this end, the components of knowledge based systems for mine ventilation and strata control design are described. The potential applications and limitations of knowledge based systems are outlined.

Introduction

Correct decisions are the key to success in any enterprise. Scope of decisions varies with the echelons of management hierarchy. The decisions of top management are strategic, relating to the long-term future of the organization. In a mineral organization, these deal with such issues as the acquisition of a new mineral property or the diversification of the business to exploit additional markets. At the operational level, a manager is concerned with decisions pertaining to day-to-day eventualities related to production activities and other short-term needs. In either case, the prerequisite is the timely availability and use of information. The difficulty involved in decision-making depends on the situational aspect. In many

cases, the decisions to be made under given conditions are fairly straight-forward and standard. This may be due to experience gained from decision-making in similar situations in the past. In fact, many decisions in operations management are either repetitive or routine.

However, there are several situations, particularly at the higher management levels, in which the decision-making procedure does not fit a standard mold, the available information is uncertain or there are no clear guidelines as to how to make the decisions. These semistructured and unstructured decision problems, defined hereafter as complex problems, require the incorporation of judgement and experience in the decision-making process. Several

problems in engineering design can fall in the latter category.

Mine engineering design is a complex problem involving subproblems which can be structured, semistructured or unstructured. Structured design problems can be handled with standard algorithmic approaches. The solution of semi- and unstructured problems, however, has posed great difficulties, in some cases, in defining the problem itself. From the early sixties, the use of computers and mathematical logic to aid managers in decision-making has taken several algorithmic and heuristic approaches. The earliest information systems (IS) were concerned with producing historical reports with little information pertaining to current and/or future operations. Most of these IS were accounting and payroll systems. These were followed by rudimentary management information systems (MIS) which focused on summarizing data from past operations and providing limited decision-oriented information to managers. Over time, the role of MIS has increased to a point where today there are systems for providing managers with the latest information. Developments in data base technology, particularly data base management systems (DBMS) and relational data base schemes, and decision support systems (DSS) have been key in the continual evolution of MIS.

In recent years, advancements in the field of Artificial Intelligence (AI), particularly Knowledge Based Systems (KBS), have made significant contributions in bringing novel computer-oriented approaches to the solution of complex problems. KBS can incorporate aspects of reasoning under

uncertainty in situations where information is incomplete or unreliable. KBS have incorporated formalized approaches such as fuzzy logic and Bayesian probability schemes to quantify incomplete 'artistic/soft' knowledge. The KBS approach has permitted the knowledge of 'experts' to be captured in computer oriented symbolic programs and bear upon the problems of users in many diverse ill-structured domains. Examples of highly publicized areas of applications of KBS include medicine (MYCIN),¹ mineral exploration (PROSPECTOR),² chemical structure identification (DENDRAL)³ and structural engineering (SACON).⁴

The flow of information in a typical IS and MIS framework with an expert system interface is shown in Figure 1. The data collected from the system and via sensors are first sifted to filter out unwanted 'noise.' The filtered data are stored in data bases and is also available online. In structured decision situations, the data are fed to algorithmic models, the output

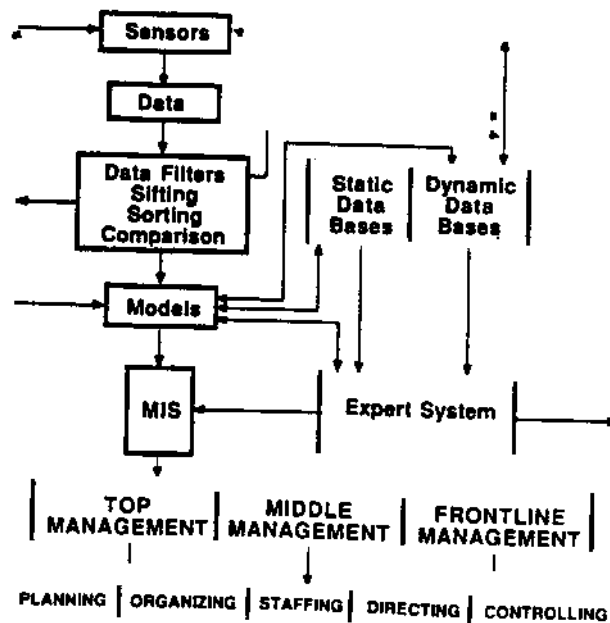


FIGURE 1. Flow of information in a management information system (MIS) with an expert system interface

from which is made available to the decision-maker in the form of information reports. In case of semi- and unstructured decision problems which defy a programmed approach, the expert system can provide the experiential and judgemental knowledge required. As shown in Figure 1, the expert system functions in close interaction with classical MIS and as such it is an integrated part of MIS - a broad epithet encompassing all systems aiding management in decision-making.⁵

The objective of this paper is to present the principles of the knowledge based paradigm and to outline its usefulness as a decision support aid for solving mineral engineering design problems. This discussion will also focus on two functionally important areas of mine engineering design: mine ventilation system design and mine strata control design.

Knowledge based systems

Knowledge based systems are sophisticated, interactive computer programs which use high quality, specialized knowledge in some narrow problem domain to solve complex problems in that domain. KBS have been referred to with a variety of names such as expert systems, intelligent assistants, epistemological systems and design and analysis systems. The two terms most popular in common usage, often used synonymously, are KBS and expert systems.

This is unfortunate because some systems which are advanced as expert systems do not have the essential elements to be considered as such. Strictly speaking, the term expert system implies that a predominant part of the knowledge in the

system has been acquired from expert practitioner(s) in the chosen field. As a result of their unique experiences, experts solve complex problems in reasonable (minimal) time using creative approaches and rules of thumb. As such, a strict or straight-forward mathematical algorithm cannot be an expert system. Further, with KBS, there is no implication of the presence of expert knowledge. The knowledge could be gathered from disparate sources in the public domain. Expert knowledge can be viewed as a particular instance of total knowledge (both expert and other). Expert systems, therefore, are a special breed of KBS where an expert(s)'s knowledge takes prominence over the public domain knowledge. The more encompassing term KBS will be used in this paper.

KBS features

There are four important aspects of KBS which need to be emphasized: (i) they are knowledge intensive, i.e. it is the fundamental hypothesis in Artificial Intelligence, the parent field of KBS, that the problem solving power of a program comes from the quality and quantity of knowledge it possesses relevant to the problem; (ii) the inference or reasoning mechanisms are human-like, i.e. the reasoning strategies adopted by the program reflect the reasoning style of the humans; (iii) the domain of application is narrow; this requirement is a consequence of the high levels of performance expected of the program; expertise is deemed to come with great depth of knowledge in some specialized area rather than general knowledge of several different fields; (iv) KBS are able to explain their line of

THE RESPIRABLE DUST CENTER

reasoning to the user, i.e. they can give justifications as to 'why' a particular line of reasoning was or is being pursued over another and explanations as to how it arrived at a certain conclusion. Clearly, problems requiring significant infusion of common sense and general knowledge for solution are not suitable for KBS applications.

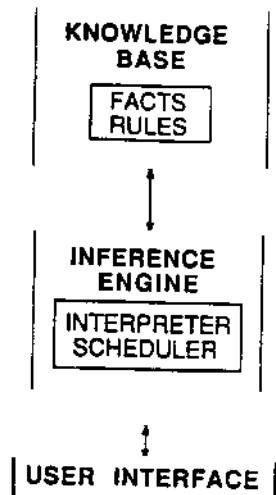


FIGURE 2. Anatomy of a knowledge based system

KBS components

There are two main parts to any KBS - the knowledge base and the inference engine (Figure 2). In addition, there are peripheral features designed to facilitate interaction with end-users (user interface), explanation of a line of reasoning (justifier), etc. The knowledge base consists of two different kinds of domain specific knowledge: (i) declarative knowledge which includes facts related to the domain and the specific problem, and (ii) procedural knowledge which contains rules (or procedures) and heuristics which generate alternate paths of reasoning. The facts and rules constitute a body of information that is widely shared, publicly

available and generally agreed upon by practitioners in the field. The heuristics, on the other hand, are private, experientially gained rules of thumb (rules of plausible reasoning, rules of good guessing, etc.). The primary role of heuristics is to aid in limiting the search for solutions to a problem. This is probably the most powerful feature of KBS.

Knowledge representation

The predominant means of representing the vast amount of problem specific knowledge in KBS has been by production rules. Production rules are of the form 'situation >> action', i.e. they are syllogisms of the form 'IF a certain situation holds THEN take a particular action'. The IF portion of the rule is called the antecedent and the THEN portion, the consequent of the rule. The reasoning mechanism of KBS (Inference Engine) uses these IF...THEN rules to arrive at a conclusion, establish the validity of a fact, etc.

Because of the inherently uncertain nature of the system knowledge, in many instances the rules may not imply strict logical implication. That is, each rule is not deemed to be categorically true or false but rather a qualified statement having a certain amount of 'strength' associated with it. The strength value could have a probability interpretation as in PROSPECTOR, or could be an ad hoc 'certainty factor' (-1 to +1, certainly false to completely true) measure, as in MYCIN.

Inference engine

The inference engine is made up of two parts: (i) an interpreter which decides on how to apply rules to infer new knowledge, and (ii) the scheduler which decides on the order in which the rules should be applied. Generally, the interpreter validates the relevant conditions of rules and performs the tasks which the rule prescribes. The scheduler maintains control of an agenda and determines which pending action should be executed next. There are two major ways in which inference engines apply reasoning strategies to arrive at plausible conclusions:

(i) Data driven reasoning/forward chaining: To illustrate this type of reasoning, consider the following three rules:

- RULE1: IF A THEN B
- RULE2: IF B THEN C
- RULE3: IF C THEN D

when it is known that A is true at a particular instance. The system starts drawing inferences on this newly asserted fact. The new fact asserted satisfies the antecedent of RULE1. This establishes fact B. Since the truth of B satisfies the antecedent of RULE2, C is established and so on.

(ii) Goal directed reasoning/backward chaining: Consider the following set of rules in the knowledge base.

- RULE1: IF (A and B) THEN C
- RULE2: IF (D and E) THEN A
- RULE3: IF (F and G) THEN B

The problem to solve may be to find out if C is true. To establish C (the consequent of RULE1), the inference engine tests if the antecedent is true. The antecedent

involves the establishment of the truth of A and B. Two subgoal problems are now set up: (i) prove truth of A and (ii) prove truth of B. Only when A and B are proven true, C is true. But proof of A and B themselves involve two more conjunctive sub-goal problems - proof of D and E, and F and G. Therefore, the truth of the facts D, E, F and G are checked in the knowledge base. If they explicitly exist in the knowledge base, then C is established, otherwise the inference engine has two options: (i) report that it does not have sufficient information to establish the truth of C, or (ii) query the user for any information regarding the truth of D, E, F and G. This is a very common reasoning process used in medical diagnosis, or any system diagnosis for that matter, when it is desired to establish if a patient has a certain disease, i.e. check if the patient has the symptoms endemic to the disease.

MYCIN (an expert system, developed at Stanford University, for providing physicians with advice on diagnosing bacterial infections) uses backward chaining for its reasoning process. The advantages over forward chaining are very apparent in this instance. If the inference mechanism had started out to establish C by looking into the knowledge base trying to find an antecedent which is true and initiating forward chaining on the fact, it could be led into blind alleys and may never realize the goal of establishing C. In a knowledge base with hundreds of rules, this could mean an inefficient and unintelligent search procedure, even if C were to be established.

This is not to imply that backward chaining would always yield better results. There are problems in which the current system knowledge is used to infer more interesting knowledge which leads the system closer to the goal. Forward chaining is ideally suited for such problems. There are also situations where even a combination of forward and backward chaining might be necessary. The choice, however, is critical.

Strict delineation between the knowledge base and inference engine is a desirable feature. If the two are intermixed, domain knowledge gets spread out through the inference engine and it becomes less clear what ought to be changed to improve the system at a later date. The result is an inflexible system. If all the task specific knowledge has been kept in the knowledge base, then it is possible to remove the current knowledge base and 'plug in' another. The explicit division thus offers a degree of domain independence. It does not mean, however, that the knowledge base and inference engine are totally independent. Knowledge base content is strongly influenced by the control paradigm used in the inference engine.

User interface

The user interface is basically a language processor which permits the end-user to communicate with the KBS in a problem/task jargon, usually some restricted variant of English. Typically, the user interface parses and interprets user questions, commands and volunteered information. Conversely, the interface formats information generated by KBS, including answers to questions, explanations and

justifications for its behavior and requests for information.⁶

KBS versus conventional programs

The utility of KBS and its superiority over conventional computer programs are not obvious. A frequently asked question is: What is the difference between a KBS and a normal program? Consider the IF...THEN statements versus the IF...THEN rules. The difference is analogous to the difference between sequential and direct access of information from disks (as far as program execution is concerned). In conventional computer programs, the IF...THEN statements are executed in a preset sequence and the execution is entirely control flow dependent. In KBS, on the other hand, it is the state of the system's current knowledge which determines its future course of execution. The system's current knowledge accesses the relevant IF...THEN rules and chooses from them the most appropriate one. Therefore, in KBS, the execution is totally knowledge dependent. A further difference emanating from the above argument is that in a KBS the control of execution is in the hands of the user, i.e. what question will be asked next, or what piece of information will be necessary next is entirely dependent on what response is given to the present question. Moreover, explanations and justifications can be requested of the system at any time. These explanations and justifications are more powerful and context dependent than information obtained by invoking HELP menus in conventional computer programs.

The knowledge base in a KBS is organized in a way that separates the knowledge about

the problem domain from the system's other knowledge, viz. general knowledge about how to solve problems in the domain - the inference engine. This aspect highlights one more important difference between KBS and conventional computer programs, viz. additional knowledge in the form of IF...THEN rules can be added to the knowledge base of a KBS without any adverse side effects in terms of system functioning. Adding an additional piece of code to a conventional computer program might prompt a major restructuring of the program.

Developments of knowledge based systems in widely different fields have shown that the same inference engine can be used in different application areas (e.g. EMYCIN). The popularity of the rule based knowledge representation approach has also contributed to the development of 'canned' reasoning strategies. Therefore, a gradual shift towards a formalized means of developing these inference engines has evolved. These inference engines interfaced with other peripheral components are being marketed under the name of 'expert system shells'. The inferencing scheme in these shells is built by assuming a certain knowledge representation scheme. Therefore, one can conclude that some of the aspects of KBS development are being algorithmized. However, development of the domain dependent knowledge base remains the key activity involving the most time and effort.

KBS for engineering design

Hitherto the dominant application area of KBS has been in diagnostic fields, i.e. weighing and classifying complex patterns

of evidence to evaluate a situation that is either abnormal (as in diseases and faults) or developable in new ways (as in mineral prospecting). But diagnosis is just one of the tasks that requires expertise. There are other tasks which are equally demanding of expertise.⁷ These include:

- (i) INTERPRETATION: analysis of data to determine its meaning and implications. Diagnosis can be considered as a major component of interpretation. But use of the term diagnosis has been reserved exclusively for evaluating maladies/abnormalities from available symptomatic data.
- (ii) PLANNING: creating programs of action to achieve goals.
- (iii) DESIGN: constructing or creating a system or object that satisfies certain stipulated requirements.
- (iv) PREDICTION: forecasting the future from a model of the present or past (or both); forecasting the values at locations where there is no data from data at known locations.

In engineering disciplines, the role of design is important. The view of design here is different from that stated above. In an engineering design problem, there are strong underpinnings of both planning and interpretation. Diagnosis also plays an important part in the design process but it is not the objective per se. The overall design process can be viewed as consisting of the following three major components:

- (i) ANALYSIS COMPONENT: this includes the planning and interpretation tasks and involves the idealization of the given problem situation to

make it amenable to engineering analysis.

- (ii) SOLUTION COMPONENT: this involves the use of major algorithmic programs to operate on the idealized model and provide results.
- (iii) INTERPRETATION COMPONENT: this involves diagnosis and interpretation of the model results to check the validity of the idealized model and hypothesize refinements (if needed) before going back to the analysis step for another iteration, if necessary.

The solution component is a structured problem and its computerization and automation in mining engineering have reached a high level of maturity. Excellent computer programs are available for the solution of, for example, finite element models of mine structures, network models of mine ventilation systems and influence function models for subsidence prediction. The complexity of these programs has grown to such an extent that, user's manuals notwithstanding, it takes months to use the program options. Even if one learns how to run the program, the user is ill-prepared for the tasks of analyzing a physical problem in terms of the model and interpreting the model output in terms of the overall design objectives and constraints. This is because the analysis and interpretation components are not structured and require experience and expertise. At the same time, there are recognized 'experts' (albeit few in number) who perform the analysis and interpretation tasks with relative ease and with great competence.

Advances in computer hardware and software have been incorporated in recent computer application packages to alleviate some of these problems. Programs have been made interactive and user-friendly. Interfaces with graphics devices have been established to aid interpretation of data and results. These approaches, however, have not addressed the real problem. The 'experts' perform better than others largely because of their greater knowledge acquired through exposure to different kinds of problem scenarios and experience gained therefrom. The requirement is to transfer the accumulated analysis and interpretation expertise of experienced people to other, less experienced users.

For example, geostatistical techniques have been used for years in ore reserve estimation. Much of the methodology has been formalized and programmed in the last two decades. The first step in any geostatistical study is the determination of the form of the spatial variability function (the variogram). The choice of the form of this function is highly judgemental and depends heavily on the knowledge of the geology of the area. Similarly, the interpretation of the results from a geostatistical investigation is also dependent on experience gained with the applications of this and other techniques in specific deposits. Without this expert analysis and interpretation, the geostatistical exercise may not provide valid information to decision makers. The tapping of this expertise and its incorporation in the knowledge base are crucial. To achieve this goal, the KBS approach seems viable.

Incorporation of expertise in programs via KBS is not new. As mentioned earlier, there has been great success in such efforts in fields such as medical diagnosis. But a significant limitation of such KBS is that they tend to be based solely on rules of experience gleaned from 'experts'. Since the solution component is a major stage in engineering design, in addition to experiential knowledge, the capability to model the behavior of the system under consideration is also necessary. This kind of system would take advantage of the synergistic efficiency afforded by using expert rules of experience and algorithmic programs (to provide information needed by a rule, e.g. pressure drop in a particular branch of a ventilation network). The integration of algorithmic programs with expert systems for analysis and interpretation would, therefore, represent a major step in enhancing design capability. A generic knowledge based system anatomy is illustrated in Figure 3.

A mining knowledge based system must have as a minimum the following features which also permit identification of programs which are not legitimate KBS.

- (i) A knowledge representation formalism and a knowledge base. The knowledge should not be mere numeric data but must include symbolic data as well.
- (ii) An inference engine which manipulates the knowledge to arrive at conclusions. The inference should not be an algorithm. If the problem has an algorithmic solution it is not necessary to build a KBS for it.

- (iii) An explanation facility capable of providing explanations (in terms of the system knowledge) as to how the system arrived at a certain conclusion or result and justifications as to 'why' a certain piece of information is being requested.
- (iv) A user interface that facilitates communication between the user and the KBS in a subset of English.
- (v) Input and output interfaces between design and analysis programs and the KBS.

Mine ventilation system design

Although the importance of mine ventilation has been recognized from the earliest days of mineral extraction, ventilation planning is, even today, more commonly considered an art rather than a science.

Ventilation system design is an engineering design problem whose solution requires the steps of perception, idealization, modeling, interpretation, feedback and control.⁸ During the analysis phase, since ventilation system design is a part of the overall mine design, consideration must be given to the interrelationships which exist between the mine infrastructure and mine ventilation system. The adequacy of the input data and their reliabilities are also of paramount importance. In the interpretation phase, an objective analysis of the output is necessary. This step may identify weak areas in the definition of the problem in which case redefinition of the problem may be in order. The solution may have undesirable elements or maybe infeasible to implement, leading to questions on the

THE RESPIRABLE DUST CENTER

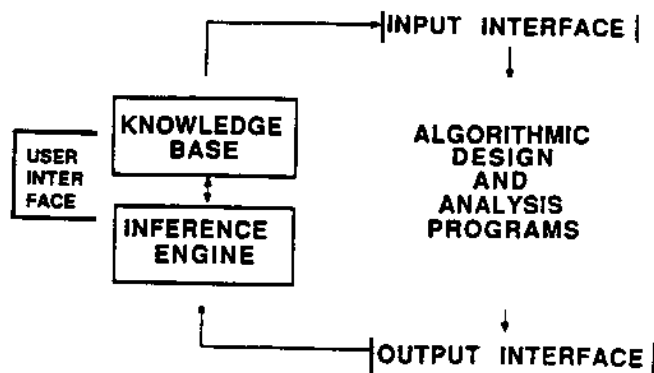


FIGURE 3. Anatomy of a knowledge based system for engineering design

design or the data. Also, the solutions, when properly analyzed and interpreted, can lead to a better definition of the problem, or superior alternatives to the problem. The design process can be visualized as an iterative process leading to improved perception, idealization, definition and solution of the problem.

The application of digital computers to solve the pressure quantity problem associated with mine ventilation systems began to make an impact only two decades ago. It is important to stress that the solution of the pressure quantity problem is only one step in the total planning process outlined before. There are important analysis steps prior to this 'solution' stage and even more important interpretation steps after the 'solution' stage. Considerable experience and expertise are needed in mine ventilation systems and mining engineering to arrive at good ventilation designs. Many benefits of computer-aided analysis are not realized in practice as this expertise is not readily available. Therefore, integration of KBS reasoning with mathematical models seems desirable. The essential elements of such a system are shown in Figure 4.

There are three major elements in the integrated system: (i) the KBS and its

input-output interfaces to the design and analysis programs (DAP); (ii) the design and analysis programs, consisting of a ventilation data base and ventilation programs, and (iii) the actual mine system which is operated on by natural (mine location, seam characteristics, methane, etc.) and cultural factors (equipment characteristics, fan operation, etc.) resulting in dust, gas, heat and humidity, etc. and from which data can be collected on a real time basis. The KBS element is the prime mover of the whole system.

In the analysis step, decisions have to be made regarding some of the following factors:

- (i) What is the problem to be addressed? Is it dust generation? Is it lack of requisite air quantities? Is it the excessive liberation of methane? Is it a combination of the above?
- (ii) Interrelationships of the problem with other mine design aspects, e.g. ground control, mining method and extraction, hydrology, regulations, etc. have to be identified.
- (iii) Since an engineering problem is rarely amenable to engineering analysis as is, the problem has to be idealized with simplifying assumptions. A major decision has to be made regarding the relevant assumptions to make so as not to sacrifice the purpose of the analysis. An appropriate model will have to be hypothesized.
- (iv) An appropriate design and analysis program will have to be selected commensurate with the availability

Follo
DAP is
stage,
follows
model,
any dis
overall
questio
followi
(i)

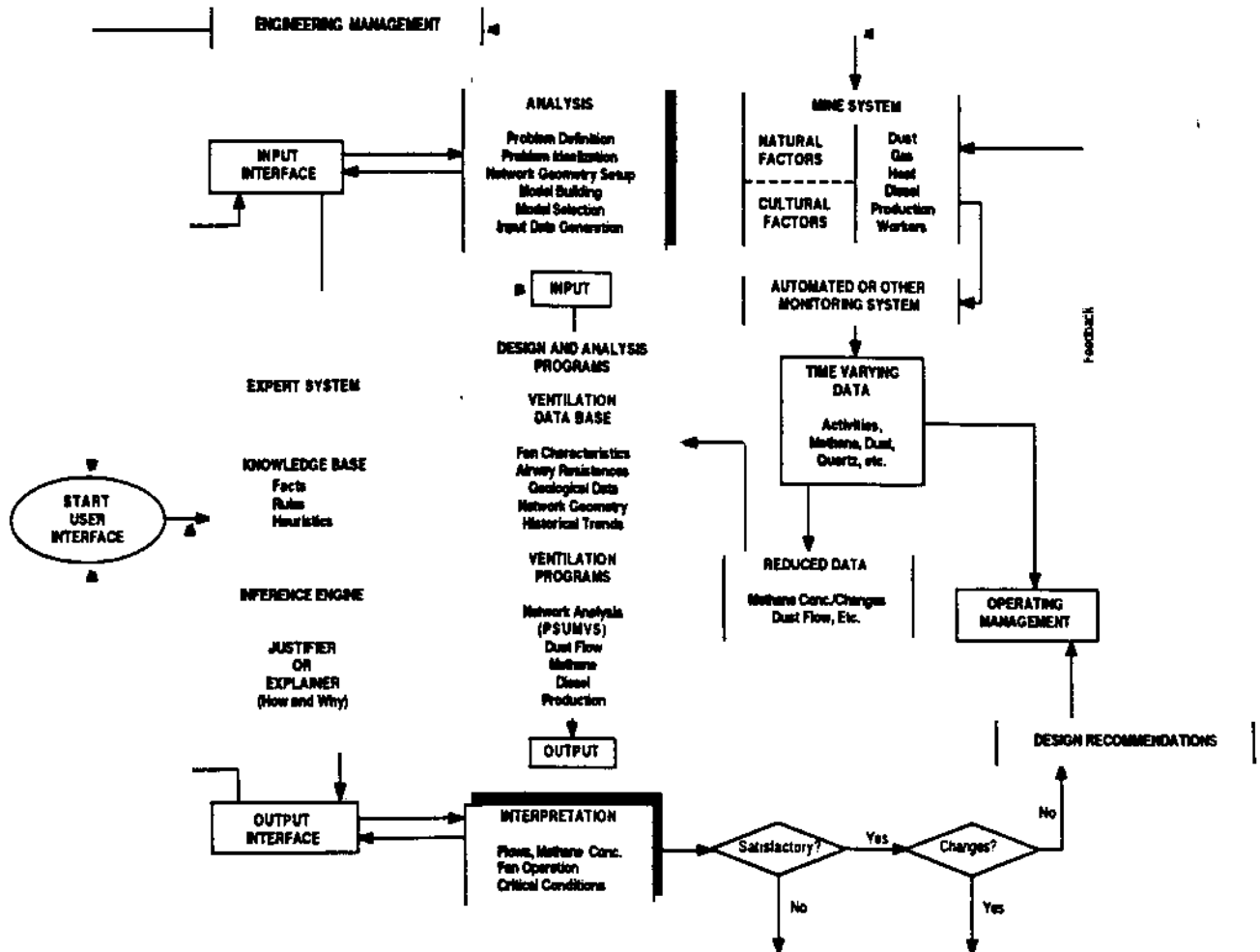


FIGURE 4. A logic flow diagram of a knowledge based system for planning mine ventilation systems

and quality of the input data and desired accuracy of results. The data necessary for the model have to be developed.

Following the analysis step, the selected DAP is executed and after this solution stage, interpretation of the output follows. In the interpretation stage the model results have to be interpreted and any discrepancies diagnosed in terms of the overall design objectives. Among the questions arising at this stage are the following:

- (i) Are the model results realistic?
Is the hypothesized model a valid

idealization of the problem situation?

- (ii) What do the flow directions, air quantity, dust and methane concentration values mean and imply? What are the fan operating conditions? Are they realistic?
- (iii) How sensitive is the solution? Are the conditions critical in any branch of the network? If so, what could be the possible reasons?
- (iv) What are the refinements which can be made to the current analysis? What other model alternatives can we choose from?

(v) Which one of the available options should be chosen?

Most of the knowledge involved in answering these questions and making these decisions is experience dependent. This knowledge can be acquired from public domain sources and from experienced mine ventilation practitioners, and incorporated in the KBS for ventilation systems. An integration of KBS and traditional algorithmic programs yields a superior decision support system for mine ventilation system design. Development of such a system is possible with the current state of system technology.⁵

Mine strata control design

Mine strata control design is another important area where an integrated approach seems to hold promise. An outline of a typical strata control design approach is shown in Figure 5. As can be seen, the overall design philosophy is still the same, i.e. it fits the standard 'analysis -- solution -- interpretation' mold.

The objective in a strata control design program is usually the selection of the location and subsequent design (construction) of access and service openings and structures. To achieve this objective, three types of information are essential: (i) knowledge of the material properties of the different rock strata in the area -- these include the compressive, tensile and shear strengths, RQD, RMR, etc., (ii) knowledge of the in-situ stress regime in the area, and (iii) knowledge of the location and frequency of major geological features like folds, faults, etc. in the area. Most of this data is collected during the exploration stage from

cored boreholes and geophysical measurements.

The above information is often not adequate to characterize the behavior of the various rock strata completely. An appropriate material behavior has to be hypothesized. Moreover, once some form of material behavior is assumed, an appropriate analysis tool has to be selected. These two aspects form the core of the ANALYSIS stage in strata control design. In this stage questions such as the following must be answered: (i) Should the design be based on empirical formulae or should a more rigorous analysis (such as Finite Element Method - FEM) be adopted? (ii) How should the material behavior be characterized? What failure criterion is most appropriate? What are the loading and boundary conditions? What will be the granularity of the analysis? (iii) From the quantity and quality of the input data available, which design and analysis program would be most suitable? Most of the reasoning in this stage is nonalgorithmic and requires considerable experience and expertise.

The solution stage, as shown in Figure 5, can be purely algorithmic, the input to which is generated in the analysis stage. Here use is made of algorithmic design and analysis programs such as a finite element analysis program for an idealized coal pillar model. The number of programs available to the user at this stage is numerous. In the mining domain, for example, one could use ADINA/BM or BMINES etc. These programs generate reams of output, usually the stresses and strain in each element of the model.

KNOWLEDGE BASED SYSTEMS

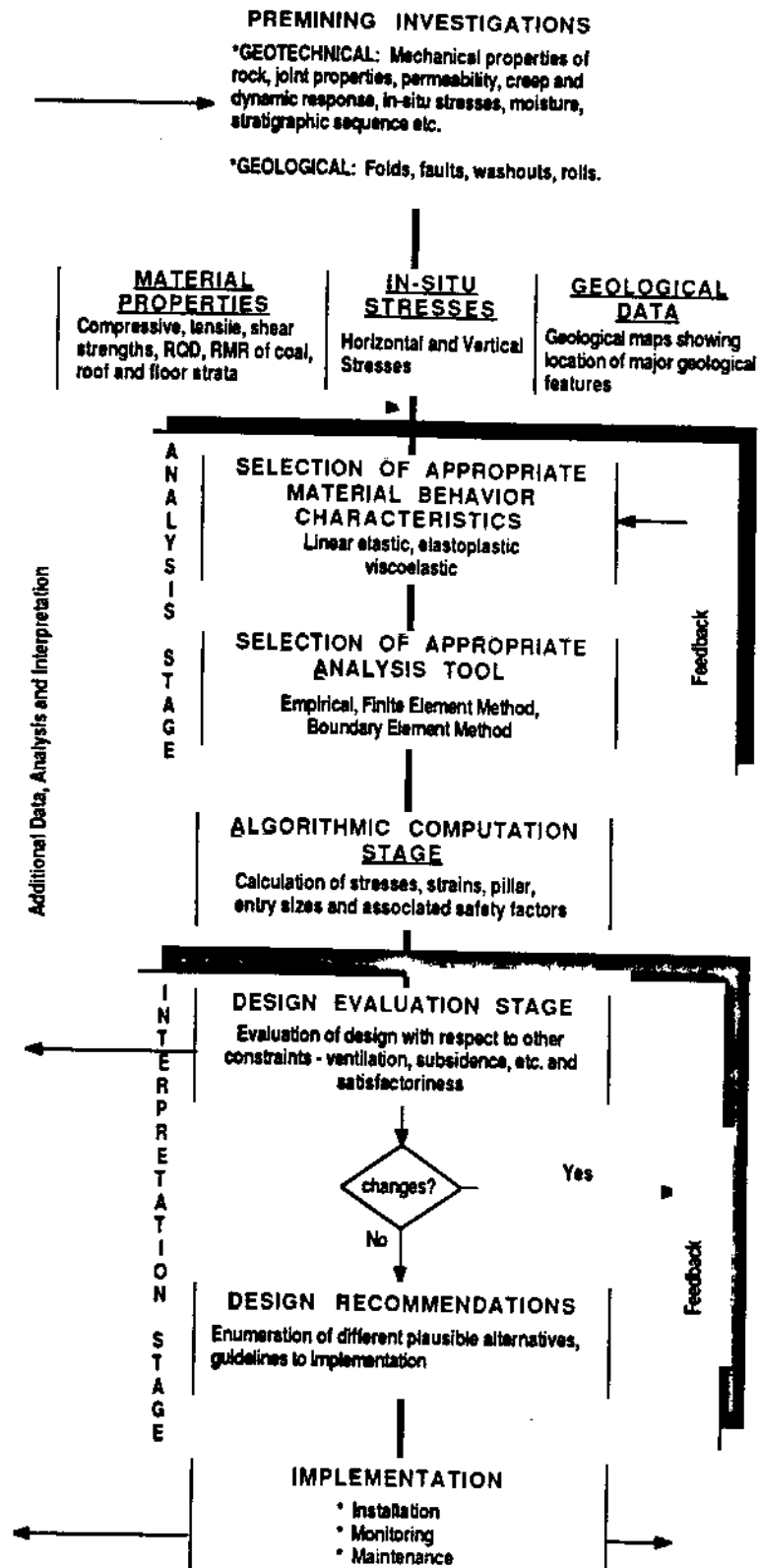


FIGURE 5. An outline of the design approach for strata control in mines

The interpretation of the output generated by the solution stage again requires considerable expertise. What do the stress and strain values in the different elements imply? Is there local failure in a certain portion of the mine? If so, what can be said of overall stability and the type of analysis procedure chosen in the analysis stage? Was it adequate? Was it representative? Is the design satisfactory with respect to the design in other areas such as the ventilation system? If there is some experimental data available, how does the model output compare with the real world scenario? Are the discrepancies due to poor material behavior idealization? If so what changes should be tried out? In this stage too, judgemental knowledge is necessary to identify the overall adequate design.

Other application areas

In addition to the two applications discussed above, there are several other areas in mining engineering which can benefit from the KBS approach. The potential for the development of a KBS for geostatistical studies was already mentioned. KBS use in the analysis of investment and risk also falls in the same category. Other major design elements in mining engineering such as electrical, drainage and haulage systems, and surface mining reclamation schemes can also benefit from KBS applications. There also are promising applications in the area of diagnosis, viz. troubleshooting and maintenance of mining machines and equipment via goal directed KBS. Development of these systems will also be

of value in computer assisted training and instruction.

Conclusion

This paper has highlighted the importance of incorporating experiential and judgemental knowledge in engineering design problems. This issue, as it relates to mine ventilation and mine strata control systems, has been outlined. It is imperative that efforts be made to formalize this 'artistic' information via knowledge engineering so that it is widely available. Nonavailability or difficulty in accessibility of expert opinion and input has severely throttled design efforts in the past. In light of this paucity, the advantages of mathematical models for design have not been fully realized. The benefits accruing from the proposed approach are:

- (i) Permanent availability of timely, high quality and diverse expertise for analysis and interpretation.
- (ii) Assistance in characterization of the problem situation and proper consideration of relevant (and critical) factors.
- (iii) Avoidance of misinterpretation of program outputs and assistance in faster convergence of the iterative design process towards the goal.
- (iv) Ability to solve problems where incomplete or uncertain data only are available.
- (v) Enhanced training of new engineers and analysts.
- (vi) Increased productivity and better designs.

It is important to evaluate the suitability of the problem for solution

through a KBS approach. A common pitfall has been the recasting of algorithmically solvable problems in the KBS mold. In looking for appropriate problems for KBS development instead of seeking problems which require expertise to solve, a common error has been to look for experts whose knowledge can be captured. A better approach is to look for engineering design problems which are demanding of knowledge and expertise. Moreover, in any problem being considered, it is essential to filter out the algorithmic portions and attempt to use the KBS approach for the judgemental and experiential portions only. KBS technology is successful only when applied in narrow, specialized domains. Extending the problem domain to such areas as overall mine design will involve large commitment of funds and efforts without any guarantee of success.

References

1. BUCHANAN, B. C. and SHORTLIFFE, E. H. Rule Based Expert Systems - The MYCIN Experiments of the Stanford Heuristic Programming Project. Addison-Wesley, Reading, MA, 1984.
2. GASCHING, J. PROSPECTOR: an expert system for mineral exploration. In: Introductory Readings in Expert Systems, Michie, D. Gordon and Breach Science Publ., New York, NY, 1982.
3. FEIGENBAUM, E. A., BUCHANAN, B. G. and LEDERBERG, J. On generality and problem solving: a case study using the DENDRAL program. Machine Intelligence 6. Edinburgh University Press, 1971.

4. BENNETT, J., CREARY, L., ENGLEMORE, R. and MELOSH, R. SACON: A knowledge-based consultant for structural analysis. Technical Report STAN-CS-78-699, Stanford University, 1978.
5. KOHLER, J. L., RAMANI, R. V., KOHARCHIK, G. J. and BHASKAR, R. A conceptual investigation of a management information system for coal mines. Final Report to U.S. Bureau of Mines. Contract #J0348005, August 1986.
6. HAYES-ROTH, F., WATERMAN, D. A. and LENAT, D. B. eds. Building Expert Systems. Addison-Wesley, Reading, MA, 1983.
7. STEFIK, M., AIKINS, J. BALZER, R., BENOIT, J., BIRNBAUM, L., HAYES-ROTH, F. and SACERDOTI, E. The organization of expert systems - a tutorial. Artificial Intelligence, 18, 1982, pp. 135-173.
8. LUXBACHER, G. W. and RAMANI, R. V. The interrelationship between coal mine plant and ventilation system design. Proc. 2nd. International Mine Ventilation Congress. Society of Mining Engineers of AIME, New York, NY, 1979, pp. 73-82.

This research has been supported by the Department of the Interior's Mineral Institute program administered by the Bureau of Mines through the Generic Mineral Technology Center for Respirable Dust under grant number G1135142.

A Comparison of the Performance of Impactors and Gravimetric Samplers in Mine Airflow Conditions

R. Bhaskar and R.V. Ramani
Department of Mineral Engineering, The
Pennsylvania State University

Abstract. While the National Academy of Sciences has stated that gravimetric sampling technology for compliance purposes is adequate, research into various aspects of respirable dust control require data on many other parameters of airborne dust. These, in turn, have created the need to use many instruments, other than personal gravimetric samplers, in mine environments for dust measurement. There is a need to evaluate the performance of these instruments under conditions of potential use.

As part of research in the Generic Technology Center for Respirable Dust, cascade impactors, gravimetric personal samplers and gravimetric samplers collecting dust using isokinetic sampling principles were employed for dust measurements under identical conditions in a mine airway. During the course of the experiments, 8-stage cascade impactors and gravimetric samplers drawing air isokinetically were located in the center of a mine airway at various stations. Two types of data were examined - concentration of dust and size distribution of the dust collected in the samplers. The data show that the amount of dust collected by an impactor is less than half the amount collected isokinetically. The size distributions of the dusts collected from the two instruments, though comparable, show a consistent difference in median diameters. The cause for this bias is examined.

The paper presents and discusses the results of the tests, including the concentrations and size distributions obtained from the two instruments for different experimental conditions. There is a need to document the performance of various dust measuring devices in mine airflow conditions.

INTRODUCTION

The sampling of airborne dust in mines can be done for several purposes. Traditionally, dust sampling has been restricted to the gravimetric measurement of airborne respirable dust to comply with the regulations governing the mining industry. Instruments such as the MRE

gravimetric sampler, and personal gravimetric samplers that have collection characteristics similar to the human respiratory system have been in use for the last two decades. Presently available instrumentation for the purpose of regulation have been considered adequate by the Committee on the Measurement and Control of Respirable Dust in Mines (National Academy of Sciences, 1980).

The increased research activity in studying the other attributes of airborne dust such as total size range concentration, particle size distribution, particle shape and elemental composition has created a need for instruments which selectively collect dust for evaluating these properties. In relation to mining, efforts have been made by various researchers to adapt instruments developed in areas of aerosol science for mining requirements with varying degrees of success as no instrument is specifically available for these purposes for use in the mines.

One instrument that has been used in mining research is the cascade impactor. The cascade impactor has been used for several decades (May, 1945) in various forms, but the development of smaller versions (Sierra Models 296 and 298) increases the scope of its use in the industry. The instrument has been used with very good results in other areas of research and has scope for extensive application in mining.

During the course of a research experiment conducted by the authors in a mine airway (Bhaskar, Ramani and Jankowski, 1986), it was decided to evaluate the sampling efficiency of cascade impactors against another instrument used to measure airborne dust. The instrument was an assembly containing a filter holder connected to a nozzle designed to draw air isokinetically. The two instruments were placed at the same location in a flowing stream of air. The study is aimed at providing potential users an understanding of the collection characteristics of the instruments so that proper precautions and inferences can be drawn from the collected data.

IMPACTORS AND GRAVIMETRIC SAMPLERS

LITERATURE SURVEY

Several studies have been conducted on the performance of impactors. Because the design of impactors vary between various brands, quantifications of errors and the limitations of the instruments have to be determined. Rubow et al. (1985) and Marple and Willeke (1976) have presented a list of operational precautions that have to be taken when collecting aerosols and interpreting the data. The authors note that precaution must be taken in the use of sampling efficiency charts when sampling conditions are different from those specified in the charts. Some of the precautions that have been studied are (Marple and Willeke, 1976);

(1) High velocity through the nozzles

The authors note that high velocity through the nozzles of the impactor stages may result in particle losses between stages and from the impaction plate due to reentrainment. The use of proper substrate coatings is suggested. A discussion of various substrates and filters has been provided by Rao and Whitby, 1978; Dzubay, Hines and Stevens, 1976; Esmen and Lee, 1980; and Lee, 1986.

(2) Inlet Losses

Studies on the sampling efficiency of the impactor in calm air conditions was studied by Agarwal (1975) and Agarwal and Liu (1980). Agarwal (1975) showed that particles up to about 100 microns can be sampled with nearly 100% efficiency in still air. However, Marple and Willeke (1976) note that there may be considerable losses on the internal surfaces of the inlet due to impaction and settling.

(3) Wall Losses

These losses occur between stages due to deposition of particles on surfaces other than the impaction plates. Rao (1975) studied the losses in various impactors and determined the losses as a function of particle aerodynamic size.

The literature survey indicates that little work has been done to evaluate the performance of the impactor under flowing air conditions as opposed to calm air conditions, particularly under mine airway conditions. While some researchers have used isokinetic sampling attachments with impactors (Courtney et al., 1986) thereby reducing sampling inefficiencies, the use of impactors without such isokinetic sampling attachments will cause data collection problems. Lee (1986) performed studies comparing the sampling efficiencies of impactors with and without isokinetic sampling attachments, for velocities under 250 fpm, both in the laboratory and in mines. His results are presented in Table 1. The amount of dust

collected isokinetically is less than that collected nonisokinetically. The data show that under mine conditions the ratio is nearly 1.0 for velocities about 100 fpm, while at 210 fpm, the value is 0.72, the ratio varying from experiment to experiment and demonstrate the need for more extensive data for drawing conclusions.

Table 1. Impactor data collected with and without isokinetic sampling nozzles (after Lee, 1986).

Test Number	Velocity (fpm)	Sample Weight Ratio*
1	97	1.02
2	103	0.97
3	150	0.87
4	192	0.74
5	195	1.03
6	205	0.96
7	210	0.72
8	230	0.77
9	230	0.88

* isokinetic to non-isokinetic sample weight. Inlet line (9" in length) losses not accounted for.

Besides the understanding of the limitation of the impactor in terms of mass measurements, it is helpful to develop relationships between dust size distribution parameters obtained from impactor data with that obtained from other size measurement instruments. One such instrument is the MICROTRAC for which the size distribution relationship is examined here.

The MICROTRAC Small Particle Size Analyzer provides a rapid method of analyzing size distributions of particles in solution form. The instrument uses the laser diffraction principle for size analysis. Studies have been performed by Dumm (1986) relating the size distribution of dust derived from the mass collected on the impactor substrates with the same dust redispersed from the substrates into solution and subject to MICROTRAC random projected area diameter size analysis. Dumm (1986) compared the median diameter (d_{50}) of two samples. The ratios of d_{50} obtained using the MICROTRAC and the d_{50} obtained from impactor data were 1.03 and 1.16 for the two samples examined by the author. This is the shape factor between the two size distributions.

EXPERIMENTAL SET-UP

The present research was conducted as part of a study on the behavior of dust clouds in mine airways. The experimental studies were conducted in the Lake Lynn Laboratory of the U.S. Bureau of Mines and have been described in a paper by

THE RESPIRABLE DUST CENTER

Bhaskar, Ramani and Jankowski 1986. The study was aimed at examining the change in dust concentration, deposition and size distribution of the dust as it traveled the length of an airway under various airflow velocities. A total of six experiments were conducted, at three velocities using dusts of two different densities. Two types of ambient concentration sampling were performed: (1) sampling of air at the center of the airway, and (2) cross-sectional sampling. In four of the six experiments, Sierra 298 cascade impactors were also used to sample the dust. A description of the instrument set-up follows.

Instrumentation

Three different instruments were used in the study: (1) MSA personal gravimetric samplers, (2) Sierra 298 8-stage cascade impactors, and (3) an isokinetic sampling arrangement. A set of one each of the three instruments were hung from a telescopic pole in the center of the airway, at three locations in experiment 3 and at four locations in experiments 4, 5 and 6.

The MSA personal gravimetric sampler is essentially the same instrument used for MSHA compliance. However, the conventional MSA pre-weighed cassette was replaced by a two piece MSA cassette holder containing a 0.2 μ m Nuclepore filter. The advantages of using this filter are the superior collection efficiency of the filter and the ease with which the deposited dust can be ultrasonically washed off its surface for size analysis. The pumps used were constant flow DuPont pumps set at 2.0 l/min.

The Sierra 298 8-stage impactor is a compact personal impactor fitted with a cowl and visor. The impactor can be operated at 2.0 l/min to yield a standard set of particle size cuts of the collected dust. To reduce the possibility of particle bounce, the mylar substrates were sprayed with a 20% petroleum jelly in toluene solution. Almost 99.5% of the dust was less than 25 μ m. The sampling time and concentration were such that no overloading of the impactors took place.

The isokinetic sampling arrangement consisted of a MSA two-piece cassette holder containing a 0.2 μ m Nuclepore filter. The cassette holder was connected to a short tube with a nozzle fitted at the other end. To ensure isokinetic sampling under the experimental conditions, special sharp-edged nozzles were designed and fabricated for use with the sampling units. The chamfer angle of the nozzle's exterior surface was less than 30°, further reducing the disturbance to the air flow at the point of sampling. A typical arrangement of the nozzle is shown in Figure 1. By adjusting the pumping rate of the sampling unit, the velocity of the air through the nozzle was matched with the velocity in the airway. This procedure ensures that a representative sample is collected.



Figure 1. Assembly for Ambient Concentration Sampling.

Dust was dispersed using a dust dispersion device at the head of the airway located at least 500 feet away from the sampling stations having impactors. Flow velocities were 365 fpm for experiment 3 and 4, and 305 fpm for experiments 5 and 6. No impactor sampling was conducted for experiments 1 and 2.

At the end of the experiments, the instruments were carefully removed from the sampling pole with minimal disturbance. The impactor as well as the total and respirable dust cassettes were transported to the lab where gravimetric and size analysis were carried out after desiccation of the samples.

DATA ANALYSIS

The total and respirable dust were desiccated and weighed and the concentration of the airborne dust cloud was determined. The impactor substrates were also desiccated and the masses on the individual substrates and back-up filter were determined.

The total and respirable dusts deposited on the Nuclepore filter were ultrasonically removed from the filter and dispersed in water. The solution was then subjected to a MICROTRAC size analysis. The size distributions of the impactor dust were determined directly from the mass of dust deposited on the individual substrates and the corresponding size cut off points for a flow rate of 2.0 lpm.

RESULTS

Two types of data were obtained from the experiments — concentration and size analysis.

Concentration

The concentration data is presented in Table 2 for the three instruments used. The last column contains the ratio of the concentration obtained

IMPACTORS AND GRAVIMETRIC SAMPLERS

Table 2. Comparison of Sampling Efficiency of Impactors in Flowing Air.

Experiment Number	C O N C E N T R A T I O N (mg/m ³)			Velocity (fpm)	Ratio of Impactors Isokinetic
	Impactors	Respirable	Isokinetic		
3	16.7	9.36	43.41	365	0.384
3	15.88	10.95	46.66	365	0.34
3	17.34	7.03	67.19	365	0.26
4	14.33	8.35	38.84	365	0.37
4	15.63	8.33	44.34	365	0.35
4	15.49	11.38	52.5	365	0.30
4	16.14	-	57.225	365	0.28
5	19.09	10.78	41.78	305	0.46
5	19.68	11.17	41.53	305	0.47
5	22.56	11.10	53.70	305	0.42
5	24.74	11.61	64.55	305	0.38
6	26.91	18.08	70.19	305	0.38
6	37.19	17.1	80.6	305	0.46
6	29.70	22.06	80.42	305	0.37
6	31.73	21.06	99.98	305	0.32

using impactors and isokinetic samplers. However, the analysis and discussion in this paper is limited to the results from the impactors and isokinetic samplers. The data are for four experiments. While semi-anthracite was dispersed in experiments 3 and 5, bituminous coal was dispersed in experiments 4 and 6. The average ratio is 0.33 for 305 fpm and 0.41 for 365 fpm indicating that with increase in velocity, the ability of the impactor to capture dust decreases. The sampling stations were located 100 to 200 feet apart and deposition between stations leads to reduction in concentration. Therefore, the concentration varies from instrument to instrument of the same type, e.g., personal samplers, depending on its proximity to the source.

Size Distribution

The size distribution of the dust obtained from impactor data and that obtained from the total dust samplers were compared and are presented in Figures 2 through 5, with one graph for each experiment. The data for the other samples collected during the study are essentially similar to the representative diagrams presented. Additional diagrams for the rest of the samples are presented in Bhaskar (1987).

The size distribution data show that, in general, the slopes of the two size distributions are similar. The d_{50} values for the 15 sets of data are presented in Table 3. The average d_{50} for isokinetically collected dust is 4.13 μm , while the d_{50} for impactor data is 4.98 μm . The ratio of the d_{50} of isokinetic sample to d_{50} of impactor sample is 0.83 which can be considered to be the shape factor between the two techniques of measurement. The value of

0.83 is, however, dependent on the dust type used and the flow velocity and therefore cannot be used as a general value. Three causes can be attributed for this difference:

- (1) The dust collected on the impactor is classified on the basis of aerodynamic sizes, while the data collected through isokinetic sampling and analyzed for size in a Microtrac are based on projected area diameters. Due to the difference in the two size measurement techniques, the median diameter difference in dust obtained by isokinetic sampling and in the impactor may be strictly a shape factor effect.
- (2) The agglomeration of particles in the air can lead to an increase in effective sizes of the particles. Therefore, smaller particles tend to grow to larger sizes. If the particles do not deagglomerate at high velocities encountered in the impactor between the stages, then they will be deposited in the upper stages leading to an apparent increase in the median size.
- (3) The deviation from isokineticity at the entrance to the impactor has to be considered. Since the particle laden air has to turn a 90° bend at least once to enter the impactor, the large particles may not be completely captured by the impactor. This will lead to a distortion in the data. One can expect a lowering of the median size due to this error.

The average median diameter (d_{50}) values for each experiment are also presented in the table. It is expected that for a given dust, an increase in flow velocity will result in larger

THE RESPIRABLE DUST CENTER

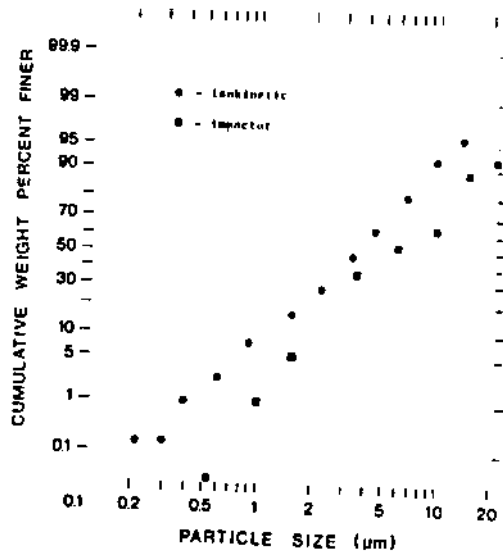


Figure 2. Size Distributions of Impactor and Isokinetic Sampling Data (Experiment 3).

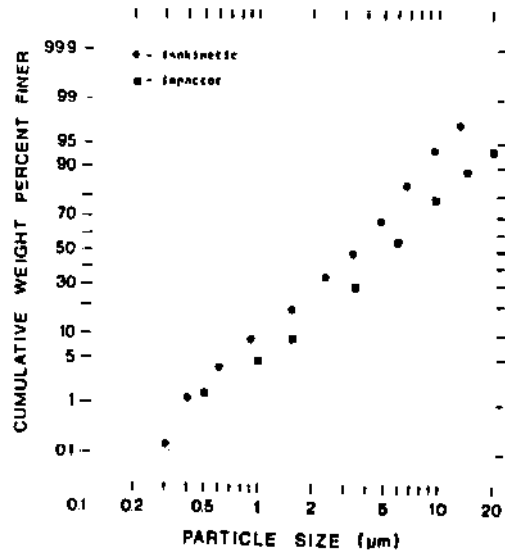


Figure 4. Size Distributions of Impactor and Isokinetic Sampling Data (Experiment 5).

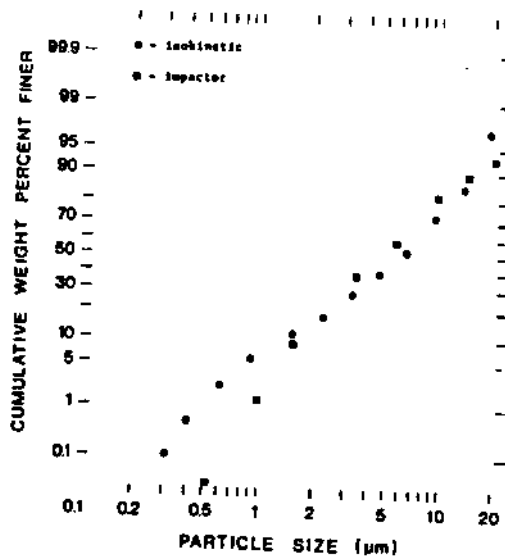


Figure 3. Size Distributions of Impactor and Isokinetic Sampling Data (Experiment 4).

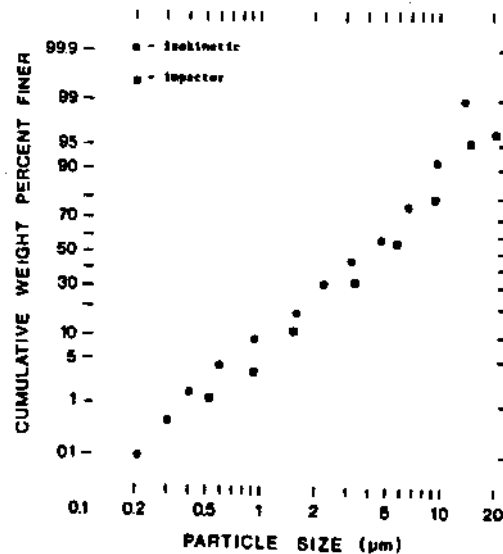


Figure 5. Size Distributions of Impactor and Isokinetic Sampling Data (Experiment 6).

IMPACTORS AND GRAVIMETRIC SAMPLERS

Table 3. Values of d_{50} for dust collected using isokinetic samples and impactors.

Experiment	Isokinetic	Impactor
3	3.2	4.9
3	2.3	4.9
3	3.8	5.2
Average	3.1	5.0
4	6.3	4.1
4	5.0	4.2
4	5.1	4.1
4	4.5	4.5
Average	5.23	4.22
5	3.2	5.8
5	3.7	5.7
5	3.6	4.5
5	4.0	6.1
Average	3.63	5.55
6	4.2	4.9
6	4.8	5.8
6	3.8	5.1
6	4.8	4.8
Average	4.4	5.15
Overall Average	4.13	4.98

dust particles being carried longer distances. In other words, in general, the d_{50} value of the dust cloud at a point will tend to be higher as the flow velocity increases. This phenomenon is not noticed in the impactor data where for experiments 3 (velocity = 365 fpm) and 5 (velocity = 305 fpm), the decrease in velocity should have resulted in a decrease in d_{50} . The opposite effect appears to be the case when comparing experiments 3 with 5 and experiments 4 with 6. One possibility is that with increase in flow velocity, more particles do not get deflected into the impactor, especially the larger particles. This will result in a lowering of the d_{50} value. Examination of the isokinetic data show that d_{50} decreases with flow velocity for experiment 4 and 6, while for experiments 3 and 5, the effect is reversed primarily due to the extremely low d_{50} (2.3 μm) for the second isokinetic d_{50} value in experiment 3.

DISCUSSION

The comparative analysis of the collection characteristics of the impactor with an isokinetic sampler has been presented in this study. The size distribution obtained using the impactor data and the MICROTRAC Small Particle Analyzer show differences in the apparent d_{50} values, resulting in the need for a shape factor to relate the two d_{50} values. On the basis of this study, which is limited in the range of velocities employed, it appears that the impactor should be used in conjunction with an isokinetic nozzle to sample airflows at higher velocities encountered in mines. Studies by Lee

(1986) show that the effect is not pronounced at low velocities (100 fpm). However, it appears that the higher the velocity, the greater the discrepancy between the impactor and isokinetic samples.

The shape factor relating the size distribution obtained using the two instruments appears to vary with flow velocities (primarily due to inlet sampling errors) and particle density.

The role of flow velocity in the sampling efficiency of impactors in flowing air can be easily reduced by using isokinetic sampling nozzles. The role of density in determining aerodynamic size distribution can be accounted for by experimentally determining the shape factor for the particular density and type of dust used. The reduction or control over the influence of these factors will enable better and more accurate interpretation of the valuable data obtained using impactors.

The study is limited and only indicative of the problems that may arise in the collection and interpretation of impactor data in mine airways. There is a need for more evaluative studies on the use of impactors in flowing air. The impactor contributes a wealth of data, especially when studying size preferential properties of dust in the characterization of various coal seams and the dust generated during mining in these seams and, therefore, deserves attention.

REFERENCES

- Agarwal, J. K. and B. Y. H. Liu, 1980, "A Criterion for Accurate Aerosol Sampling in Calm Air," *Am. Ind. Hyg. Assoc. J.*, Vol. 41, pp. 191-197.
- Agarwal, J. K., 1975, "Aerosol Sampling and Transport," Ph.D. Thesis, University of Minnesota, Particle Technology Laboratory, Publ. No. 265.
- Bhaskar, R., 1987, "Spatial and Temporal Behavior of Dust in Mines--Theoretical and Temporal Studies," unpublished Ph.D. Thesis, The Pennsylvania State University (forthcoming).
- Bhaskar, R., R. V. Ramani and R. A. Jankowski, 1986, "Experimental Studies on Dust Dispersion in Mine Airways," SME Preprint No. 86-140, under review by Society of Mining Engineers for the Transactions.
- Courtney, W. G., L. Cheng, and E. F. Divers, 1986, "Deposition of Respirable Coal Dust in an Airway," *Proc. Intl. Symp. on Respirable Dust in the Mineral Industries*, Univ. Park, PA. Proceedings in print by ACGIH.
- Dumm, T. F., 1986, "An Evaluation of Techniques for Characterizing Respirable Coal Dust," M.S. Thesis, The Pennsylvania State University.

THE RESPIRABLE DUST CENTER

Dzubay, T. G., L. E. Hines and R. K. Stevens, 1976, "Particle Bounce Errors in Cascade Impactors," Atmos. Environ., Vol. 10, pp. 229-234.

Esmen, N. A., and T. C. Lee, 1980, "Distortion of Cascade Impactor Measured Size Distributions Due to Bounce and Blow-off," Amer. Ind. Hyg. Assoc. J., Vol. 41, No. 6, pp. 410-419.

Marple, V. A. and K. Willeke, 1976, "Impactor Design," Atmos. Environ., Vol. 10, pp. 891-896.

May, K. R., 1945, "The Cascade Impactor: An Instrument for Sampling Coarse Aerosols," Jl. Sci. Instrum., Vol. 22, pp. 187-195.

National Academy of Sciences, 1980, "Report of the Committee on Measurement and Control of Respirable Dust," Report NMAB-363, National Academy of Sciences, Washington, DC.

Rao, A. K. and K. T. Whitby, 1978, "Non-ideal Collection Characteristics of Inertial Impactors - II. Cascade Impactors," Jl. Aerosol Sci., Vol. 9, pp. 87-100.

Rao, A. K., 1975, "An Experimental Study of Inertial Impactors," Ph.D. Thesis, Univ. of Minnesota.

Rubow, K. L., V. A. Marple, J. Olin and M. A. McCawley, 1985, "A Personal Cascade Impactor: Design, Evaluation and Calibration," Particle Technology Lab Publ. No. 469, Mech. Engr. Dept., Univ. of Minnesota.

ACKNOWLEDGEMENTS

This research has been supported by the Department of the Interior's Mineral Institute program administered by the Bureau of Mines through the Generic Mineral Technology Center for Respirable Dust under grant number G1135142.

III
CHARACTERIZATION
OF DUST PARTICLES

Abstr
on re
evalu
labor
measu
pared
sizin
filte
The l
sedir
autor
agree
good,
attri
used.
obtai
labor

sampl
Agair
alth
some
degre
lead
distr

cont:
"resj
fine;
deter
of ti
eval
syste
dust
meast
thes
coll
coll
exam
data
have
the
do
buti
dust
purp
to e

Particle Size Distribution of Airborne Dust in Coal Mines

T.F. Dumm and R. Hogg

Department of Mineral Engineering, Mineral Processing
Section, The Pennsylvania State University

Abstract. Procedures for particle size analysis on respirable dust from coal mines have been evaluated. Using respirable dusts dispersed in a laboratory dust chamber, size distributions measured using cascade impactors have been compared with the results of a variety of laboratory sizing methods performed on samples collected on filters placed side-by-side with the impactors. The laboratory techniques included centrifugal sedimentation, laser diffraction/scattering and automatic particle counting. The general agreement among the various methods was very good, with systematic differences which can be attributed to the different definitions of size used. Simple conversion factors have been obtained which can be used to transform the laboratory data to equivalent aerodynamic sizes.

Similar comparisons have been made on samples collected in underground coal mines. Again, the results are in quite good agreement although small discrepancies were observed in some cases. These have been attributed to some degree of agglomeration in the airborne dust, leading to slightly coarser apparent distributions in the impactor samples.

INTRODUCTION

A primary goal of mine ventilation is the control of airborne dust, especially in the "respirable" size range, typically defined as finer than about 5 to 10 μm . It follows that determination of the amount and characteristics of the respirable dust is an important factor in evaluating the performance of ventilation systems. Particle size information on airborne dust in mines is commonly obtained by *in-situ* measurements using cascade impactors. However, these tend to be inconvenient for routine data collection and the alternative approach of collecting samples in the mine, on filters for example, and returning them to the laboratory for detailed analysis is very attractive. Questions have often been raised, on the other hand, as to the appropriateness of this approach. How well do such laboratory methods describe the distribution of aerodynamic diameter of the airborne dust particles in the mine environment? The purpose of the work described in this paper was to evaluate some laboratory sizing methods and to

compare the results of such measurements with the size data obtained by the direct, *in-situ* method.

PARTICLE SIZE ANALYSIS ON RESPIRABLE DUST

A variety of instrumentation is available for determining the size distribution of respirable dust particles. Typically these are based on one or another of a few general principles such as sedimentation, light scattering, inertial impaction, etc. The measured size of a particle will depend on the principle and specific technique used to determine it. If all particles were perfect spheres, or some other uniform shape, it would be possible to correlate the sizes measured by all techniques through simple geometric laws. However, since dust particles do not have uniform shapes, and because particle sizing devices may have detection or measurement limitations, conversion factors are generally needed to correlate sizes measured by different techniques.

In practice, all sizing techniques have a limited range of applicability. For respirable dust particles, the lower size limit is often a critical factor. This lower limit may represent a measurement limit below which useful information cannot be obtained, or, more seriously, a detection limit below which particles are not even observed. Methods subject to detection limits provide size data which are based on the implicit assumption that the entire sample is coarser than the limit. This can lead to highly significant errors, especially since there is generally no simple procedure for testing this assumption. The results of such measurements should be regarded as questionable whenever there are significant quantities of material close to the lower limit.

Sedimentation methods are very reliable and widely used for size analysis on fine powders. Their range of applicability for coal particles (with density $\rho=1.5\text{g/cm}^3$) is from about 90 μm to 1 μm using gravity settling. This range can be extended to about 0.05 μm using centrifuges. For the most part, these are measurement limits only, i.e. the amount of material finer than the limit is determined, but no further information on the size distribution of this undersize material is given. The principal defects of the

THE RESPIRABLE DUST CENTER

sedimentation methods are that the procedures tend to be time consuming and relatively large samples are needed.

Electrical sensing methods, such as the Coulter Counter, are based on measurement of the electrical resistance of a small aperture containing an electrolyte solution. This resistance depends on the amount of electrolyte present in the orifice. Displacement of the electrolyte by a particle results in a resistance change which is proportional to particle volume. The electrical sensing methods suffer from a detection limit at about 0.5 to 1 μm . Finer particles are completely excluded from the measured distribution.

Light scattering methods have become increasingly popular for fine particle sizing in recent years - largely due to the availability of laser optics and the powerful microprocessors needed for data analysis. The Leeds and Northrup Microtrac Small Particle Analyzer (SPA) uses a combination of Fraunhofer diffraction and right angle scattering to determine particle size in the 0.1 to 40 μm range. Again, the lower limit is one of detection, and finer particles are not included in the reported distribution.

Microscopy is especially attractive for fine particle characterization, since particles are observed directly and information on shape, morphology and composition can be obtained in addition to size data. Microscopic examination is invaluable for qualitative evaluation of particle systems, but there are serious defects in its use for the quantitative determination of size distributions. Sampling problems and the need to count extremely large numbers of particles generally more than compensate for the potential advantages of this approach. In practice, microscope sizing methods are invariably associated with lower detection limits.

Cascade impactors are commonly used for measuring the particle size distribution of airborne dust. These are size-selective, multi-stage, sampling devices through which a stream of dust-laden air is drawn at a fixed rate. The air and dust pass through a series of progressively smaller nozzles, each situated directly above an impaction plate. At any given stage, particles with sufficient inertia (determined by the velocity of flow through the nozzle) strike the plate and are removed from the airstream. Finer particles remain entrained in the air and pass on to the next (higher velocity) stage. The final stage consists of a fine filter which collects all undersize particles. Cascade impactors can provide very reliable size data and are subject to measurement limits only. Because of their sensitivity to disturbance during use and their susceptibility to overloading, however, they are rather inconvenient for routine data collection in mines.

EXPERIMENTAL

Materials

The materials used in this investigation were standard respirable dusts prepared from Pennsylvania coals: a medium volatile bituminous

coal, from the Lower Kittanning seam, (designated 1192M) and an anthracite coal, from the Primrose seam, (designated 867). Details of the preparation and characterization of these dust samples have been given elsewhere (Dumm and Hogg, 1986a).

Procedures

Laboratory Sizing. Since each of the laboratory sizing methods involved the use of particles in liquid suspension, dispersion of the dust in a suitable liquid medium was a critical factor.

DISPERSION PROCEDURE: The dust particles were dispersed in an aqueous solution containing 0.2% by weight of a wetting agent (aerosol OT) and 0.1% by weight of a dispersant (sodium metaphosphate) and adjusted to pH 8 using sodium hydroxide. Deagglomeration was accomplished by placing the suspension in an ultrasonic bath for two minutes, with stirring. Particle dispersion was verified by visual examination of a drop of the suspension under an optical microscope.

LADAL PIPET CENTRIFUGE: Sedimentation size analysis was performed using a LADAL, pipet-withdrawl centrifuge system. Details of the procedures used have been given elsewhere (Dumm and Hogg, 1986b).

MICROTRAC SPA: The procedure for particle size analysis using this instrument has been described in a previous publication (Dumm and Hogg, 1986c).

COULTER COUNTER: Analyses were performed using a Coulter Counter Model TA following the Count Mode operating procedure recommended by the manufacturer. Dispersed particles were diluted into Isoton II electrolyte solution and passed through a 140 μm aperture. A total of about 400,000 counts were taken and data were collected in all 16 channels. The instrument was calibrated with 10.02 μm diameter latex spheres and set so that this size corresponded to the boundary between channels 8 and 9.

SCANNING ELECTRON MICROSCOPY: Analyses were carried out on a Japanese Electron Optical Ltd. (JEOL) Model 50A scanning electron microscope interfaced to a Digital Equipment Corporation (DEC) PDP-11/20 minicomputer. The computer program used for the automated particle characterization was the Computer Evaluation of Scanning Electron Microscope Images (CESEMI) program (Hoover, et al., 1975). Samples were prepared by passing a sufficient quantity of a dilute suspension of the dispersed dust through a 0.1 μm pore size, 25 mm diameter polycarbonate Nuclepore filter to produce a uniform distribution of the particles on the flat surface of the filter. Size analysis was performed at a magnification of 500X.

Airborne Dust. Comparisons of the laboratory and *in-situ* size analyses were obtained by sampling standard dust dispersed in a laboratory dust chamber and on samples collected in underground mines.

PARTICLE SIZE DISTRIBUTION

DUST CHAMBER: Airborne dust was prepared in the laboratory by loading about 1-2 g of dust into a TSI Model 3400 Fluidized Bed Aerosol Generator, passing it through a TSI Model 3012 Aerosol Neutralizer and then directing it into an Elpram Systems Inc., Aerosol Test Chamber. Cascade impactor analyses of the dust were performed using an Andersen 1 cfm cascade impactor and an Anderson (formerly Sierra) Model 298 personal cascade impactor. Assembly and operation of the impactors was according to the manufacturer's recommended procedure. Bulk samples were also taken from the chamber using a Nuclepore Open-Face filter system, operating side-by-side with the impactors, at an air-flow rate of 2 l/min.

MINE SAMPLES: Dust samples were collected from the return airways in three underground mines designated as mines A, B, and C, using modified personal samplers, Nuclepore Open-Face filters and Andersen Model 298 cascade impactors. The sampling procedures etc., have been described elsewhere (Dumm and Hogg, 1986c; Lee, 1986).

RESULTS AND DISCUSSION

Particle Size in Liquid Suspension

The measured particle size distributions for standard respirable dust 1192 M dispersed in water are compared in Figure 1. As pointed out previously, most of these techniques are subject to lower detection limits which can lead to significant errors in the measured distribution,

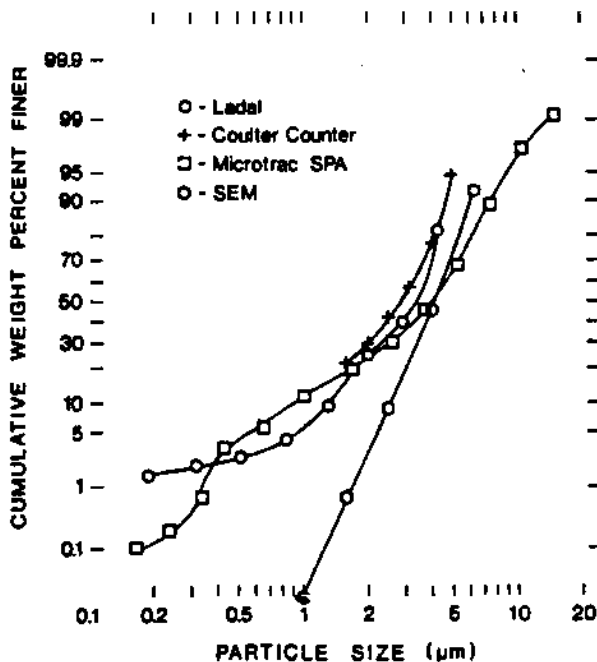


FIGURE 1. Particle size distributions for standard dust 1192M obtained using various techniques.

particularly at fine sizes, close to the limit. This problem is especially severe for the Coulter Counter for which the detection limit in this case was about 1.6 μm . Centrifugal sedimentation, which has no detection limit, indicated that over 20% by weight of the dust was finer than this size. For comparison purposes, therefore, we have corrected the Coulter distribution by adding the undersize material (estimated from the LADAL data) and renormalizing the distribution using

$$F(x) = u + (1-u)F'(x) \quad (1)$$

where $F(x)$ is the corrected cumulative size distribution, $F'(x)$ is the apparent distribution, read directly from the instrument, and u is the estimated undersize ($< 1.6 \mu\text{m}$) fraction. The corrected form is given in Figure 1. A similar correction could have been applied to the Microtrac SPA data, but was considered to be unnecessary due to the very small amount of undersize ($< 0.12 \mu\text{m}$ for the SPA) estimated. The application of such a correction to the SEM data was not attempted because the detection limit for this system is not clearly defined.

The results shown in Figure 1 indicated that the measured size distributions have similar shape but are shifted to smaller or larger sizes depending on which sizing method was used. These differences have been attributed to the different definitions of "size" employed. In a separate series of experiments, using very narrow size fractions of coal, we have investigated these variations and determined size conversion factors using sedimentation size (Stokes diameter) as the standard (Dumm, 1986). The results are given in Table 1.

Table 1

Size Conversion Factors, Based on Stokes Diameter, Obtained From Experiments on Narrow Size Fractions

Method	Size Definition (x_{method})	Conversion Factor $\gamma = x_{\text{method}} / x_{\text{Stokes}}$
Sedimentation	Stokes diameter	1.0
Coulter Counter	Volume diameter	0.97 ± 0.05
Microtrac SPA	Random projected area diameter	1.29 ± 0.11
SEM	Stable projected area diameter	1.50 ± 0.12

Application of the conversion factors from Table 1 to the measured size distributions for respirable dusts 1192M and 867 leads to the normalized distributions (corrected to Stokes diameter) shown in Figures 2 and 3. It is clear that the general agreement between sedimentation, electrical sensing (when corrected for undersize) and light scattering is very good. The slight deviations in the tails of the distribution, which are somewhat exaggerated by the scales used in plotting, probably reflect the detection limit

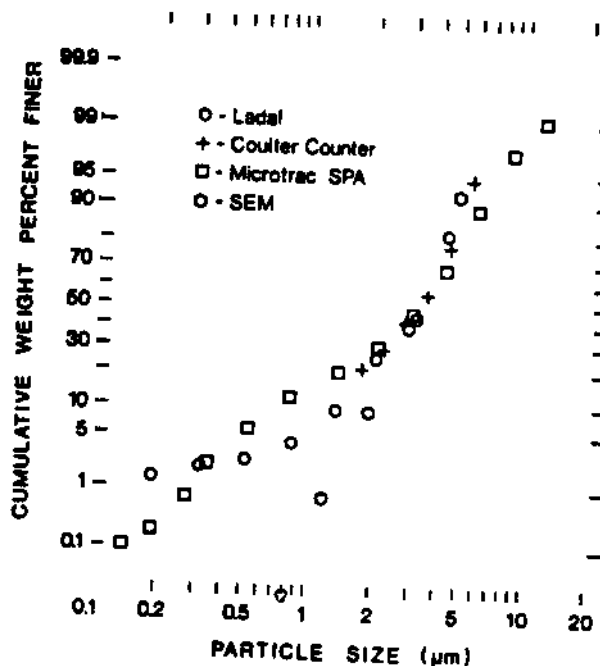


FIGURE 2. Distribution of Stokes diameter for standard dust 1192M obtained by applying conversion factors to the results obtained by different techniques.

of the Microtrac SPA. The SEM data show very significant departures from the other techniques. This is probably the result of poor counting statistics due to failure to resolve large numbers of submicron particles and leading to an effective detection limit in the 0.5 to 1 µm range.

Airborne Dust

Dispersion of fine particles in air is considerably less amenable to precise control than is dispersion in liquids. In particular, there is no guarantee that dispersion is not accompanied by some degree of classification, e.g. preferential loss of coarse particles from the air-stream. A comparison of Microtrac SPA analyses of standard dust 1192M from a bulk sample and from a filter sample collected after dispersion in the Elpram Aerosol Test Chamber is shown in Figure 4. The excellent agreement indicates complete dispersion of the dust in the chamber with minimal loss of coarse material in the aerosol generator.

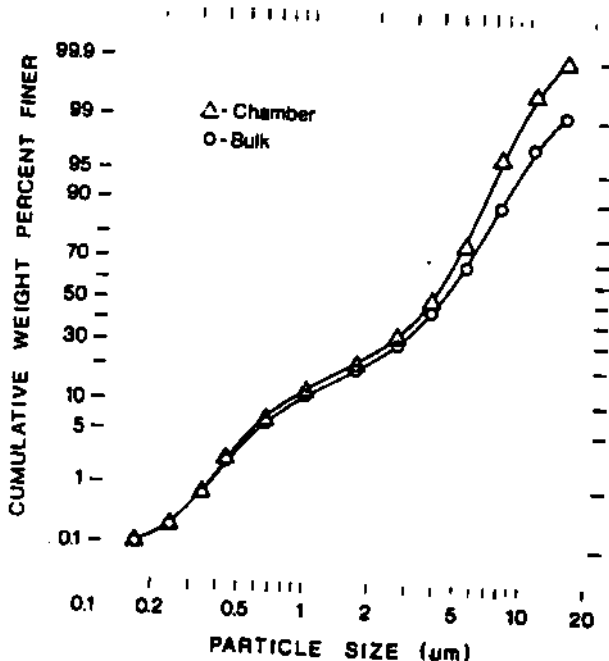


FIGURE 4. Comparison of Microtrac SPA size distributions for standard dust 1192M as prepared and following dispersion in a laboratory dust chamber and collection on an open-face filter.

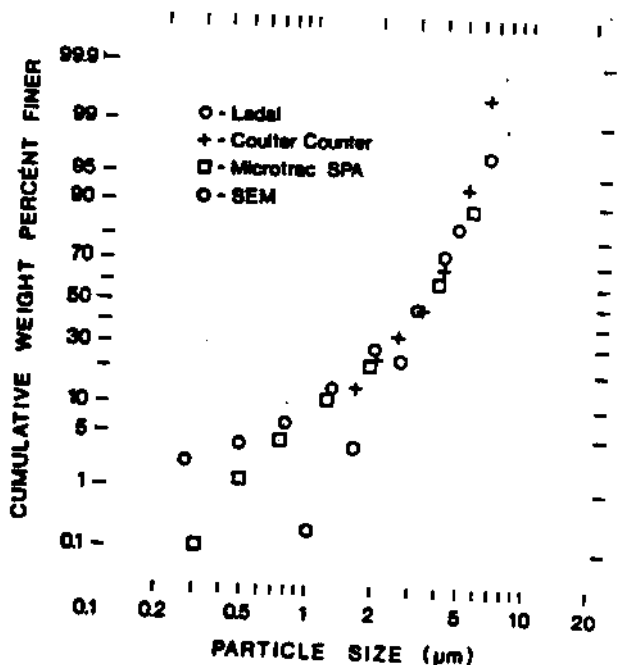


FIGURE 3. Distribution of Stokes diameter for standard dust 867 obtained by applying conversion factors to the results obtained by different techniques.

Cascade impactor analyses of standard dust 1192M are shown in Figure 5. The results show good reproducibility even when different instruments are used. Comparison of these distributions with the data shown previously in Figures 1, 2 and 4, again shows a definite similarity in the shapes of the distributions with a lateral shift due to the definition of "size."

Direct comparison of the impactor data with sedimentation leads to a conversion factor of 1.21 ± 0.02 for the two dust samples. Since aerodynamic diameter is defined using an arbitrary density of unity, the conversion factor for aerodynamic to Stokes diameter can be expected, on theoretical grounds, to be equal to the square root of the solid density. The value of 1.21 obtained here would correspond then to a density of about 1.46 g/cm³ which is quite reasonable for coal.

PARTICLE SIZE DISTRIBUTION

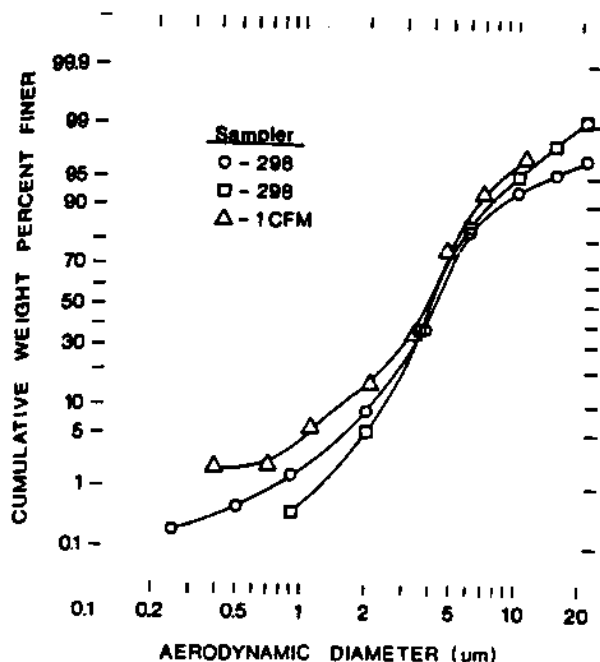


FIGURE 5. Aerodynamic size distribution of standard dust 1192M dispersed in a dust chamber and sampled using Andersen Model 298 and 1CFM cascade impactors.

If aerodynamic diameter is used as the standard for respirable dust, the conversion factor for size data obtained by sedimentation would be $1/1.21=0.83\pm 0.01$. Similarly, comparison of the impactor data with the Coulter Counter, Microtrac SPA and SEM results in factors of 0.79 ± 0.06 , 1.10 ± 0.09 and 1.19 ± 0.17 , respectively for converting data from these instruments to an equivalent aerodynamic size.

Samples of airborne dust from underground coal mines were collected by three different techniques: a modified personal sampler (MSA Gravimetric Dust Sampling Kit), Nuclapore Open-Face Filters, and Andersen Model 298 cascade impactors. The personal sampler separates the dust, using a cyclone, into a coarse and a "respirable" fraction. Size analyses were performed on both fractions using the Microtrac SPA. The overall size distribution can be obtained by combining the data for comparison with the filter samples and cascade impactors.

A comparison of the personal sampler with the open-face filter is shown in Table 2, which gives Microtrac SPA size distributions for two personal samples and two filters located in close proximity in a return airway in Mine C. The close agreement among the four distributions indicates that the procedures are reproducible and not subject to significant bias. The overall size distributions and those of the respirable fractions are shown in Figure 6.

For direct comparison with cascade impactor results, it is necessary to convert the Microtrac SPA sizes into equivalent aerodynamic diameters using the conversion factor of 1.10 obtained previously. The results of such comparisons are shown in Figures 7, 8, and 9 for three different

Table 2

Comparison of Overall Dust Size Distributions for Samples Collected from Mine C Using Modified Personal Samplers and Open-Face Filters

Particle Size, μm	Cumulative Weight Percent Finer			
	Filter Samples		Personal Sampler	
	1	2	1	2
42.21	100.0	100.0	100.0	100.0
29.85	96.0	90.4	91.2	88.6
21.10	87.8	78.7	79.4	76.6
14.92	71.6	62.6	61.5	59.1
10.55	55.6	46.5	46.0	45.3
7.46	41.3	34.3	35.4	35.0
5.27	27.6	22.6	24.2	24.2
3.73	18.9	14.7	15.5	16.4
2.63	11.4	8.8	10.2	10.6
1.69	6.8	5.1	5.5	6.1
1.01	3.8	2.5	3.0	3.1
0.66	1.3	0.8	1.1	1.1
0.43	0.1	0.3	0.1	0.3
0.34	0.0	0.1	0.4	0.1
0.24	0.0	0.0	0.0	0.02
0.17	0.0	0.0	0.0	0.0

mines. In general, the overall distributions, as determined by the two different techniques, agree quite well although the impactor distributions tend to be slightly coarser, especially for the samples from mines B and C. These discrepancies have been attributed to the presence of agglomerates in the airborne dust (Dumm and Hogg, 1986c; Dumm, 1986). Such agglomerates

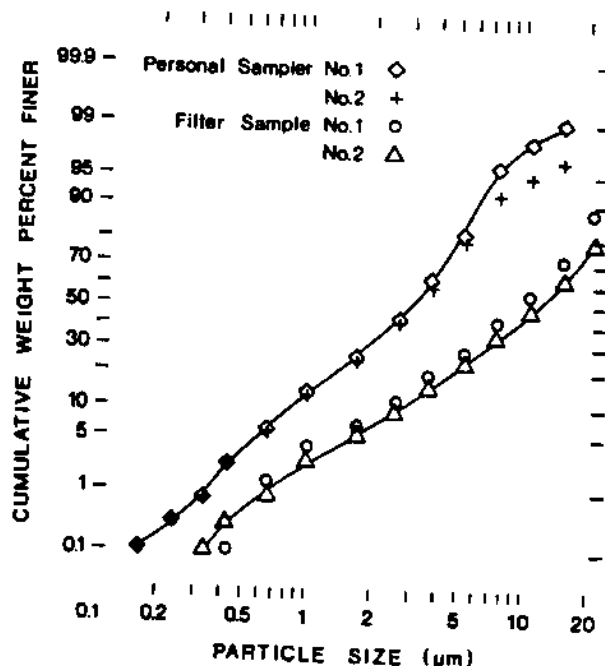


FIGURE 6. Microtrac SPA size distributions of coal dust collected at Mine C using personal samplers (respirable fraction) and open-face filters (total dust).

THE RESPIRABLE DUST CENTER

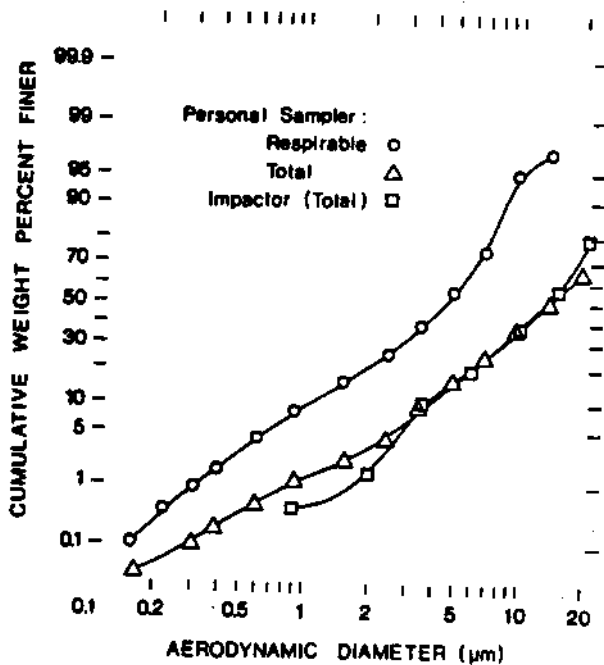


FIGURE 7. Distributions of aerodynamic diameter of dust collected in Mine A using a modified personal sampler (respirable fraction and total dust) and an Andersen Model 298 cascade impactor.

would be registered as coarse particles in a cascade impactor but would be broken up by dispersion in liquid.

It is interesting to note that the size distributions of the airborne dust from the three

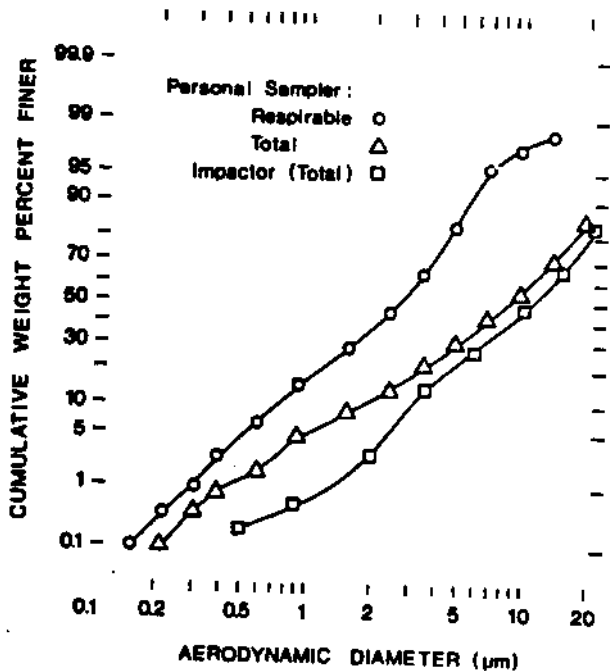


FIGURE 8. Distributions of aerodynamic diameter of dust collected in Mine B using a modified personal sampler (respirable fraction and total dust) and an Andersen Model 298 cascade impactor.

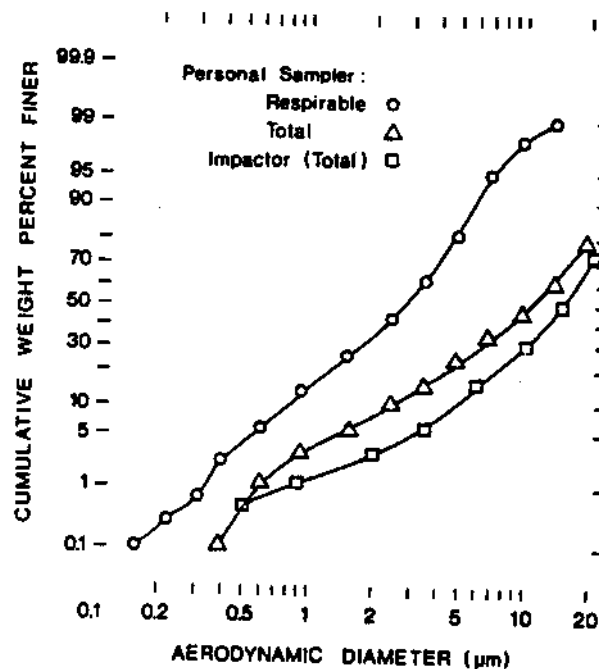


FIGURE 9. Distributions of aerodynamic diameter of dust collected in Mine C using a modified personal sampler (respirable fraction and total dust) and an Andersen Model 298 cascade impactor.

mines were quite similar, probably because of the natural classification effects of gravity settling etc. The respirable fractions were also similar for the mine dusts and for the standard dust 1192M indicating that the latter simulates actual mine dust quite well.

CONCLUSIONS

Based on the results of these investigations, the following general conclusions can be drawn:

1. Different laboratory sizing procedures used to analyze particles dispersed in liquid or in air, give consistent results provided proper allowance is made for the different definitions of size used and for the existence of detection limits for some techniques.
2. The Microtrac SPA is especially appropriate for the analysis of respirable dust. Samples of as little as 0.1 mg of dust can be analyzed quite accurately, the analysis is simple and rapid, and the lower detection limit at about 0.1 μm does not lead to significant errors. Centrifugal sedimentation would also be highly appropriate, perhaps even more so than the Microtrac since there are no detection limits involved. However, the large sample size required (~1g) render this technique impractical for routine analyses. Because of the fairly coarse detection limit (~0.8 μm) the Coulter Counter is not recommended for the analysis of respirable dust. Our results indicate that about 10% of the

PARTICLE SIZE DISTRIBUTION

respirable component of mine dust is finer than this size. Scanning electron microscopy (SEM) is not generally suitable for particle size analysis on respirable dust, due to the problems associated with poor resolution of submicron particles and the need to count extremely large numbers of particles to obtain reasonable estimates of the numbers of large particles present.

3. Microtrac SPA analyses of dust collected using modified personal samplers or simple filters offers a useful and reliable alternative to *in-situ* analysis using impactors. It is important to recognize, however, that the SPA has a lower detection limit at about 0.1 μm . For samples which are found to contain significant quantities in the 0.1 to 0.2 μm range, further investigation using, for example, cascade impactors would be recommended.

ACKNOWLEDGEMENTS

The work described in this paper was supported by the Mineral Institutes program by Grant No. G1135142 from the Bureau of Mines, U.S. Department of Interior, as part of the Generic Mineral Technology Center for Respirable Dust.

REFERENCES

- Dunn, T.F., 1986, "An Evaluation of Techniques for Characterizing Respirable Coal Dust", M.S. Thesis, The Pennsylvania State University, University Park, Pa.
- Dunn, T.F. and Hogg, R., 1986a, "Standard Respirable Dusts", Proceedings International Symposium on Respirable Dust in the Mineral Industries, The Pennsylvania State University.
- Dunn, T.F. and Hogg, R., 1986b, "Estimation of Particle Size Distributions Using Pipet-Withdrawal Centrifuges", Particle Characterization, Vol. 3, pp. 122-128.
- Dunn, T.F. and Hogg, R., 1986c, "A Procedure for Extensive Characterization of Coal Mine Dust Collected Using a Modified Personal Sampler", Proceedings International Symposium on Respirable Dust in the Mineral Industries, The Pennsylvania State University.
- Hoover, M.R., White, E.W., Lebedzik, J. and Johnson, G.G., Jr, 1975, "Automated Characterization of Particulates and Inclusions by Computer-Controlled SEM/Probe", Proceedings of the Microbeam Analysis Society, Tenth Annual Conference, August 11-15.
- Lee, C., 1986, "Statistical Analysis of the Size and Elemental Composition of Airborne Coal Mine Dust", Ph.D. Thesis, The Pennsylvania State University, University Park, Pa.

Distribution of Sulfur and Ash in Ultrafine Coal

T.F. Dumm and R. Hogg

Department of Mineral Engineering, Mineral Processing Section,
The Pennsylvania State University

ABSTRACT

A procedure for evaluating the size/specific gravity distribution of ultrafine coal and the distributions of sulfur and ash with respect to particle size and specific gravity is described. The procedure is essentially an extension of the conventional coal washability technique in which special precautions are taken to ensure particle dispersion in the heavy organic liquids, centrifuges are used to obtain adequate separation rates, and micromesh sieves are used for size separation at fine sizes. An example of the application of this technique to the evaluation of the extent of liberation of sulfur and ash in a coal sample ground to 90% passing 200 mesh (74 μ m) is described.

INTRODUCTION

In order to determine the potential for deep cleaning of coal by fine grinding to liberate sulfur and ash-forming minerals, it is necessary to obtain data on the distributions of these species by size and specific gravity. In conventional coal processing operations, this information is obtained by means of a standard "washability" analysis. Attempts to extend this procedure to ultrafine coal, however, have generally been unsatisfactory and have often led to unreliable and inconsistent results [1]. The present authors have described a modified washability procedure in which cumulative specific gravity fractionation is combined with sub-sieve size analysis (by laser diffraction/light scattering) to determine the particle size/specific gravity distribution of ultrafine coal [2]. Unfortunately, because this technique does not involve separation of the individual fractions, only limited information can be obtained on the specific distributions of sulfur and ash.

The objective of the work described in this paper was to develop and evaluate a procedure for size and specific gravity fractionation of ultrafine coal and to use conventional analyses for sulfur and ash to determine their relative distribution in the coal. The procedure is essentially a simple extension of the standard washability analysis [3] but incorporating special precautions for treating ultrafine particles.

EXPERIMENTAL

Material

The material used in the development and evaluation of the ultrafine coal fractionation procedure was a medium volatile bituminous coal from the Lower Kittanning seam. A sample of the coal (nominally - $\frac{1}{4}$ inch), obtained from the Penn State Coal Data Base, was ground to 90% passing 200 mesh by the following two-stage grinding procedure: About 2 kg of the as-received coal were ground to about 30% passing 200 mesh in a Model 4-E Quakertown mill ("coffee grinder"). About 1 kg of this product was then ground to about 90% passing 200 mesh in a Holmes Model 300 Pulverizer.

Specific Gravity Fractionation

Separation into specific gravity fractions was accomplished by centrifugation in heavy organic liquids obtained from American Chemical Inc., Coranpolis, PA. Approximately 3 g samples of the coal were

DISTRIBUTION OF ULTRAFINE COAL

dispersed in 500 ml Teflon bottles containing 300 ml of the appropriate liquid to which 2% by weight of the surfactant Aerosol OT (nonaqueous) had been added to ensure adequate dispersion of the particles. The heavy liquid suspensions were subjected to a 1-2 minute ultrasonic treatment for deagglomeration of the fine particles prior to separation. The bottles were centrifuged at 1000 rpm in an International Equipment Co., Model K centrifuge. Separation times were established by visual examination of the suspension, i.e., centrifugation was continued until the central portion of the bottle was essentially clear. Times ranging from about 5 hours up to 20 hours (for the lighter fractions which contain many near-gravity, fine particles) were found to be necessary for complete separation. The float and sink fractions were collected using the pinch-clamp technique described in a previous publication (2). The solid particles were separated from the liquid using 0.2 μ m pore size Nuclepore polyester membrane filters.

Size Separation

After drying and weighing, the individual specific gravity fractions were removed from the filters and dispersed in an aqueous solution of 0.2% by weight Aerosol OT, 0.1% sodium metaphosphate and 0.1% Daxad 11 KLS, in distilled water. Ultrasonic treatment was used to aid in removal of the particles from the filter membrane and for deagglomeration. The resulting suspensions were wet-screened at 200, 270 and 400 mesh using conventional woven-wire screens and using the dispersing solution only to wash the particles. Further classification of the -400 mesh material was accomplished using electroformed micromesh screens, (Buckbee Mears Co., St. Paul, MN) by the following procedure:

The -400 mesh filtrate was allowed to stand for 10 to 15 minutes in a 500 ml beaker. A 43 mm diameter electroformed screen was placed into a Nuclepore filter holder and clamped in place. A slight vacuum was applied to the micromesh sieve using an aspirator. The solution in the beaker was carefully decanted through the sieve and collected in a 500 ml filter flask. The settled particles in the beaker were then redispersed with about 50 ml of dispersing agent, given a few more minutes to stand, and decanted through the sieve. This decanting process was repeated two or three times depending on the quantity of the settled particles and density of the liquid after each decantation. In order to remove as many near-size particles as possible, the settled particles were poured onto the sieve. The Tygon tubing leading from the filter flask to the filter holder was clamped by hand, and a small amount (~ 10 ml) of dispersing solution was added to the particles in the holder. While providing an agitation to the slurry in the filter holder, the clamp on the tubing was gently released providing a small amount of suction for removing the undersize particles while at the same time minimizing the formation of a filter cake on the screen. When all of the fluid had passed through the screen more dispersing liquid was added and the process was continued until the fluid leaving the filter holder was clear. The undersize particles were then placed into suitable beakers and given time to settle for the next decantation through a smaller screen. The oversize particles were rinsed from the micromesh screen and filtered onto a 0.2 μ m Nuclepore filter.

Sulfur and Ash Analyses

The total sulfur content of each size/specific gravity fraction was determined using a Leco sulfur analyzer (Laboratory Equipment Corp., St. Joseph, Mich.).

THE RESPIRABLE DUST CENTER

Ash contents were determined by the standard ASTM procedure [4]. When there was insufficient material in a fraction (less than ~ 0.1 g) to determine the ash content by this procedure, a modified ash analysis was used. In the modified procedure, a small amount (5-50 mg) of the sample to be ashed was dispersed in approximately 20 ml of dispersing solution and deposited onto a 25 mm 0.2 μ m Nuclepore membrane filter of known weight.

The coal and filter were reweighed on a Mettler M3 microbalance to obtain the weight of deposited coal. The filter was then placed into a clean porcelain crucible, which was put into a muffle furnace and ashed according to the ASTM recommendations. When ashing was complete, the crucible was removed and the ash was dispersed in the crucible using dispersing solution and ultrasonic agitation. The contents of the crucible were poured onto a tared Nuclepore membrane filter and reweighed to determine the weight of ash.

RESULTS AND DISCUSSION

Approximately 35 grams of coal was separated into specific gravity fractions of 1.3 float, 1.3x1.6, 1.6x2.0, 2.0x2.5, 2.5x2.95 and 2.95 sink. The specific gravity fractions were then sieved at sizes of 74, 53, 38, 26, 17, 10 and 6 μ m. The resulting size/specific gravity distribution along with the corresponding ash and sulfur for each size/specific gravity fraction are shown in Table I. In some instances, it was not possible to determine the ash or sulfur content because there was an insufficient amount of material in the fraction. In performing the mass balance and plotting some of the data, therefore, reasonable estimates of these undetermined values were made based on values obtained for the other size fractions of that particular specific gravity. From a mass balance of the data, the calculated sulfur content of the coal was 2.05% compared to the actual of 2.45%. The calculated ash content of the coal was 9.60% and the actual ash content was 9.70%.

The size distributions obtained on each specific gravity fraction are shown in Figure 1. As expected, this figure shows that there is an obvious trend in the size distributions with increasing specific gravity. The 1.3 float size distribution is quite coarse and narrow while the 2.5x2.95 fraction has the finest and broadest distribution. The 2.95 sink material, which appeared to be mostly liberated pyrite, did not follow the trend and was coarser and narrower than the 2.5x2.95 fraction.

The weight percents of coal in each size/specific gravity fraction is presented as a block diagram in Figure 2. This figure clearly shows that the 1.3 float and 1.3x1.6 fractions comprise almost 90 percent of the total weight of the coal. The remaining 10 percent is distributed fairly evenly throughout the higher specific gravity fractions. The size distribution within each specific gravity fraction is approximately normally distributed allowing for the fact that the +74 μ m and -6 μ m fractions are the widest intervals.

Figure 3 shows the weight percent sulfur versus mean particle size for each specific gravity. It can be seen from the figure that there is very little change in sulfur content as particle size decreases within the 1.3 float and 1.3x1.6 specific gravity fractions. However, there do appear to be slight decreases in the sulfur contents of the larger size fractions of the higher specific gravity fractions.

The sulfur content in each size/specific gravity fraction, expressed as a percent of the total sulfur in the coal, is presented as a block diagram in Figure 4. With the sulfur distribution expressed this way, it can be seen that the distribution is bimodal and that the largest concentration of sulfur occurs in the very fine, high specific gravity fractions. Despite the fact that the sulfur concentrations in the 1.3x1.6 specific gravity fraction is relatively low (~ 1%), this fraction actually

DISTRIBUTION OF ULTRAFINE COAL

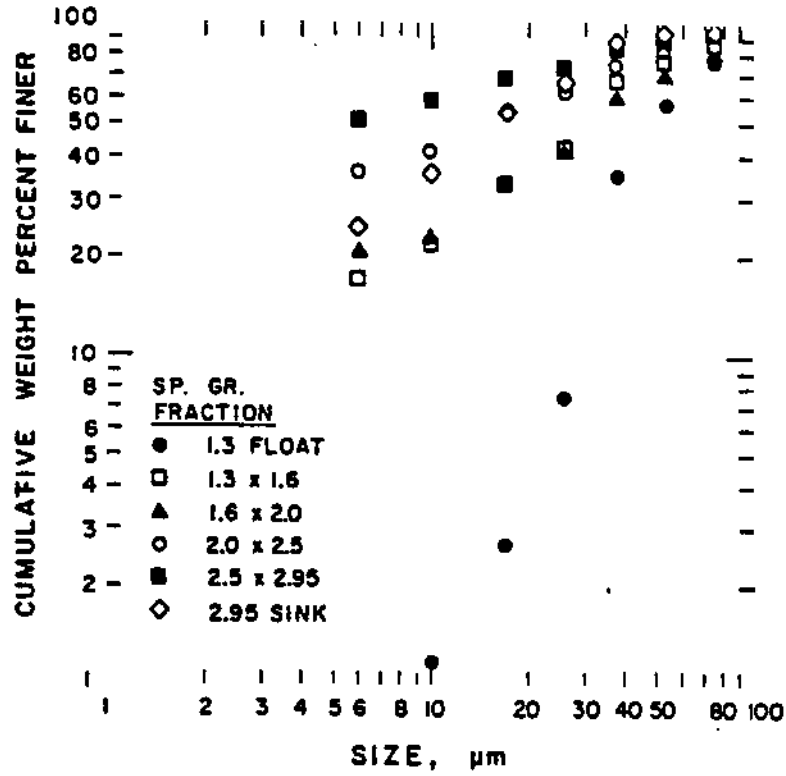


FIG. 1. Particle size distributions of the individual specific gravity fractions.

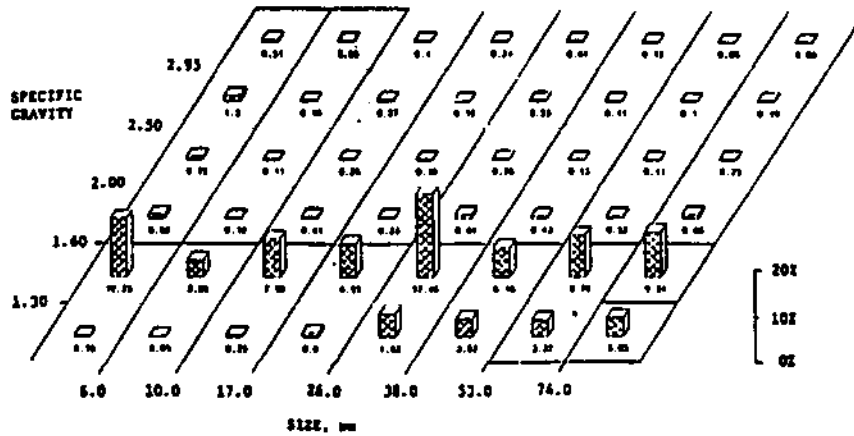


FIG. 2. Size-specific gravity distribution of the ground coal.

THE RESPIRABLE DUST CENTER

TABLE I. Size-specific gravity distribution with corresponding ash and sulfur values of the ground coal.

SPECIFIC GRAVITY	+74 μm			53 x 74 μm			38 x 53 μm		
	<u>Wt. %</u>	<u>ZA</u>	<u>ZS</u>	<u>Wt. %</u>	<u>ZA</u>	<u>ZS</u>	<u>Wt. %</u>	<u>ZA</u>	<u>ZS</u>
1.3 FLOAT	3.85	1.65	0.81	3.32	1.39	0.85	3.62	1.27	0.73
1.3 x 1.6	9.34	9.48	0.97	8.77	8.04	0.96	6.15	6.99	1.04
1.6 x 2.0	0.86	36.5	1.52	0.52	34.5	1.93	0.43	32.7	1.92
2.0 x 2.5	0.25	68.3	1.42	0.11	58.4	-	0.13	60.5	-
2.5 x 2.95	0.19	76.2	-	0.10	72.3	-	0.11	77.5	-
2.95 SINK	<u>0.08</u> <u>14.58</u>	71.1	27.6	<u>0.06</u> <u>12.88</u>	-	31.3	<u>0.12</u> <u>10.56</u>	64.9	40.0

SPECIFIC GRAVITY	26 x 38 μm			17 x 26 μm			10 x 17 μm		
	<u>Wt. %</u>	<u>ZA</u>	<u>ZS</u>	<u>Wt. %</u>	<u>ZA</u>	<u>ZS</u>	<u>Wt. %</u>	<u>ZA</u>	<u>ZS</u>
1.3 FLOAT	4.63	1.22	0.79	0.80	0.92	0.83	0.25	1.51	1.04
1.3 x 1.6	17.46	5.33	0.93	6.95	3.74	0.95	7.96	3.35	0.95
1.6 x 2.0	0.84	31.6	2.09	0.33	28.4	2.00	0.41	29.4	2.03
2.0 x 2.5	0.26	56.9	4.15	0.16	54.0	-	0.26	58.7	3.60
2.5 x 2.95	0.23	71.3	7.54	0.12	69.2	-	0.27	66.9	8.02
2.95 SINK	<u>0.44</u> <u>23.86</u>	67.6	42.3	<u>0.24</u> <u>8.60</u>	66.8	41.6	<u>0.40</u> <u>9.55</u>	67.0	43.1

SPECIFIC GRAVITY	6 x 10 μm			-4 μm			<u>EWt. %</u>	<u>FAZ</u>	<u>ZSZ</u>
	<u>Wt. %</u>	<u>ZA</u>	<u>ZS</u>	<u>Wt. %</u>	<u>ZA</u>	<u>ZS</u>			
1.3 FLOAT	0.05	-	-	0.15	-	-	16.7	0.22	0.14
1.3 x 1.6	3.55	3.11	0.99	12.25	3.03	1.07	72.4	3.96	0.70
1.6 x 2.0	0.12	28.6	2.37	0.88	19.3	2.02	4.4	1.32	0.09
2.0 x 2.5	0.11	59.5	-	0.72	51.5	2.94	2.0	1.14	0.06
2.5 x 2.95	0.18	64.6	8.38	1.20	60.4	8.78	2.4	1.57	0.20
2.95 SINK	<u>0.25</u> <u>4.26</u>	66.3	45.9	<u>0.51</u> <u>15.70</u>	63.9	39.4	<u>2.1</u> <u>100.0</u>	<u>0.86</u> <u>9.60</u>	<u>1.39</u> <u>2.05</u>

DISTRIBUTION OF ULTRAFINE COAL

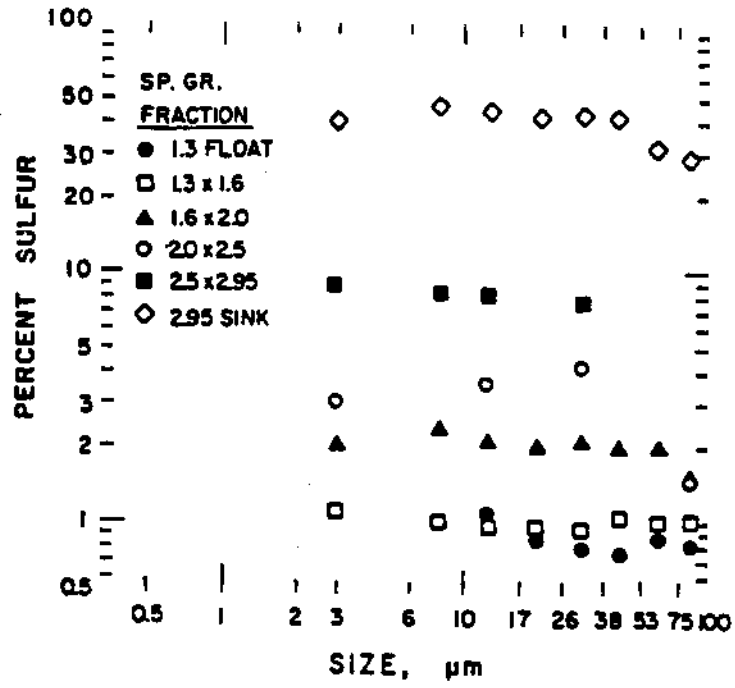


FIG. 3. Variation in sulfur content with particle size for the different specific gravity fractions.

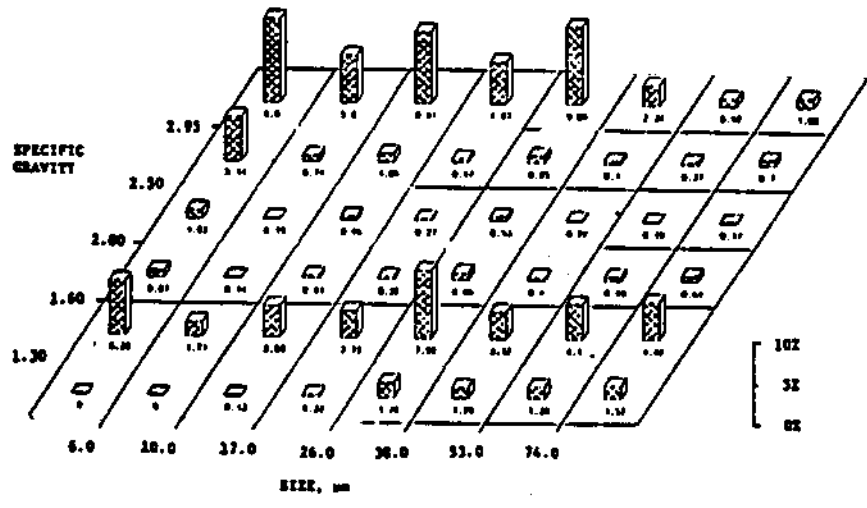


FIG. 4. The distribution of sulfur content (expressed as percent of total sulfur) with respect to size and specific gravity.

THE RESPIRABLE DUST CENTER

contains about one-third of the total sulfur, simply because it is the dominant fraction by weight. In order to gain a better understanding of the sulfur distribution in the coal, further specific gravity fractionation between 1.3 and 1.6 specific gravities would be necessary. Also, it would be of considerable interest to determine the sulfur forms in these lower, but most abundant specific gravity fractions. This information could be used to determine at what size liberation of pyrite is complete and only organic and sulfate sulfur remain.

The ash content is plotted versus mean particle size for each specific gravity in Figure 5, which shows, that there is a significant change in ash content with size for each specific gravity fraction except the 1.3 float. The scatter associated with the ash content values of the higher specific gravity fractions is due to the fact that only small quantities of material were available for analysis. The decrease in ash content in the 1.3x1.6 specific gravity fraction could be explained by liberation of locked ash particles at the finer sizes. It would appear that the inherent ash content of the 1.3x1.6 fraction is about three percent. Again, however, further specific gravity fractionation of the 1.3x1.6 interval would be necessary in order to fully evaluate the ash distribution.

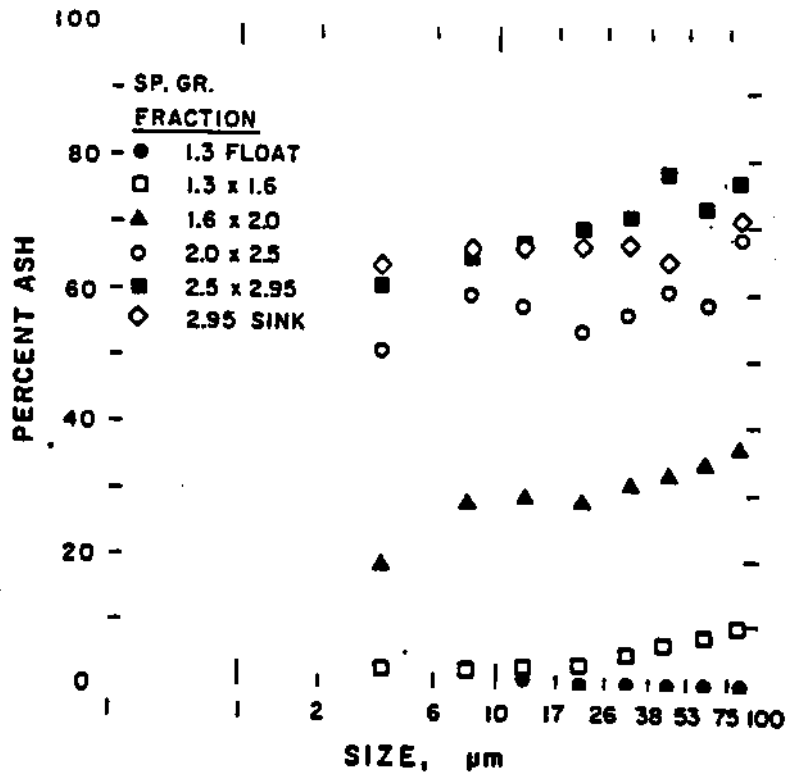


FIG. 5. Variation in ash content with particle size for the different specific gravity fractions.

DISTRIBUTION OF ULTRAFINE COAL

The ash distribution is shown in Figure 6 as a block diagram. This shows that over 40 percent of the total ash in the coal occurs within specific gravity fractions less than 1.6. Also, about 20% of the ash in the coal is associated with particles which are smaller than 6 μ m in size. In particular, the 2.5x2.95, -6 μ m fraction, which appeared to be mostly fine clay, contributes a significant amount of ash. Otherwise, the percent of total ash is fairly evenly distributed in the specific gravity fractions greater than 1.6.

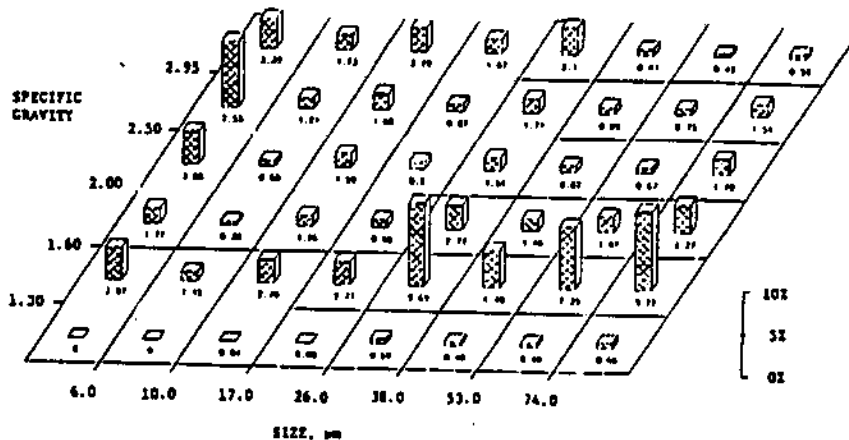


FIG. 6. The distribution of ash content (expressed as percent of total ash) with respect to size and specific gravity.

A more conventional representation of the coal washability is shown in Figure 7. In this figure, the data are compressed to give the product characteristics which would result from any given specific gravity separation. Representation in this form is very useful for estimating the performance of gravity separation processes and for specifying operating conditions. However, the block diagrams given in Figures 2, 4 and 6 provide considerably more information on how separations might be effected and on the potential for further grinding to increase liberation or for the use of staged separation processes.

CONCLUSIONS

A size/specific gravity distribution and the associated sulfur and ash distributions were determined for a medium volatile, Lower Kittanning coal crushed to 90% minus 74 μ m. From the results, it would appear that the conventional washability technique can indeed be extended to include subsieve particles, however, certain precautions must be observed.

The centrifugation time can be considerable (up to 20 hours at 1000 rpm) for the very small, near-gravity particles to separate, particularly in the 1.3 and 1.6 specific gravity fractionations. Care must be taken to ensure that the particles are dispersed in the heavy liquids and that they remain dispersed while separating. Also, the solids content of the particles in suspension should be kept as low as possible (preferably less than ~ 1% by weight) to reduce the chance of agglomeration.

Care must also be taken to keep the particles well dispersed during subsieve size fractionation. Having well dispersed suspensions allows easy passage of undersize particles through a micromesh sieve by decanting the top part of the suspension. Some patience must be exercised in removing the near-size particles because this process will take more time than the removal of the finer sizes.

THE RESPIRABLE DUST CENTER

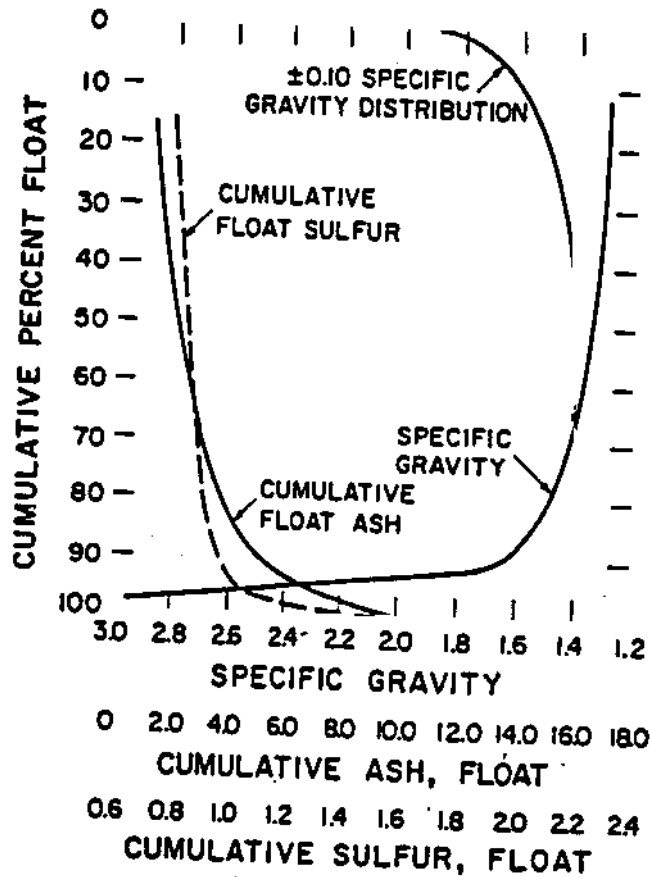


FIG. 7. Washability curves for the ground coal.

Although the washability procedure for ultrafine coals is more time consuming and requires more analytical care, the results yield much information on the distribution of sulfur and ash in the coal. The specific gravity intervals of choice are arbitrary and it appears from this study that for this particular coal, more specific gravity fractionation should be performed between the 1.3 and 1.6 intervals. Finally, although 35 grams of coal were fractionated, there still resulted some size/specific gravity intervals which had very little material in them. In order to improve the accuracy of the subsequent sulfur and ash analyses for this particular coal, more feed coal (100-200 grams) would have to be processed.

ACKNOWLEDGEMENTS

The work described in this paper was supported, in part, under The Mineral Institutes program by Grant No. G1135142 from the Bureau of Mines, U.S. Department of the Interior as part of the Generic Mineral Technology Center for Respirable Dust.

DISTRIBUTION OF ULTRAFINE COAL

REFERENCES

1. H.C. Cho, Liberation of Coal Macerals, M.S. Thesis, The Pennsylvania State University, (1986).
2. T.F. Dumm, R. Hogg, Washability of Ultrafine Coal, Paper Presented at the AIIME Annual Meeting, Denver, CO., Preprint No. 87-136, (1987).
3. Annual Book of ASTM Standards, Designation D4371-84, 5.05, (1985).
4. Annual Book of ASTM Standards, Designation D3174, 5.05, (1985).

Surface Characterization for Coal Processing

R. Hogg and S. Chander

Department of Mineral Engineering, Mineral Processing Section,
The Pennsylvania State University

INTRODUCTION

The behavior of particulate systems in general is determined by the properties of the solid and fluid phases and of the interfaces between them. As particle size is reduced, the interfacial effects become increasingly important until, in colloidal systems, they become completely dominant. Interfacial phenomena are especially important in coal processing for a variety of reasons. Because coal is naturally hydrophobic and its density is low, surface forces begin to dominate over gravity at relatively coarse sizes. Coal is thermodynamically unstable in the presence of air, so that surface oxidation occurs readily leading to important variations in surface properties with time and environment. These effects are further compounded by the inherent heterogeneity of the material.

Surface characteristics and properties play a significant role in most aspects of coal processing. Comminution, for example, is a process of creating new surface, while agglomeration involves the reduction of surface area and is usually controlled by surface forces. Both solid-solid and solid-liquid separations are influenced by interfacial phenomena. Gravity separations are usually performed in a liquid phase and are affected by the wetting characteristics of the various solids present and by the need to ensure proper dispersion of the individual particles. Froth flotation, of course, separates particles on the basis of differences in surface characteristics. Chemical processes such as leaching generally involve interfacial reactions whose rates depend on surface area and may be influenced by electrochemical effects in the electrical double layer at the solid-liquid interface, or by adsorption of reactant and/or product species from solution. Solid-liquid separations and associated processes such as flocculation are strongly dependent on the nature and properties of the solid-liquid interface.

In characterizing solid surfaces, it is important to consider first the surface area, since this determines the relative importance of the interfacial effects. The structure and chemical composition of the surface may depend on the distribution of different petrographic constituents and impurities such as finely disseminated mineral matter, on the extent of surface oxidation, and on adsorption from the environment. These, in turn, will generally determine the surface properties which define particle behavior. Since the relationships between structure etc., and properties are not generally known, it is usually necessary to measure properties such as wettability and electrical charge directly.

SURFACE CHARACTERIZATION

SURFACE AREA

It is convenient to consider two contributions to the surface area of a particulate solid; external and internal surface. The external surface is determined by the geometry (size and shape) of the particles as modified by surface roughness. Internal surface refers to the contribution of pores, cracks, etc., within the individual particles, and is particularly important in coal, which is typically highly porous. The distinction between internal and external surface is generally somewhat arbitrary and may depend on the method of measurement.

Geometric Surface Area

The external surface area of a particulate material can be evaluated from a knowledge of the particle size distribution and the particle shape. For a single particle, or a system of identical particles, of size x the volume specific surface S_v (surface area per unit volume) is given by

$$S_v = \frac{k_s x^2}{k_v x^3} \quad (1)$$

where k_s and k_v are the appropriate shape factors which relate the linear dimension x to the surface area and the volume of the particle, respectively. Since these factors are not generally known, except for simple shapes, they are often combined into a single, specific surface shape factor k_{sv} (equal to k_s/k_v) such that Equation 1 reduces to

$$S_v = \frac{k_{sv}}{x} \quad (2)$$

For spherical particles of diameter x , $k_{sv} = 6$, and Equation 2 can be used to define a specific surface mean diameter, \bar{x}_{sv} such that

$$\bar{x}_{sv} = \frac{6}{S_v} \quad (3)$$

In a real powder with a range of particle sizes, the specific surface area can be obtained by integration over all sizes. If the shape factors are independent of size, this leads to

$$S_v = k_{sv} \int_0^{\infty} x^{-1} q(x) dx \quad (4)$$

where $q(x)$ is the particle size density function such that $q(x)dx$ is the volume fraction of particles whose diameter lies between x and $x+dx$.

Equation 4 can be used to evaluate the specific surface area of a particulate material by numerical integration using measured size data. Alternately, if the size distribution can be shown to conform to a specific mathematical function, the integral can often be evaluated to yield a direct relationship between specific surface and the parameters of the distribution. (Hogg, 1980). It is important to recognize that such relationships generally lead only to an estimate of the external surface area, and may be subject to significant error due to:

- i) imprecise knowledge of the shape factors and their possible variation with size.
- ii) incomplete information on the size distribution, especially in the fine sizes which tend to dominate the surface area.

Nevertheless, these relationships can be useful. Comparison of calculated with directly measured areas, for example, can give information on surface roughness, porosity etc.

THE RESPIRABLE DUST CENTER

External Surface Area

External surface area can be obtained directly from measurements of the permeability of a packed bed of powder to a fluid (gas or liquid). This approach is based on the assumptions that the pores in a packed bed can be treated as a bundle of capillaries with some effective mean radius, and that fluid flow is laminar through each pore. Flow through the bed can then be described by the well-known Carman-Kozeny equation (Carman, 1956; Kozeny, 1927) which relates flow rate at a given applied pressure to the porosity of the bed and the external surface area of the particles.

Commercially available equipment for the measurement of specific surface area by gas (air) permeametry includes the Fisher-Sub-Sieve Sizer which uses a system of calibrated jets and a manometer to determine gas flow rate at fixed pressure through a specially prepared powder bed, and the Blaine Permeameter which uses liquid displacement to force a fixed volume of gas through a particle bed. Preparation of the bed is critical for both instruments, and standardized procedures must be followed. Liquid permeameters can also be used (Allen, 1981) to estimate external surface area for relatively coarse particles.

Total Surface Area

Gas Adsorption: Gas adsorption measurements can be used to determine the total (external plus available internal) surface area of solids. At the interface between a solid and a gas, there is an imbalance of intermolecular forces. Attractive forces exist which are opposed by the thermal motion of the gas molecules. The net result is a tendency for gas molecules to accumulate in the vicinity of the surface, i.e. to adsorb. The extent to which a given gas at a given temperature and pressure is adsorbed onto the surface of a solid is in direct proportion to the surface area. If the specific relationship between gas pressure and amount adsorbed - the adsorption isotherm - is known, adsorption data can be used to evaluate the surface area of the solid.

Various empirical and semi-theoretical models are used to describe adsorption isotherms. The well-known Brunauer, Emmett and Teller (BET) isotherm (Brunauer et al., 1938) is based on the assumption that adsorption takes place reversibly at specific sites on the solid surface and that multiple adsorbed layers can be formed, by successive adsorption, in a process similar to condensation of the gas at the surface. The BET model leads to the following expression for the adsorption isotherm:

$$\frac{p}{v(p_0 - p)} = \frac{1}{v_m C} + \frac{(C-1)}{v_m C} \frac{p}{p_0} \quad (5)$$

where p_0 is the saturation pressure of the gas and C is a constant which denotes the strength of the adsorption of the first layer relative to that of subsequent layers. If the volume of gas adsorbed is measured at a series of pressures and, from the data, a plot is made of the quantity $p/v(p_0 - p)$ versus the relative pressure p/p_0 , a straight line should be obtained. From the slope S , and the intercept I at $p=0$, the monolayer volume and the constant C can be obtained from $v_m = 1/(I+S)$ and $C = 1+I/S$. It is generally found that, for the physical adsorption of gases such as nitrogen on typical mineral surfaces, the BET equation applies for pressures ranging from 5% to 30% of the saturation pressure.

When, as is often the case in practice, the constant C is large, corresponding to strong adsorption of the first layer, drastic simplification of the BET equation is possible. Under these conditions, Equation (5) reduces to

$$\frac{v}{v_m} = \frac{p_0}{p_0 - p} \quad (6)$$

and the monolayer volume v_m can be calculated from a single determination

SURFACE CHARACTERIZATION

of the volume adsorbed at some pressure. This equation forms the basis of the so-called single point techniques for surface area measurement. It should be emphasized that Equation (6) is valid only when C is large, so that the single-point determinations should be used with care. If possible, the validity of this approximation should be tested by determination of several points on the isotherm before the single-point method is accepted, say for routine work.

For highly porous materials like coal, and where total surface area is important, the BET type of gas adsorption models are not appropriate because:

- i) adsorption equilibrium is not attained at the temperatures normally used for measurements
- ii) the BET model is inappropriate due to the finite (and small) size of the pores.

The Dubinin-Kaganer-Radushkevich (DKR) Adsorption Isotherm (Dubinin, 1955; 1960) which has found increased application in recent years for determining surface area of coals, is a semi-empirical expression of the form,

$$\ln (v/v_m) = -B(\ln p_0/p)^2 \quad (7)$$

where B is constant. The DKR equation is particularly useful at very low relative pressures, where the BET isotherm is inapplicable, and has been applied to the adsorption of CO_2 on coals at room temperature (Mahajan and Walker, 1978).

Once the monolayer volume v_m is known, the surface area of the solid can be calculated from:

$$S = 0.289 \sigma_0 V_m \quad (8)$$

where S is the total surface area of the sample (m^2), V_m is the monolayer volume (cm^3) and σ_0 is the area occupied by a single adsorbed molecule (\AA^2). The molecular area for nitrogen is generally accepted to be 16.2\AA^2 ; values for other gases are available in the literature (Sutherland, 1967; Kantro et al., 1967).

An alternative approach for the application of gas adsorption measurements for surface characterization makes use of the observation that, when fractional surface coverage v/v_m is plotted against relative pressure p/p_0 for a single gas on a variety of solids, a single characteristic isotherm is obtained. Based on this concept, de Boer et al. (1956; 1964) developed the so-called "t-plot" technique in which the quantity v/v_m is interpreted in terms of the thickness t of the adsorbed film. t is assumed to be uniquely related to relative pressure for any particular gas and extensive tabulations are available (de Boer et al., 1956; Lippens et al., 1964; Adamson, 1982).

The t-plot is obtained by plotting the measured volume of gas adsorbed at different relative pressures against the corresponding t values, obtained from the tables. The resulting plot should be a straight line whose slope is proportional to surface area. Deviations from linearity can give additional information on the morphology of the surface, the presence of microspores etc., (Mikhail et al., 1968).

Gas adsorption isotherms can be measured experimentally by volumetric, gravimetric, or continuous-flow (chromatographic) techniques. In the volumetric approach (Emmett, 1940) the solid is first outgassed, usually by heating in high vacuum, and then exposed to a known quantity of the adsorbing gas. The amount adsorbed is determined from the difference between the measured equilibrium pressure and the calculated value based on the quantity of gas admitted and the system volume.

THE RESPIRABLE DUST CENTER

Gravimetric methods involve direct measurement of the weight of gas adsorbed at different pressures. This approach is rarely used for surface area determination. The continuous-flow techniques (Nelsen and Eggersten, 1958) use gas chromatography to measure the change in composition of a mixture of the adsorbate gas (usually nitrogen) and a non-adsorbing carrier gas (usually helium) after passing over a sample of the powder. Advantages of the continuous-flow method are that the measurement is direct rather than by difference and that the need for troublesome, high-vacuum systems is eliminated. Disadvantages are that the systems are inherently expensive and that they are less suited than the volumetric types for studies of hysteresis effects etc., which can provide useful information on pore structures and the nature of the internal surface. Gas adsorption procedures have been described in some detail by Allen (1981).

Gas adsorption measurements can provide useful, but sometimes ambiguous, information on the characteristics of coal surfaces. For example, nitrogen adsorption typically indicates internal surface areas of the order of 1 to 10 m²/g depending on the coal. CO₂ adsorption, on the other hand, often gives values which are ten or more times larger on the same coal. The discrepancy has been attributed to the considerably more rapid diffusion of CO₂ into extremely fine pores at the higher temperatures which can be used for this gas (Mahajan and Walker, 1978). However there is also evidence that CO₂ adsorption can cause irreversible changes in coal structure, suggesting that there may be a specific chemical affinity of the gas for the solid.

Adsorption from Solution: In principle, it should be possible to use adsorption at the solid-liquid interface to determine surface area in much the same way as gas adsorption is used. If dye or other large molecules are used as the adsorbing species, such that they do not penetrate the micropores, this method could also be used to estimate the external (accessible) surface area of porous solids such as coal. In practice, however, a number of problems are encountered due to the greater complexity of the adsorption phenomenon, competition between solvent and solutes for surface sites and the effects of solution composition on the interaction forces responsible for adsorption (Somasundaran and Fuerstenau, 1966; Wakamatsu and Fuerstenau, 1968). Probably as a result of complications such as these, surface areas measured by adsorption from solution tend to be inconsistent and often do not agree with values obtained by gas adsorption. Nevertheless, a number of methods have been described in the literature and are discussed at some length by Allen (1981).

PORE STRUCTURE

Gas adsorption measurements can be used to obtain information on total pore volume, pore size distribution etc., from studies of hysteresis in the adsorption-desorption isotherms (Cranston and Inkley, 1957) or from non-linearities in the t-plot (Mikhail et al., 1968). These methods are particularly useful for pores in the 30 to 300Å size range (Pierce, 1953; Mahajan and Walker, 1978). Very small pores can be investigated by "molecular probing", i.e. by comparing apparent pore volumes obtained using gases of different molecular size (Spencer, 1967).

Larger pores (>300Å) are usually studied by means of mercury porosimetry. Since most solids, including coal, are not wetted by mercury, external pressure must be applied to force the liquid to penetrate the pores. For a pore of radius r, the required pressure p is given by a form of the Laplace equation (Washburn, 1921):

$$p = \frac{-2\gamma \cos \theta}{r} \quad (9)$$

where γ is the surface tension of the liquid (480 ergs/cm² for mercury) and θ is the contact angle (about 140° for mercury on most solids).

SURFACE CHARACTERIZATION

Experimentally, the volume of mercury which enters the pores is measured as a function of progressively increasing pressure, leading to a direct estimate of the cumulative (volume) distribution of pore radius. Commercial porometers are available which can operate at pressures up to 100,000 psi, corresponding to pore radii of about 10Å. Such pressures, however, can lead to disruption of the solid. Mercury porosimetry has been discussed at length in the literature (Allen, 1981; Scholten, 1967; Rootare and Nyce, 1971).

SURFACE COMPOSITION AND STRUCTURE

The chemical and physical nature of the surfaces of coal particles can have very significant effects on their behavior during processing, especially in view of the inherent heterogeneity of coals, the potential for alteration of surface functional groups due to oxidation, and the presence of finely disseminated mineral matter.

Surface Analysis

The objectives of surface analysis of a solid are determinations of composition (elemental, mineralogical, etc.), structure (atomic geometry, vacancies, morphology, etc.), and molecular and electron dynamics of surface atoms. Surface analysis of solids is, unfortunately, not an easy task because in real solids, the properties of the material often deviate from their ideal bulk values, for depths of up to a micron, in a spatially inhomogeneous manner.

A large number of instrumental methods, see listing in Table 17.1, is now available for surface analysis of solids in which an excitation signal (electrons, photons or ions) is used and the emission from the solid (electrons, photons and ions) is detected and measured. The analysis of surface layers is achieved by either limiting the excitation signal such that only the surface layers are penetrated or by measuring a signal which comes from surface layers only (the signal from atoms beneath the surface is absorbed by the solid). The thickness of the material which generates a signal to be measured by the detector is called the escape depth. The escape depth, which can vary from a few angstroms to a micron, is an indicator of the thickness of the layer of the surface being probed by the measurement technique. When the escape depth is small, the technique can be considered as a true surface analysis method. The escape depth is a complex function of the type and energy of the excitation signal and the absorption characteristics of the solid.

The type of analysis technique to be used depends upon the objective of the analysis, that is, how the information is to be used. Unlike the physical methods of surface characterization (surface area, pore volume, etc.) which may be used for routine characterization, chemical methods are used mainly as research tools. Therefore, only the broad principles, capabilities and limitations of these methods are given in this chapter. The purpose of this discussion is to make the reader aware of the availability of a large number techniques for surface analysis of solids. Many of the instruments are commercially available and the reader must refer to additional literature (books (Casper and Powell, 1982), review articles (Chander, 1981; Fuerstenau and Chander, 1982; Giesekke, 1983) and manufacturer's guides) once the need for a certain kind of surface analysis has been established.

Surface Structure: Relatively large-scale features can be investigated by microscopy, using optical microscopes down to about 1 μm or scanning electron microscopes to about 100Å. Optical reflectance measurements are used extensively in coal characterization, but the results are generally interpreted in terms of bulk rather than surface characteristics.

Diffraction Methods such as low energy electron diffraction (LEED) and

THE RESPIRABLE DUST CENTER

reflection high energy electron diffraction (RHEED) can be used to obtain information on the atomic structure of the surface layers (Adamson, 1982; Casper and Powell, 1982). Essentially, a diffraction pattern is obtained much as with conventional x-ray diffraction. However, due to the low penetrating power of low-energy electrons or by using glancing incidence of a high energy electron beam, the pattern obtained is indicative of periodicity etc., in the surface rather than in the bulk solid.

Surface Composition: It is obvious that the composition of the surface layers will significantly affect the surface properties. Impurity levels in the surface may be quite different from those in the bulk due to adsorption or to segregation within individual particles. Indeed, impurities whose bulk concentration is too low for detection could play a dominant role in determining surface characteristics. Examples of such cases are very common in mineral processing systems. It is well known, for instance, that surface oxidation has very important effects in sulfide flotation; surface hydroxylation in oxide minerals largely determines the electrical charging of such particles in water. Flotation of coals depends strongly on the nature of surface functional groups.

A number of techniques is available for determining the chemical composition of surface layers. An energy dispersive spectrophotometer attached to a scanning or transmission electron microscope can be used to determine the spatial distribution of elements in the surface layers of a specimen. The electron microprobe attachment to a scanning electron microscope can be used to identify surface species over an area of about one square micron. In Auger electron spectroscopy, an incident electron beam is used to excite surface atoms leading to the emission of so-called Auger electrons (Brundle, 1982). The emission spectrum is characteristic of the particular atom. Auger spectroscopy is used primarily for the identification of surface species. Auger and LEED capability are often combined in a single instrument.

Electron spectroscopy for chemical analysis (ESCA), also known as x-ray photoemission spectroscopy (XPS), and ultraviolet photoemission spectroscopy (UPS) are techniques based on principles similar to Auger spectroscopy, except that x-ray or ultraviolet radiation is used for excitation. Because of the smaller escape depth of emitted electrons (10-50Å), the technique is suitable for analysis of surface layers.

Infrared (IR), Fourier transform infrared (FTIR), Raman, nuclear magnetic resonance (NMR) and electron spin resonance (ESR) spectroscopy can be used to evaluate the structure and binding of adsorbed layers (Adamson, 1982; Little, 1966; Fuerstenau and Chander, 1982).

Ellipsometry has been widely used in investigations of surface films. In this technique, an incident beam of plane polarized light is elliptically polarized on reflection from the surface. From the phase shift and the relative amplitude of the parallel and perpendicular components, the thickness and density of the film can be evaluated (Archer, 1964).

Photo-acoustic spectroscopy (PAS) is a technique in which a photo-acoustic signal is generated when the sample absorbs electromagnetic radiation of a specific wavelength. The absorbed energy is converted into thermal waves that produce acoustic waves in the gas surrounding the sample and are detected by a microphone. Fourier transform infrared PAS has been used for coal characterization (Vidrine, 1980) and the spectrum shows comparable, if not better, resolution compared to the diffuse reflectance IR spectra of coal obtained under similar conditions. One of the main advantages of PAS is that the analysis does not require any special sample preparation.

It should be emphasized that the above techniques can give information on the physical structure and chemical composition of the surfaces and adsorbed films, but that the relationships between these characteristics and the actual response in the various fine coal processing methods are not

SURFACE CHARACTERIZATION

generally known. Consequently, these should be regarded as largely qualitative tools for investigating differences in properties and departures from normal behavior. At present, they have very little predictive capability.

Composition of Coal Surfaces

Coals are generally analyzed either for the moisture, ash and volatile matter content or for elemental (C, H, N, S and O) content. Sometimes composition of minerals in the ash is also determined. Only in recent years, since it has become necessary to process fine coals more effectively, the need to characterize surfaces of coals is being fully recognized. Of major importance to coal processing is the nature and concentration of functional groups containing oxygen. The oxygen-containing functional groups include $-\text{COOH}$, $=\text{CO}$, $-\text{OCH}_3$ and both alcoholic and phenolic $-\text{OH}$. There is some evidence for peroxide and esteroxygen and heterocyclic oxygen. The methods which could be employed to determine these functional groups may be divided into two groups:

- Spectroscopic methods
- Chemical methods

Spectroscopic methods include IR, FTIR, PAS and Raman Spectroscopy and are described in a previous section of this chapter. These methods have been used to determine the nature of functional groups in coals. (Fuerstenau and Chander, 1982; Glesekke, 1983). Chemical methods include various titration procedures in which the amount of a chemical reagent reacted per unit weight of coal is determined. By selecting the chemical reagent, which will react with a specific functional group, both the type and concentration of functional groups can be determined. For example, concentration of acidic groups can be determined by neutralization with a base (NaHCO_3 , Na_2CO_3 , NaOH , etc.). Alternatively, surface groups can be reacted to form products which can be identified and whose concentration can be determined by standard analytical techniques. Some examples are given below:

a) Carboxylic groups may be determined by their methylether derivatives. Methylation may be carried out by diazomethane in the presence of a Broensted acid, such as HCl or in the presence of a Lewis acid such as BF_3 , or in methanol. Phenolic- OH may also be estimated by this method if methylation in ether is followed by saponification to eliminate interference from $-\text{COOH}$.

b) Carbonyl functional groups can be transformed into an oxime derivative by alcoholic hydroxylamine chlorohydrate and monitored by the liberation of HCl .

c) Phenolic groups and hydroxyls can be measured most accurately by acetylation and subsequent hydrolysis of the acetylated sample with barium hydroxide.

d) Carbon dioxide evolved when coal is heated with a suitable catalyst (such as copper carbonate or copper sulfate) is a measure of carboxyl groups. Other reducing agents such as amalgamated Zn with HCl , LiAlH_4 and NaBO_2 attack different groups differently and may be used for characterization.

SURFACE PROPERTIES

The properties of coal surfaces in general, and of the coal-water interface in particular, play a prominent role in most of the operations used in coal processing. The stability and rheology of coal-water slurries, froth flotation, flocculation, and solid-liquid separation processes such as thickening and filtration are obvious examples. Other processes such as

THE RESPIRABLE DUST CENTER

heavy medium and other gravity separations may also depend on surface properties through their effects on wetting characteristics etc. It follows that the design and control of the various processing operations and their successful integration into a coal cleaning circuit may depend heavily on our ability to evaluate and control surface properties.

Surface Free Energy (Surface "Tension")

The surface tension, or surface free energy, of a liquid is a fundamental, thermodynamic quantity which can be defined unambiguously and measured quite easily (Adamson, 1982). Thus, the surface tension γ of a liquid is generally defined as

$$\gamma = \left(\frac{\partial G}{\partial A} \right)_{T, P, n_i, E} \quad (10)$$

where G is the Gibbs free energy of the system and A is the surface area. The partial derivative is expressed under conditions of constant temperature T , pressure P , chemical composition n_i , and electrical potential E .

Equation (10) describes the work involved in a reversible change in surface area. Such a process can readily be carried out on liquids, but it is not generally possible to vary the surface area of a solid reversibly. Consequently, while there is no doubt that there are surface energies associated with solids, the concept of surface energy as analogous to surface tension in liquids is of quite limited practical value (Guggenheim, 1967).

Changes in the free energy of solid-fluid interfaces, on the other hand, can often be measured, at least indirectly, and provide useful relationships for the description and correlation of various interfacial phenomena such as wetting and adsorption.

Wettability

The three kinds of wetting phenomena which might occur in a system containing a solid, a liquid and a gas phase are: adhesional wetting, spreading wetting and immersional wetting. Adhesional wetting is the process of formation of a three phase contact, spreading wetting is the process of displacement of the gas by the liquid on the surface of the solid and immersional wetting is the process of transfer of the particle from gas into the liquid phase. The free energy changes for the three wetting processes can be represented by the following relations:

Adhesion: $\Delta G_A = \gamma_{SL} - \gamma_{SG} - \gamma_{LG}$

Spreading: $\Delta G_S = \gamma_{SL} - \gamma_{SG} + \gamma_{LG}$

Immersion: $\Delta G_I = \gamma_{SL} - \gamma_{SG}$

where γ_{SL} , γ_{SG} , and γ_{LG} are the respective surface free energies of the solid/liquid, solid/gas and liquid/gas interfaces. For a more detailed discussion of wetting phenomena, see Blake (1984). The importance of these phenomena in capture of coal dust particles by water sprays has been discussed by Chander et al. (1986).

The spreading coefficient is defined as the negative free energy change ($-\Delta G_S$) in the displacement process. In general, for the replacement of phase 1 by phase 2 at the solid surface, the spreading coefficient S_{12} is given by:

$$S_{12} = \gamma_{1S} - \gamma_{1S} - \gamma_{2S} \quad (11)$$

If S_{12} is positive, phase 2 will displace phase 1 and vice versa.

SURFACE CHARACTERIZATION

The quantities γ_{1S} and γ_{2S} are not generally known, but the difference between them can be expressed in terms of the contact angle θ , which is defined, for a gas-liquid-solid system as the angle, measured in the liquid phase, at which the liquid surface meets that of the solid. An analogous definition can be made for a solid in contact with two immiscible liquids. The contact angle can be related to the interfacial tensions through Young's equation:

$$\gamma_{1S} = \gamma_{2S} + \gamma_{12} \cos \theta \quad (12)$$

and Equations (11) and (12) can be combined to give

$$S_{12} = \gamma_{12} (\cos \theta - 1) \quad (13)$$

It should be noted that Equations (11) and (12) apply only when the contact angle is finite. If $(\gamma_{12} - \gamma_{25}) > \gamma_{12}$ there is no stable three-phase contact and $S_{12} > 0$.

The displacement of one liquid by another at a solid surface can be expressed by (Hogg, 1980):

$$S_{12} = \gamma_1 \cos \theta_1 - \gamma_2 \cos \theta_2 \quad (14)$$

where γ_1 and γ_2 are the surface tensions of the two liquids and θ_1 and θ_2 are the contact angles of the separate liquids with respect to a common gas phase. Equation (14) is particularly useful in that the displacement process can be predicted knowing only the properties of the individual liquids, provided they are immiscible.

Wetting behavior can be significantly affected by changes in the various interfacial tensions due to adsorption. For a solid-liquid-gas system, for example, in which the liquid may be a solution and the gas may be a mixture (e.g., air), γ_{LG} may be affected by adsorption from either the gas or the liquid, and γ_{LS} may be affected by adsorption from the liquid. Any slight solubility of the gas in the liquid could lead to changes in γ_{LS} and γ_{LG} , while volatility of the liquid could affect γ_{SG} and γ_{LG} .

The effects of adsorption on the interfacial tensions can be described by the Gibbs adsorption isotherm:

$$d\gamma = - \sum_i \Gamma_i d\mu_i \quad (15)$$

where Γ_i and μ_i are, respectively, the adsorption density and chemical potential of species i in the system. Equation (15) is quite general, but its application requires a knowledge of the adsorption behavior of the various species present in the different phases. Some generalizations can be made, however. Positive adsorption of any species will always tend to reduce the interfacial tension. Thus, by rearranging Equation (12):

$$\cos \theta = \frac{\gamma_{SG} - \gamma_{LS}}{\gamma_{LG}} \quad (16)$$

it can be seen that positive adsorption at the solid-gas interface should increase contact angle (decrease wettability) while adsorption at the solid-liquid and/or liquid-gas interfaces will decrease contact angle (improve wettability). So-called wetting agents are typically surfactants which adsorb readily at solution interfaces, reducing γ_{LG} and/or γ_{LS} . Their effects are often attributed primarily to the reduction of γ_{LG} , but solid/surfactant specificity indicates that reduction in γ_{SL} may also be important. It has recently been shown, for example, that a given surfactant can have quite different effects on the wettability of coals of different rank (Chander et al., 1986b).

THE RESPIRABLE DUST CENTER

Measurement of Wetting Characteristics: Contact angle provides a useful measure of the wettability of solids. Various techniques are available for the experimental determination of contact angles (Adamson, 1982; Neuman and Good, 1976).

Direct observation of sessile drops using a microscope and goniometer arrangement is simple and quite accurate. An alternative approach makes use of the captive-bubble technique, in which the solid is immersed in liquid and a gas bubble, formed at the tip of a syringe, is brought into contact with the solid surface. This method gives good control over the gas phase and can readily be used to obtain both advancing and receding angles. For small drops, which can be assumed to be spherical in shape, contact angles can be calculated from the dimensions (height or volume and radius).

When the solid is available only as a fine powder, it may be possible to compact the material into a flat disk and use one of the techniques described above. However, it may be very difficult to obtain a sufficiently smooth surface. Several other methods are available to determine wetting characteristics of powders including: displacement pressure, capillary rise, immersion/sink time, bubble pick-up, induction time, imbibition time, etc. Each technique measures a somewhat different property and, therefore, quantitative correlations between different measurements are difficult.

The displacement pressure method is very similar to that used in mercury porosimetry. The pressure needed to force a non-wetting liquid, or prevent a wetting liquid from entering the pores of a packed bed is given by Equation (9). By comparing the experimental pressure for the liquid of interest with that for one which completely wets the solid ($\theta = 0$), the contact angle can be estimated from:

$$\cos \theta = p \gamma_0 / p_0 \gamma$$

where p_0 and γ_0 refer to the wetting liquid.

A variation of the displacement pressure is the capillary rise method (Crowl and Wooldridge, 1987). In this case, the powder whose wetting behavior is to be determined is placed in a tube which has a filter paper or porous disc at one end. The porous-end of the tube is placed in contact with the surface of the wetting solution. The liquid rises into the tube by capillary forces against gravity. The height of the liquid rise or weight of liquid in the bed is taken as a measure of wettability.

An immersion/sink time procedure was used by Walker et al. (1952) to determine the effect of surfactant on wetting of coal dusts. In this procedure, a small quantity of powder (~ 1 g) is dropped onto the surface of surfactant solutions of different concentrations. The most dilute concentration in which the powder would sink 'instantaneously' is determined. In this way, the effectiveness of various surfactants for wetting powders can be compared. Other investigators modified this technique in different ways. Some investigators measure the time for wetting a given amount of powder, whereas others measure a wetting rate. Mohal and Chander (1986) have recently described a technique in which wetting rate is measured as a function of time, from which information regarding the heterogeneity of the powder can be obtained. The technique is especially useful for heterogenous materials like coal.

In the same study, these investigators describe a method of imbibition time measurements to determine wetting characteristics of powders. Imbibition time is defined as the time between the instant a particle first contacts a liquid-gas interface and the instant when the particle detaches from the interface and becomes engulfed in the liquid. The method provides a means to determine a distribution of wettability for an assembly of heterogeneous particles. Samples from different coals were observed to give different distributions of imbibition times.

SURFACE CHARACTERIZATION

Prediction of Wetting Behavior: Characteristics such as spreading coefficient, contact angle, etc., are useful for describing and correlating wetting behavior. However, since they depend on the interaction between the phases, they provide little or no predictive capability. Zisman (1964) developed an empirical approach which can be used to estimate contact angles. He showed that, for a given solid and a homologous series of liquids, there is a linear relationship between γ_{LG} and $\cos\theta$. Furthermore, a similar relationship was found to hold approximately for any series of liquids. The intercept of the line at $\cos\theta=1$ ($\theta=0$) is termed the critical surface tension γ_c and is characteristic of the solid. It follows that any liquid for which $\gamma_{LG} < \gamma_c$ will wet the solid spontaneously. The values of γ_c for coals seem to be fairly constant at about 45 ergs/cm² (Parekh and Aplan, 1978). It is interesting to note that the slope of the linear relationship appears to vary with rank.

A more theoretical approach to the prediction of contact angles was taken by Girifalco and Good (1957; 1960; 1964) and later extended by Fowkes (1964). The latter considered that interfacial tensions result from contributions due to various kinds of intermolecular forces. Thus,

$$\gamma = \gamma^d + \gamma^m + \gamma^H + \dots \text{ etc.} \quad (18)$$

where γ^d is the contribution due to dispersion forces, γ^m is that due to metallic bonding, γ^H refers to hydrogen bonding, etc. The relative importance of each contribution will depend on the nature of the phase. For non-polar liquids such as hydrocarbons, it is reasonable to assume that $\gamma = \gamma^d$ since the intermolecular forces will be dominated by dispersion forces. Similarly, when a polar and a non-polar phase are in contact, it can be expected that interactions between the phases are due to dispersion forces only. Fowkes demonstrated that, for such systems, simple relationships can be derived for evaluating dispersion force contributions to the various interfacial tensions involved in wetting phenomena and for predicting contact angles etc.

Unfortunately, the applicability of the Fowkes approach to mineral systems, including coal, appears to be limited. The interactions between water and the surfaces of oxides, silicates etc., almost certainly include important contributions from hydrogen bonding as well as dispersion forces. Even for coal, which is normally regarded as a non-polar substance, the presence of surface functional groups and inherent mineral matter may lead to a significant degree of hydrogen bonding with water.

Electrical Charge

It is a general rule that differences in electrical potential usually exist at the interface between two phases. Such effects are especially important in aqueous suspensions of solid particles where their existence leads to disproportionation of charged species (ions) adjacent to a charged surface. When such a surface is in contact with an electrolyte solution, oppositely charged ions - counter ions - are attracted to it resulting in the formation of an electrical double layer at the interface. Because of mixing effects due to thermal motion in the liquid, the counter ions form a diffuse layer of charge extending out into the solution. The electrical potential decays from its value at the interface - the surface potential - to zero in the bulk solution, far away from the surface. Details of the electrochemistry of the double layer are given in most standard texts on colloid and surface chemistry (e.g., Kruyt, 1952).

The charge at a solid-water interface can arise in a variety of ways. In the case of sparingly soluble salts such as silver iodide, the charge results from disproportionate adsorption of the constituent ions - known as potential determining ions - at the interface. In the ideal case, this leads to a simple relationship between the surface potential and the activities of the potential determining ions - the Nernst equation (Kruyt, 1952):

$$\psi_0 = \frac{RT}{F} \ln \frac{a}{a_0} \quad (21)$$

where ψ is the surface potential, R is the gas constant, T is the absolute temperature, F is Faraday's constant, a is the activity of the potential determining ion in solution and a_0 is the activity at which the surface is uncharged. a_0 defines the point of zero charge (PZC) of the solid. For such solids, the surface potential is completely defined by the activity of the potential determining ions relative to the PZC.

For oxide minerals, whose surfaces are probably hydroxylated in the presence of water, there is considerable experimental evidence that surface potentials are controlled by the activities of H^+ and OH^- , i.e., by pH. Consequently, these are often regarded as the potential determining ions for oxide systems. The surfaces of oxides have been discussed at length by Healy and Fuerstenau (1965), Parks (1965) and Healy and White (1978).

For certain types of minerals, especially the aluminosilicates, the surface charge may be fixed by substitutions in the solid crystal during its original formation. For example, substitution of Ca^{+2} or Fe^{+2} for Al^{+3} , or of Al^{+3} for Si^{+4} leads to a residual negative charge on the crystal. Ideally, the charge on such surfaces is fixed by the degree of substitution in the solid and is independent of conditions in solution; there is no point of zero charge. The surface potential, on the other hand, is free to vary according to the concentration of different ionic species in solution (Kruyt, 1952).

The clay minerals are often given as examples of fixed-charge surfaces. However, it should also be recognized that these minerals have structures which are finite in one direction only. Ideally, the crystal would be an infinite sheet. The edges of actual clay platelets will have unsatisfied valences which probably become hydroxylated in water and behave much like oxide surfaces. Thus, a clay particle in water will have face areas with fixed (negative) charge and edge areas whose potential varies with the pH of the solution. The edges will generally be positively charged in acid solutions and negatively charged in base (van Olphen, 1977). It has been estimated (Williams and Williams, 1978) that the edges of kaolin clay particles are uncharged at about pH 7.

Surface potentials on coal also appear to depend on pH (Wen and Sun, 1977; Arnold and Aplan, 1986). In this case, the surface charge probably results from acid-base dissociation of surface groups such as carboxylates, with additional contributions from orientation of water molecules and preferential adsorption of certain ions on the hydrophobic surface. The apparent point of zero charge for coals varies between pH 2 and pH 7 depending on rank, degree of oxidation etc. (Arnold and Aplan, 1986). From the nature of the variation in potential with pH, it seems quite unlikely that Equation (21) is applicable to coal-water interfaces. Perhaps, complete dissociation of ionogenic groups occurs at alkaline pH's and the potential remains constant. Similar behavior is observed for other naturally hydrophobic solids such as molybdenite and graphite containing ionogenic surface groups (Chander et al., 1975). The surface properties of coal may also be affected by the adhesion of very fine particles, particularly of clay minerals. Although attempts have been made to demineralize coals by chemical dissolution methods, care must be exercised because the effects of chemical treatments on surface functional groups of coal are not fully known.

Zeta Potential

Characterization of the electrical effects at particle surfaces is usually accomplished by means of electrokinetics measurements. These involve evaluation of the relative motion of the solid and solution phases in an electric field. The measurements most commonly used for coal and mineral systems are electrophoresis, in which an applied electric field causes

SURFACE CHARACTERIZATION

migration of the solid particles relative to the solution, and streaming potential, where the particles are fixed, in a packed bed, and an electric field is established in response to forced motion of the solution.

The basic principle underlying these techniques is that relative motion of the solid and fluid phases causes the diffuse double layer to be stripped away from the interface. The results of electrokinetics measurements are commonly represented in terms of the so-called zeta-potential which is defined as the potential difference between the bulk solution and a hypothetical plane, close to the interface, at which shearing of the fluid is considered to begin. It is known from hydrodynamics that fluids do not slip at solid surfaces. In the usual continuum treatments of fluid flow, this leads to a condition of zero relative velocity at the surface. At the molecular level, however, the fluid cannot be treated as a continuum and there is considerable uncertainty as to what is actually meant by the "plane of shear". The problem may be compounded by the presence of relatively immobile adsorbed layers at the interface and by the electrostatic interactions between the charged surface and the ions in the double layer. Thus, it is conceivable that the location of the shear plane, and hence the precise definition of the zeta-potential, may themselves depend on charge and potential in the double layer.

In streaming potential measurements, the relative motion gives rise to a convective electric current in the direction of flow which is opposed by a conduction current through the solution. At steady-state, this leads to an electrical potential gradient across the bed of particles. If the streaming potential E is measured as a function of applied pressure P , the zeta-potential ζ can be estimated (Overbeek, 1952) from:

$$\zeta = \frac{4\pi\mu\lambda}{\epsilon} \left(\frac{E}{P}\right) \quad (22)$$

where λ is the conductivity, μ the viscosity, and ϵ the dielectric constant of the solution.

In the case of electrophoresis, the charged particles and the layer of oppositely charged fluid in the double layer are attracted towards the appropriate electrodes. The relative motion of particles and fluid is opposed by viscous forces, and a steady state can be established where the electrical and viscous forces just balance. The zeta-potential can be determined from measurements of the electrophoretic velocity v_E for a given potential E , applied between electrodes a distance L apart, using (Overbeek, 1952):

$$\zeta = \frac{\pi\mu L}{f\epsilon E_a} v_E \quad (23)$$

where f is a correction factor whose value is 1/6 for particles which are small compared to the double layer thickness (Huckel, 1924) and 1/4 for very large particles (Smoluchowski, 1903). Many practical cases fall in the intermediate range for which extensive tabulations are available (Loeb et al., 1960).

Streaming potential measurements are usually carried out using systems designed and constructed in the laboratory (Fuerstenau, 1956; Somasundaran and Kulkarni, 1973). Various instruments are available commercially for measuring electrophoretic mobilities. For the most part, these use the microelectrophoresis technique in which the motion of individual particles is observed directly through a microscope as a function of the potential applied across the ends of the cell. Problems arising due to the simultaneous establishment of an electroosmotic flow of fluid adjacent to the cell walls are minimized by careful choice of the position in the cell at which the particles are observed (Overbeek, 1952).

THE RESPIRABLE DUST CENTER

SUMMARY

The complete characterization of the surfaces of coals and associated minerals is obviously impractical and, in fact, rarely necessary. At the same time, however, surface phenomena can have important effects in most aspects of coal processing and some knowledge of surface characteristics is generally useful for the design and operation of coal cleaning processes. The extent to which characterization should be undertaken will usually depend on the nature and magnitude of the problems encountered in processing a particular coal or performing a specific operation.

Surface characterization may involve evaluation of surface area (external and internal) and pore structure, investigation of the physical and chemical nature of the surface regions, and determination of surface properties such as wetting behavior and surface charge. The various techniques available for measuring surface characteristics are outlined in this chapter; the reader is referred to the sources listed in the bibliography for details on specific procedures, etc.

It is well known that surface characteristics, and their variation due to weathering and oxidation of coal, can significantly affect behavior during processing. However, surface characterization has not generally been regarded as necessary to the operation of coal preparation plants. This may change as the use of physical cleaning methods is extended to finer sizes. Characterization of the surfaces of coal and its associated minerals, especially fine clays, could become a requirement for the proper control of fine coal processing operations.

This research has been supported by the Department of the Interior's Mineral Institute program administered by the Bureau of Mines through the Generic Mineral Technology Center for Respirable Dust under grant number G1135142.

REFERENCES

- Adamson, A.W., 1982, *Physical Chemistry of Surfaces*, 4th Ed., New York, Wiley - Interscience.
- Allen, T., 1981, *Particle Size Measurement* 3rd Ed., London, Chapman and Hall.
- Archer, R.J., 1964, *Ellipsometry in the Measurement of Surfaces and Thin Films*, ed. E. Passaglia, R.R. Stromberg, and J. Fruger, J., Nat. Bur. Std. Misc. Publ. No. 256, p. 255.
- Arnold, B.J. and Aplan, F.F., 1986, "The Effect of Clay Slimes on Coal Flotation, Part II: The Role of Water Quality", *Int'l. J. Miner. Proc.* 17: 243-260.
- Blake, T.D., 1984, "Wetting", in *Surfactants*, ed. Th.F. Tadros, pp. 221-225, New York, Academic Press.
- Brunauer, S., Emmett, P.H., and Teller, E., 1938, "Adsorption of Gases in Multimolecular Layers", *J. Am. Chem. Soc.*, 60: 309-319.

SURFACE CHARACTERIZATION

- Brundle, C.R., 1982, "Ultra-High Vacuum Techniques of Surface Characterization", in *Industrial Applications of Surface Analysis*, ed. L.A. Casper and C.J. Powell, pp.13-32. ACS Symposium Series No.199, Washington, D.C., ACS.
- Carman, P.C., 1956, *Flow of Gases Through Porous Media*, London, Butterworths.
- Casper, L.A. and Powell, C.J., eds. 1982, *Industrial Applications of Surface Analysis*, ACS Symposium Series No. 199, Washington, D.C., ACS.
- Chander, S., Wie, J.M. and Fuerstenau, D.W., 1975, "On the Native Floatability and Surface Properties of Naturally Hydrophobic Solids", *AIChE Symp. Series*, 71 (150): 183-188.
- Chander, S., Mohal, B.R. and Aplan, F.F., 1986, "Wetting Characteristics and Their Significance in Dust Abatement", *Colloids and Surfaces*, in press.
- Chander, S., 1981, "X-Ray Techniques in Mineral Science and Engineering", *Trans. Indian Institute of Metals*, 34: 390-397.
- Cranston, R.W. and Inkley, F.A., 1957, "The Determination of Pure Structures from Nitrogen Desorption Isotherms" in *Advances in Catalysis*, Vol. 9., ed. A. Farkas, pp 143-154, New York, Academic Press.
- Crowl, V.T. and Wooldridge, W.D.S., 1967, "A Method for the Measurement of Adhesion Tension of Liquids in Contact with Powders", *S.C.I. Monograph* 25, pp. 200-212, London, Society of Chemical Industry.
- de Boer, J.H., Lippens, B.C., Linsen, B.G., Broekhoff, J.C.P., van den Heuvel, A., and Osinga, Th. J., 1966, "t-Curve of Multimolecular Nitrogen Adsorption", *J. Coll. Interf. Sci.*, 21: 405-414.
- Dubinin, M.M., 1955, "Investigation of the Porous Structure of Active Carbons by Complex Methods, Quart. Rev., 9: 101-114.
- Dubinin, M.M., 1960, "The Potential Theory of Adsorption of Gases and Vapors for Adsorbents with Energetically Nonuniform Surface", Chem. Rev., 60: 235-241.
- Emmett, P.H., 1940, 12th Report of the Committee on Catalysis, Chapter 4 in *Physical Adsorption in the Study of the Catalysis Surface*, New York, Wiley.
- Fowkes, F.M., 1964(a), "Dispersion Force Contributions to Surface and Interfacial Tensions, Contact Angles and Heats of Immersion", in *Contact Angle, Wettability and Adhesion*, *Advances in Chemistry Series*, No. 43, pp. 99-111, Washington, D.C., ACS.
- Fowkes, F.M., 1964(b), "Attractive Forces at Interfaces", Ind. Eng. Chem., 56: 40-52.
- Fuerstenau, D.W., 1956, "Measuring Zeta Potentials by Streaming Potential Techniques", Trans. AIME, 205: 834-835.
- Fuerstenau, D.W. and Chander, S., 1982, "Surface Characterization in Mineral Processing", in *Industrial Applications of Surface Analysis*, ed. L.A. Casper and C.J. Powell, ACS Symp. Series 199, pp. 283-312, Washington, D.C., ACS.
- Giesekke, E.W., 1983, "A Review of Spectroscopic Techniques Applied to the Study of Interactions Between Minerals and Reagents in Flotation Systems, Int'l. J. Miner. Proc., 11, 19-56.

THE RESPIRABLE DUST CENTER

- Girifalco, L.A. and Good, R.J., 1957, "A Theory for the Estimation of Surface and Interfacial Energies I. Derivation and Application to Interfacial Tension", J. Phys. Chem., 61: 904-909.
- Good, R.J., and Girifalco, L.A., 1960, "A Theory for Estimation of Surface and Interfacial Energies. III. Estimation of Surface Energies of Solids from Contact Angles", J. Phys. Chem., 64: 561-565.
- Guggenheim, E.A., 1967, Thermodynamica, pp. 166-167, Amsterdam, North Holland.
- Healy, T.W. and Fuerstenau, D.W., 1965, "Oxide-Water Interface. Interrelation of the Zero Point of Charge and the Heat of Immersion", J. Coll. Interf. Sci., 20: 376-386.
- Healy, T.W. and White, L.R., 1978, "Ionizable Surface Group Models of Aqueous Interfaces", Adv. Coll. Interf. Sci., 9: 303-345.
- Hogg, R., 1980, "Characterization of Mineral Surfaces", in Fine particles Processing, Vol. 1, ed. P. Somasundaran, pp.492-524, New York, AIME.
- Huckel, E., 1924, "Die Kataphorese der Kugel", Physik. Z., 25: 240.
- Kantro, D.L., Brunauer, S., and Copeland, L.E., 1967, "BET Surface Areas - Methods and Interpretations", in The Solid - Gas Interface, Vol. 1, ed. E. A. Flood, New York, Marcel Dekker.
- Kozeny, J., 1927, Ber. Wien, Akad., 136A: 271.
- Kruyt, H.R., ed. 1952, Colloid Science, Vol. 1, Amsterdam, Elsevier.
- Lippens, B.C., Linsen, B.G. and de Boer, J.H., 1964, "Pore Systems in Catalyst. I. Adsorption of Nitrogen", J. Catalysis, 3: 32-37.
- Little, L.H., 1966, Infrared Spectra of Adsorbed Molecules, New York, Academic Press.
- Loeb, A.L., Overbeek, J.Th.G., and Wiersema, P.H., 1960, The Electrical Double Layer Around a Spherical Colloid Particle, Cambridge, MA, MIT Press.
- Mahajan, O.P. and Walker, Jr., P.L., 1978, "Porosity of Coals and Coal Products", in Analytical Methods for Coal and Coal Products, Vol. 1, ed. C. Karr Jr., pp. 125-162, New York, Academic press.
- Mikhail, R.S., Brunauer, S., and Bodor, E.E., 1966, "Investigations of a Complete Pore Structure Analysis I. Analysis of Micropores", J. Coll. Interf. Sci. 26: 45-53.
- Mohal, B.R. and Chander, S., 1986, "A New Technique to Determine Wettability of Powders - Imbibition Time Measurements", Colloids and Surfaces, in press.
- Nelsen, F.M., and Eggersten, F.T., 1958, "Determination of Surface Area. Adsorption Measurements by a Continuous Flow Method", Anal. Chem., 30: 1387-1390.
- Neuman, A.W. and Good, R.J., 1976, Surface Colloid Techniques, New York, Plenum Press.
- Overbeek, J. Th.G., 1952, in Colloid Science, Vol. 1, ed. H.R. Kruyt, Amsterdam, Elsevier.

SURFACE CHARACTERIZATION

- Parekh, B.K. and Aplan, F.F., 1978, "The Critical Surface Tension of Wetting of Coal", in Recent Developments in Separation Science, ed N.H. Li, R. G. Long, S. A. Stern, and P. Somasundaran, pp. 107-113. West Palm Beach, FL, CRC Press.
- Parks, G.A., 1965, "The Isoelectric Points of Solid Oxides, Solid Hydroxides and Aqueous Hydroxo Complex Systems", Chem. Rev., 65: 177-198.
- Pierce, C., 1953, "Computation of Pore Sizes from Physical Adsorption Data", J. Phys. Chem., 57: 149-152.
- Rootare, H.M. and Nyce, A.C., 1971, "Use of Porosimetry in the Measurement of Pore Size Distribution in Porous Materials", Int. J. Powder Metall., 7: 3-111.
- Scholten, J.J.F., 1967, "Mercury Porosimetry and Allied Techniques", in Porous Carbon Solids, ed. R.L. Bond, pp. 225-249, New York, Academic Press.
- Smoluchowski, J., 1903, "Contribution a la Theorie de L'endomuse Eletrique et de quelques Phenomenes Correlatifs", Bull. Intern. de L'Academie des Sciences de Cravocie, 3: 182.
- Somasundaran, P. and Fuerstenau, D.W., 1966, "Mechanisms of Alkyl Sulfonate Adsorption at the Alumina - Water Interface", J. Phys. Chem., 70: 90-96.
- Somasundaran P., and Kulkarni, R.D., 1973, "A New Streaming Potential Apparatus and Study of Temperature Effects Using it", J. Coll. Interf. Sci., 45: 591-600.
- Spencer, D.H.T., 1967, "Use of Molecular Probes in the Characterization of Carbonaceous Material", in Porous Carbon Solids, ed. R.L. Bond, pp. 87-154, New York, Academic Press.
- Sutherland, J.W., 1967, "Usefulness of Measurements of the Physical Adsorption of Gases in Characterizing Carbons", in Porous Carbon Solids, ed. R.L. Bond, pp. 1-63, New York, Academic Press.
- Vidrine, D.W., 1980, "Photoacoustic Fourier Transform Infrared Spectroscopy of Solid Samples", Appl. Spectroscopy, 34: 314-319.
- van Olphen, H., 1977, An Introduction to Clay Colloid Chemistry, 2nd Ed., New York, Wiley.
- Wakamatsu, T. and Fuerstenau, D.W., 1968, "The Effect of Hydrocarbon Chain Length on the Adsorption of Sulfonates at the Solid/Water Interface", in Adsorption from Aqueous Solution, Advances in Chemistry Series No. 79, pp. 161-171, Washington, D.C., ACS.
- Walker, Jr., P.L., Peterson, E.E. and Wright, C.C., 1952, "Surface Active Agent Phenomena in Dust Abatement", Industrial and Engineering Chemistry: 44: 2389-2392.
- Washburn, E.W., 1921, Proc. Nat. Acad. Sci., 7: 115.
- Wen, W.W., and Sun, S.C., 1977, "An Electrokinetic Study on the Amine Flotation of Oxidized Coal," Trans. AIME., 262: 174-180.
- Williams, D.J.A., and Williams, K.P., 1978, "Electrophoresis and Zeta Potential of Kaolinite," J. Coll. Interf. Sci. 65: 79-87.
- Zisman, W.A., 1964, "Relation of Equilibrium Contact Angle to Liquid and Solid Constitution," in Contact Angle, Wettability and Adhesion, Advances in Chemistry Series, No. 43, pp. 1-51, Washington D.C., ACS.

Wetting Behavior of Coal in the Presence of Some Nonionic Surfactants

S. Chander, B.R. Mohal and F.F. Aplan

Mineral Processing Section, Department of Mineral Engineering, The Pennsylvania State University

ABSTRACT

The wetting behavior of coal has been determined in the presence of nonyl and octyl series of nonionic surfactants containing polyethoxy groups of different sizes. The wetting behavior was determined by a modified Walker technique and contact angle measurements. The results show that the wetting rate of coal varies with coal rank, structure of the hydrocarbon chain and number of ethoxy groups in the hydrophilic group of the surfactant. A close relationship has been observed between the wetting rates and the short-time advancing contact angles.

INTRODUCTION

Nonionic surfactants are used in many applications to improve wettability of solids. They can be used as dispersing agents [1] or dust suppressants [2-5] and to control the flotation, flocculation, filtration and flowability of particulates. This study was undertaken to study the effect of a series of nonionic surfactants on the wetting behavior of coal. Two series of surfactants, namely, ethoxylated nonyl and octyl phenols were used. The nonyl phenol series contains a linear hydrocarbon chain containing nine carbon atoms $(\text{CH}_3(\text{CH}_2)_8-\text{C}_6\text{H}_4-(\text{OC}_2\text{H}_4)_n)$, where n is the number of ethoxy groups). The octyl phenol series contains a branched hydrocarbon chain containing eight carbon atoms $((\text{CH}_3)_3\text{CCH}_2\text{C}(\text{CH}_3)_2-\text{C}_6\text{H}_4-(\text{OC}_2\text{H}_4)_n)$.

Initial wetting rates — modified Walker technique

Walker et al. [6] developed a sink test to determine the wettability of coal particles. In this technique, coal particles are dropped individually onto the surface of surfactant solutions of different concentrations, and the most dilute concentration in which coal would sink "instantaneously" is determined. This technique is a variation of a procedure initially developed by Draves and Clarkson [7] to determine the effect of surfactants on wettability of cotton fibers.

WETTING BEHAVIOR OF COAL

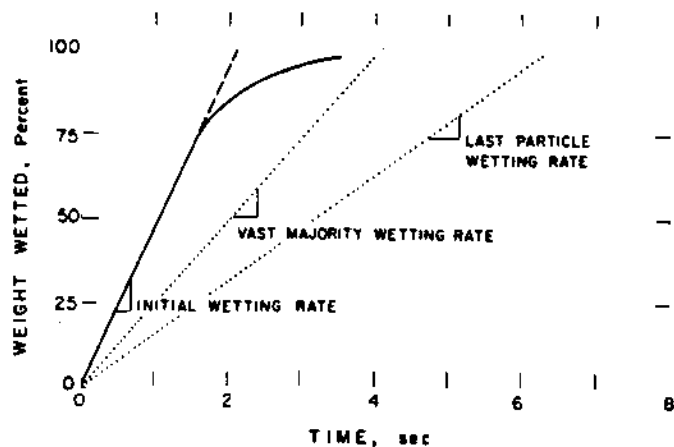


Fig. 1. The amount of a HVA-bituminous coal wetted by a $4 \times 10^{-4} M$ Triton X-100 solution versus time in a typical wetting rate measurement.

In this procedure commonly known as the Draves test, the concentration of a surfactant required to give a 'sink time' of 25 s is determined.

Other investigators have used slight variations of the Walker method to study the wetting of fine particles [8-12], by measuring the time for wetting a given amount of powder. There are differences in the manner in which the time of wetting is measured, however. Some investigators measure the time for the last trace of coal to disappear [8,11] whereas others determine the time for the vast majority of particles to sink [10]. Some investigators report a wetting rate [11] which is a value calculated on the basis of the time for the 'last traces of particles to sink'. The differences in choice of criterion for wetting can result in different values for wetting rates as illustrated in Fig. 1 which is based upon our measurements of the amount of powder wetted as a function of time. The procedure for wetting rate measurements is described in the next section. The technique in which time for disappearance of the 'last traces of particles' is determined gives the smallest value for the wetting rate, while the technique in which the time for wetting of the 'vast majority' of particles is determined will give intermediate rates. The terms 'last traces of particles' and 'vast majority of particles' are usually not defined explicitly and can lead to large differences in wetting rates measured by different investigators. Since our measurements show that the wetting rates for an assembly of powder decreases with time, we have used the initial wetting rates to compare the wetting behavior of coal in solutions of different surfactants.

EXPERIMENTAL METHODS AND MATERIALS

Wetting rate — modified Walker technique

To avoid some of the inherent difficulties associated with the measurement of time for wetting of powders, as discussed in the previous section, we have

WETTING RATE MEASUREMENT APPARATUS

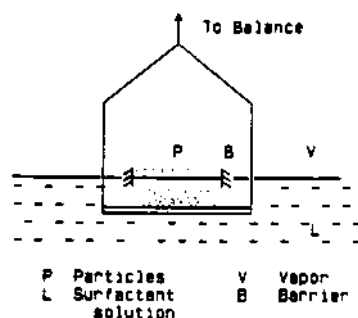


Fig. 2. A schematic diagram for the wetting rate measurement apparatus.

modified the Walker method. In this method, shown schematically in Fig. 2, a 40 mg sample of $250 \times 150 \mu\text{m}$ coal was dropped on the surface of a surfactant solution and the amount of coal imbibed into the liquid was measured by placing the pan of a Cahn electrobalance beneath the liquid surface. The initial wetting rates were determined from measurements of the amount of coal wetted as a function of time, as illustrated in Fig. 1. The rate of wetting was found to be independent of the amount of the coal sample in the range 20–100 mg. The data reported for the wetting rates is an average of at least four replicate measurements in which the coefficient of variation was about 0.08.

Contact angles

The sessile drop contact angles were measured on carefully selected samples, avoiding those with cracks, locked particles of pyrite, mineral occlusions, etc. The coal was polished following the procedure of Gutierrez et al. [13]. Briefly, the procedure consisted of a rough polish on a series of emery papers followed by wet polishing on rotating laps (250 rpm) using, successively, 0.3 and $0.05 \mu\text{m}$ levigated Linde Alumina. The samples were washed thoroughly with water to remove any adhering alumina particles and stored under distilled water. The contact angles were usually measured within ten minutes of sample preparation. Surgeon's gloves were used for the entire polishing sequence and all specimen handling was done with gloves or glass forceps to avoid contamination. The apparatus used for measuring the contact angle was the Ramé-Hart Model A-100 Contact Angle Goniometer.

Advancing contact angles

The advancing contact angle measurements were made by observing the advance of the three-phase perimeter on a polished surface of coal. A drop of the surfactant solution (diameter $\sim 2 \text{ mm}$) was dropped from a height of 1 cm

WETTING BEHAVIOR OF COAL

TABLE 1

Proximate and ultimate analysis of coal samples

	HVA-bit.	Sub-bit.	Anthracite
Moisture	3.2%	10.24%	1.5%
Proximate analysis (dry basis %)			
Ash	8.47	6.64	8.2
VM	38.16	40.00	5.3
FC	53.37	53.36	86.4
Ultimate analysis (DAF basis %)			
C	81.94	75.42	94.3
H	5.70	5.15	2.3
N	1.54	0.84	0.9
S	2.12	0.35	0.6
O	8.7	18.22	1.9
Cl	-	0.22	-

from a Gilmont microsyringe onto the polished specimen. The height of 1 cm was chosen to obtain a free falling drop. The progression of the drop was recorded using a Spin Physics Model SP2000 High Speed Motion Analysis System. The contact angle was measured during the period when the movement of the three-phase contact attained a constant velocity. This was taken to be the advancing contact angle.

Coal and reagents

The three coal samples used in this investigation were: a HVA-bituminous coal from the Upper Freeport seam obtained from the Penn State Data Bank (PSOC 1361p), a sub-bituminous-A coal from Wyoming also obtained from the Penn State Data Bank (PSOC 512), and an anthracite coal obtained from Reading, PA. Proximate and ultimate analysis of the coal samples are given in Table 1. The coal samples were crushed and screened to obtain a $250 \times 150 \mu\text{m}$ fraction which was then used for the wetting tests.

The ethoxylated nonyl phenols (Triton N series) and octyl phenols (Triton X series) were obtained from Rohm and Haas and some of their properties are given in Table 2.

RESULTS AND DISCUSSION

Wetting rates

The initial wetting rates for a HVA-bituminous coal as determined by the modified Walker technique are given as a function of surfactant concentration

TABLE 2

Surfactant properties and parameters of coal wettability

Surfactant	No. of ethoxy groups	HLB	C_{CMC}^a (M)	C_{cr}^b (M)	C_{cr}/C_{CMC}	Slope ^c
Nonyl Phenols						
N-60	6	10.9	2.7×10^{-5}	5.4×10^{-6}	0.20	7.9
N-101	9-10	13.4	3.3×10^{-5}	8.2×10^{-6}	0.25	14.5
N-111	11	13.8	6.0×10^{-5}	1.8×10^{-5}	0.30	13.7
N-150	15	15.0	9.3×10^{-5}	4.5×10^{-5}	0.48	8.2
Octyl Phenols						
X-45	5	10.4	(1.17×10^{-4})	4.3×10^{-5}	0.37	14
X-114	7-8	12.4	(2.1×10^{-4})	5.7×10^{-5}	0.27	21.7
X-100	9-10	13.5	2.2×10^{-4}	1.3×10^{-4}	0.59	34.0
X-102	12-13	14.6	—	9.0×10^{-5}	—	25.4

^aThe C_{CMC} value given in parentheses are from the literature [14], other values were obtained in this investigation.

^bCritical wetting rate concentration, see text.

^cSlope of the log surfactant concentration-initial wetting rate plot, see text.

in Fig. 3. The surfactants used in this series of tests were ethoxylated nonyl phenols with varying number of oxyethylene groups, the properties of which are given in Table 2. In the range investigated, the wetting rate increases linearly with the logarithm of concentration. The minimum concentration at which wetting occurs, obtained by extrapolating the wetting rate versus logarithm of concentration plots, is referred to as the critical wetting concentration, C_{cr} . In practical application in controlling wettability, C_{cr} would determine the minimum amount of surfactant needed to wet a given powder. Concentrations greater than C_{cr} will give higher rates of wetting. The C_{cr} values for various surfactants in the nonyl phenol series are shown by vertical arrows in Fig. 3 and are tabulated in Table 2.

The initial wetting rates, normalized with respect to the critical wetting concentration, are given in Fig. 4 for the nonyl phenol series and in Fig. 5 for the octyl phenol series of surfactants. The error bars for replicate measurements are given in Fig. 5, but are omitted from other figures for purpose of clarity. The results in Figs 4 and 5 show that the concentration dependence of wetting rates, measured in terms of the slope of the wetting rate versus log concentration, first increases and then decreases with an increase in the number of ethoxy groups. The slopes are given in the last column of Table 2. With the exception of Triton X-102, the C_{cr} increases with increase in the number of ethoxy groups. The ratio, C_{cr}/C_{CMC} , depends upon the number of ethoxy groups in the hydrophilic group of the surfactant and the nature of the hydrophobic group. This

WETTING BEHAVIOR OF COAL

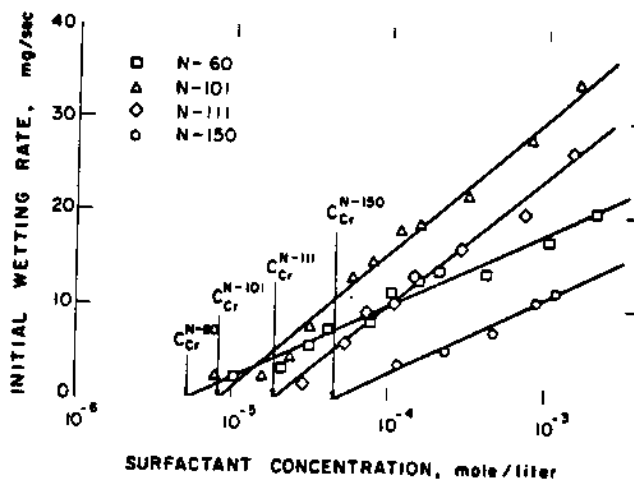


Fig. 3. The initial wetting rates for HVA-bituminous coal for various ethoxylated nonyl phenols.

is considered to reflect the importance of the adsorption phenomena at various interfaces in the three-phase system. These results are discussed later in the section on contact angles. The maximum in the slope occurs at about 9-10 ethoxy groups per molecule, or an HLB value of 13.5, for both the nonyl and the octyl phenol series of surfactants.

The initial wetting rates for three different coals, namely, an anthracite, a HVA-bituminous and a sub-bituminous, are given as a function of surfactant concentration in Fig. 6 for Triton N-101 and in Fig. 7 for Triton X-100. The effectiveness of the surfactant in wetting coal clearly depends upon both (a) the coal rank and (b) the type of surfactant. For example, the rate of wetting for Triton N-101 follows the order:

HVA-bituminous > anthracite > sub-bituminous

whereas for Triton X-100, the order is:

anthracite \geq HVA-bituminous > sub-bituminous

These differences in the effect of surfactants on wetting rates are attributed to differences in the adsorption behavior of surfactants on the surface of coal and are discussed in the following section.

Contact angles — sessile drop

The sessile drop contact angles for HVA-bituminous and anthracite coals are given in Fig. 8 for Triton N-101 and in Fig. 9 for Triton X-100. As the concentration of the surfactant is gradually increased, the contact angle first increases and then decreases. The critical wetting concentration (C_{cr}) as

THE RESPIRABLE DUST CENTER

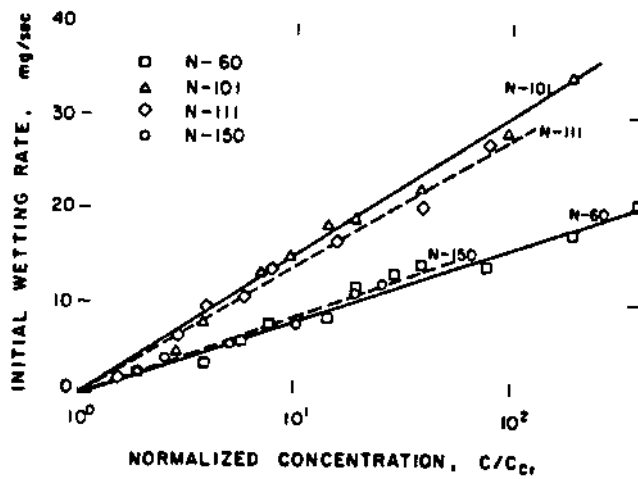


Fig. 4. The initial wetting rates for a HVA-bituminous coal as a function of normalized concentration for various ethoxylated nonyl phenols.

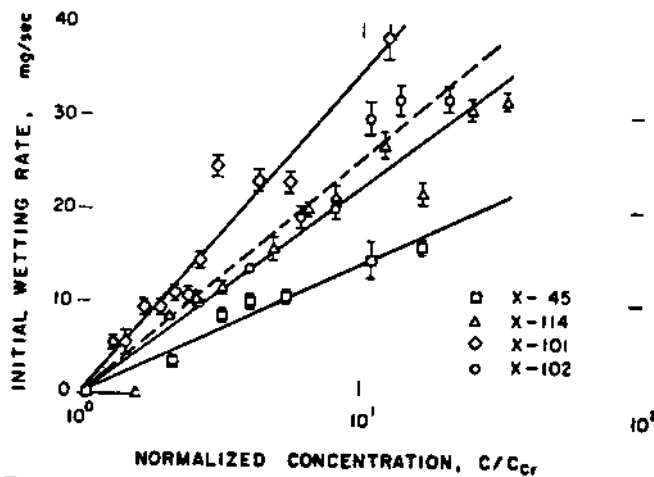


Fig. 5. The initial wetting rates for HVA-bituminous coal as a function of normalized concentrations for various ethoxylated octyl phenols.

determined by wetting rate tests (Table 2) for these surfactants are shown by vertical arrows in both the figures.

The increase in contact angles at low concentration can be used to explain the zero wetting rate at concentrations below C_{cr} . At these concentrations the surfactant adsorbs on the hydrophilic sites at the coal surface through the polar head groups thus making coal more hydrophobic and non-wettable. Since coal consists of a distribution of hydrophilic sites on a hydrophobic surface [13], it is likely that at low surfactant concentrations, adsorption occurs simultaneously through hydrophobic interactions between the hydrocarbon chain and

WETTING BEHAVIOR OF COAL

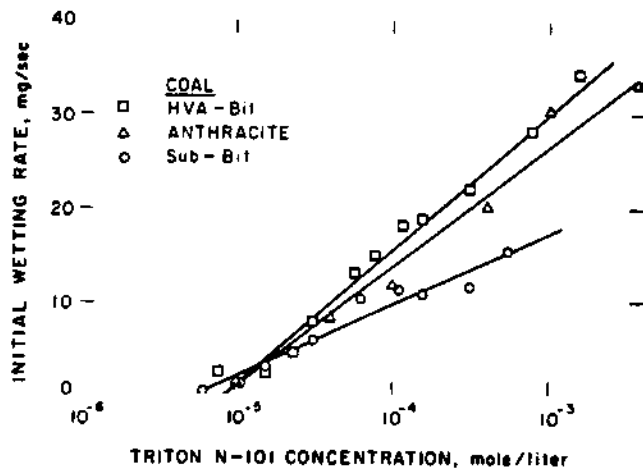


Fig. 6. The initial wetting rates for various coals as a function of Triton N-101 concentration.

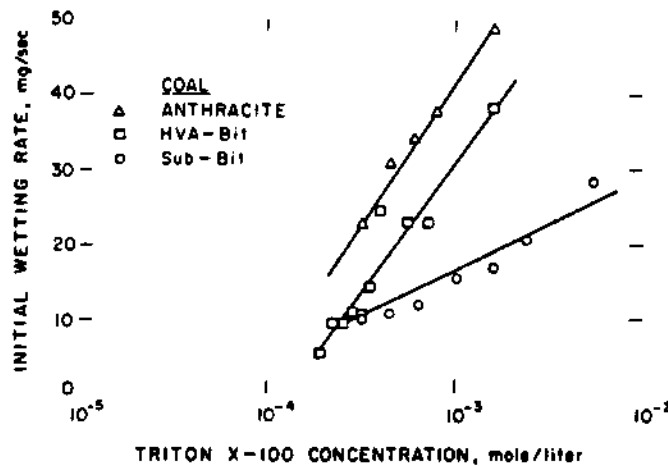


Fig. 7. The initial wetting rates for various coals as a function of Triton X-100 concentration.

the hydrophobic coal and through polar interactions between the ethoxylated group in the adsorbed molecule and the hydrophilic sites at the surface of coal. At high surfactant concentrations, the surfactant molecules adsorb through hydrophobic chain interactions with a resultant decrease in contact angle and an increase in the rate of wetting. A direct correspondence between the wetting rates and the contact angles is not observed, however. For example, for Triton N-101 wetting occurs as soon as the concentration is such that the contact angle begins to decrease from its maximum value which is 75° for the HVA-bituminous coal and 70° for the anthracite. For Triton X-100, the contact angle must be reduced to ~55° for the HVA-bituminous coal and to ~50° for the anthracite coal before wetting is observed. Furthermore, on the basis of a

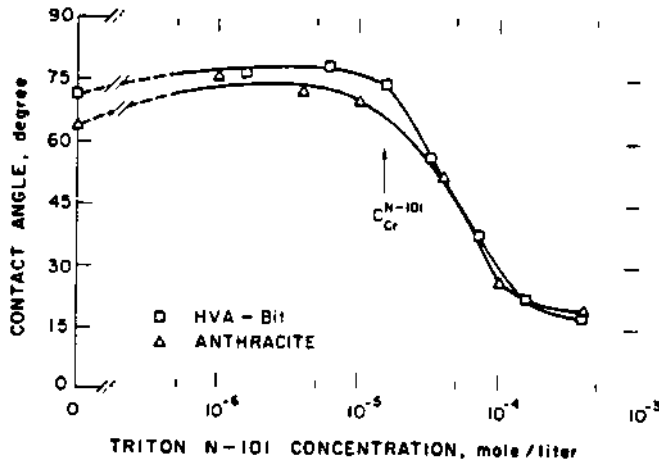


Fig. 8. The sessile drop contact angles for a HVA-bituminous coal and an anthracite coal as a function of Triton N-101 concentration.

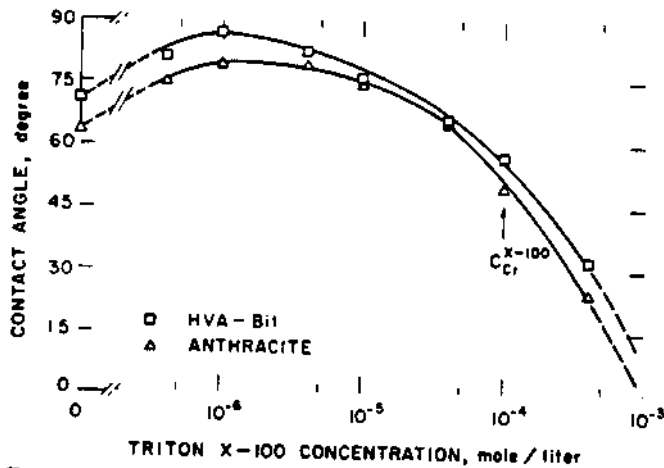


Fig. 9. The sessile drop contact angles for a HVA-bituminous coal and an anthracite coal as a function of Triton X-100 concentration.

thermodynamic analysis, involving the concept of immersional wetting ($W_I = \gamma_{SL} - \gamma_{SV} = -\gamma_{LV} \cos \theta$), a large effect on wetting rate is not expected when contact angle changes from $\sim 75^\circ$ to $\sim 50^\circ$.

Contact angles — advancing

In an attempt to explain these observations, advancing contact angles were measured and the results are presented in Fig. 10. From the concept of immersional wetting the free energies involved in transfer of particles from air into

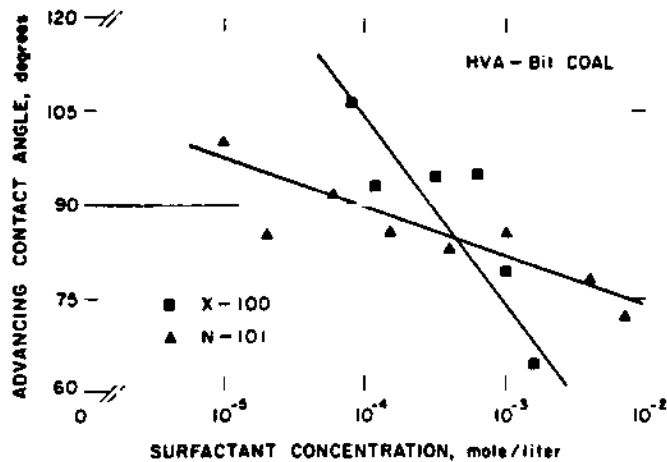


Fig. 10. The advancing contact angles for a HVA-bituminous coal as a function of concentration for Triton N-101 and Triton X-100.

an aqueous solution, wetting is expected when the contact angle is less than 90° . The results in Fig. 10 show that the effect of surfactant concentration on the advancing contact angle is very different for the two surfactants. In fact, the higher slope of the contact angle versus concentration plot for Triton X-100 than for Triton N-101 is in agreement with the slopes of the wetting rate versus concentration plots for these two surfactants. The minimum concentrations needed to decrease the advancing contact angles below 90° is higher for Triton X-100 ($\sim 3 \times 10^{-4} M$) than for Triton N-101 ($\sim 10^{-4} M$). The C_{cr} values for the above surfactants are $1.3 \times 10^{-4} M$ and $\sim 1 \times 10^{-5} M$, respectively. These relate reasonably well but more importantly the slopes of the curves for the two surfactants (cf. Figs 4 and 5) for the wetting tests can be related to the slope of the curves in Fig. 10. Thus the concentration dependence of wetting rates can be explained in terms of the effect of surfactant concentration on advancing angles.

SUMMARY

On the basis of the results reported in the previous section, it may be concluded that the wetting of coal particles depends upon the nature of interactions between coal surface and the surfactant. At low concentrations, the surfactant adsorbs through the polar ethoxy head group making coal non-wettable. Most likely, the hydrocarbon chains lie parallel to the surface resulting in an increased free energy of adsorption due to hydrophobic interactions between the hydrocarbon chain of the surfactant and the hydrophobic surface of coal. With increasing concentration, the contact angle decreases and the rate of wetting of coal increases. At higher concentrations, the orientation of

adsorbed molecules is likely to be such that the polar ethoxy groups are oriented towards the solution.

The wetting behavior of coals by surfactant solutions varies with the coal rank because the nature of coal-surfactant interactions depends upon both the properties of the surfactant and type of hydrophilic and hydrophobic sites on the coal surface. Thus, the effectiveness of a given surfactant as a wetting agent for coal may be expected to vary with coal rank. For a HVA-bituminous coal, Triton-N-101 was found to be a superior wetting agent whereas for an anthracite coal, Triton X-100 was superior.

The results of wetting rate measurements correlate very well with the advancing contact angles. A comparison of the effect of surfactant concentration on wetting rate shows that the slope of the wetting rate versus logarithm of concentration plot for Triton X-100 is greater than the slope for Triton N-101 (cf. Figs 4 and 5). The slope of the advancing contact angle versus logarithm of concentration plots for Triton X-100 is also significantly greater than the slope for Triton N-101. Wetting is observed for conditions when the advancing contact angle decreases below about 100° . Thermodynamically, wetting is expected when the contact angle would be less than 90° . The slight difference is probably due to: (1) the differences in geometry of the system (the contact angles are measured on a polished surface whereas the wetting rate measurements are made with particles dropped onto an air/solution interface); (2) the effect of particle-particle interactions at the interface on wetting rate measurements. (More recently, through direct observation of a particle at interfaces, we have observed that the time of wetting of a particle is influenced by the presence of another particle at the interface.)

ACKNOWLEDGEMENTS

The authors acknowledge the support from the Mineral Institutes Program under Grant No. G1135142 from the Bureau of Mines, U.S. Department of the Interior, as part of the Generic Mineral Technology Center for Respirable Dust, The Pennsylvania State University. The support from the National Science Foundation, under equipment Grant No. CPE-8406276 is also acknowledged.

REFERENCES

- 1 G.D. Parfitt, *Dispersion of Powders in Liquids*, 3rd edn, Applied Science Publishers, Barking, 1982.
- 2 Anon., *Rock Prod.*, 65 (August 1962) 92-96.
- 3 R. Harold, *Coal Age*, 84 (June 1979) 102-105.
- 4 T. Kobrick, *U.S. Bur. Mines Inf. Circ.*, 8458 (1969) 123-131.
- 5 P. Green, *Coal Age*, 87 (August 1982) 72-75.
- 6 P.L. Walker, E.E. Peterson and C.C. Wright, *Ind. Eng. Chem.*, 44 (1952) 2389-2392.

WETTING BEHAVIOR OF COAL

- 7 C.Z. Draves and R.C. Clarkson, *Am. Dyestuff Reporter*, 20 (March 1931) 109-116.
- 8 N. Feldstein, U.S. Bureau of Mines OFR 127-81, 1981, 47 pp., NTIS PB 82-104654.
- 9 M.M. Papić and A.D. McIntyre, *Coal Age*, 78 (June 1973) 85-87.
- 10 J.A. Kost, G.A. Shirey and C.T. Ford, U.S. Bureau of Mines OFR 30-82, 1980, 188 pp., NTIS PB 82-183344.
- 11 J.O. Glanville and J.P. Wightman, *Fuel*, 58 (1979) 819-822.
- 12 S. Garshve, S. Contreras and J. Goldfarb, *Colloid Polym. Sci.*, 256 (1978) 241-250.
- 13 J.A. Gutierrez-Rodriguez, R.J. Purcell Jr. and F.F. Aplan, *Colloids Surfaces*, 12 (1984) 1-25.
- 14 E.H. Crook, D.B. Fordyce and G.F. Trebbi, *J. Phys. Chem.*, 67 (1963) 1987-1994.

Surfactant Adsorption and Wetting Behavior of Freshly Ground and Aged Coal

B.R. Mohal and S. Chander

Department of Mineral Engineering, Mineral Processing Section,
The Pennsylvania State University

ABSTRACT

The adsorption and wetting behavior of freshly ground and aged coals has been determined in the presence of a nonionic surfactant. The amount of surfactant adsorption changes with the concentration and "age" of the coal. The freshly ground coal has smaller amounts of adsorption at lower surfactant concentrations than the "aged" coal whereas at large surfactant concentrations, the order is reversed. In the latter case, more surfactant is adsorbed on fresh coal than on the "aged" coal. It is proposed that at low concentrations, the surfactant adsorbs through both hydrophobic and hydrophilic interactions with the molecule lying parallel to the surface, whereas at higher concentrations surface micelles form at the hydrophobic sites. The wetting behavior correlates well with the adsorption behavior.

INTRODUCTION

Nonionic surfactants have many applications in the coal and mineral processing industry. They can be used as dispersing agents to modulate flotation, flocculation and filtration of particulates (1). They can also be used to increase the wettability of hydrophobic solids such as coal and can hence be used as dust suppressants (2,3). Although the adsorption of representative nonionic surfactants such as Triton N-101 (an ethoxylated nonylphenol with 9.5 moles of ethylene oxide and HLB equal to 13.4) have been studied extensively on substrates such as calcium carbonate (4), silica (5) carbon black (6) and graphite (7), very few studies are available for coals. Coals differ from other substrates with respect to two important characteristics: 1) coal are porous and 2) coals consist of a patchwork of hydrophobic and hydrophilic sites (8). Since the adsorption characteristics of a surfactant are influenced significantly by the nature of the substrate the characteristics of the coals must be taken into consideration.

Kinetics of surfactant adsorption is likely to have a major influence on the wetting of coal, since the coal particles are wetted in a

few seconds or less (9). Equilibrium adsorption measurements are normally carried out for a period ranging from of 2 to 18 hours to achieve equilibrium (4,5). For porous solids such as coal, the surfactant molecules can diffuse into the pores of the coal thereby showing a much greater adsorption than would be possible on the external surface only. Therefore for wetting studies in which the coal particles are wetted in a few seconds, the wetting test data might not be directly relatable to equilibrium adsorption measurements. In addition, it is well known that coal particles undergo disintegration when being agitated during the adsorption tests. The disintegration and dissolutions of dissolved species (10) is a function of time and would therefore have an influence on the equilibrium adsorption results. The influence of the dissolution of species from coal probably does not exist during the time frame of a few seconds during which wetting occurs. Thus the rapid adsorption studies become even more important to understand the mechanisms of surfactant-coal interactions during rapid processes such as wetting.

In this investigation, rapid adsorption measurements have been made to study the influence of aging on wetting behavior of coals in the presence of surfactants. It is well known that oxidation or aging of coal increases the relative proportion of the hydrophilic sites of coal and effect their floatability (11). These studies have been conducted to determine the effect of the relative amounts of hydrophobic to hydrophilic sites on coal on the mechanism of surfactant adsorption.

EXPERIMENTAL MATERIALS AND METHODS

Coal and Reagents

The two coal samples used in this investigation were: a HVA bituminous coal from the Upper Freeport seam (PSOC 1361p) and a sub-bituminous A coal from Colorado (PSOC 1382p), both were obtained from the Penn State Coal Data Bank. The analysis of the coals are given in Table 1. The coal samples were crushed and screened to obtain a 250 x 150 μm fraction used for the tests. For the aging tests coal samples were aged in ambient air for a period of one week.

The surfactant used in this investigation was an ethoxylated nonyl phenol (Triton N-101) obtained from Rohm and Haas. Conductivity water (18 mohm cm^{-1}) obtained from a Millipore Milli-Q water system was used

for the adsorption experiments. Distilled water from a tin lined Barnstead still equipped with a Q baffle system was used for the wetting experiments.

Surfactant Adsorption

For adsorption measurements a 10 g sample of 250 x 150 μm coal was deslimed over a 150 μm screen in distilled water. The coal was then placed in an agitated vessel and enough water added to make up the volume to 300 ml. A liquid sample was continuously withdrawn through a 10 μm filter with the help of a peristaltic pump and transferred to the spectrophotometer. A schematic of the apparatus is shown in Figure 1. At the start of the experiment the solution in the flow cell was referenced as the blank using an HP 8451A Diode Array Spectrophotometer. The UV spectra in the range 190-300 nm was then monitored every 1.2 seconds. A known quantity of surfactant (1-5 ml depending on the desired concentration) was injected 10 seconds after the solution was referenced. The adsorption test was carried out typically for about 6-7 hours. The coal was then filtered, dried and weighed. The surfactant Triton N-101 has two absorbance peaks at 224 nm and 276 nm due to the phenol. In the concentration range investigated the 224 nm peak was

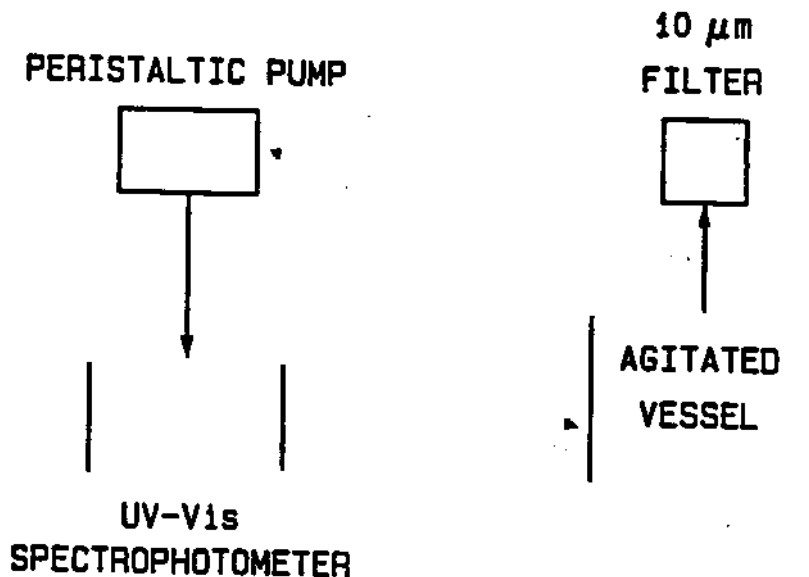


Fig. 1. Schematic of the setup for adsorption measurements.

ADSORPTION AND WETTING BEHAVIOR OF COAL

TABLE 1

Analysis of the coal samples

	<u>HVA-bituminous</u>	<u>Sub-bituminous</u>
H ₂ O	3.2 %	13.03 %
Proximate analysis (Dry basis %)		
Ash	8.47	5.65
VM	38.16	34.20
FC	53.37	47.12
Ultimate analysis (DAF basis %)		
C	81.94	75.19
H	5.7	5.04
N	1.54	2.01
S	2.12	0.40
O (Diff)	8.7	17.37
Surface area (250 μm x 150 μm fraction)		
N ₂ (BET) cm ² /g	3,300.0	2530.0*
Blaine cm ² /g	618.0	1942.0

* Estimated from Esposito (13)

TABLE 2

Free Energy and Area Per Molecule for Adsorption of Ethoxylated Nonyl Phenol

Concentration Range	ΔG Kcal/mole	area per molecule, Å ² -----basis-----		
		CO ₂ (DF)	N ₂ (BET)	Blaine
<u>Sub bituminous</u>				
<u>Fresh</u>				
Conc. < CMC	-9.07	6,400	70	33.7
Conc. > CMC	-8.07	2,400	26	20.0
<u>Aged</u>				
Conc. < CMC	-10.03	60,000	66	50.6
Conc. > CMC	-8.07	35,700	39	30.2
<u>HVA bituminous</u>				
<u>Fresh</u>				
Conc. < CMC	-9.19	105,000	151	28.2
Conc. > CMC	-7.83	42,000	61	11.4

THE RESPIRABLE DUST CENTER

linear and had a stronger absorbance than the 276 nm peak. Due to greater sensitivity of the former peak it was used for the adsorption isotherms.

Wetting Rate of Powders by the Modified Walker Method

In the Modified Walker Test a 30 mg sample of 250 x 150 μm coal was dropped on the surface of a surfactant solution and the amount of coal wetted by the liquid was measured by placing the pan of a Cahn electrobalance beneath the liquid surface. The initial wetting rates were determined from measurements of the amount of coal wetted as a function of time. The rate of wetting was found to be independent of the amount of the coal sample in the range 20-100 mg. The data reported for the wetting rates is an average of at least four replicate measurements in which the coefficient of variation was about 0.08. Additional details of the measurements are given elsewhere (9,12).

RESULTS AND DISCUSSION

Adsorption Kinetics

The absorbance at a wavelength of 224 nm of a solution containing 3×10^{-5} M (initial concentration) Triton N-101 is shown in Figure 2 with and without the addition of a HVA bituminous coal sample. The solution (without coal) reached 90 % of the equilibrium value in about 40 seconds and 100% in about 5 minutes after the addition of the surfactant. A constant absorbance thereafter showed negligible adsorption of the surfactant on the sides of the tubes or the agitated vessel.

In the experiment in which coal was present in the solution the absorbance first increased rapidly after the addition of the surfactant and then it started to decrease as the surfactant adsorbed on coal. The maximum absorbance was lower than the case where no coal was present. The plot of the absorbance vs. \sqrt{t} after the initial rapid adsorption is linear for a certain time period that ranged from about three to seven hours depending on the surfactant concentration. The mechanism of adsorption in this time period is considered to be that of slow diffusion into the pores of coal. Extrapolation of the linear diffusion curve to short times gives the amount of surfactant adsorbed at the external surface as shown in Figure 2. The absorbance becomes constant

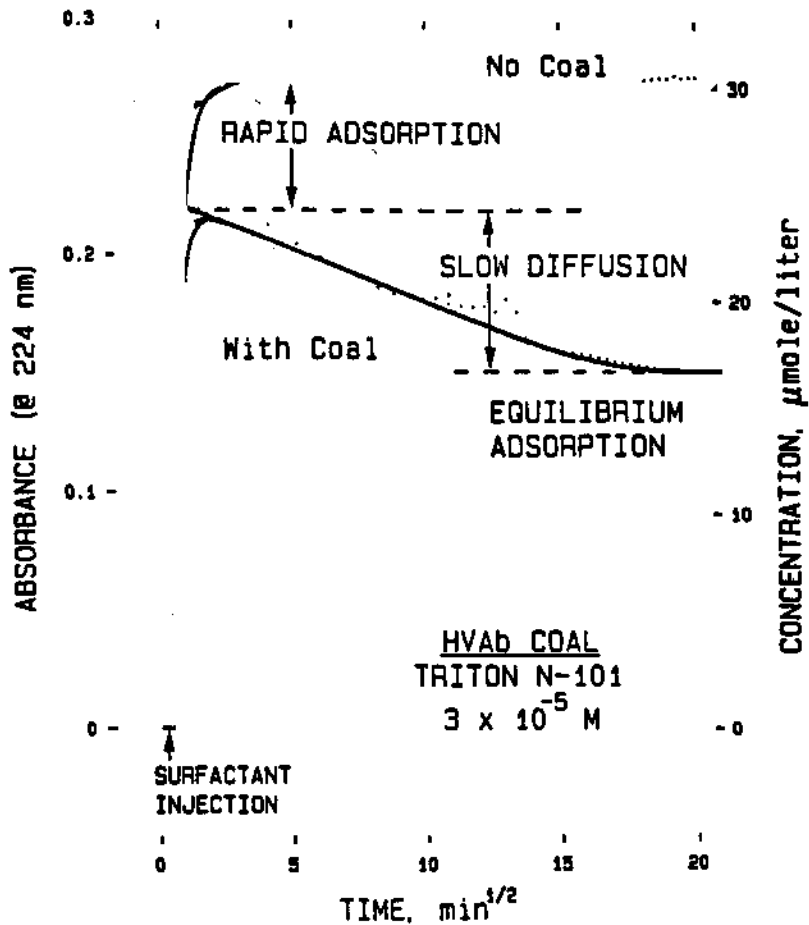


Fig. 2. Absorbance of a solution containing Triton N-101 with and without the presence of a HVA bituminous coal.

at longer times indicating equilibrium adsorption at the inner surface of the pores. The results of this aspect of the investigation will be reported elsewhere. Since different amounts of surfactant may be adsorbed depending upon the time for which adsorption is allowed to occur the amount of surfactant adsorbed during "Rapid" adsorption on the external surface was chosen as the parameter for comparison. The external area was measured using the Blaine surface area measurement device, so that the adsorption density at the external surface could be determined.

Disintegration and Dissolution of Coal During Surfactant Adsorption

It is well known that various soluble species are leached out from coal in an aqueous environment (10). These soluble species have an absorbance in the UV range and therefore can interfere in the determination of surfactant concentration using UV spectrophotometry. In order to determine the effect of the soluble leached species from coal on the absorbance measurements the spectra of the solution containing an aged

THE RESPIRABLE DUST CENTER

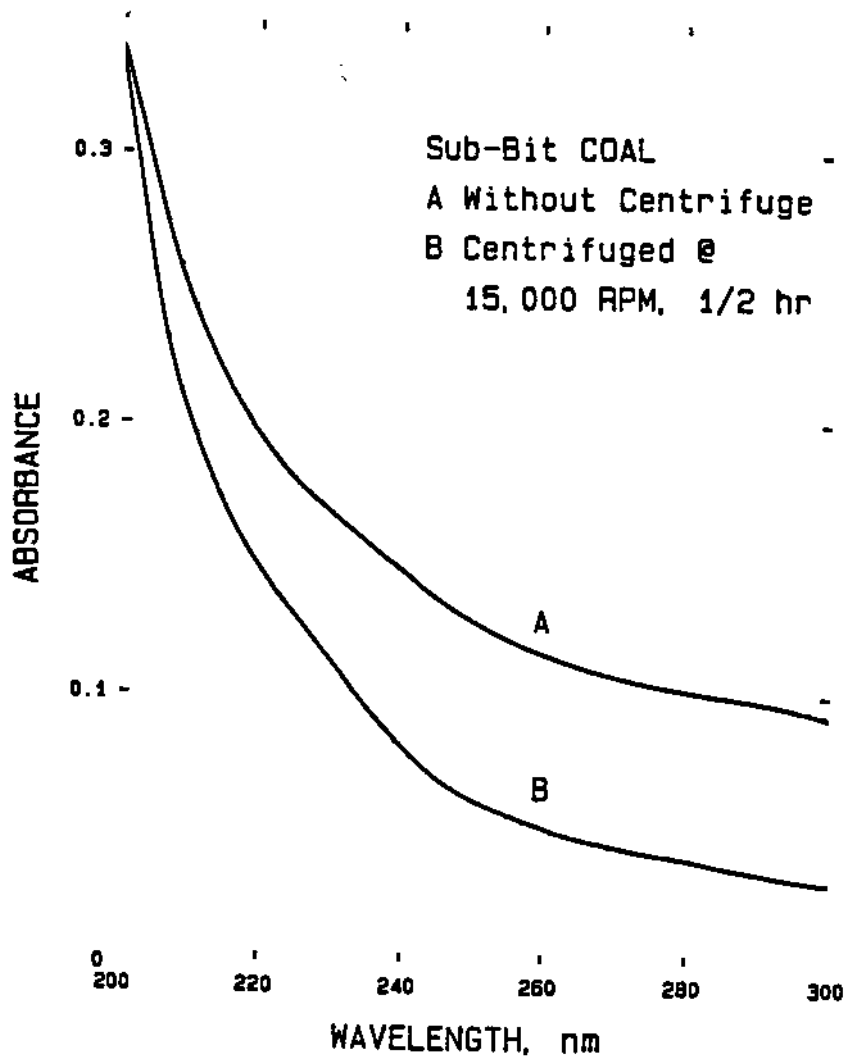


Fig. 3. Spectrum of a solution containing an aged sub-bituminous coal A) before centrifugation and B) after centrifugation at 15,000 RPM for 1/2 hour.

sub-bituminous coal was measured after equilibration for 2 1/2 hours and is shown as curve A in Figure 3. The spectra of the same solution after centrifugation at 15,000 RPM for 1/2 hr is shown as curve B in Figure 3. The decrease in the absorbance of the solution after centrifugation indicates that some fines are also being produced but they are not the sole cause for the increase in background absorbance. The amount of fines produced and the species dissolved depend upon the surfactant concentration as shown in Figure 4. In this figure the absorbance at 298 nm is plotted as a function of Triton N-101 concentration at various times of equilibration. Similar plots would result for other wavelengths also. The results at 298 nm were selected to minimize the effect of Triton N-101 absorbance on the spectra. At concentrations

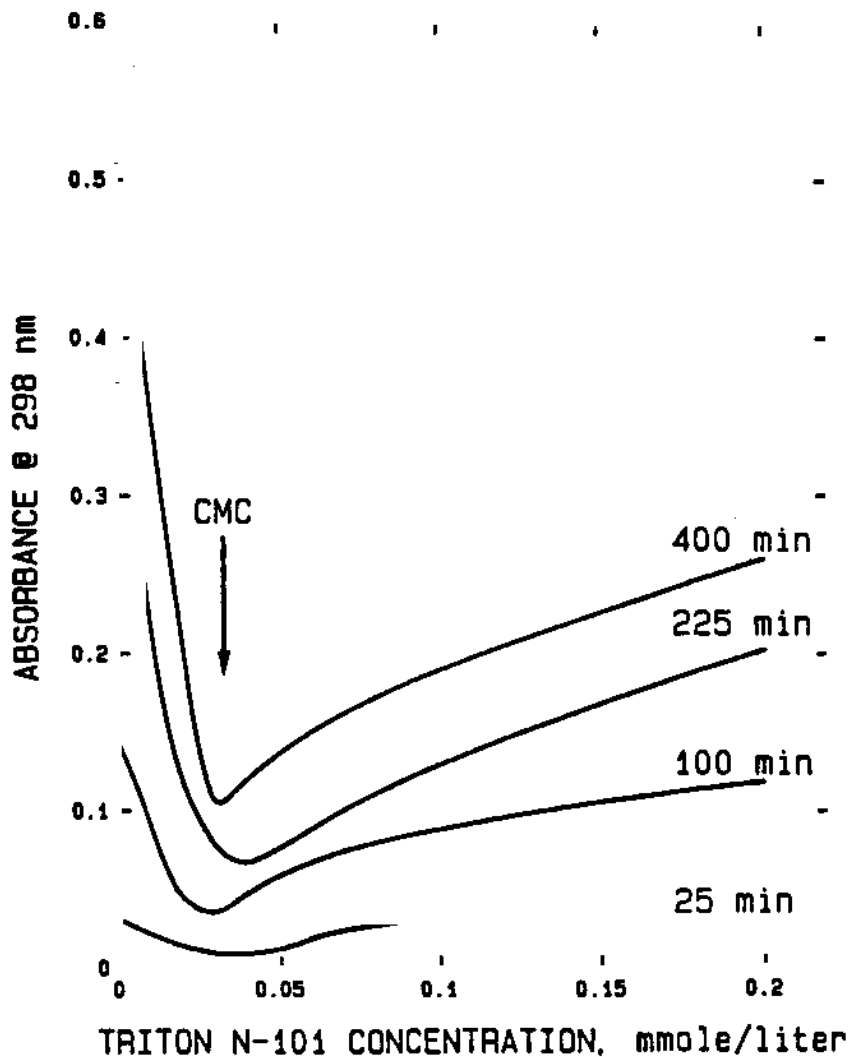


Fig. 4. Background absorbance at 298 nm for an aged sub-bituminous coal as a function of the Triton N-101 concentration.

below CMC the background absorbance decreases with increase in concentration whereas at concentrations above CMC the background absorbance increases.

For concentrations lower than the CMC the greater quantities of the monomer present in the solution tend to block the pores and slow the dissolution and disintegration of coal. For concentrations greater than the CMC the micelles can solublize the leached species and lead to an increase in the extent of dissolution and disintegration. The leaching is time dependant and therefore to minimize the interference from the leached species the "Rapid" adsorption on the external surface was chosen for subsequent experimentation.

THE RESPIRABLE DUST CENTER

Adsorption Isotherms

The rapid adsorption isotherms for Triton N-101 are given in Figure 5 for the fresh and aged sub-bituminous coal and in Figure 6 for the HVA bituminous coal. The corresponding Langmuir plots are given in Figure 7 and 8, respectively. The aged sub-bituminous coal adsorbs a greater amount of surfactant at concentrations less than the CMC and adsorbs a lesser amount at concentrations greater than the CMC than the freshly ground sample. The break in the Langmuir plot near the CMC indicates two modes of adsorption. For concentrations less than the CMC the adsorption is due to monomers, whereas for concentrations greater than the CMC the adsorption is due to "surface micelles". At longer times the adsorption continues to occur by diffusion of monomers into the pores of the coal as stated in a previous section.

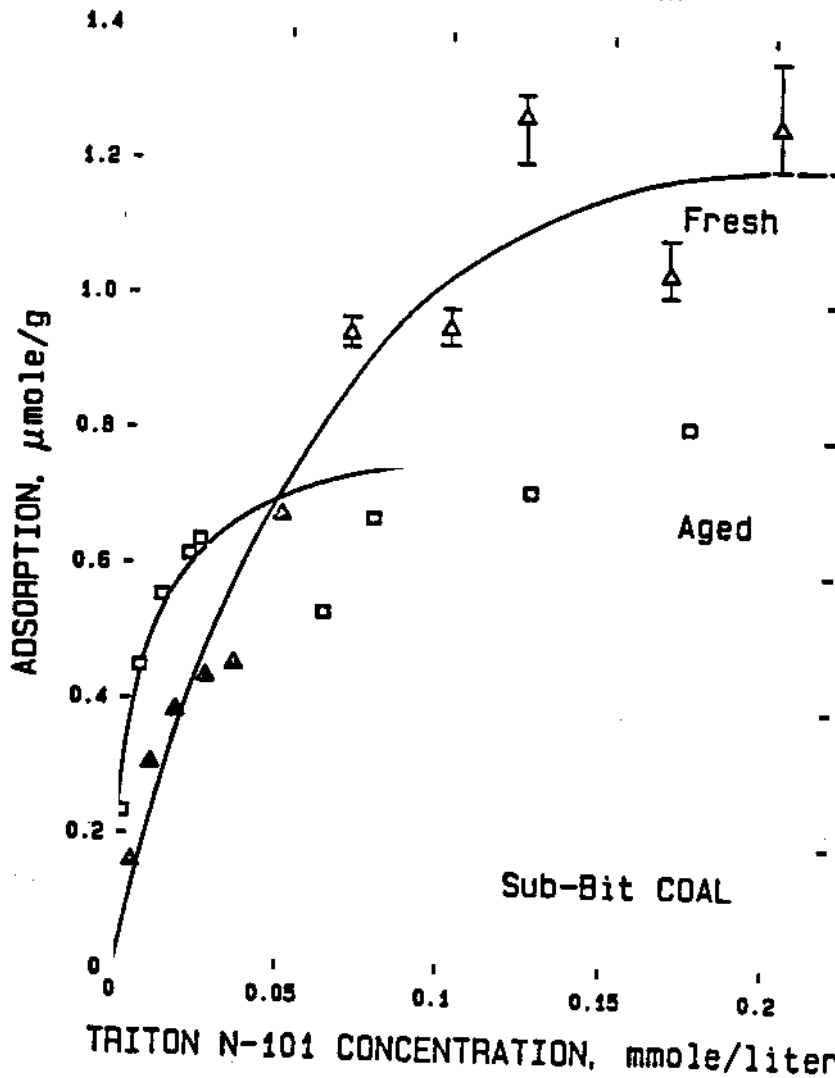


Fig. 5. Adsorption of Triton N-101 versus equilibrium concentration for a (Δ) freshly ground and (\square) aged sub-bituminous coal. (For filled symbols error bars are less than symbol size)

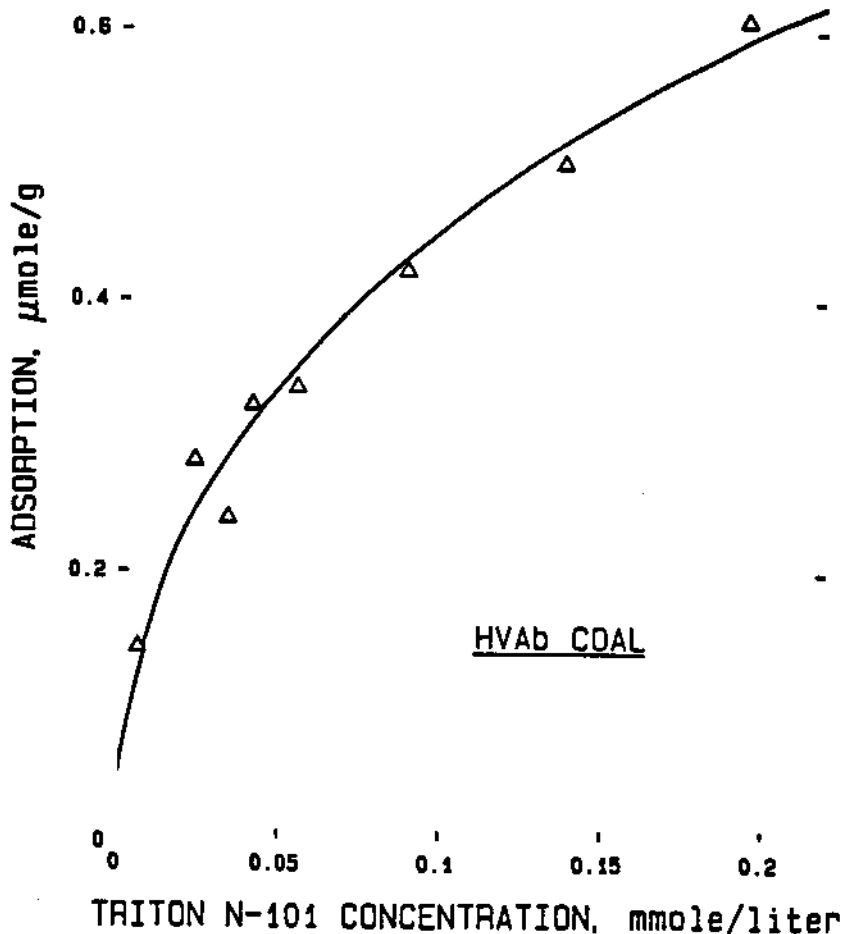


Fig. 6. Adsorption of Triton N-101 versus equilibrium concentration for a HVA bituminous coal.

At concentrations lower than the CMC the surfactant can adsorb on both the hydrophobic and hydrophilic sites of coal. The schematic of a surfactant molecule adsorbing on a hydrophobic substrate is shown in Figure 9. The adsorption on the hydrophobic sites is due to the hydrocarbon chain and the adsorption on the hydrophilic sites is due to hydrogen bonding between the substrate and the ethylene oxide part of the molecule. The free energy of adsorption for the aged coal surface is greater than the free energy of adsorption for the fresh coal surface for concentrations lower than the CMC as shown in Table 2. Since both types of adsorption (hydrocarbon chain interaction and hydrogen bonding) may take place simultaneously at low surfactant concentrations, the total adsorption would depend upon the relative proportion of hydro-

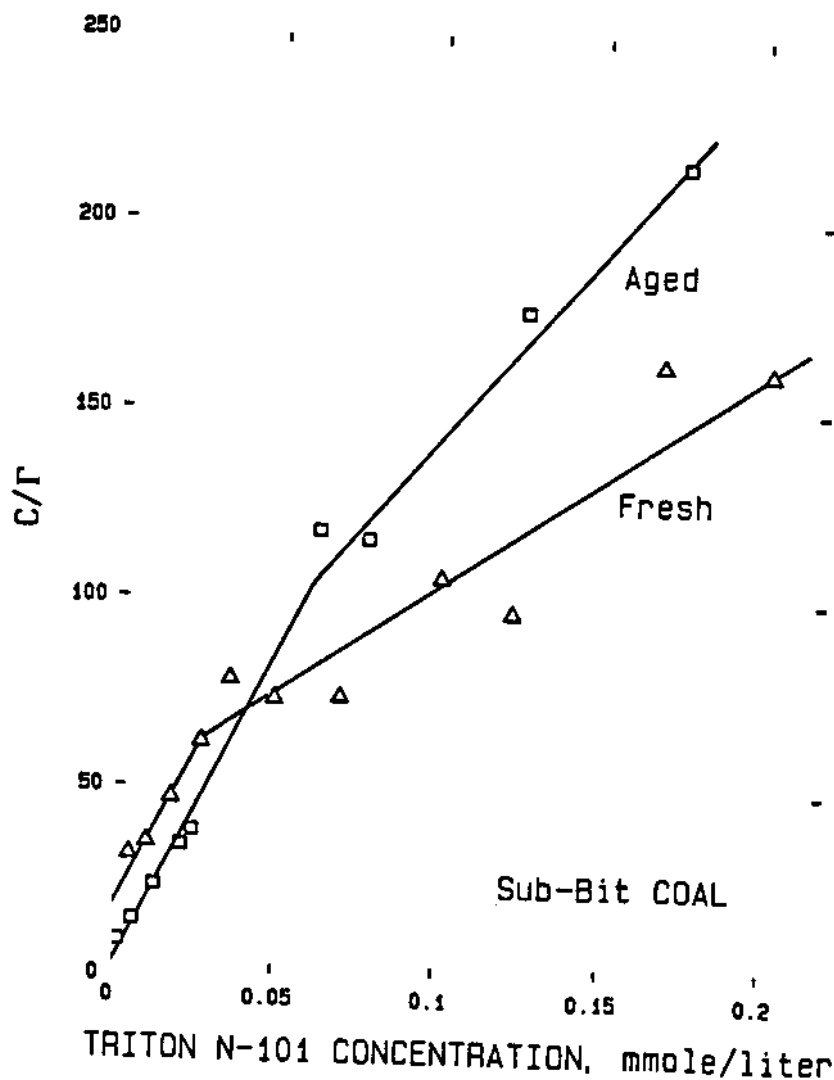


Fig. 7. Langmuir plot for adsorption of Triton N-101 on (Δ) freshly ground and (\square) aged sub-bituminous coal.

phobic and hydrophilic sites. The results show that the aged coal with a greater proportion of hydrophilic sites adsorbs a greater amount of surfactant as compared to the freshly ground coal.

At concentrations greater than the CMC, the relatively small area per molecule ($11.4 \text{ \AA}^2/\text{molecule}$ for the surfactant on the HVA bituminous coal and $20 \text{ \AA}^2/\text{molecule}$ for the sub-bituminous coal) as shown in Table II is much greater than what can be accounted for by a monolayer adsorption. The cross sectional area for Triton N-101 is about 56 \AA^2 (14) for the vertical orientation. Adsorption in multilayers might be considered but the shape of the adsorption isotherm is Langmuirian. Alternatively, one may consider that the micelles present in solution might attach through colloidal interaction but this mode is considered less likely

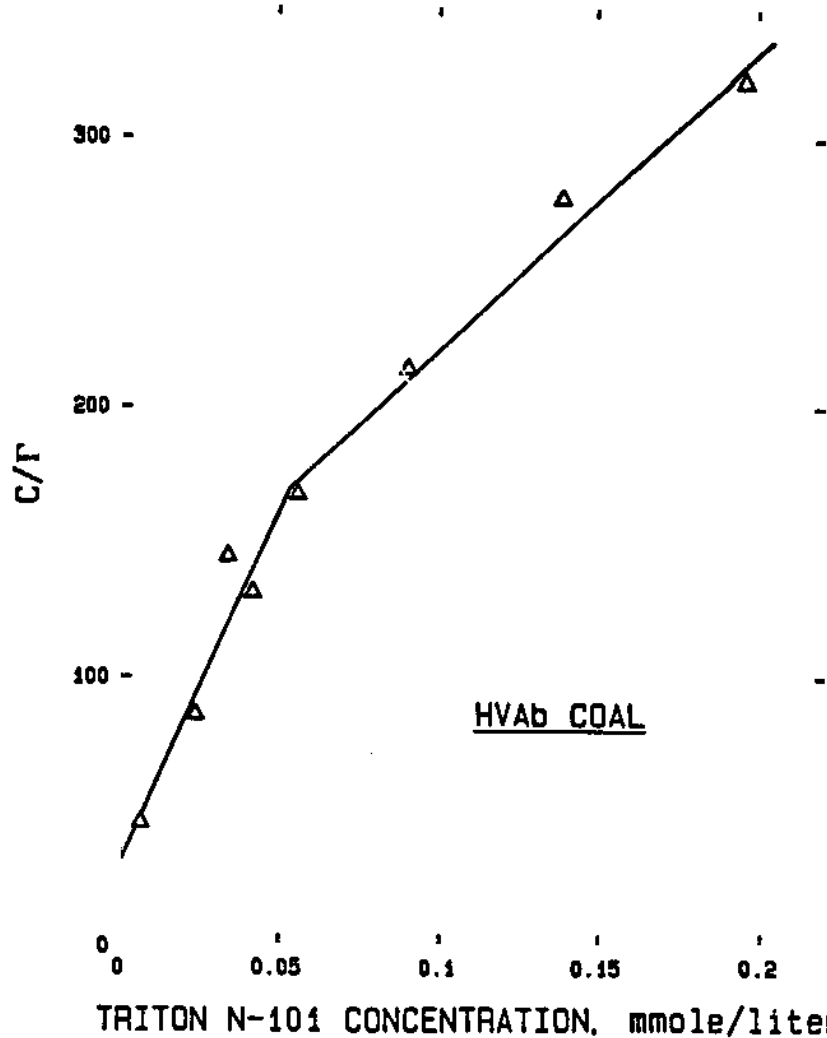


Fig. 8. Langmuir plot for adsorption of Triton N-101 on a HVA bituminous coal.

because the coal is hydrophobic whereas the micelle is hydrophilic. Therefore the concept of a "surface micelle" has been proposed in this investigation. A surface micelle is formed by a mechanism in which the surfactant adsorbs on the hydrophobic coal surface by hydrocarbon chain interaction in the horizontal orientation. More molecules can adsorb on this first layer due to hydrocarbon chain interaction by a mechanism very similar to the formation of a micelle in the bulk solution as shown in Figure 9b-d. The surface micelle can be considered to be equivalent of half a micelle with the hydrophilic portion (ethoxylated part) exposed to water. Coal particles are wetted very easily at these surfactant concentrations as discussed in the paragraphs that follow. The interaction energies for the surfactant at concentrations greater than the CMC with the three substrates : aged sub-bituminous coal, freshly ground sub-bituminous coal and a HVA bituminous coal are very

THE RESPIRABLE DUST CENTER

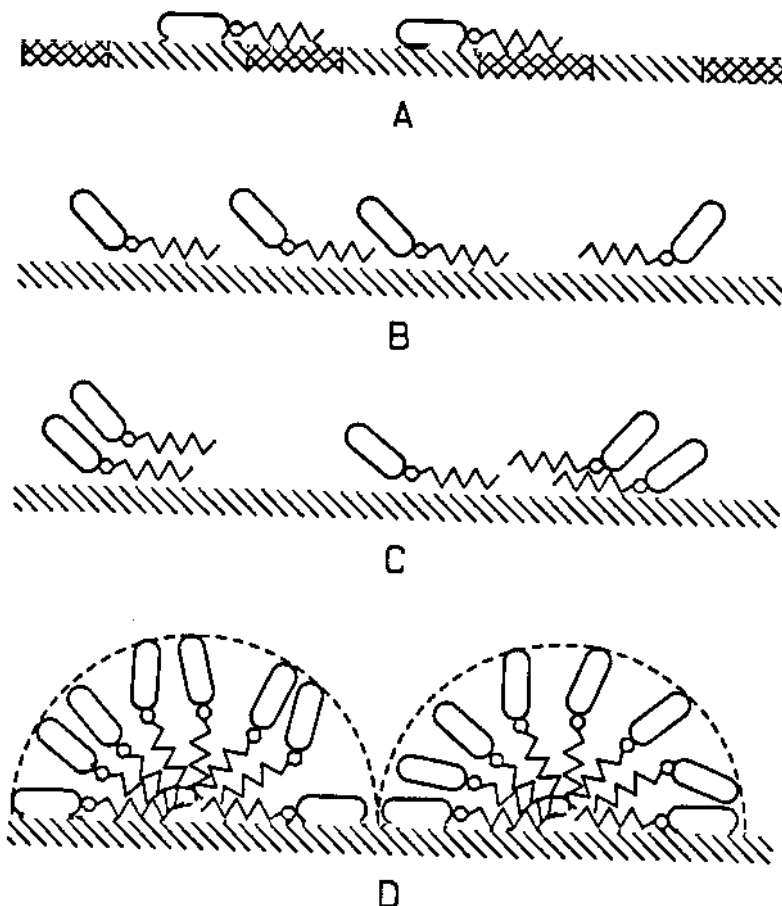


Fig. 9. A) Surfactant adsorption on a patchwork of hydrophobic and hydrophilic sites.
B) Surfactant adsorption on a predominantly hydrophobic surface.
C) Growth of Surface Micelles on hydrophobic sites.
D) Schematic of a surface micelle.

similar as shown in Table 2 which is consistent with the hypothesis that surface micelles are formed at energetically, similar sites which we consider to be the hydrophobic sites. Since the aged coal has a smaller number of hydrophobic sites the adsorption on it is less as shown in Figure 5 (at concentrations greater than CMC).

Wetting Rates

The initial wetting rates are shown in Figure 10 for fresh and aged sub-bituminous coals and in Figure 11 for fresh and aged HVA bituminous coal. The results show that there is an increased wetting of aged coal

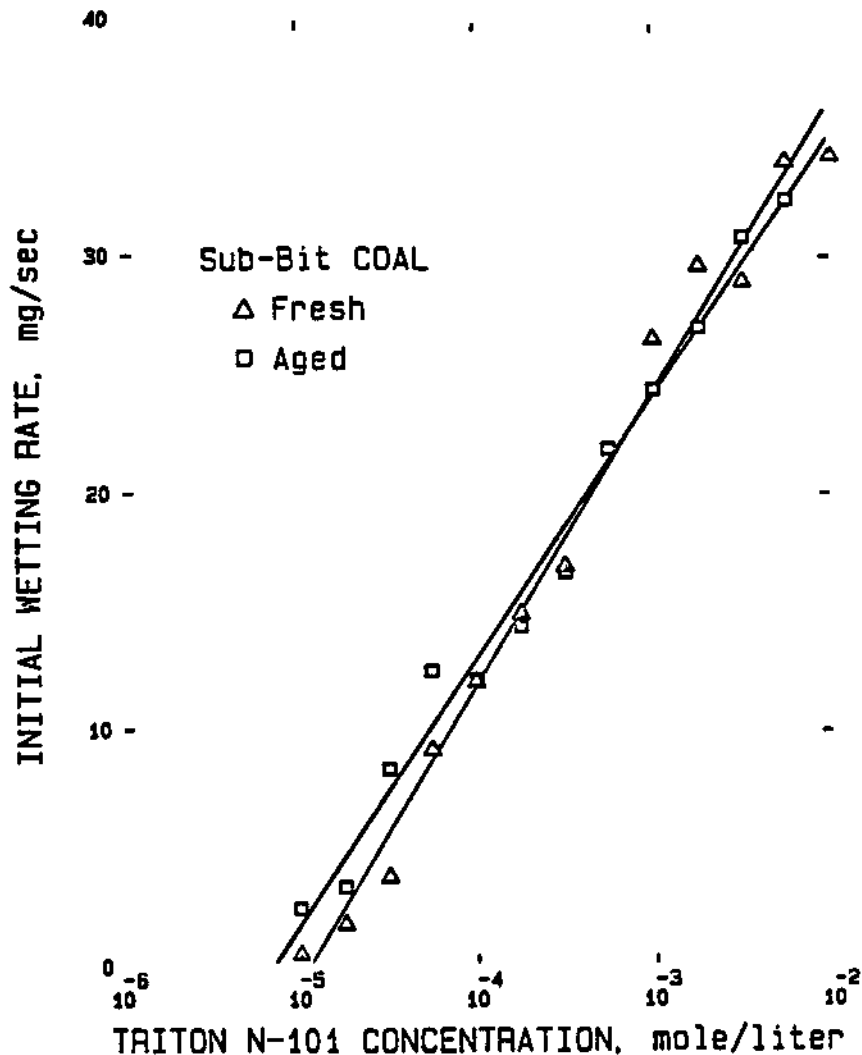


Fig. 10. Initial wetting rate vs. concentration for a (△) freshly ground and (□) aged sub-bituminous coal.

at low concentrations of the surfactant for both the sub-bituminous and the HVA bituminous coals. These results correlate well with the results in Figure 5 where at concentrations below the CMC the aged coal adsorbed a greater amount of the surfactant than the freshly ground coal. Wetting of the coal in this low concentration range implies the adsorption of the surfactant onto the hydrophobic coal surface by the hydrophobic chain such that the hydrophilic portion of the surfactant extends outwards, as represented in Figures 9b and c. At higher surfactant concentrations, the wetting rate of aged coal is less than that of the freshly ground sample for both the coals. These results also correlate with the effect of aging on adsorption densities. As stated in the previous section, the aged coal have a smaller density surface micelles which gives rise to a smaller rate of wetting.

THE RESPIRABLE DUST CENTER

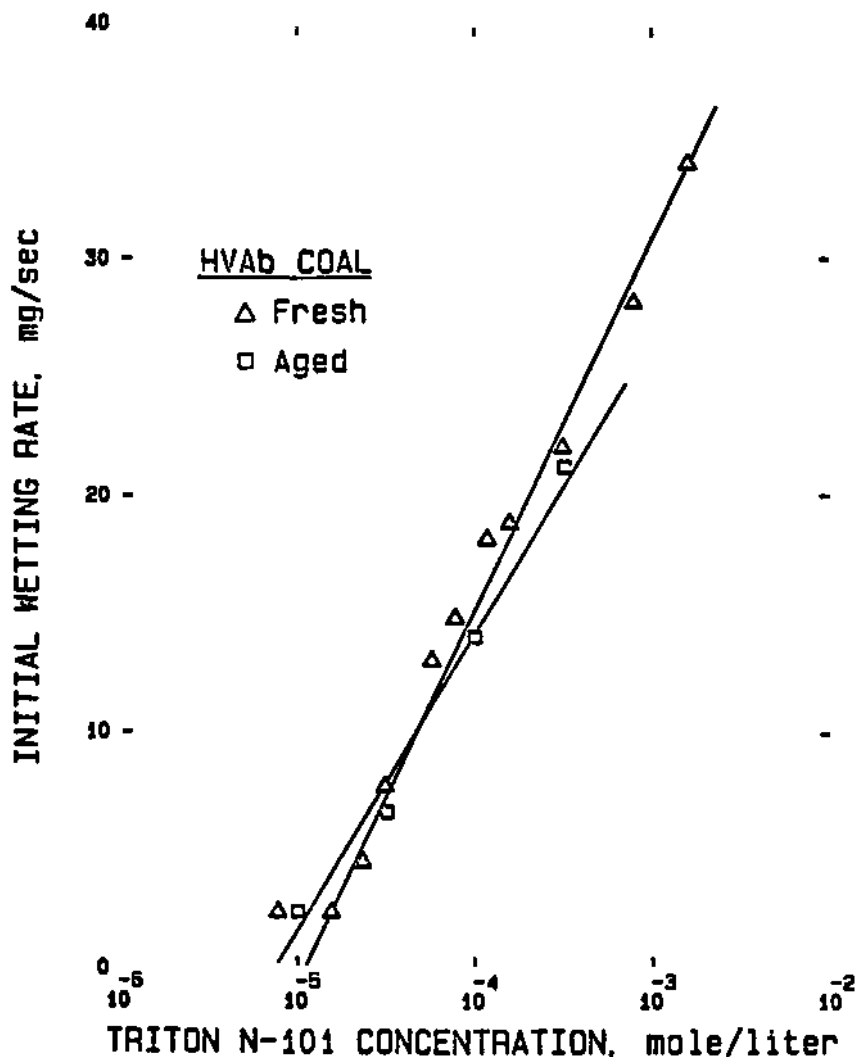


Fig. 11. Initial wetting rate vs. concentration for a (Δ) freshly ground and (\square) aged HVA bituminous coal.

SUMMARY

The adsorption of ethoxylated nonyl phenol on coal may be summarized as follows: rapid adsorption of the surfactant on the external surface; slow equilibration by diffusion of the surfactant into pores and adsorption on the internal surface. For coals investigated in this study the pores accessible by nitrogen in surface area determinations are available for surfactant adsorption also. The break in the Langmuir plot near the CMC indicates two different modes of adsorption. For concentrations below the CMC the adsorption is due to surfactant monomers. For concentrations above the CMC the adsorption is through the formation of surface micelles at the external hydrophobic surface and as monomers at the internal surface.

ADSORPTION AND WETTING BEHAVIOR OF COAL

This investigation shows that the presence of the surfactant affects the dissolution of species from coals. Significantly greater amount of soluble species leach out from the aged sub-bituminous coal as compared to the freshly ground coal. The amount of dissolved species depends upon the surfactant concentration with a dissolution minima at the CMC. For concentrations below the CMC, an increase in concentration of the monomer prevents the dissolution of the soluble species whereas for concentrations above the CMC the surfactant micelles can solublize the dissolving species and thus promote dissolution.

As compared to the freshly ground coal the aged coal adsorbs a greater amount of surfactant at concentrations less than the CMC and adsorbs a lesser amount at concentrations above the CMC. The effect of aging on surfactant adsorption can be explained if it is considered that the monomers adsorb (at conc. $<$ CMC) on both hydrophilic and hydrophobic sites whereas the surface micelles form (at conc. $>$ CMC) only at the hydrophobic sites. The wetting rates correlate very well with the adsorption results for both the HVA bituminous and the subbituminous coals.

ACKNOWLEDGEMENTS

The authors acknowledge the support from the Mineral Institutes Program under Grant No. G1135142 from the Bureau of Mines, U.S. Department of the Interior, as part of the Generic Mineral Technology Center for Respirable Dust, The Pennsylvania State University.

REFERENCES

1. G.D. Parfitt, Dispersion of Powders in Liquids, Applied Science Publishers, Third Ed., 1982.
2. R. Harold, Coal Age 84, No. 6 (June 1979) 102-105.
3. Anon., Rock Products, 65 No. 8 (August 1962) 92-96.
4. H. Kuno and R. Abe, Kolloid Zt., 177 (1961) 40-50.
5. D.N. Furlong and J.R. Aston, Colloids and Surfaces, 4 (1982) 121-129.
6. H. Kuno, R. Abe and S. Tahara, Kolloid Zt., 198 (1964) 77-81.
7. V.N. Moraru, F.D. Ovcharenko, L.I. Kobylinskya and T.V. Karmazina, Kolloid Zh., 46 (1984) 1148-1153.

THE RESPIRABLE DUST CENTER

8. J.A. Gutierrez-Rodriguez, R.J. Purcell Jr. and F.F. Aplan, *Colloids and Surfaces*, 21 (1984) 1-25.
9. B.R. Mohal and S. Chander, *Colloids and Surfaces*, 21 (1986) 193-203.
10. D.W. Fuerstenau and Pradip, *Colloids and Surfaces*, 4 (1982) 229-243.
11. J.A. Gutierrez-Rodriguez and F.F. Aplan, *Colloids and Surfaces*, 21 (1984) 27-51.
12. S. Chander, B.R. Mohal and F.F. Aplan, *Colloids and Surfaces*, (in press).
13. C. Esposito , M.S. Thesis, The Pennsylvania State University, 1986.
14. L. Hsiao, H.H. Dunning and P.B. Lorenz, *J. Phys. Chem.*, 60 (1956) 657-660.

Photoacoustic Spectroscopy of Quartz: Chopping Frequency Dependence, Saturation Phenomenon and Quantitative Analysis

M.S. Seehra, P.S. Raghootama and L. Cheng
Physics Department,
West Virginia University

ABSTRACT

The four major IR bands of α -quartz at 1080, 797, 693 and 488 cm^{-1} are studied at room temperature by FTIR-Photoacoustic Spectroscopy. Using Rosencwaig-Gersho theory, equations for the PAS signal q for the thermally thin and thermally thick cases are derived and it is shown how thin to thick transition occurs and leads to saturation as the sample mass is increased. For sample mass < 2 mg, q is proportional to sample mass thus defining the region for quantitative analysis. The dependence of q on the chopping frequency f is found to vary as $q \sim f^{-n}$ with $n \approx 0.9$ for quartz, in good agreement with the RG theory.

INTRODUCTION:

The technique of photoacoustic spectroscopy (PAS) is becoming an important tool for investigating the IR properties of materials.¹⁻⁸ This technique offers several advantages over the standard IR or FTIR spectroscopy (where samples usually need to be mixed with KBr and made into pellets): First, no special sample preparation is required in PAS; Second, opaque or light scattering substances can be studied by PAS; And third, depth profiling

of the samples is possible by changing the chopping frequency of the incident radiation. Despite these advantages, PAS has not yet reached the same level of acceptance as FTIR spectroscopy in quantitative analysis of samples because problems of saturation usually encountered in PAS are not yet fully resolved.

A detailed theory of the PAS in solids was first proposed by Rosencwaig and Gersho (RG).¹ There are three important length scales in this theory: the sample length l ; the optical absorption length $\mu_B = \beta^{-1}$, where β is the absorption coefficient of the sample; and the thermal diffusion length $\mu_S = (2\kappa/\rho c \omega)^{1/2}$, where κ is the thermal conductivity, ρ is the density, c is the specific heat and $\omega = 2\pi f$ is the chopping frequency. As f increases, μ_S decreases. This results in a decrease in the PAS signal since, now, a smaller volume of the sample contributes to the signal.

In this paper, we report the results of our recent studies on the PAS spectroscopy of α -quartz (hereafter referred to as quartz). The four prominent bands near 1080, 797, 693 and 488 cm^{-1} have been investigated as to their dependence on the chopping frequency and the sample mass leading to the saturation phenomenon. These results are compared with the predictions of the RG theory. Although the cases of thermally thick ($l \gg \mu_S$) and thermally thin ($l \ll \mu_S$) samples have been discussed in literature, (e.g. by Teng and Royce⁹ and Holter and Perkampus¹⁰ respectively) how one case merges into the other as the sample size is increased has not received adequate attention. Using the general result of the RG theory, we derive expressions for the two cases, compare our results with the theoretical predictions and demonstrate the conditions under which PAS can be used as a quantitative technique. We also study the chopping frequency dependence of the PAS signal for the cases when the chopping frequency f of the sample equals f_0 , the chopping frequency of the reference signal and when $f \neq f_0$. A good agreement with the theory is obtained. These results are presented and discussed in this paper.

Theoretical Considerations:

In order to put the experimental results in proper perspective, we briefly outline some of the important theoretical results based on the RG theory. For the thermally thick case ($l \gg \mu_B$) and for opaque samples (β large or $\mu_B \ll l$), the RG theory yields the following result for the PA signal Q

$$Q = \frac{C_s \beta \mu_B}{\sqrt{2} f} \left[\frac{(\beta \mu_B - 2) - i \beta \mu_B}{(\beta \mu_B)^2 - 2i} \right] \quad \text{--- (1)}$$

where

$$C_s = \frac{I_0 \gamma P_0 K_g}{2\pi l_g \rho_g c_g T_0 (\rho_g c_g + \rho_s c_s)} \quad \text{--- (2)}$$

In the above, g and s respectively refer to gas and sample in the PAS cell and other symbols have their usual meanings in the RG theory. If only the amplitude of the signal is detected, as in our work, then $q = |Q|$ is the observed signal and from Eq. (1), it follows that

$$q_s = \frac{C_s}{f} F(\beta \mu_B) \quad \text{--- (3)}$$

where

$$F(\beta \mu_B) = \left[\frac{(\beta \mu_B)^2}{(\beta \mu_B)^2 + 2(\beta \mu_B) + 2} \right]^{1/2} \quad \text{--- (4)}$$

Eq. (3) is, for example, discussed in Ref. 9 and applies to the thermally thick case.

For the thermally thin case ($l \ll \mu_B$), one can follow a similar procedure as above and show that

$$q_s = \frac{C_s}{f} F(\beta \mu_B) \cdot [1 - e^{-\beta l}] \quad \text{--- (5)}$$

Although in Ref. (10), an equation similar to Eq. (5) is given, it is shown only here, for the first time, that the function $F(\beta\mu_s)$ given by Eq. (4) is exactly the same for the thermally thick and thermally thin cases. This has important consequences when discussing the saturation phenomenon.

In actual experiments, the signal is referenced against a standard absorber such as carbon black for which $\beta\mu_s \gg 1$. The function $F(\beta\mu_s)$ then equals unity and referenced signal q is then given by

$$q(\text{thin}) = C_o \cdot \frac{f_o}{f} \cdot F(\beta\mu_s) \cdot [1 - e^{-\beta l}] \quad \text{--- (6)}$$

and

$$q(\text{thick}) = C_o \cdot \frac{f_o}{f} \cdot F(\beta\mu_s) \quad \text{--- (7)}$$

where f_o is the chopping frequency of the reference and

$$C_o = \frac{\rho_g C_g + \rho_r C_r}{\rho_g C_g + \rho_s C_s} \quad \text{--- (8)}$$

For very thin sample such that $\beta l \ll 1$, $q(\text{thin})$ is proportional to βl , the absorbance. For thick sample so that $\beta l \gg 1$, Eq. (6) reduces to Eq. (7), leading to the saturation phenomenon. An important consequence of Eq. (6) is that PAS signal is proportional to absorbance βl for the thermally thin case. Of course if $f = f_o$, then the only frequency dependence is the implicit dependence in the function $F(\beta\mu_s)$ through the frequency dependence of μ_s .

Pertinent Experimental Details:

The FTIR-PAS was carried out on Mattson Instruments Cygnus 100 FTIR spectrometer in conjunction with MTEC PAS cell. Normally, averages of 32

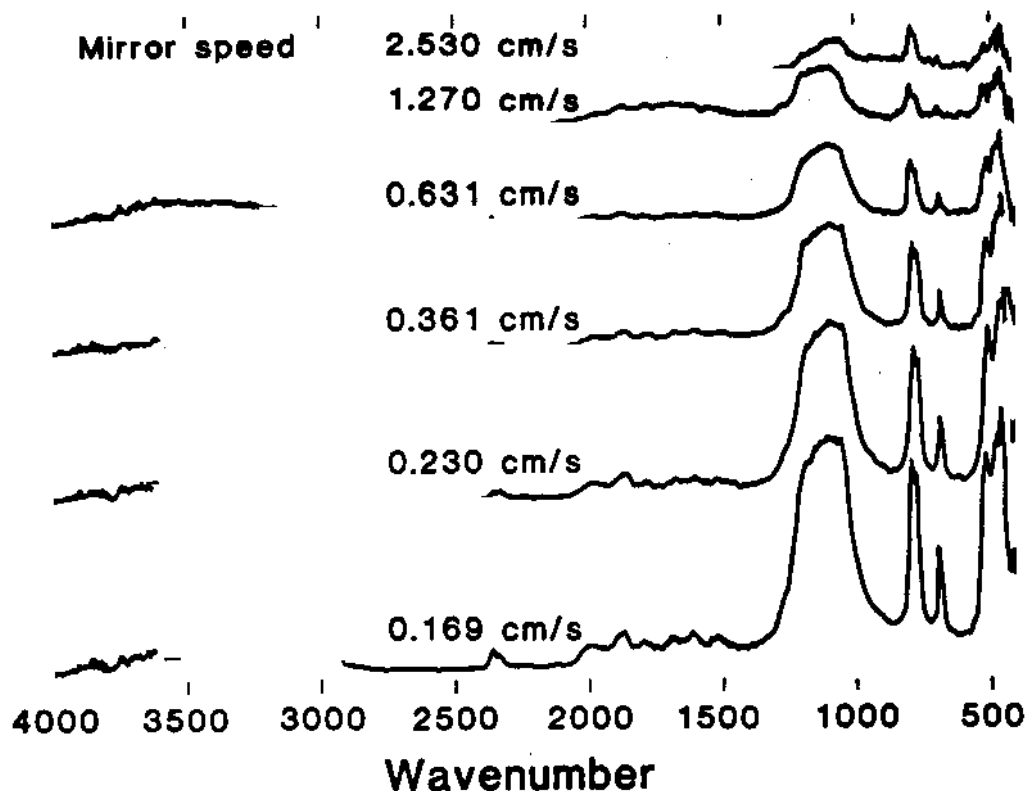


Fig. 1. Reproduction of the PAS signal of quartz at different mirror speeds.

scans at 8 cm^{-1} resolutions were recorded. The carbon black was dried at 200°C before it was used as the reference sample. McClelland³ has discussed in some detail major experimental aspects of the PAS. The powder sample of silica was obtained from Dr. W. E. Wallace of the National Institute of Occupational Safety and Health (NIOSH) and it had particle size $< 5 \mu\text{m}$. All spectra were taken at room temperature.

Experimental Results and Discussion:

Fig. 1 shows the photoacoustic spectra of quartz taken at different mirror speeds and under the condition $f \neq f_0$. From the mirror speed $V(\text{cm/s})$, the chopping frequency $f = V\nu$ can be determined for each spectral wave number ν in cm^{-1} . The decrease in the intensity of the peaks with increasing mirror speeds (or f) is obvious from fig. 1. These measurements refer to thermally thick case since the PAS sample cell was nearly filled with the sample. The

reference chopping frequency f_0 here corresponds to the lowest mirror speed.

The normalized intensity of the four major bands of quartz at 1080, 797, 693 and 488 cm^{-1} as a function of the chopping frequency f is shown in Fig. 2. Here $f \neq f_0$ and intensity refers to the area under the bands. The solid lines are theoretical fits to Eq. (7), where C_0 is evaluated by normalization at the lowest f and values of β for the various bands of quartz are from the work by Spitzer and Kleinman¹¹ ($\beta \cong 960, 295, 55, 715 \text{ cm}^{-1}$ for the 1080, 797, 693 and 488 cm^{-1} bands respectively and corresponding $\mu_s (\mu\text{m}) \cong 85, 100, 106$ and 126 respectively at 0.169 cm/s mirror speed). There is a general agreement between

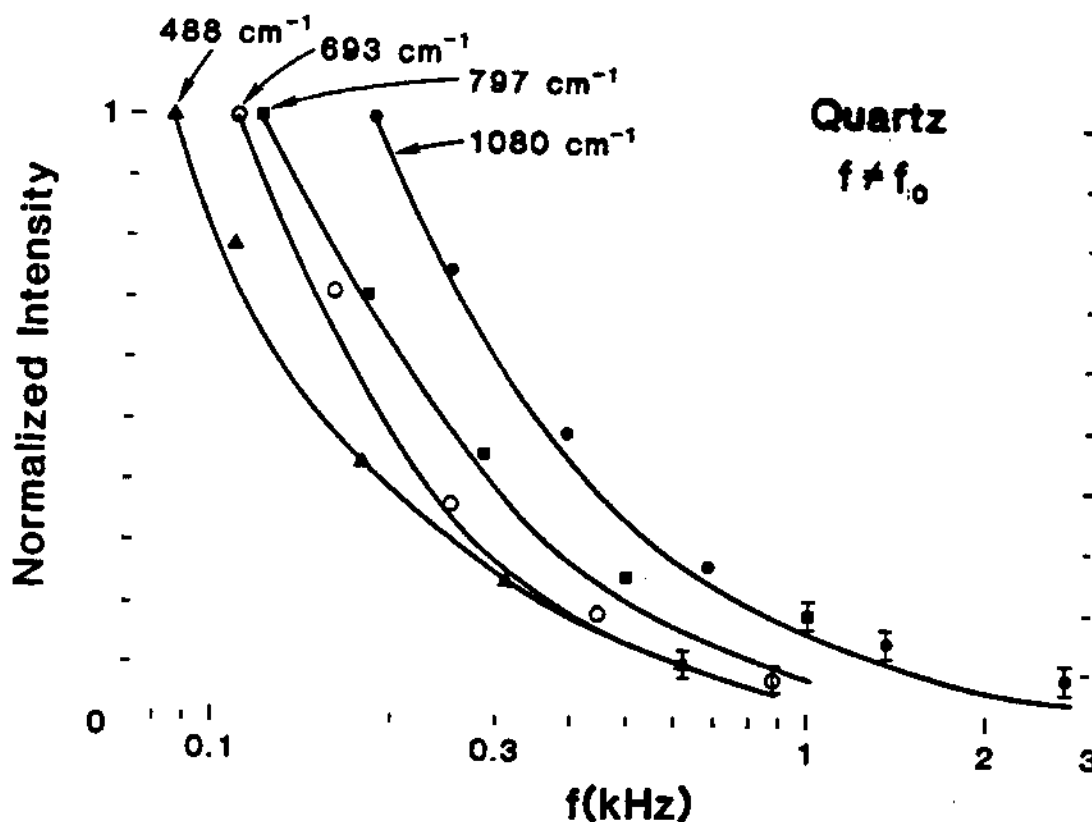


Fig. 2. Normalized intensity (area under bands) of the four bands of quartz as a function of the chopping frequency f . and f_0 corresponds to the lowest mirror speed = 0.169 cm/s in each case. The solid lines are fits to Eq. (7). μ_s was calculated using $\rho = 2650 \text{ kg/m}^3$, $c = 745 \text{ J/kg K}$ and $\kappa = 7.61 \text{ W/mK}$ for quartz.

theory and experiment, except for chopping frequencies above 1 kHz, where experimental values are a bit higher than the predictions.

In the case $f = f_0$, the frequency dependence is only due to the factor $F(\beta\mu_s)$. In this case, the comparison between theory and experiment is shown in Fig. 3 for the three bands. The data for the lowest band at 488 cm^{-1} is not shown because of the excessive noise. Excellent agreement is observed, suggesting that values of β used in the fit are correct.

Another way of plotting the data of Fig. 2 is shown in Fig. 4 as a log-log plot of q vs f . The slope of these plots, denoted by index n , vary

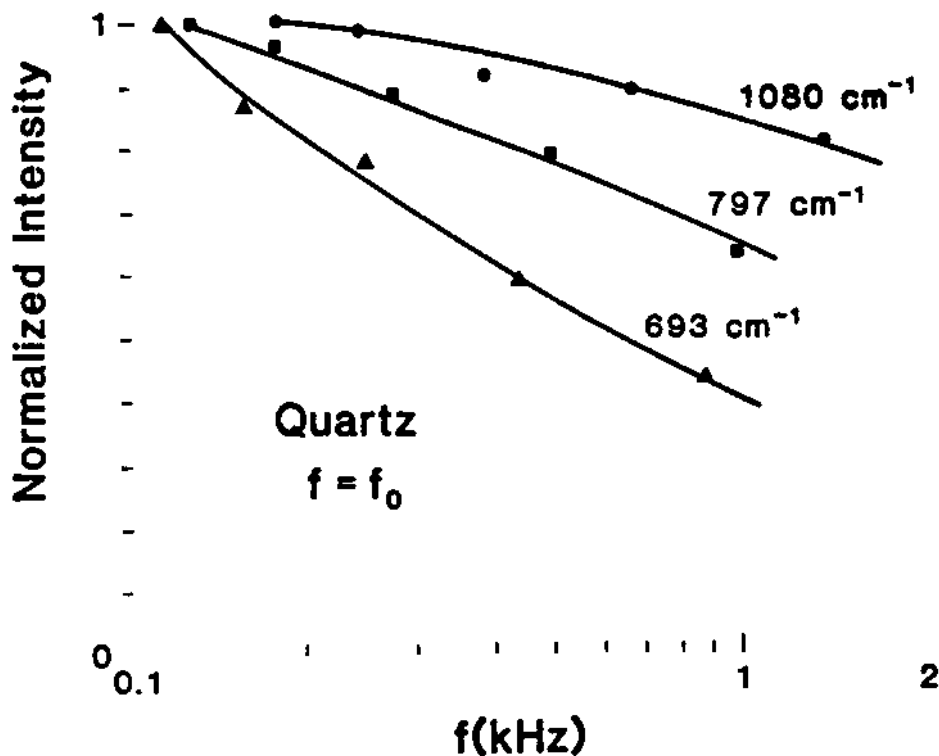


Fig. 3. Normalized intensity of three bands of quartz as a function of chopping frequency f . Here $f = f_0$ i.e. the signal from the sample and carbon black were taken at the same mirror speeds. The solid lines are fits to Eq. (7) with $f = f_0$.

between 0.82 for the 693 cm^{-1} band to 0.95 for the 797 cm^{-1} band. In the limit that $\beta\mu_s \gg 1$ and $f \neq f_0$, Eq. (7) yields $q \sim f^{-1}$ and for $\beta\mu_s \ll 1$, $q \sim f^{-3/2}$. For quartz $\beta\mu_s \gg 1$ for various bands and hence value of n near 1 observed here are quite understandable.

The saturation behavior of the three bands is shown in Fig. 5, where we have plotted the PAS intensity of a band against the sample mass. The solid line is a fit to Eq. (6) where all the dependence on the sample mass is contained in the term $e^{-\beta\mu}$ and the curve was normalized at one point. We note that μ is proportional to mass since the base area of the sample cup is constant in each case. The saturation limit is given by Eq. (7) and here it

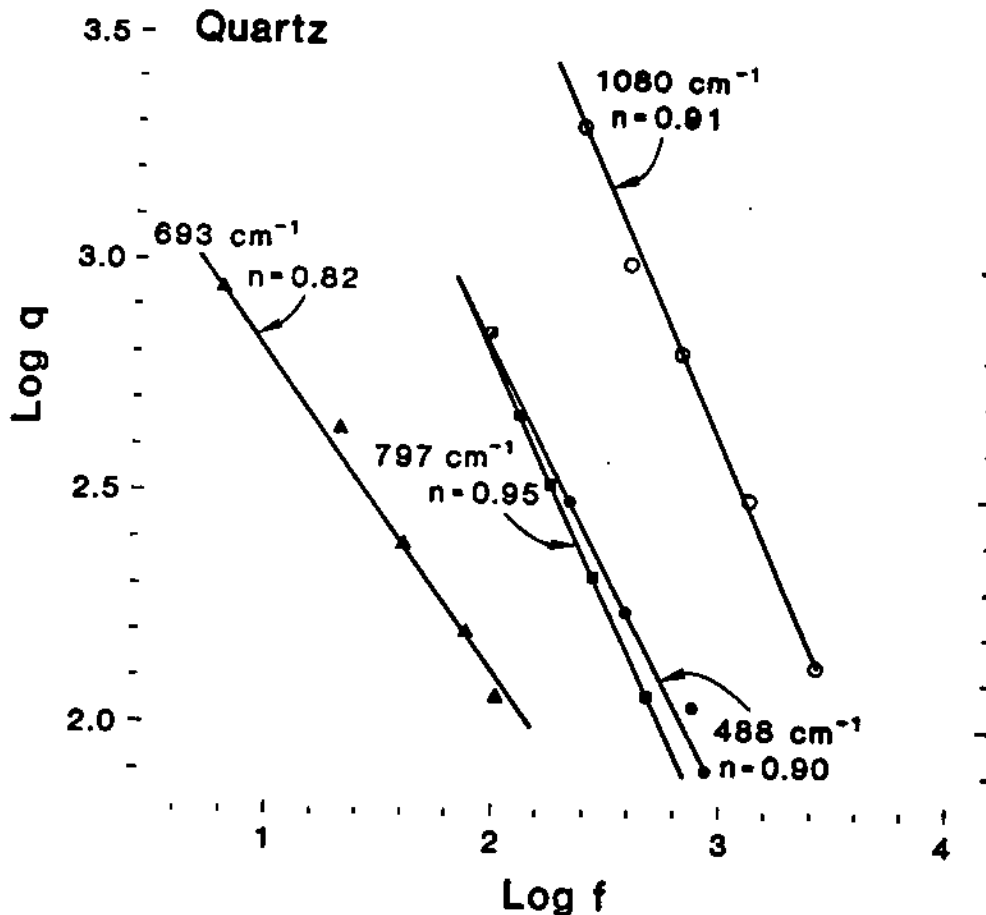


Fig. 4. Plot of Log q versus Log f to determine n in the equation $q \sim f^{-n}$.

The experimental values of n for various bands are shown. The data were at the lowest mirror speed.

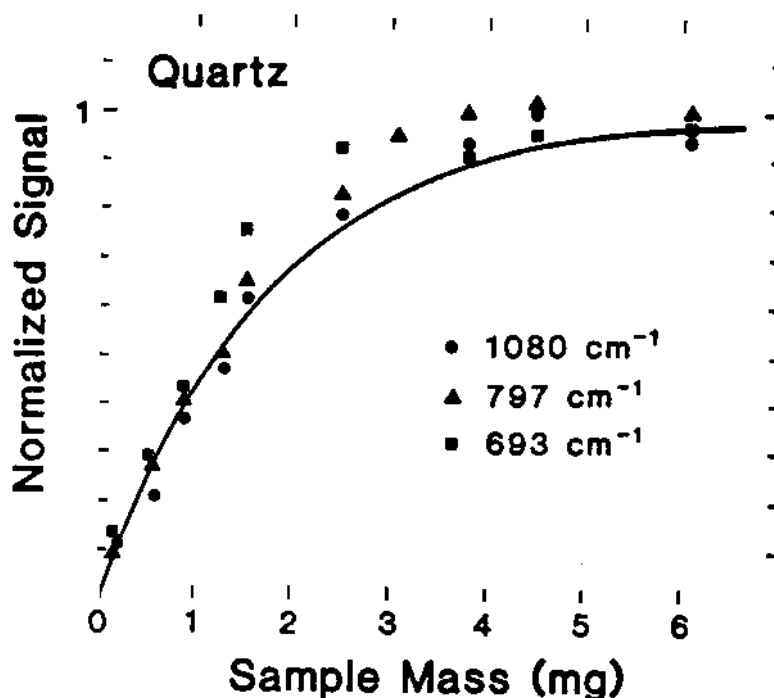


Fig. 5. Normalized PAS signal (area under bands) against sample mass of quartz for the three bands indicated. The solid line is fit to Eq. (6) and the saturated value is normalized to unity. The data were taken at the lowest mirror speed.

is normalized to unity. It is clear that major features of the data are well described by Eq. (6). For small masses, the PAS signal does measure the absorbance βl of the sample. For quartz, near saturation is observed for sample masses > 2 mg.

For the narrowest band of quartz viz. band at 693 cm^{-1} , we have compared the signal for PAS and standard FTIR transmission spectroscopy using the KBr pellet method as a function of the sample mass and the results are shown in Fig. 6. It is evident that the two techniques coincide for small sample masses. This is the region where PAS can be used for quantitative determination of quartz in unknown samples e.g. in mine dusts. Of course the major advantage of PAS is that no sample preparation is necessary unlike the case of FTIR spectroscopy.

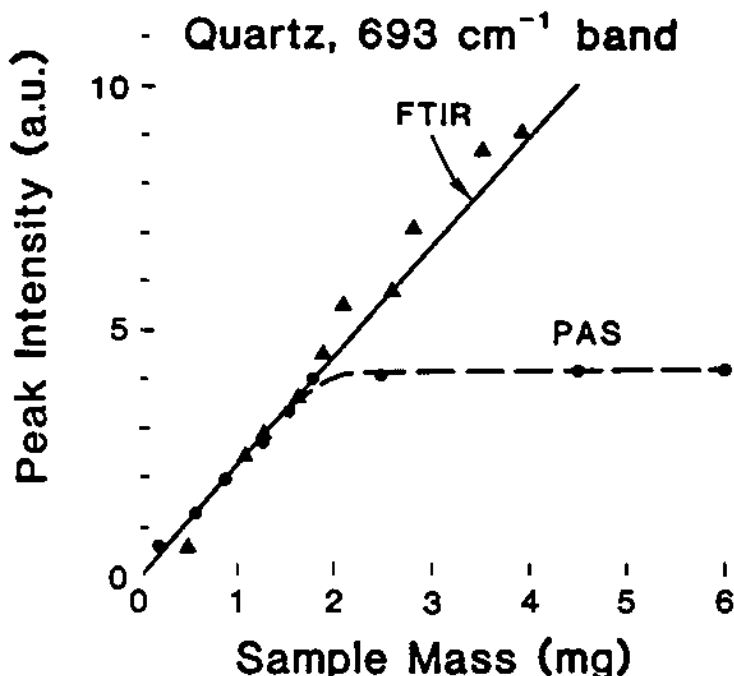


Fig. 6. Peak intensity (area under the band) of the narrowest band of quartz at 693 cm^{-1} in arbitrary units (a.u.) versus sample mass. The data is shown both for the standard FTIR technique and the PAS technique. The solid lines are drawn through the points as guides. The FTIR and PAS techniques agree for sample mass $< 2\text{ mg}$.

Concluding Remarks:

The major limiting factor for the use of PAS in quantitative analysis has been the saturation phenomenon. In this work, we have shown how the PAS signal for the thermally thin case (Eq. (6)) leads to the PAS signal for the thermally thick case (Eq. (7)) as the sample mass (or length l) is increased. This has led to an enhanced understanding of the saturation phenomenon and provided the limits under which PAS can be used for quantitative analysis. This and the chopping frequency dependence of the PAS signal in quartz has provided additional verification of the correctness of the RG theory.¹²

Acknowledgements:

This work was supported in part by a grant awarded to MSS by the U.S. Bureau of Mines under the Generic Technology Center for Respirable Dust, Grant No. G1135142. We thank Dr. W. E. Wallace of NIOSH for providing the sample of quartz used in this work and for many useful discussions.

REFERENCES

1. A. Rosencwaig and A. Gersho, *J. Appl. Phys.* 47, 64 (1976); For general review, see A. Rosencwaig, "Photoacoustic and Photoacoustic Spectroscopy" (John Wiley and Sons, New York, 1980); and A. Rosencwaig, "Advances in Electronics and Electron Physics" 46, pp 207-311 (1978).
2. L. W. Burggraf and D. E. Leyden, *Anal. Chem.* 53, 759 (1981).
3. J. F. McClelland, *Anal. Chem.* 55, 89A (1983).
4. N. C. Fernelius, *J. Appl. Phys.* 52, 6285 (1981); *J. Opt. Soc. Am.* 70, 480 (1980).
5. P. Poulet, R. Unterreiner and J. Chambron, *J. Appl. Phys.* 51, 1738 (1980).
6. N. Teramae and S. Tanaka, *Appl. Spectros.* 39, 797 (1985).
7. C. F. Kirkbright, *J. de Physique C6*, 99 (1983).
8. B. Mongeau, G. Rousset and L. Bertrand, *Can. J. Phys.* 64, 1056 (1986).
9. Y. C. Teng and B. S. H. Royce, *Appl. Opt.* 21, 77 (1982).
10. A. Holter and H.-H. Perkampus, *Appl. Spectros.* 39, 278 (1985).
11. W. G. Spitzer and D. A. Kleinman, *Phys. Rev.* 121, 1324 (1961).
12. For a detailed exposition of the RG theory, see the M.S. thesis of L. H. Cheng entitled "Theory of Photoacoustic Spectroscopy and Spectra of Quartz", West Virginia University, 1987 (unpublished).

Oxygen Effects on Free Radicals and Cytotoxicity of Freshly Crushed Coal

N.S. Dalai¹, B. Jafari¹, M.M. Suryan¹ and V. Vallyathan²

¹Department of Chemistry, West Virginia University

²Pathology Section, National Institute of Occupational Safety and Health, Morgantown, WV

The biologic events leading to coal workers' pneumoconiosis (CWP) are not yet fully understood. There is no good correlation between toxicity studies or animal models with human epidemiologic and pathologic data. Several studies have shown that the severity and prevalence of the CWP in miners correlate strongly with the rank and type of the coal mined. However this has not been found to be the case with laboratory animal models or in vitro studies. In 1980 Russian scientists Artemov and Resnik suggested that the discrepancy may be related to the excessive amount of short-lived free radicals present in freshly generated coal mine dust. Because of their short life, such free radicals would be absent in the "stale" coal dust used in most animal experiments. To test this hypothesis we have undertaken a systematic study of the generation, reactivity with oxygen and biological significance of free radicals in coal dust.

Electron spin resonance (ESR) was used as a technique for the direct detection of radical production and kinetics of decay. ESR signals from the newly generated radicals decreased with time on exposure to oxygen or when stored in biological buffers at a rapid rate. In vitro biological tests were carried out which suggest that the reaction between the newly generated radicals and oxygen plays a significant role in the sample's cytotoxicity.

Materials and Methods

ESR measurements were made at X-band (~9.7 GHz) using a computer-controlled Bruker ER200D ESR spectrometer. The two coals studied in detail were obtained from the Pennsylvania State University Coal Depository. These were, a bituminous sample, PSOC-1172 (72% carbon) and an anthracite sample, PSOC 867 (95% carbon). Coal particles of several millimeter (mm) dimensions were evacuated to a pressure of $\sim 10^{-3}$ mm Hg typically overnight. Without exposure to air, these particles were ground in an agate mortar with an agate pestle for about 30 minutes and then sieved through a 20 μ m mesh filter before ESR measurements or cytotoxicity studies. As an index of cytotoxicity, hemolysis was measured according to the method of Harrington, with minor modifications. Sheep erythrocytes (2%) were incubated with test samples at 37°C for one hour, and the hemoglobin released was quantitatively estimated photometrically. Additionally, release of alveolar macrophage enzyme lactate dehydrogenase (LDH) was estimated after incubation of the macrophages with the coal particles at different time intervals after the grinding. Enzyme activity was assayed according to the method of Wroblewski and LaDue and expressed as percent of enzyme released in 2 hours per million cells with 1 mg of coal.

Results and Discussion

Figure 1 shows EPR spectra of freshly ground coals. Fig. 1(a) shows the ESR spectra for the bituminous coal, demonstrating that grinding indeed causes an increase in the concentration of the coal-based organic free radicals. Fig. 1(b) shows the decay of the free radicals from the two coal samples as a result of admitting a low pressure of oxygen into the ESR sample tube, demonstrating the reactivity of oxygen with the coal-based radicals.

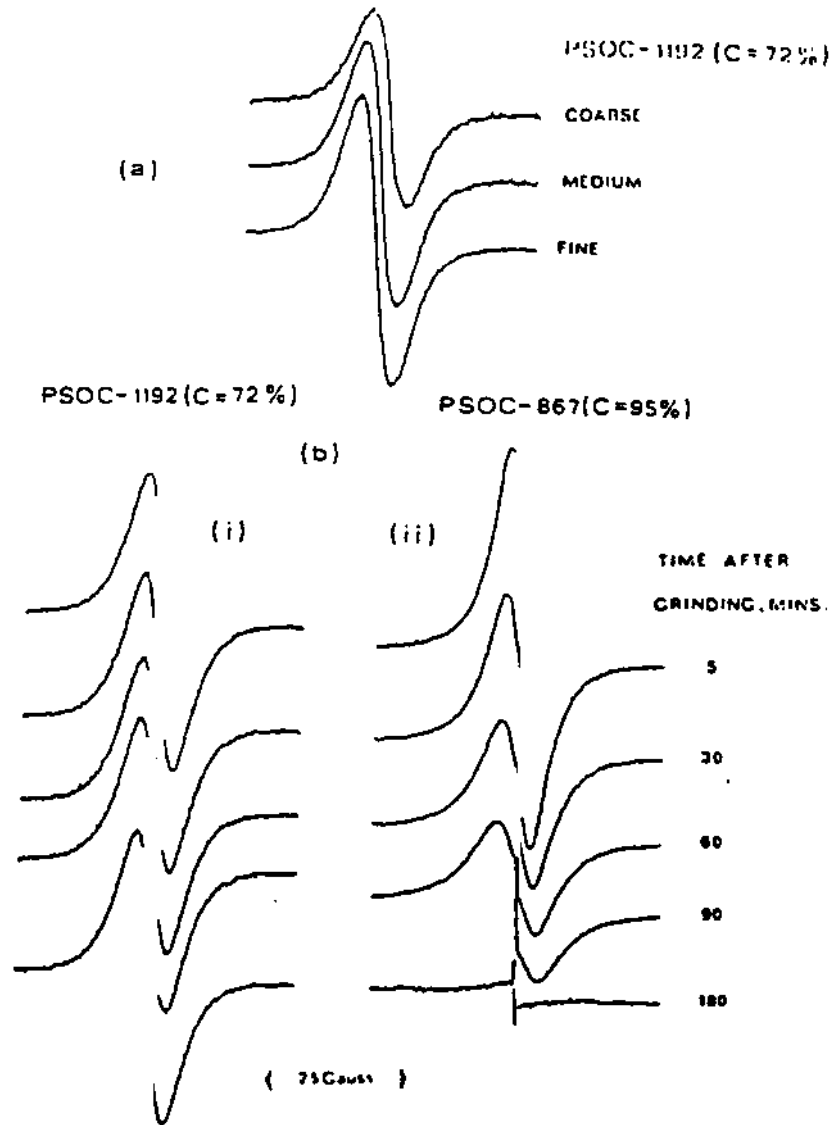


Figure 1. Time dependence of ESR spectra of crushed coal particles.

Figure 2 shows a plot of the decay of the coal-based radicals when the anthracite sample was crushed in air and then kept in air.

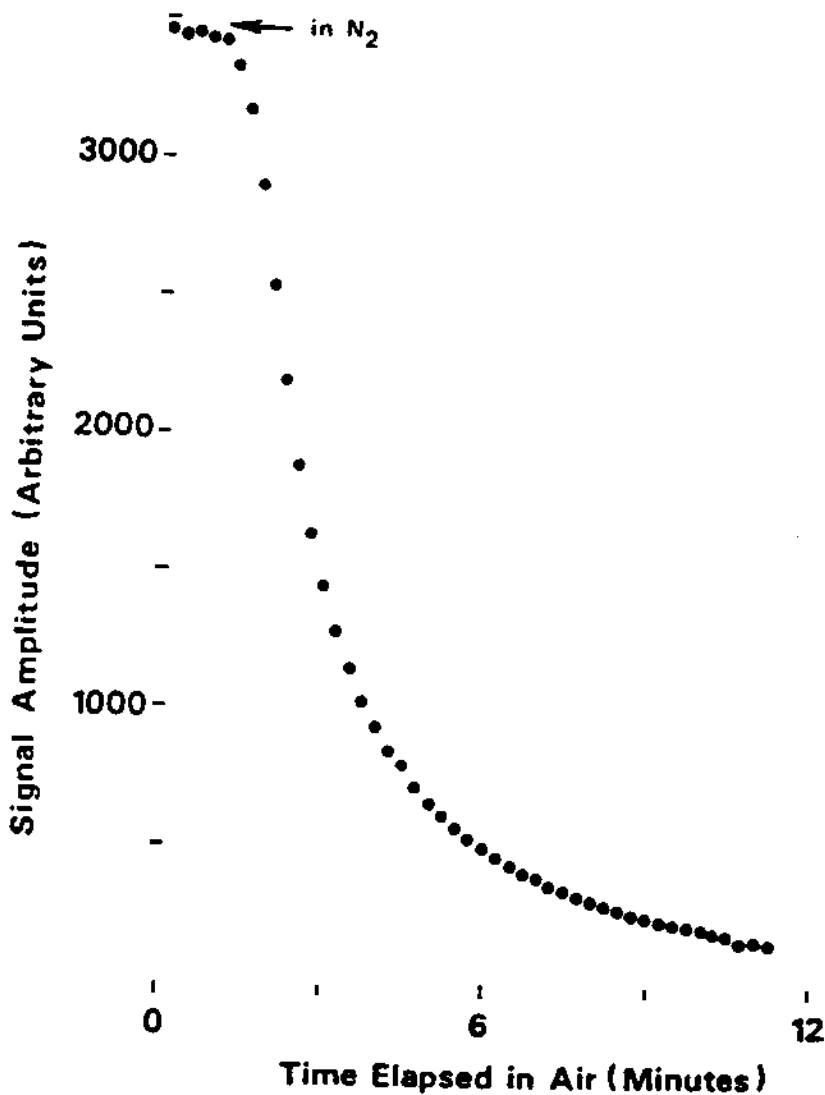


Figure 2. A plot showing time dependence of the concentration of radical-oxygen complexation.

Figure 3 shows a bar-type graph of the time dependence of the hemolysis caused by a 2 mg per ml of coal dust. The time refers to the time elapsed after the dust preparation. The results show that the cytotoxicity of the freshly ground coal dust is the highest when it is just produced and it decreases on storing the dust in either air or in a phosphate buffer solution.

EFFECT OF CRUSHING COAL ON CYTOTOXICITY

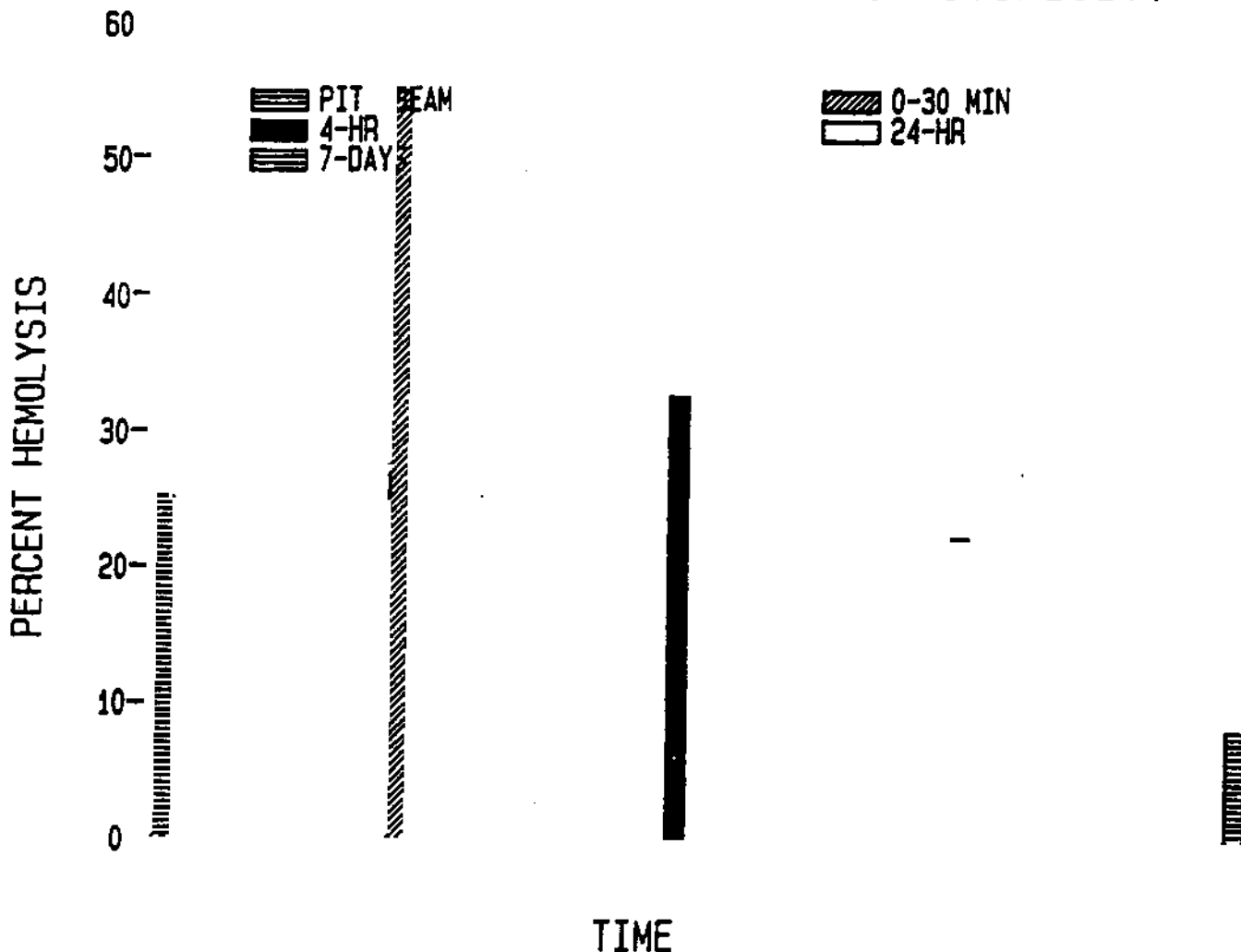


Figure 3. A bar graph of time dependence of hemolysis caused by freshly crushed anthracite coal.

The cytotoxic activity of the coal dust was found to be decreased partially by superoxide dismutase while catalase inhibited the toxicity completely. More detailed studies of the mechanism of this inhibitory action are currently in progress.

We believe that the results summarized above and to be presented in fuller detail at the conference, could provide a novel mechanism for understanding the primary steps in the biochemical mechanism of CWP. Moreover the methodology for the radical production under controlled environment and the reactivity studies will be of general interest of all interested in the toxicology of free radical-oxygen complexes.

Role of Reactive Oxygen Radicals in Silica Cytotoxicity

V. Vallyathan¹, X. Shi², N.S. Dalal² and W. Irr¹

¹Pathology Section, National Institute for Occupational Safety and Health, Morgantown WV
and ²Chemistry Department, West Virginia University

Inhalation of crystalline silica is associated with a biphasic biologic response of acute cell injury and chronic pulmonary fibrosis. Dust induced cell membrane injury leading to the release of lysosomal enzymes and cell death has been implicated as the initial important biologic event triggering the fibrosis. However, it is also possible other biologic reactions could alternatively, or in addition to these enzyme related cytotoxicity reactions, alter the normal functioning of cells. It is well known that phagocytic activation results in the production of oxygen radicals which are highly cytotoxic to cells. In healthy lung, protection against the toxic effects of the normal balanced biologic reactions are provided by a number of defense systems including antioxidants. In disease or conditions of overproduction of oxygen radicals, biochemical protection may be overwhelmed with resultant cellular injury.

Our recent observations have shown that reactive oxygen radicals (ROR) are generated during grinding of crystalline silica. We hypothesized that these newly generated RORs may cause cell injury, lipid peroxidation, or even damage to macromolecules such as DNA. Biochemical aberrations caused by the inhalation of crystalline silica with ROR at occupational settings might overwhelm cellular and antioxidant defense systems of the lung leading to injury and subsequent fibrosis.

To test this hypothesis, we have investigated the generation and decay of ROR produced by crystalline silica using electron spin resonance (ESR) and investigated its toxicity with conventional biologic tests at various time intervals after grinding. We also studied the decay of these newly generated RORs in buffer and the effect of antioxidants and scavengers in the abolition of cellular damages.

Crystalline silica with a particle size of 0.2 to 5 μm was obtained from the Generic Respirable Dust Technology Center, Penn State University, State College, PA. NIOSH crystalline silica with a particle size of less than 5 μm was used in all the tests as a positive control. As negative controls titanium dioxide or barite were used as non-toxic inert dusts. Silica was ground in an agate mortar with a pestle for 30 min and sieved through a 20 μm mesh filter before using in the ESR and biologic tests. For investigations on decay and toxicity of ROR during exposure to air and buffer, stock samples of ground silica were studied at time intervals of 0-30 min., 4 hrs, and 1, 2, 3, 7 and

REACTIVE OXYGEN RADICALS

14 days after grinding. ESR spectra were obtained at X-band (9.7 GHz) using a Bruker ER 200D ESR spectrometer. For the efficient detection and specific identification of ROR we used a spin trap 5, 5-, dimethyl-1-pyrroline-N-oxide (DMPO). In addition, we also used ethanol as a secondary radical trap to further verify hydroxy radicals.

As an index of cytotoxicity, hemolysis was measured according to the method of Harrington, with minor changes. Sheep erythrocytes (2%) were incubated with test samples at 37°C for one hour, and the hemoglobin released was quantitatively estimated with positive and negative controls. As an additional measure of cellular cytotoxicity, release of enzyme lactate dehydrogenase (LDH) was estimated after incubation of alveolar macrophages with freshly ground silica. Enzyme activity was assayed according to the method of Wroblewski and LaDue and was expressed as percent of enzyme released.

The particle characteristics and size of crystalline silica generated by grinding varied greatly between samples. Therefore, quantitative analysis of each sample generated was treated independently for the evaluation of ROR decay and cytotoxicity after exposure to air and storage in buffer. The mean particle size of fresh ground silica was considerably larger than the NIOSH standard with less than 5 μm particles. NIOSH silica with smaller particle size was more cytotoxic than the freshly ground silica.

When crystalline silica was ground in 0.1M DMPO, an ESR spectrum with a typical DMPO-OH adduct was obtained. This $\cdot\text{OH}$ radical signal was also increased with more grinding. Studies with ethanol, as a secondary trap, further characterized the ESR signal as $\cdot\text{OH}$ radical. The newly generated ESR signal showed slow decay when exposed to air and a dramatic decay in phosphate buffer.

The two cytotoxic evaluations showed consistent results with degree of cytotoxicity correlations to ESR signals ROR reactivity and its decay during time intervals tested. Freshly ground crystalline silica induced a significantly greater hemolysis and release of LDH within 0-30 min after grinding than at later time intervals. Cytotoxicity of silica samples exposed to ambient air showed a gradual decrease of toxicity over two weeks. Phosphate buffer storage of freshly ground silica resulted in a rapid loss of cytotoxicity and ESR signal.

Studies on the effect of exogenous scavengers showed differential inhibitory effect of the cytotoxicity. Superoxide dismutase and sodium benzoate provided a partial protection to the cytotoxic effect, while catalase completely abolished the cytotoxic effect of silica. The newly generated ROR was also completely scavenged by boiling silica in water.

The results presented here support a role of ROR in silica toxicity, which may be significantly greater in occupational exposures where the inhaled dust contained freshly fractured silica particles. Sandblasting and silica flour mill operations create worksite atmospheres with great quantities of freshly fractured respirable silica particles and are associated with particularly high risk of acute silicosis.

THE RESPIRABLE DUST CENTER

This project represents a collaborative effort between NIOSH and West Virginia University. The University's contribution was supported in part by a grant from the Bureau of Mines through the Generic Mineral Technology Center for Respirable Dust. We would like to thank Julia Martin for technical assistance and Lunette Utter for secretarial assistance.

This research has been supported by the Department of the Interior's Mineral Institute program administered by the Bureau of Mines through the Generic Mineral Technology Center for Respirable Dust under grant number G1135142.

Mutagenicity of Diesel Exhaust Particles and Oil Shale Particles Dispersed in Lecithin Surfactant

W.E. Wallace^{1,2}, M.J. Keane¹, C.A. Hill² and J. Xu³

¹National Institute for Occupational Safety and Health,
Division of Respiratory Disease Studies,
Morgantown, WV

²West Virginia University

³Shanxi Medical College, Taiyuan, Shanxi, China

Diesel exhaust particulate material from exhaust pipe scrapings of two trucks, diluted automobile diesel exhaust particulate material collected on filters, and two oil shale ores were prepared for the Ames mutagenicity assay by dichloromethane (DCM) extraction, by dispersion into 0.85% saline, or by dispersion into dipalmitoyl lecithin (DPL) emulsion in saline. Salmonella typhimurium TA98 was used to detect frameshift mutagens in the samples. Samples of diesel soot gave positive mutagenic responses with both DCM extraction and DPL dispersion, with the DPL dispersion giving higher results in some cases. The results suggest that possible mutagens associated with inhaled particles may be dispersed or solubilized into the phospholipid component of pulmonary surfactant and become active in such a phase.

INTRODUCTION

The Ames *Salmonella*/microsome assay (Ames et al., 1975) has been shown to be a useful test for detecting genotoxic properties of various agents. Hundreds of specific chemicals have been screened (McCann et al., 1975), and the test has been applied for many types of environmental samples. Airborne mutagenic agents, for example, have been found in urban air (Chrisp and Fisher, 1980; Hughes et al., 1980; Rosenkranz et al., 1978), in diesel engine exhausts (Huisinigh et al., 1978), and in the byproducts of coal combustion processes (Chrisp et al., 1978).

Samples of airborne particles are typically collected on membrane filters, and undergo a rigorous extraction procedure with organic solvents and/or ultrasonic agitation (Clark and Hobbs, 1980). Often extracts are transferred to another solvent that is compatible with the assay system. These extraction procedures, while efficient from an analytical perspective, are not physiologically plausible. The questions that present themselves are whether a demonstrated mutagen can be taken up in vivo and whether the process is quantitatively or qualitatively different from the above laboratory procedure (Wallace et al., 1984).

When a particle of respirable size is inhaled to the alveolar region of the lung, its first physiological contact is with pulmonary surfactant that lines the inner surfaces of the alveoli. This surfactant is an aqueous fluid containing proteins, phospholipids, and other components (R. J. King, 1982). The principal phospholipid constituent is L-alpha-phosphatidylcholine, beta,gamma-dipalmitoyl, or dipalmitoyl lecithin (DPL) (L. C. King et al., 1981).

The objectives of this study were to determine whether mutagenic compounds can be transferred to a fluid representative of the phospholipid component of pulmonary surfactant and whether the results of mutagenicity testing following such preparation are comparable to the results of preparatory procedures using organic solvents. These

objectives were intended to address the question of *in vivo* biologic availability of mutagenic hydrophobic respirable particles deposited in the acinar region of the lung and to test a preparatory procedure for mutagenicity assays of respirable particles that takes account of that question (Wallace et al., 1986).

The fluid used was dipalmitoyl lecithin emulsified in physiological saline. Several substances not expected to exhibit mutagenic activity were also assayed to screen for possible false positive results.

MATERIALS AND METHODS

Diesel soot (D1) was obtained by scraping the inside of the exhaust pipe of a large diesel truck at the West Virginia University Medical Center. The soot was collected immediately after the engine was stopped. Magnetic particles were removed with a magnet. Diesel soot (D2) was provided by Dr. Trent Lewis of the National Institute for Occupational Safety and Health (NIOSH) Division of Biomedical and Behavioral Science. The soot was generated by a stationary diesel engine, and was over 1 yr old at the time used. The particulate matter was scraped from the inside of filter bags. Dusts D1 and D2 were stored in sterile jars at -10°C . Diesel soot (D3) was provided courtesy of Dr. Roger McClellan of the Lovelace Inhalation Toxicology Research Institute (ITRI). Exhaust particulate material was collected by high-volume sampling on filters in a dilution tunnel diluting the exhaust of a General Motors 5.7-l engine operated on a Federal Test Procedure Cycle, and the filter was stored at -80°C . Paraho oil shale (OS1) and Scottish oil shale (OS2) were provided by Dr. James Jackson of Los Alamos National Laboratory (LANL). The ores were ground to fine powders with mortars and pestles, and stored in sterile vials at -10°C .

Dipalmitoyl Lecithin Emulsion, 10 mg/ml

For this preparation, 100 mg L-alpha-lecithin, beta,gamma dipalmitoyl (DPL) (Calbiochem, La Jolla, Calif.) was weighed into a sterile 50-ml centrifuge tube, 10 ml of 0.85% physiological sterile saline (PSS) was added, and the liquid was sonicated 10 min at 40 W (Heat Systems-Ultrasonics, Plainview, N.Y.). The probe was wiped with 95% ethanol and was covered with Parafilm during the sonication.

Dichloromethane Extraction

For this, 2.5 mg of each particulate material was suspended in 2.5 ml of dichloromethane (DCM) (Mallinckrodt, St. Louis, Mo.) in sterile 15-ml glass centrifuge tubes and sonicated in a water bath (Branson, Shelton, Conn.) for 30 min at room temperature. Tubes were placed in a dry bath at 45°C , 2.7 ml dimethyl sulfoxide (DMSO) (Baker, Phillipsburg, N.J.) was added, and the DCM was evaporated under nitrogen, until 2.5 ml of liquid remained.

DPL Dispersion

For this, 2.5 mg of each particulate material was weighed into a sterile glass centrifuge tube, 2.5 ml of 10 mg DPL/ml saline was added, and the tube was placed in a water bath for 60 min at 37°C . PSS dispersion was similar to DPL dispersion, except PSS was used.

Samples extracted with DCM were diluted 1:2 and 1:4 with DMSO; samples dispersed with DPL or PSS were diluted likewise with PSS. Particulate matter was not removed in any of the assays except the experiments involving sedimentation, as described below. Negative controls were DMSO, PSS, and DPL. Positive controls were technical-grade trinitrofluorenone (TNF) (Aldrich, Milwaukee, Wis.), 1 mg/ml, for experi-

ments without S9, and 2-aminoanthracene (2AA) (Aldrich, Milwaukee, Wis.), 2.5 mg/ml, for the experiment with S9.

For experiments that involved separation of dispersed or extracted diesel soot into a liquid phase and a sedimented phase, samples were centrifuged 10 min at $2000 \times g$ after the extraction or dispersion procedure. The supernatant was removed and diluted as above, and the sediment resuspended in either DMSO or PSS, vortexed, and diluted as above. For experiments that involved filtration of the supernatant from centrifugation of dispersed or extracted diesel soot, samples were first dispersed or extracted and then centrifuged as above. The supernatant was then filtered through an $0.2\text{-}\mu\text{m}$ syringe filter (Millipore, Bedford, Mass.). The filtrate was then diluted as above for assay.

The Ames *Salmonella*/microsome assay was used for mutagenesis testing, and the S9 mixture was prepared as described by Ames et al. (1975). The preincubation test was used as the assay system. In brief, 0.1 ml of each sample, 0.5 ml PSS or S9 mixture, and 0.1 ml of TA98 culture was added to a $16 \times 100\text{-mm}$ plastic culture tube, and all sample tubes were rotated in a 37°C incubator for 90 min. Samples were then mixed with 2 ml top agar supplemented with biotin (0.05 mM) and histidine (0.05 mM), and mixtures were poured into Vogel-Bonner minimal media plates and incubated 48 h at 37°C . Revertant colonies were counted with an electronic counter (Artek, Farmingdale, N.Y.); plates containing visible diesel particles were hand counted to assure that only *Salmonella* colonies were counted. Since diesel soots D1 and D2 had been shown by previous work in this laboratory to be mutagenic to TA98 without S9, this tester strain was used exclusively, and S9 activation was used in only one experiment.

RESULTS

Figure 1 shows the results for D1 for each of three preparation media: dichloromethane, physiological saline, and dipalmitoyl lecithin emulsified in saline. Mutagenic response increases with dose in all cases. The responses of DPL-dispersed samples and the DCM-extracted samples both substantially exceed the response of the saline-dispersed samples. The results from duplicated experiments show that the response in revertants per plate is generally higher for DPL-dispersed than for DCM extracted samples. An additional experiment was done to see the effect, if any, of S9 microsomal fraction on the samples prepared by the three methods. The S9 fraction suppressed the mutagenic response in all the samples, especially those dispersed in DPL. Potential reasons for this have not yet been investigated. The S9 fraction also elevated the controls. This is not unexpected, noting that some histidine may be present in the liver homogenate.

As shown in Fig. 2, diesel soots D2 and D3 both met the criterion for mutagenicity (response producing an increase equal to two or more

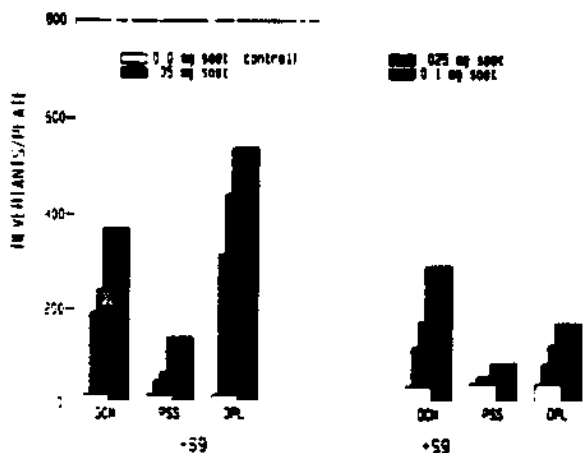


FIGURE 1. Mutagenic response versus extraction or dispersion medium for diesel soot D1 with and without S9 microsomal activation.

times the control for at least one concentration tested, and a positive dose related response at three concentrations) (Ames et al., 1975). The responses from OS1 and OS2 were similar for all three preparation media; OS1 minimally meets the criterion for mutagenicity with DCM extraction, but otherwise the responses for all preparation media were very weak. The mutagenic responses of both positive and negative controls were typical for the TA98 tester strain in all experiments.

To examine whether DPL was acting as an extracting agent or as a

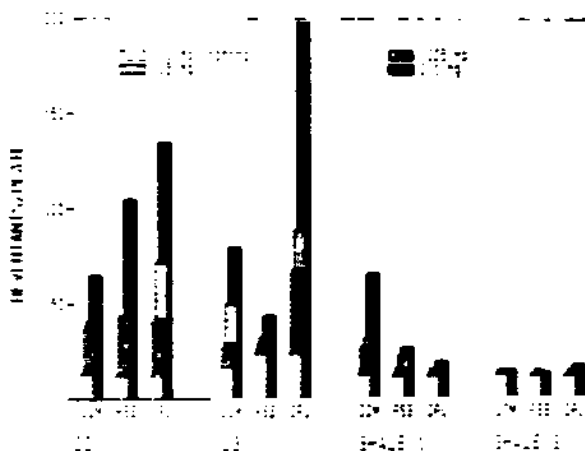


FIGURE 2. Mutagenic response versus extraction medium for diesel soot D2 and D3, and oil shales OS1 and OS2.

solubilizing or dispersing agent in this system, samples were centrifuged 10 min at $2000 \times g$ after the DCM extraction or DPL dispersion procedures. The supernatants were transferred to vials, and the sediments were resuspended in DMSO or saline, respectively, for the DCM-extracted or DPL-dispersed samples. Figure 3 shows that virtually all of the mutagenic activity for the DCM-extracted samples is in the supernatant, but the greater activity lies with the sediment phase in the DPL-prepared samples. To investigate whether the mutagenic activity in the supernatant was due to dissolved or dispersed soot fractions, a set of samples were subjected to this same procedure of DCM extraction or saline or DPL-saline dispersion and subsequent centrifugation. The supernatant fraction from the centrifugal separation was filtered through a $0.2\text{-}\mu\text{m}$ filter. The filtrates were then assayed. Figure 4 shows that this filtration removed all mutagenic activity from the DPL-saline-prepared sample supernatants.

An experiment was performed to determine the effect of varying DPL emulsion concentration (the concentration of dipalmitoyl lecithin emulsified in saline) on the mutagenic response of diesel soot D1 dispersed in the emulsion. Figure 5 shows that the response increases with increasing DPL concentration up to 7 mg DPL/ml saline, where the effect levels off.

Another experiment showed that mutagenic response is essentially constant for unseparated sample D1 incubated for times of 1, 2, 4, and 8 h in dispersion in 10 mg DPL/ml saline at 37°C ; the dispersion times do not include the 90 min associated with the preincubation procedure.

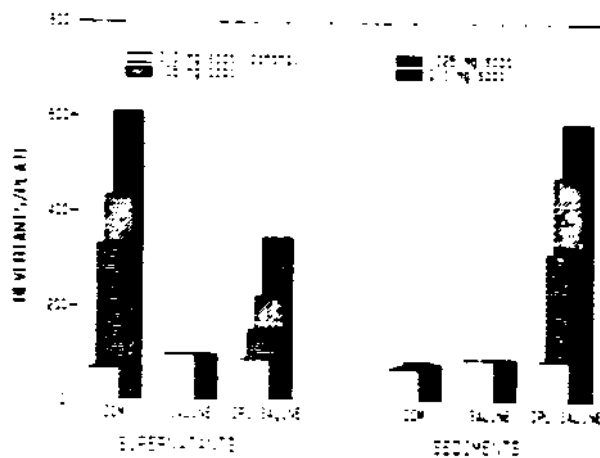


FIGURE 3. Mutagenic response for supernatant and $2000 \times g$ sediment phases of diesel soot D1 versus extraction or dispersion medium.

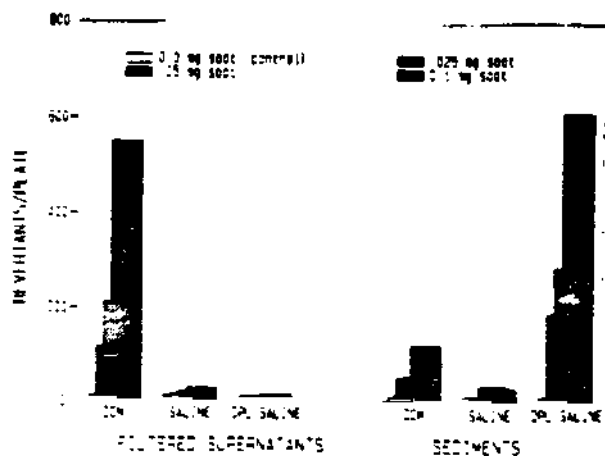


FIGURE 4. Mutagenic response for filtered supernatant and 2000 x g sediment phases of diesel soot D1 versus extraction or dispersion medium.

DISCUSSION

From this study it seems clear that mutagenic agents from some diesel soots can express mutagenic activity when dispersed in phospholipid emulsion that resembles a major component of pulmonary surfactant. It is especially surprising that the response in many cases is greater than that using extraction with organic solvents. This seemingly is contradictory to the findings of L. C. King et al. (1981) and Brooks et al. (1981), who found, respectively, mild response with lung lavage

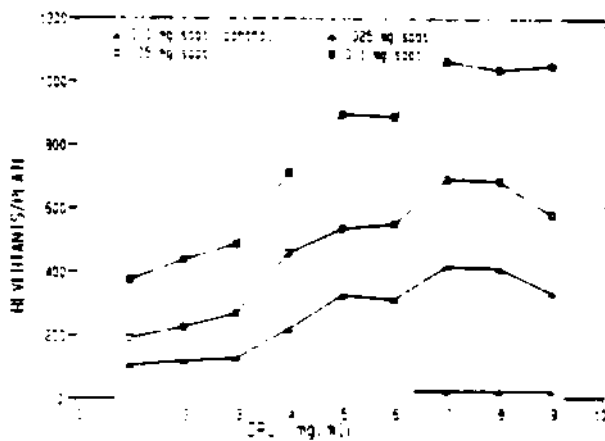


FIGURE 5. Mutagenic response versus lecithin concentration in emulsion for diesel soot D1, without S9 activation.

fluid extracts and no response with both lavage fluid and DPL extracts of diesel particulate material. However, one crucial difference between this work and those studies is that in this work particulate materials were not removed by filtration or sedimentation before the assay. Their studies used several hours to several days of incubation with extractants, but this would not appear to be the basis for the differences in results (L. C. King et al., 1981; Brooks et al., 1981).

In the experiment where samples were separated into a supernatant and a sedimented phase, both fractions were assayed. After 2000 × g centrifugation, most of the mutagenic activity was found in the sediment for DPL-dispersed samples, in contrast to DCM-extracted samples. Filtration of the supernatants removed the remaining mutagenic activity from the DPL-dispersed sample supernatant. It therefore appears that the supernatant-fraction mutagenicity of the DPL-dispersed samples is due to very fine dispersed particles, which might be removed by the separation procedures used in other studies (L. C. King et al., 1981; Brooks et al., 1981). DPL may be solubilizing the diesel soot, rather than extracting a soluble fraction.

Since the majority of mutagenic response with DPL-dispersed samples is with the sedimented material, this is evidence that the DPL may facilitate interaction of diesel soot particles with the *Salmonella* auxotrophs. Microscopic examination of D1 revealed most particles were less than 1 μm in diameter, consistent with published data on other diesel exhaust particulate material (Cheng et al., 1984). This is very fine but still sizeable relative to bacteria (less than 2 μm in length). Since the TA98 auxotrophs have cell-wall defects (Ames et al., 1973), these defects may allow contact of the plasma membrane with particles or agents adsorbed on particles.

These results suggest a research premise that components of pulmonary surfactant provide a solubilization mechanism for hydrophobic or sparingly water-soluble respirable particulate material that deposits in the acinar regions of the lung. Such solubilization might affect one or more steps in the chain of exposure from contact to uptake to metabolism and interaction with genetic material within the cell.

In any case, this sample shows that surrogate physiological fluid is capable of efficient delivery of mutagenic agents from particles to tester cells. Additional research is needed to elucidate the mechanisms involved.

REFERENCES

- Ames, B. N., Lee, F. D., and Durston, W. E. 1973. An improved bacterial test system for the detection and classification of mutagens and carcinogens. *Proc. Natl. Acad. Sci. USA* 70:782-786.
- Ames, B. N., McCann, J., and Yamasaki, E. 1975. Methods for detecting carcinogens and mutagens with the *Salmonella*/mammalian microsomal mutagenicity test. *Mutat. Res.* 31:347-364.

THE RESPIRABLE DUST CENTER

- Brooks, A. L., Wolff, R. K., Royer, R. E., Clark, C. R., Sanchez, A., and McClellan, R. O. 1981. Deposition and biological availability of diesel particles and their associated mutagenic chemicals. *Environ. Int.* 5:263-268.
- Cheng, Y. S., Yeh, H. C., Mauderty, J. L., and Mokler, B. V. 1984. Characterization of diesel exhaust in a chronic inhalation study. *Am. Ind. Hyg. Assoc. J.* 45:547-555
- Chrisp, C. E., and Fisher, G. L. 1980. Mutagenicity of airborne particles. *Mutat. Res.* 76:143-164.
- Chrisp, C. E., Fisher, G. L., and Lammert, J. E. 1978. Mutagenicity of filtrates from respirable coal fly ash. *Science* 199:73-75.
- Clark, C. R., and Hobbs, C. H. 1980. Mutagenicity of effluents from an experimental fluidized bed coal combustor. *Environ. Mutagen.* 2:101-109.
- Hughes, T. J., Pellizzari, E., Little, L., Sparacino, C., and Kolber, A. 1980. Ambient air pollutants: Collection, chemical characterization and mutagenicity testing. *Mutat. Res.* 76:51-83.
- Huisingh, J., Bradow, R., Jungers, R., Claxton, L., Zweidinger, R., Tejada, S., Bumgarner, J., Duffield, F., Waters, M., Simmon, V. F., Hare, C., Rodriguez, C., and Snow, L. 1978. Application of short term bioassay to the characterization of diesel particle emissions. *Environ. Sci. Res.* 15:381-418.
- King, L. C., Kohan, M. J., Austin, A. C., Claxton, L. D., and Huisingh, J. L. 1981. Evaluation of the release of mutagens from diesel particles in the presence of physiological fluids. *Environ. Mutagen.* 3:109-121.
- King, R. J. 1982. Pulmonary surfactant. *J. Appl. Physiol.* 53:1-8.
- McCann, J. E., Choi, E., Yamasaki, E., and Ames, B. N. 1975. Detection of carcinogens as mutagens in the *Salmonella*/microsome test: Assay of 300 chemicals. *Proc. Natl. Acad. Sci. USA* 72:5135-5139.
- Rosenkranz, H. S., McCoy, E. C., Anders, M., Speck, W. T., and Bickers, D. 1978. The use of microbial assay systems in the detection of environmental mutagens in complex mixtures. *Environ. Sci. Res.* 15:3-42.
- Wallace, W. E., Keane, M., Vallyathan, V., Ong, T.-M., and Castranova, V. 1984. Pulmonary surfactant interaction with respirable dust. In *Proc. Coal Mine Dust Conf., Morgantown, West Virginia, October, 1984*, ed. S. Peng, pp. 180-187. National Technical Information Service Report PB86 169380/AS. Springfield, Va.: NTIS.
- Wallace, W. E., Keane, M., and Ong, T.-M. 1986. Lecithin surfactant extraction of mutagenic compounds from diesel particulates. *Toxicologist* 6:227 (Abstr. 25th Anniversary Meeting of the Society of Toxicology).

Received August 25, 1986

Revised October 31, 1986

Accepted as revised November 13, 1986

The Authors gratefully thank Dr. Wen-Zong Whong for preparation of the TA98 cultures, Eugene Regad for assistance with the graphics, Dale Bates for technical assistance, and Dr. James Jackson of Los Alamos National Laboratory, Dr. Trent Lewis of NIOSH, and Dr. Roger McClellan of Lovelace Biomedical and Environmental Research Institute, Inhalation Toxicology Research Institute for graciously providing samples. ITRI samples were collected under U.S. Department of Energy contract DE-AC04-76EV01013.

This research has been supported by the Department of the Interior's Mineral Institute program administered by the Bureau of Mines through the Generic Mineral Technology Center for Respirable Dust under grant number G1135142.

A Method for Resuspending Particles Deposited on Filters

V.A. Marple and K.L. Rubow
Mechanical Engineering Department,
University of Minnesota

Filter samplers are one of the simplest methods and, in some instances, one of the only methods that can be used to obtain samples of particulate matter suspended in a gaseous medium. Once collected, particles are normally analyzed directly on the filter by gravimetric, chemical or microscopic techniques. However, it is sometimes desirable to resuspend the particles in an airstream for analysis. This would be the case if the size distribution of the particles were to be measured using one of many particle sizing techniques such as inertial classifiers, optical particle counters or the TSI Aerodynamic Particle Sizer (APS).

A technique has been recently developed whereby one can resuspend particles from filter samples in an airstream. The technique has been used for the resuspension of coal dust from filters. The resuspended particles were then introduced into the APS. This development was necessary since an APS can not be taken directly into an underground coal mine. For this application, particle samples are collected on membrane filters in the underground mines. The mass concentration of the particles determined through gravimetric analysis. The particle size distribution was then determined by resuspending the particles and passing them through a TSI Aerodynamic Particle Sizer (APS). Excellent agreement has been obtained between the size distribution directly measured underground with a cascade impactor and that measured from the resuspended particles. For this experiment, an open-faced filter sampler was placed adjacent to the cascade impactor in the mine. The particles collected on the filter were resuspended in the laboratory and measured with the APS.

A venturi aspirator is used in the apparatus developed for resuspending the particles. The venturi has a small diameter capillary tube placed in the venturi throat. High velocity air flow is passed through the venturi, thereby, creating a low pressure region at the exit of the capillary tube. The low pressure draws air through the tube. The filter with deposited particles is located at the inlet to the capillary tube where the air flow into the capillary resuspend the particles. Once airborne, the particles are deagglomerated as they pass through the high velocity air flow in the venturi throat.

An Impactor with Respirable Penetration Characteristics and Size Distribution Capabilities

V.A. Marple and K.L. Rubow
Mechanical Engineering Department,
University of Minnesota

In our laboratory several impactors have been developed in the past which have penetration characteristics that approximate that of the ACGIH or the British MRC respirable curves. In these impactors the large nonrespirable particles are collected on an impaction plate of a multiple round nozzle stage where the nozzles are of different diameters. The principle for designing a respirable cut impactor is quite simple in that the respirable curve is divided into two or more segments and the nozzles are designed with the correct diameters and number of nozzles to have collection characteristics with 50% cutpoints at the center of each segment. The particles not collected on the impaction plates are then collected upon a filter. These particles represent the respirable fraction of the aerosol. Therefore the respirable curve is approximated in a stepwise fashion with the approximation becoming better as the respirable curve is divided up into increasing numbers of segments. It has generally been felt that three segments is satisfactory for most cases.

A new version of the respirable impactor has recently been developed in our laboratory. This impactor approximates the ACGIH respirable curve in three steps at a flow rate of 30 liters per minute. However, unlike previous models where all of the particles larger than the three cut points designated by the three steps are collected upon one impaction plate, a separate impaction plate is now used for each of the three cut sizes. To approximate the respirable curve in three steps, the cut sizes must be 2.2, 3.5 and 5.8 microns diameter. Therefore, on each of these stages the particles collected will be the mass of particles that are larger than these three cut sizes. By determining the mass of particles collected on each of these three stages plus that on the after-filter using Gravimetric techniques, some information can be obtained on the size distribution of the aerosol being sampled. Furthermore, the impaction plates of the three stages are rotated and the nozzles are placed in such a position such that a uniform deposit is obtained on each of the impaction plates. Therefore, the deposits collected are suitable for X-ray fluorescence analysis or other types of analysis where a uniform deposit is required.

Under normal use, the particles which penetrate the impaction stages are collected upon a filter and these are considered to be the respirable particles in the aerosol. This impactor, however, contains an adapter so that the penetrating particles may be passed directly through a cascade impactor such as a Micro-Orifice Uniform Deposit Impactor (MOUDI). Therefore, the respirable fraction of the aerosol can be divided into distinct size fractions from .05 μm up to the upper size of the respirable curve (about 10 μm), for further size distribution analysis or chemical analysis of particles in specific size ranges.

Crossflow Influence on Collection Characteristics of Multinozzle Micro-orifice Impactor

C. P. Fang and V.A. Marple
Department of Mechanical Engineering,
University of Minnesota

For lower stages of multinozzle micro-orifice impactors, as many as two thousand nozzles are uniformly arranged within a cluster diameter of 1.06 inches. In the impaction region the mass flowrate of the spent air increases along the radius and reaches a maximum at the periphery. This crossflow can significantly deflect the air jets of the outer nozzles, hence the characteristics of impaction changes.

Investigators in heat transfer and fluid mechanics have studied the influence of crossflow on jet deflection and found the dimensionless deflection of the jet centerline X/D_n is a function of $(S/D_n)(1/m)$. only, here X is downstream coordinate measured from the center of the jet orifice, S is the jet-to-plate distance, D_n is the orifice diameter and m is the jet/crossflow mass flux ratio defined as:

$$m = \frac{\rho_j V_j}{\rho_\infty V_\infty}$$

where ρ is the air density, V is the velocity and the subscripts j and ∞ represent jet and crossflow respectively.

To apply the results of the heat transfer investigation to multinozzle impactors, assumptions must be made: (1) mass flux is uniform over the cluster area; (2) the crossflow velocity is uniform between the nozzle plate and impaction surface at a specific radius; (3) $\rho_j = \rho_\infty$. Therefore, at the periphery we obtain:

$$\left(\frac{S}{D_n}\right) \left(\frac{1}{m}\right) = \frac{D_n N}{4D_c}$$

where N is the number of nozzles and D_c is the cluster diameter. It is interesting to note that at the periphery this parameter is independent of S/D_n .

Impactor calibration data shows that the geometric standard deviation of the collection efficiency curve increases with increase of $D_n N/4D_c$ and 100% collection efficiency can not be guaranteed when $D_n N/4D_c > 1.2$. Therefore, a design criterion of $D_n N/4D_c < 1.2$ is recommended.

Fragment Size Distributions from Simple Fracture of Coal and Rock

C.J. Tsai, D.Y.H. Pui, R. Caldow, K. Olson and B. Cantrell

Particle Technology Laboratory, Mechanical Engineering
Department, University of Minnesota

The amount of new surface generated during fracture of coal and rock has been found to be directly proportional to the amount of energy associated with the fracture. To confirm this and study the relationship between the new surface and dust aerosol formed during fracture the U.S. Bureau of Mines has conducted experiments simulating fracture as it occurs during mining operations. In addition to fracture energy measurements, fragment size distributions were determined over a size range of 0.5 microns to 1 inch. The size measurements accounted for the mass of the original sample. Material studied was Illinois No. 6 coal, coal from the Taggart seam of Virginia, and Berea Sandstone. The experiment employed a chamber to confine sample fracture fragments and a combination of particle measuring systems. Measurement methods included aerodynamic sizing of entrained dust aerosol with optical counting and inertial impaction techniques, physical sizing of non-airborne fragments by sieving, and optical sizing of fragments using optical counting and scanning electron microscopy.

Results of the size distribution measurements indicate that a single size distribution law does not adequately describe the entire fragment size distribution. A combination of two size distributions, such as the Rosin-Rammler and log-normal distributions, is necessary to describe this size distribution. New surface created by fracture is primarily found in particulate between 2 and 50 microns with a mean size of 12 microns. It was also found that the specific energy of fracture can be linearly related to the concentration of aerosol in this size range.

Only a small fraction, between 0.02 and 0.16 pct, of the dust particles generated during fracture become airborne. The remainder adhere to the new surface created during fracture. An entrainment fraction, defined for a given particle size is the ratio of the mass of airborne particles to that of the total particles generated in that size range. This experimental entrainment fraction is related to the Van der Waals adhesion force and the electrostatic forces operating during fracture and is used to derive empirical parameters to model these two processes.

Measuring the Size Distribution of Diesel Exhaust and Mine Dust Aerosol Mixtures with the Microorifice Uniform Deposit Impactor

K.L. Rubow, V.A. Marple, D.B. Kittleson and C. Fang
Particle Technology Laboratory, Mechanical Engineering
Department, University of Minnesota

Under contract to the U.S. Bureau of Mines, a study was conducted to investigate the feasibility of using the microorifice uniform deposit impactor (MOUDI) to measure the size distribution of aerosols containing various mixtures of coal dust and diesel exhaust particles. The project objective was to determine if the mass concentration of diesel exhaust particles, in an airborne mixture of coal dust and diesel exhaust particles, could be determined on the basis of the size distribution of the two aerosols. In general, the mass of diesel exhaust particles is in the submicrometer size range while that of the coal particles lie in the larger size ranges.

The MOUDI is a cascade impactor with small diameter nozzles to obtain small cutsizes and rotating impaction plates to avoid particle overloading of the deposit. For this study, a 7 stage version was used. At the sample flow rate of 30 L/min, the cutsizes were 0.10, 0.23, 0.70, 1.0, 2.6, 4.9 and 10 μm .

Size distributions of aerosols generated in the laboratory and in several underground coal mines were measured. The primary emphasis of the laboratory tests was to ascertain if the diesel exhaust particles could be separated from the coal dust, regardless of mass fraction of the diesel exhaust particles in the total aerosol mixture. Diesel exhaust, from a Caterpillar Type 3304 NA diesel engine, was mixed with coal dust generated with a TSI Model 3400 fluidized bed dust generator. Experiments showed the size distributions of the mixed aerosols exhibited two definite modes with the minimum between the two modes in the 0.7 to 1.0 μm size range. Distinct modal separation was obtained as the mixture fraction of the diesel exhaust aerosols was varied from 3% to 98%.

The field study was conducted in three underground coal mines, two utilizing diesel-powered equipment and the third exclusively using electric equipment. Sampling sites were selected to obtain a wide variety in the diesel exhaust and dust aerosol concentrations. Size distribution data showed these aerosols are bimodal. The mass median aerodynamic diameters of the diesel particulate mode and the coal dust mode were approximately 0.15 μm and 3 to 10 μm , respectively. The results, in all cases, clearly show a separation between the two modes in the 0.7 to 1.0 μm size range with the minimum in the vicinity of 0.8 μm . The separation was found to be independent of mass fraction of the diesel exhaust particles, total particle concentration and sampling site.



Detection of Receptor and Synthesis Antagonists of Platelet Activating Factor in Human Whole Blood and Neutrophils Using Luminol-Dependent Chemiluminescence

K. VanDyke¹ and V. Castranova²

¹Department of Pharmacology and Toxicology, West Virginia University and ² Division of Respirable Disease Studies, National Institute for Occupational Safety and Health, Morgantown, WV

INTRODUCTION

A soluble mediator has been described which is released from activated rabbit leukocytes and induces histamine secretion from rabbit platelets (Barbaro and Zvaifler, 1966; Siraganian and Osier, 1971). This factor has been isolated, characterized and named platelet activating factor, PAF (Benveniste *et al.*, 1972). PAF has since been chemically identified as 1-*O*-alkyl-2-acetyl-*sn*-glyceryl-3-phosphocholine (Benveniste *et al.*, 1979; Demopoulous *et al.*, 1979).

PAF is a lipid mediator of broad biological activity. It causes smooth muscle contraction, contraction of lung tissue and decreased FEV₁; while enhancing capillary permeability thus causing edema (Pinkard, 1983). In addition, PAF is a chemo-attractant and can lead to inflammation.

PAF has been reported to stimulate the release of lysosomal enzymes, leukotriene B₄, and lipid metabolites from neutrophils (Smith *et al.*, 1983; Shaw *et al.*, 1981; Lin *et al.*, 1982; O'Flaherty *et al.*, 1984). The objective of the present investigation was to further characterize PAF-induced stimulation of granulocytes and to develop a bioassay, i.e. chemiluminescence, for screening PAF receptor antagonists and inhibitors of PAF-induced activation of granulocytes. The possible use of the chemiluminescence assay to monitor PAF synthesis by human granulocytes is also described.

METHODS

Blood was drawn from healthy volunteers into a blood storage bag containing CPD anticoagulant. Granulocytes were partially purified by dextran sedimentation and further purified by centrifugal elutriation as described previously (Jones *et al.*, 1980). Granulocytes obtained by this procedure were approximately 95 percent pure. The number of granulocytes in this preparation was determined using an electronic cell counter (Coulter Model Z₁, Coulter Instrument Co., Hialeah, FL). Isolated granulocytes were used to monitor membrane potential, hydrogen peroxide and superoxide release, oxygen consumption, calcium uptake and, in some cases, chemiluminescence. Studies of PAF receptor antagonists were conducted using neutrophils isolated by density centrifugation. Briefly, blood was layered onto Mono-Poly-Resolving Medium (Flow Laboratories, McLean, VA) and centrifuged at 22 °C and 300 g for 30 min. Neutrophils collected from the second band of this gradient were at least 90 percent pure.

Transmembrane potential (E_m) of human granulocytes was measured fluorometrically at 37 °C at an excitation wavelength of 622 nm and an emission wavelength of 665 nm using the fluorescent probe, Di-S-C₃(5) (Jones *et al.*, 1980). Samples contained 0.66 μg ml⁻¹ Di-S-C₃(5) and 2.3 × 10⁷ cells in 3 ml of HEPES-buffered

medium (145 mM NaCl, 5 mM KCl, 10 mM Na HEPES, 5 mM glucose, and 1 mM CaCl₂; pH-7.4).

Hydrogen peroxide release was measured by monitoring the fluorescence of scopoletin at 37 °C at an excitation wavelength of 350 nm and an emission wavelength of 460 nm (Root *et al.*, 1975). Samples contained 1×10^7 cells in 2.5 ml of HEPES-buffered medium containing 2.5 μM scopoletin and 40 μg ml⁻¹ horseradish peroxidase (165 units mg⁻¹).

Superoxide anion release was measured by monitoring cytochrome C reduction spectrophotometrically at 550 nm at 37 °C (Babior *et al.*, 1973). Samples contained 1×10^7 cells suspended in 2.5 ml of a HEPES-buffered medium containing 1.2×10^{-4} M cytochrome C.

Oxygen consumption was measured at 37 °C using a Clark electrode (Castranova *et al.*, 1980). Samples contained 6.5×10^5 cells suspended in 1.7 ml of HEPES-buffered medium.

Calcium transport was monitored at 37 °C by measuring the uptake of ⁴⁵Ca by granulocytes. Briefly, cells (2.5×10^7) were suspended in 1.5 ml of HEPES-buffered medium. At zero time, 7.5 μCi of ⁴⁵Ca was added and a 200 μl sample of this suspension placed immediately over a 100 μl cushion (dibutyl phthalate-mineral oil, density = 1.025 g ml⁻¹). This sample was centrifuged in an air-fuge (Eppendorf Model 5412, Brinkman Instrument, Westbury, NY) and the supernatant and cushion removed by suction. The cell pellet was dissolved in 100 μl of 0.1 percent Triton X-100, mixed with 10 ml of Aquasol (New England Nuclear, Boston, MA) and counted in a liquid scintillation counter. In this manner, uptake was monitored by taking cell samples at various time intervals.

Chemiluminescence generated from purified granulocytes was measured at 37 °C using a liquid scintillation counter operated in the out-of-coincidence mode (Trush *et al.*, 1978). Briefly, granulocytes (1×10^6 cells) were suspended in 5 ml of HEPES-buffered medium containing 1×10^{-8} M luminol.

Whole blood chemiluminescence was monitored at 37 °C using a luminometer (Berthold Model LB 9500T, Berthold Instrument Inc., Wildbad, W. Germany) linked to a computer data handling system (Edinboro *et al.*, 1985). Briefly, whole blood was diluted 1:50 in HEPES-buffered medium (500 μl) containing 1.12×10^{-4} M luminol.

PAF was obtained from Bachem (Torrance, CA). This PAF was used as a mixture containing 60 percent C₁₈ and 40 percent C₁₉. PAF was dissolved in 1 percent bovine serum albumin diluting with HEPES-buffered medium.

RESULTS AND DISCUSSION

The present study characterizes the effects of PAF on the membrane potential, ionic permeability, and respiratory burst activity of human granulocytes. Furthermore, these responses to PAF are compared to those for a known stimulant of phagocytes, i.e. the chemotactic agent FMLP. These results are summarized in Table 1.

Table 1. Characteristics of PAF Stimulation of Human Neutrophils: Comparison to Stimulation with FMLP¹

Response	PAF	FMLP
Chemiluminescence	+	+++
Superoxide release	+	+++++
Oxygen consumption	0	+++
H ₂ O ₂	++	+++++
Depolarization	+++	+++
Increased P _{Ca}	0	++
Increased P _{Na}	+++	+++

¹ Responses to maximal doses of stimulant, i.e., 1×10^{-5} M PAF and 1×10^{-7} M FMLP. The relative magnitude of enhancement is signified by +. No response is signified by 0.

PLATELET ACTIVATING FACTOR

PAF induces a rapid but transient depolarization of the granulocyte plasma membrane. This depolarization peaks within 15 s in response to a maximal dose of PAF (1×10^{-5} M). This response is short-lived with the membrane potential repolarizing to the resting level within 90 s. PAF fails to alter membrane potential in the absence of extracellular sodium. However, PAF-induced depolarization is unaffected by removal of extracellular calcium. These results suggest that the PAF-induced change in membrane potential is the result of a transient increase in sodium permeability but not calcium permeability. Indeed, measurement of ^{45}Ca uptake indicates that calcium transport of granulocytes is not enhanced by PAF. The effect of PAF on the membrane potential of human granulocytes is dose-dependent. Responses can be measured between doses of 10^{-7} to 10^{-5} M with an ED_{50} of 2.5×10^{-6} M. At doses of PAF above 2.5×10^{-5} M, the magnitude of the response declines. This PAF-induced depolarization is similar in magnitude and time course to that produced by FMLP. However, unlike FMLP, PAF does not produce a delayed fall in fluorescence signal below the resting level. It has been shown that this fall is the result of myeloperoxidase- H_2O_2 dependent oxidation of the fluorescent probe (Castranova and Van Dyke, 1984; Whittin *et al.*, 1981). Thus, in contrast to FMLP, PAF may not stimulate the release of myeloperoxidase from granulocytes. Furthermore, while PAF enhances only sodium permeability, FMLP increased both sodium and calcium permeability of granulocytes.

FMLP is a known stimulant of respiratory burst activity in human granulocytes, i.e. FMLP stimulates large changes in oxygen consumption, secretion of superoxide anion and H_2O_2 , and chemiluminescence. In comparison, stimulation by PAF is smaller and less complete. PAF-induced secretion of superoxide anion is only 20 percent of that induced by FMLP and H_2O_2 release in response to PAF is only 50 percent of the FMLP level. In further contrast to FMLP, PAF does not enhance oxygen consumption of granulocytes and PAF-induced chemiluminescence is only 30 percent of that seen with FMLP stimulation. It is interesting that as with stimulant-induced depolarization, PAF- and FMLP-induced chemiluminescence is dependent on the presence of extracellular sodium, i.e. little chemiluminescence is seen if external sodium is replaced by potassium.

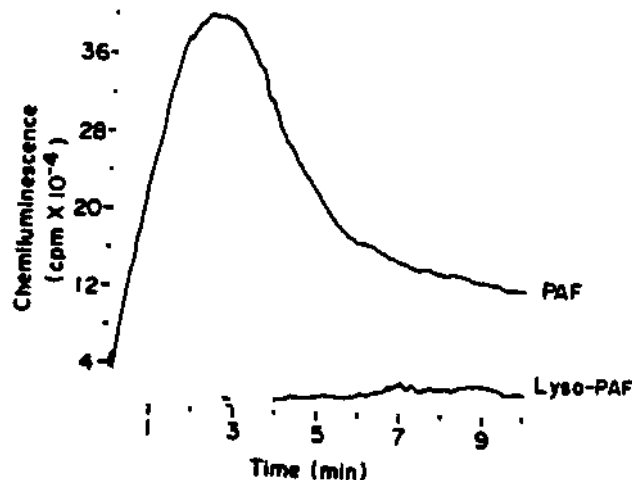


Figure 1. Chemiluminescence generated from human whole blood in response to 1×10^{-5} M PAF or lyso-PAF

Chemiluminescence has proven to be a simple and rapid method to monitor the effects of PAF on granulocytes. In contrast to other parameters studied, chemiluminescence can be monitored with whole blood. This eliminates the time involved in cell purification. An example of PAF-induced chemiluminescence in whole blood is given in Figure 1. PAF-stimulated chemiluminescence generated from purified granulocytes exhibits a time course which is similar to that of the whole blood response. However, the magnitude of the response is somewhat larger with purified cells because of quenching of light by red blood cells in the whole blood assay. In addition, the ED₅₀ for PAF is higher, i.e. 9×10^{-5} M in the whole blood system because of non-specific binding to cells other than granulocytes.

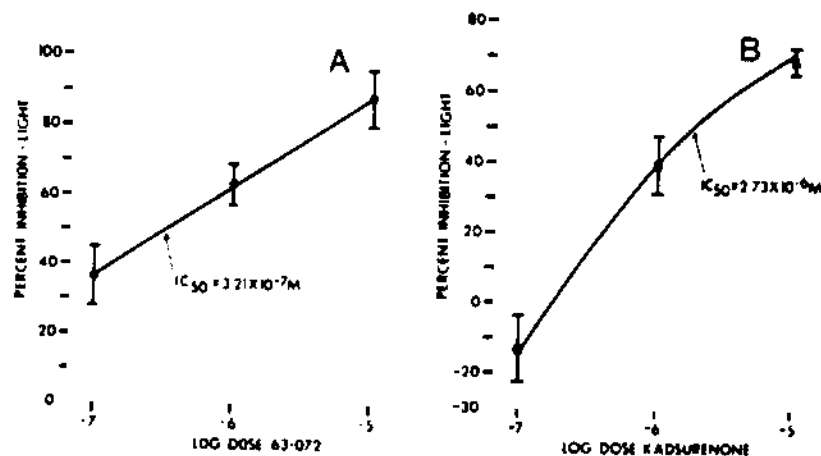


Figure 2. Dose-response curves for inhibition of PAF-induced chemiluminescence from purified granulocytes by 63-072 (A) or kadsurenone (B). Granulocytes were stimulated with 1×10^{-5} M PAF

Table 2. Effect of Inhibitors on PAF-Induced Chemiluminescence in Human Neutrophils

Inhibitor	Maximal inhibition ¹	IC ₅₀ ²
63-072	88%	3.2×10^{-7} M
Kadsurenone	70%	2.7×10^{-6} M
NDGA	62%	-
Indomethacin	20%	-

¹ Maximal inhibition was measured at an inhibitor dose of 1×10^{-5} M

² IC₅₀ is the inhibitor concentration which results in 50 percent of maximal inhibition.

The effects of PAF-receptor antagonists on PAF-induced chemiluminescence are shown in Figure 2. 63-072, an inhibitor synthesized by Sandoz Research Institute, is a potent inhibitor of PAF causing an 88 percent decrease in PAF-induced chemiluminescence at 1×10^{-5} M with an IC₅₀ of 3.2×10^{-7} M. Kadsurenone, a Merck compound, is less potent causing 70 percent inhibition at 1×10^{-5} M with an IC₅₀ of 2.7×10^{-6} M. The lipoxygenase pathway seems to be much more important in the generation of PAF-induced chemiluminescence than the cyclo-oxygenase pathway, since nordihydroguaiaretic acid (NDGA) is an effective inhibitor of PAF-stimulated chemiluminescence while indomethacin is not very effective (Table 2).

The effect of lyso-PAF on chemiluminescence is shown in Figure 1. Note that lyso-PAF, the inactive metabolite of PAF, does induce chemiluminescence in leukocytes. Compared to PAF, the response to lyso-PAF is delayed and of decreased magnitude.

This delay suggests that lyso-PAF may be used by the cells as a substrate to synthesize PAF and that it is this newly formed PAF which induces chemiluminescence. This hypothesis is supported by the following evidence. Calcium has been shown to be essential for the conversion of lyso-PAF to PAF and our data indicate that addition of EDTA, a calcium chelator, to the cell suspension inhibits chemiluminescence in response to lyso-PAF by 75 percent while decreasing the response to PAF by only 50 percent. It is interesting that there seems to be a wide interpersonal variation in the ability of leukocytes to synthesize PAF from lyso-PAF, i.e. the delay before initiation of chemiluminescence following lyso-PAF treatment ranges from 15 s to 4.5 min with an average delay of 1.5 min (n=75).

In conclusion, the data from this investigation indicate the PAF is not only a secretory product of granulocytes but is also an activator of these cells. PAF induces an increase in sodium permeability in these phagocytes as well as sodium dependent depolarization and generation of chemiluminescence. The chemiluminescence assay has proved to be useful in screening inhibitors of activation and PAF-receptor antagonists. In addition the chemiluminescence assay may also prove useful in monitoring synthesis of PAF from lyso-PAF.

REFERENCES

- Babior, B.M., Kipnes, R.S., and Curnette, J.T. (1973). 'Biological defense mechanisms: The production by leukocytes of superoxide, a potential bactericidal agent', *J. Clin. Invest.*, **52**, 741-744.
- Barbaro, J.F., and Zvaifler, G.F. (1966). 'Antigen induced histamine release from platelets of rabbits producing homologous PCA antibody, (3137)', *Proc. Soc. Exp. Biol. Med.*, **122**, 1245-1247.
- Benveniste, J., Henson, P.M., and Cochrane, C.G. (1972). 'Leukocyte-dependent histamine release from rabbit platelets', *J. Exp. Med.*, **136**, 1356-1377.
- Beneveniste, J., Tence, M., Varenne, P., Bidault, J., Bouillet, C., and Polonsky, J. (1979). 'Platelet activating factor', *Comptes Rendus hebdomadaires des seances Acad Sci Paris*, **289D**, 1037-1040.
- Castranova, V., Bowman, L., Reasor, M.J., and Miles, P.R. (1980). 'Effects of heavy metal ions on selected oxidative metabolic processes in rat alveolar macrophages', *Toxicol. Appl. Pharmacol.*, **53**, 14-24.
- Castranova, V., and Van Dyke, K. (1984). 'Analysis of oxidation of the membrane potential probe Di-S-C₃(5) during activation', *Microchem. J.*, **29**, 151-161.
- Demopoulos, C.A., Pinckard, R.N., and Hanahan, D.J. (1979). 'Platelet activating factor', *J. Biol. Chem.*, **254**, 9355-9358.
- Edinboro, L.E., Van Dyke, K., Peden, D., Castranova, V., and Wierda, D. (1985). 'Studies of luminol-dependent whole-blood chemiluminescence induced by platelet-activating factor (PAF)', *Microchem. J.*, **31**, 261-271.
- Jones, G.S., Van Dyke, K., and Castranova, V. (1980). 'Purification of human granulocytes by centrifugal elutriation and measurement of transmembrane potential', *J. Cell Physiol.*, **104**, 425-432.
- Lin, A.H., Morton, D.R., and Gorman, R.R. (1982). 'Acetyl-glycerol ether phosphorylcholine stimulates leukotriene B₂ synthesis in human polymorphonuclear leukocytes', *J. Clin. Invest.*, **70**, 1058-1063.
- O'Flaherty, J.T., Wykle, P.L., Thomas, M.J., and McCale, C.E. (1984). 'Neutrophil degranulation responses to combinations of aradidonate and platelet activating factor', *Res. Comm. Chem. Path. Pharmacol.*, **43**, 3-23.
- Pinckard, R.N. (1983). 'Platelet activating factor', *Hosp. Prac.*, **19**, 67-76.
- Root, R.K., Metcalf, J., Oshino, N., and Chance, B. (1975). 'H₂O₂ release from human granulocytes during phagocytosis. I. Documentation, quantitation, and some regulating factors', *J. Clin. Invest.*, **55**, 945-955.
- Shaw, J.O., Pinckard, R.N., Ferrigni, K.S., McManus, L.M., and Hanahan, D.J. (1981). 'Activation of human neutrophils with 1-O-hexadecyl/octadecyl-2-acetyl-glycerol-3-phosphorylcholine (platelet activating factor)', *J. Immunol.*, **127**, 1250-1255.
- Siraganian, R.P. and Osler, A.G. (1971). 'Destruction of rabbit platelets in the allergic response of sensitized leukocytes', *J. Immunol.*, **106**, 1244-1251.
- Smith, R.J., Bowman, B.J., and Iden, S.S. (1983). 'Characteristics of 1-O-hexadecyl and 1-octadecyl-2-O-acetyl-sn-glycerol-3-phosphorylcholine stimulated granule enzyme release from human neutrophils', *Clin. Immunol.*, **28**, 13-28.

THE RESPIRABLE DUST CENTER

- Trush, M.A., Wilson, M.E., and Van Dyke, K. (1978). 'The generation of chemiluminescence (CL) by phagocytic cells'. In M. Deluca (ed.) *Methods in Enzymology*, Academic Press, New York, Vol.57, pp. 462-494.
- Whitin, J.C., Clark, E.R., Simons, E.R., and Cohen, H.J. (1981). 'Effects of the myeloperoxidase system on the fluorescent probes of granulocyte membrane potential', *J. Biol. Chem.*, 256, 8904-8906.

Acknowledgement

Generic Mineral Technology Center for Respirable Dust,
BOM - G1175142

Measurement of Superoxide Release from Single Pulmonary Alveolar Macrophages

K.A. DiGregorio, E.V. Cilento and R.C. Lantz

Department of Mineral Engineering, West Virginia University

K. A. DIGREGORIO, E. V. CILENTO, AND R. C. LANTZ. *Measurement of superoxide release from single pulmonary alveolar macrophages*. Am. J. Physiol. 252 (Cell Physiol. 21): C677-C683, 1987.—An electrooptical method was developed to quantify superoxide (O_2^-) release from single rat pulmonary alveolar macrophages (PAM) during adherence to the bottom of a culture dish. This was done by measuring the reduction of nitro blue tetrazolium (NBT) to a diformazan precipitate at 550 nm from videorecorded images of individual cells. Temporal changes in cell optical density, which are proportional to the mass of diformazan produced, were calculated from videophotometric measurements of the change in light intensity over individual cells. Total diformazan produced increased 78 and 126% with an increase in NBT from 0.5 to 1.0 and 2.0 mg/ml, respectively. Total diformazan produced and maximum rate of production among individual PAM varied two- to threefold providing strong evidence for heterogeneity in O_2^- production. Specific inhibition of O_2^- production by superoxide dismutase, iodoacetate, and chlorpromazine significantly reduced the total diformazan produced and maximum rate of diformazan production. Hydrogen peroxide was not involved in NBT reduction, since catalase alone did not significantly change diformazan production. This novel method to quantify O_2^- release from single PAM should be valuable in analyzing heterogeneity and single cell kinetics of O_2^- production, in assessing the effects of exposure of cells to particulates on O_2^- release, and in relating release to electrophysiological measurements.

rat; nitro blue tetrazolium; macrophage heterogeneity; single cell kinetics

PULMONARY ALVEOLAR MACROPHAGES (PAM) protect the lungs by phagocytizing foreign debris and bacteria (24). This process involves ingestion as well as destruction of foreign matter. Phagocytosis is usually accompanied by a respiratory burst that increases cellular oxygen consumption and glucose metabolism in the hexose monophosphate shunt (7), which leads to the release of highly reactive oxygen metabolites at the surface of the plasma membrane (6, 27). These agents have been implicated in the killing of bacteria by phagocytes (22), but have also been shown to be toxic and have been linked to cancer, emphysema, arthritis, diabetes, and other diseases (17, 22, 30). Toxic effects may be a result of either an abnormally low production of metabolites, resulting in damage to lung tissue by respirable bacteria and dusts, or an abnormally high production, resulting in direct damage to lung tissue by metabolites themselves.

The initial oxygen metabolite is thought to be super-

oxide anion (O_2^-), produced from the reduction of oxygen by NADPH oxidase (6). Superoxide can readily dismutate to form hydrogen peroxide and, subsequently, other antimicrobial agents: hydroxyl radical (OH^\bullet), singlet oxygen (O^1), and hypochlorous acid ($HOCl$) (7, 22).

Two important areas of current interest concern the activation of the superoxide generating system (7, 18) and the heterogeneity of superoxide production among cells (19). Studies on groups of cells, separated into subfractions according to cell density, suggest that phagocytes from different subpopulations are heterogeneous in terms of superoxide production (19). However, significant variability may also exist among individual cells within each subfraction (15). Absolute quantitation of variability with a population can only be performed by making measurements on individual cells.

Evidence suggests that activation of phagocytes to produce superoxide occurs in response to changes in electrical potential across the cell membrane (18, 23). However, although electrophysiological measurements have been made on individual cells (14), measurement of superoxide production has only been possible on large numbers of cells in culture (22, 24). Therefore, no techniques are presently available to measure electrophysiological changes and superoxide release simultaneously on the same cell.

As such, the purpose of this study was to develop an electrooptical technique to quantitatively measure the release of superoxide from single cells in culture. Development of this methodology would be useful in analyzing heterogeneity among cells and in studying the dynamics of superoxide production by single cells. Ultimately, this approach combined with measurement of transmembrane electrical changes simultaneously on the same cell should prove valuable in understanding the production of superoxide and other metabolites by PAM. The method reported in this study uses electrooptical techniques to measure nitro blue tetrazolium (NBT) reduction to a diformazan precipitate as an indicator of superoxide production by single PAM stimulated by adherence. Specificity of the technique for superoxide was tested using either known blockers of superoxide production or superoxide dismutase (SOD), which leads to superoxide dismutation.

MATERIALS AND METHODS

Solutions. Lavage fluid contained 145 mM NaCl, 5 mM KCl, 1.9 mM NaH_2PO_4 , 9.35 mM Na_2HPO_4 , and 5 mM

glucose at pH 7.4. Resuspension fluid consisted of 140 mM NaCl, 5 mM KCl, 1.5 mM CaCl₂, 5 mM glucose and 10 mM Na-N-2-hydroxyethylpiperazine-N'-2-ethanesulfonic acid (HEPES) at pH 7.4. Lavage and resuspension fluids are those used in previous work (12, 23). NBT, SOD, catalase, iodoacetate (IOD), chlorpromazine (CHL), and bovine serum albumin (BSA) were purchased from Sigma Chemical and dissolved in resuspension fluid. NBT was added to the resuspension fluid, warmed to 25–30°C, and stirred to obtain soluble NBT solutions at concentrations of 0.5, 1.0, and 2.0 mg/ml. SOD (3,100 U/mg protein) was purchased in a suspension of 3.8 M (NH₄)₂SO₄, separated from (NH₄)₂SO₄ by centrifugation at 13,000 g for 3 min, and dissolved in resuspension fluid. SOD, catalase, and BSA were added to 3 ml NBT solution in culture dishes containing PAM to obtain a final concentration of 100 µg/ml. Iodoacetate and chlorpromazine were added to culture plates to obtain final concentrations of 10 mM and 50 µM, respectively (10, 13, 26).

Surgical preparation. PAM were obtained from male Long-Evans hooded rats (Charles River) weighing between 250–300 g using the tracheal lavage method developed by Myrvik et al. (25). Briefly, anesthesia was administered by intraperitoneal injection of pentobarbital sodium (0.1 g/kg body wt), the diaphragm was severed, the animal was exsanguinated, and a 15 g needle was inserted through an incision in the trachea. Fresh lavage fluid (7 ml, 4°C) was injected into the lung through the needle and slowly withdrawn to obtain cells. A total of 80 ml of lavage fluid was collected by repeating this process 12 times. PAM collected were centrifuged at 500 g for 5 min at 4°C and resuspended in ice-cold HEPES-buffered medium. After a second wash, PAM were resuspended in ~6 ml of HEPES-buffered medium at pH 7.4 and placed in an ice-water bath. It has been shown in other studies that as much as 99% of lavaged rat cells are macrophages (21) and that 85–95% of PAM obtained by lavage are viable (12, 32).

Experimental design. An aliquot of 400 µl of the cell suspension (2–5 × 10⁵ cells) was added to 3 ml of NBT solution at 37°C in a tissue culture dish (Falcon 3001). A layer of paraffin oil (37°C) was placed on top of the aqueous layer to reduce evaporation. The remaining cell suspension was kept in an ice-water bath until needed.

The culture dish, containing PAM and NBT, was placed on a temperature-controlled (37°C) heating element located on the stage of an Olympus (model IMT) inverted light microscope and transilluminated at 550 nm, the peak absorbance wavelength for turbidimetric assay of insoluble diformazan in aqueous solutions (5, 26). A field of at least six PAM was randomly selected such that the cells were well separated from each other. The microscope image was televised using a low-light level Cohu (model 4410) silicon-vidicon television camera and videorecorded for 40 min using a ¾ in. Sony (model V05600) videocassette recorder. The complete system operates essentially as a vertical densitometer.

Temporal changes in light intensity over single PAM were determined by playing back previously videorecorded images through an IPM (model 204A) video pho-

tometric analyzer. The analyzer generates two windows, with size and position in the video image user selectable, which act as phototransistors sensitive to changes in average light intensity in the window area. The output voltage from each window was filtered (0.23 Hz) to reduce signal noise, digitized (12 bit) using a Keithley DAS (model 520) every 10 s for 40 min, and stored on an IBM PC-XT. This procedure was repeated to obtain measurements from at least six PAM in each videorecorded image.

Background light intensity variation was determined in regions of the image containing no cells. After correction for any background variation, optical density (OD) for each cell at each time interval was calculated using a Beer-Lambert equation. The incident intensity was calculated as the average of the initial 3 intensity values, representing 20 s of base line. OD was then converted to mass of diformazan using the Beer-Lambert equation in which OD is equal to the product of an extinction coefficient, concentration, and pathlength.

This system is analogous to a vertical spectrophotometer so that OD is independent of the vertical distribution of the absorbing material (29). Although the Beer-Lambert equation is strictly true for dilute compounds in solution, it is also used for densitometric and turbidimetric measurements where the extinction coefficient is measured for the insoluble product (1). The molar extinction coefficient for insoluble diformazan in buffered aqueous solutions at neutral pH is 30,000/M·cm (5). Since concentration is mass per unit volume and in this system volume is the product of the area of the cell and the pathlength, the pathlength effectively cancels out in the equation. Therefore, the OD value calculated was multiplied by the window area and the molar extinction coefficient to determine the mass of diformazan produced.

Calibration of the electro-optical system, using neutral density filters, showed that OD was linear over the range of 0 to 0.7 OD units (Fig. 1). For comparison, OD for diformazan production from cells was typically <0.3 OD units.

Temporal changes in cumulative mass of diformazan produced for each cell (*M*), exhibited a time delay followed by an exponential-like increase to an asymptotic maximum value (*MAX*). The data were fit to the following equation

$$M = \text{MAX}[1 - \exp(-(t - t_d)/T)]$$

where *t* is the time in s; *t_d* the delay time measured between stimulation and detection of diformazan production in s; and *T* the time constant. The total diformazan produced, *MAX*, was determined by averaging the last minute of diformazan data, and *t_d* was estimated by observing the point at which diformazan production increased significantly above base line. A value for *T* was determined by fitting the data to the log-linearized form of this equation. The maximum (initial) rate of diformazan production, *R*, was calculated from the derivative of the equation at time *t_d*, that is, as *MAX/T*. The main parameters of interest in this study were the total diformazan produced, *MAX*, and the maximum rate of pro-

SUPEROXIDE RELEASE FROM SINGLE MACROPHAGES

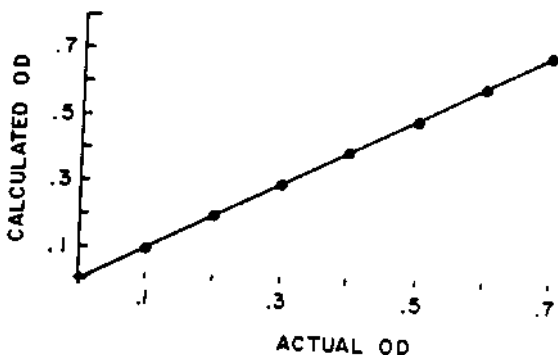


FIG. 1. Calibration of electrooptical system at 550 nm using neutral density filters. Light intensity was measured and optical density (OD) calculated using Beer-Lambert law. System response was linear up to 0.7 units.

duction, R .

To establish the methodology and to determine the best NBT concentration to use in the culture dish, cells from 3 animals were examined at each of 3 NBT concentrations, 0.5, 1.0, and 2.0 mg/ml.

Specificity of the assay for superoxide was determined by addition of 1) SOD, which competes with NBT for superoxide by catalyzing the dismutation of superoxide to hydrogen peroxide and oxygen (22); 2) iodoacetate, which inhibits the release of superoxide by blocking regeneration of NADPH needed for NADPH oxidase (10, 26); 3) chlorpromazine, which inhibits superoxide release by competing with oxygen for the NADPH oxidase (13); and 4) BSA, a nonspecific protein. To eliminate animal variation all inhibitors were tested on cells from each of four animals.

Because SOD dismutates superoxide to H_2O_2 , the effect of catalase alone (CAT) and catalase with SOD (S-C) on NBT reduction was tested in four additional animals. Catalase catalyzes the degradation of H_2O_2 to oxygen and water, thereby preventing H_2O_2 from reacting further with superoxide to produce other oxygen metabolites (30).

Experiments were analyzed using ANOVA at the 95% confidence level. When significant differences were found, the Newman-Keuls test was used to determine the significant differences among means.

RESULTS

The production of diformazan, indicated by the progressive darkening of PAM at 10, 20, and 40 min compared with *time 0*, is illustrated in photographs taken from televised images of PAM shown in Fig. 2. A window (white box) generated by the photoanalyzer is shown in the image at *time 0*. Since the PAM attach to the dish surface and spread during the 40 min, as illustrated by the increase in cell area as time progresses, the window size used for measurements was adjusted to the cell area at the end of the experiment. To evaluate whether spreading effects OD, experiments were done without NBT in the culture medium. No change in OD was seen due to spreading alone. Experiments done with and without an oil layer showed no differences.

The average mass of diformazan produced vs. time for six PAM from each of three animals at each NBT

concentration is shown in Fig. 3. The cumulative mass of diformazan produced increased in an exponential-like manner with time to an asymptotic maximum by 40 min. Increasing NBT concentration from 0.5 to 1.0 or 2.0 mg/ml increased both the total diformazan produced (78 and 126%, respectively) and the maximum rate of diformazan production (72 and 148%, respectively). Concentrations >2.0 mg/ml led to NBT precipitation that interfered with measurement of diformazan production. Therefore, to maximize detection of diformazan, 2.0 mg/ml NBT was used in all subsequent experiments. These data fit the equation very well; coefficients of determination (r^2) for individual cells ranged from 0.91 to 0.97.

Importantly, it also should be noted that statistical analysis of total diformazan produced (MAX) and rate of production (R) revealed that PAM used immediately after washing provided results similar to cells that were maintained in an ice-water bath for up to 4 h. System reliability and repeatability were excellent based on repeated measurement on one cell with either window ($\pm 2\%$). Importantly, for all control cells (102 PAM), including those analyzed with 0.5 and 1.0 mg/ml NBT, only one did not release superoxide to produce diformazan.

Heterogeneity among individual cells analyzed in the same culture dish was demonstrated by the fact that diformazan production varied widely among PAM from the same animal and under the same experimental conditions. For example, total diformazan produced and maximum rate of diformazan production are given for individual PAM at 2.0 mg/ml NBT in Table 1. Values for MAX and R from individual PAM varied two- to threefold and coefficients of variation ranged from 31 to 42%. Similar variation was found among PAM at 0.5 and 1.0 mg/ml NBT and for PAM exposed to inhibitors (see below).

Specificity for reduction of NBT by superoxide was tested using five treatments in each animal: 1) control (NBT alone); 2) SOD; 3) BSA; 4) IOD; and 5) CHL. MAX and R were significantly inhibited ($P < 0.01$) by each treatment compared with control (Fig. 4). SOD, IOD, and CHL inhibited MAX by 48, 51, and 43%, respectively, when compared with control. Interestingly, BSA, a nonspecific protein, also decreased MAX (58%). R was inhibited 49% by SOD, 41% by IOD, 60% by CHL, and 65% by BSA when compared with control. The equation also fit the data obtained from the inhibitor experiments. However, 13 of 96 PAM exhibited complete inhibition of superoxide production and another 13 PAM showed a very small linear production of diformazan. For the 13 PAM showing a small production, 4 were treated with BSA and 9 with SOD, whereas for cells that showed complete inhibition 5 were from BSA, 4 from CHL, and 4 from IOD. Again, heterogeneity among individual PAM exposed to inhibitors in the same dish was also apparent since some cells showed no production (complete inhibition), whereas others that produced diformazan exhibited up to a 10-fold variation in MAX and R .

Since SOD only inhibited diformazan production by 49%, the effect of H_2O_2 and its oxygen metabolites on NBT reduction was examined. Addition of reagent grade

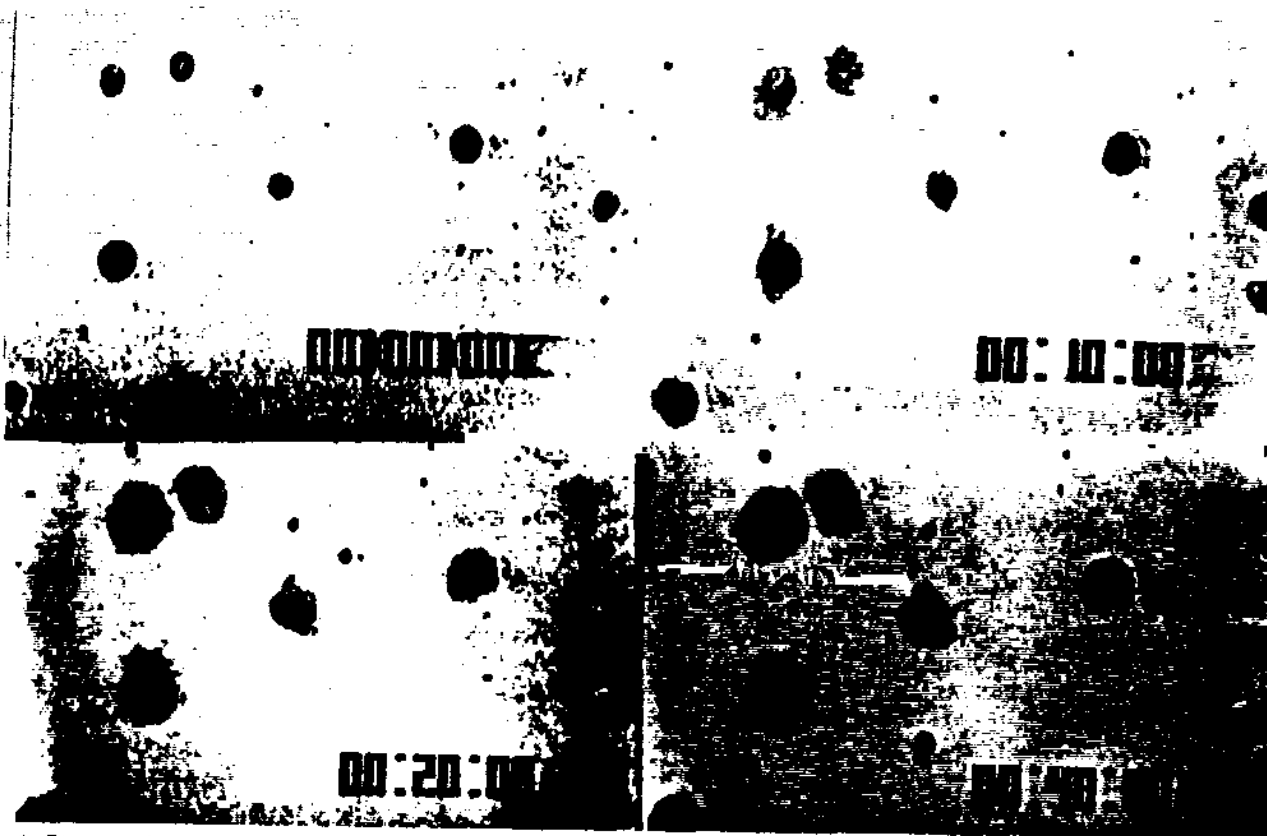


FIG. 2. Photographs of pulmonary alveolar macrophages (PAM) taken from video monitor at 0, 10, 20, and 40 min. Progressive darkening of cells is due to diformazan precipitate. One photoanalyzer window (white box) is shown at 0. PAM spreading is apparent but did not affect optical density.

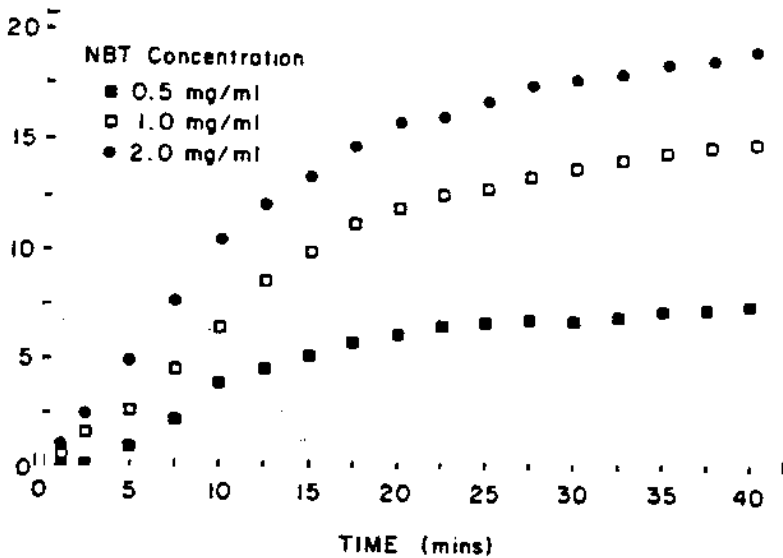


FIG. 3. Cumulative mass of diformazan produced with time for nitro blue tetrazolium (NBT) concentrations of 0.5, 1.0, and 2.0 mg/ml. Each curve represents an average of 16 cells, 6 from each of 3 animals.

O₂ to NBT solution alone did not result in production of diformazan. Production of diformazan by H₂O₂ or its analogs tested using catalase alone showed no significant differences from control cells (Fig. 5). Also, because SOD dismutates superoxide to H₂O₂, the effects of SOD and catalase together (S-C) were tested. The inhibition of MAX and R produced by S-C (60 and 57%) were not significantly different from SOD alone (49 and 48%). Importantly, the inhibition of MAX and R by SOD in this set of experiments was very similar to the previous experiments with IOD, CHL, and BSA. Heterogeneity

was also apparent among PAM treated with catalase, SOD, and S-C; 12 of 72 cells were completely inhibited (7 from S-C and 5 from SOD).

DISCUSSION

To measure the release of superoxide from individual cells, several qualities of the chemical probe and the measuring system used to detect superoxide are desirable. After reacting with superoxide, the probe should change its light absorbance properties and should become im-

SUPEROXIDE RELEASE FROM SINGLE MACROPHAGES

TABLE 1. Total diformazan produced and initial rate of diformazan production

	Total Diformazan Production, fmol			Diformazan Production Rate, 10 ⁻³ fmol/s		
	A1	A2	A3	A1	A2	A3
	8.8	12.6	9.6	10.6	20.9	9.4
	12.4	17.0	16.8	13.7	42.2	22.7
	13.6	17.1	20.3	14.0	17.4	22.0
	13.5	22.7	22.5	14.6	21.5	24.8
	23.9	23.9	25.8	22.7	23.0	27.6
	25.5	30.5	26.0	24.8	26.0	31.1
Means	16.3	20.6	20.2	16.7	25.2	22.9
± SD	±6.8	±6.4	±6.2	±5.6	±8.8	±7.4
COV	42%	31%	31%	34%	35%	32%

Measurements for 6 individual pulmonary alveolar macrophages from each of 3 animals (A1, A2, A3). COV, coefficient of variation.

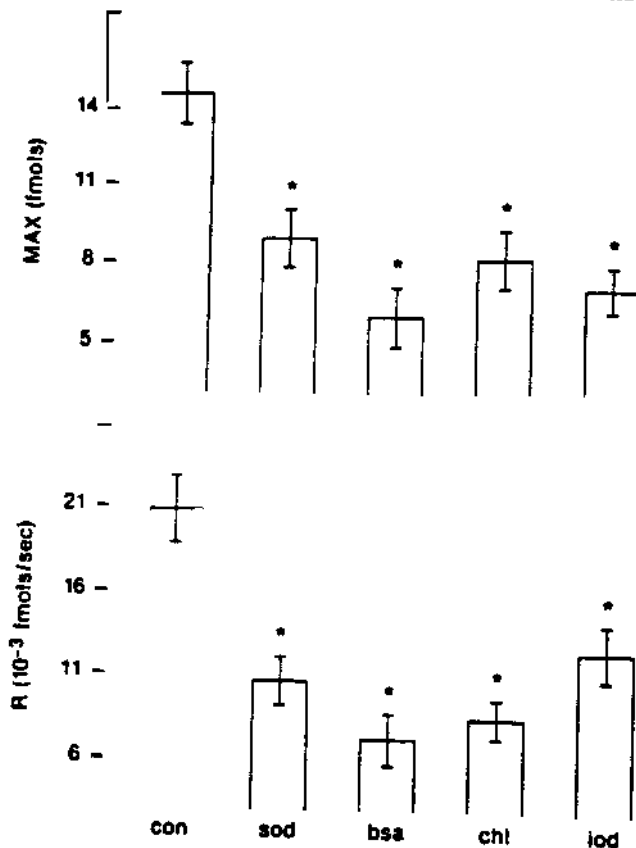


FIG. 4. Top: total diformazan produced (MAX); and bottom: maximum rate (R) of diformazan production in presence of superoxide dismutase (SOD), bovine serum albumin (BSA), iodoacetate (IOD), and chlorpromazine (CHL) as compared with control (CON). Values are means ± SE of 24 cells. * P < 0.01.

mobile at the site where it is produced. The response of the probe and the measuring system should be sensitive enough to detect production of superoxide from single cells and should be linearly related to the production of superoxide. The measuring probe should be specific for superoxide release. Although no perfect system exists, the electrooptical system described in this study using NBT adequately meets these requirements. NBT, in the presence of a strong reducing agent such as superoxide, is reduced to an insoluble diformazan precipitate at the reaction site that absorbs maximally at 550 nm. Attempts to use cytochrome c that produces a soluble, diffusible

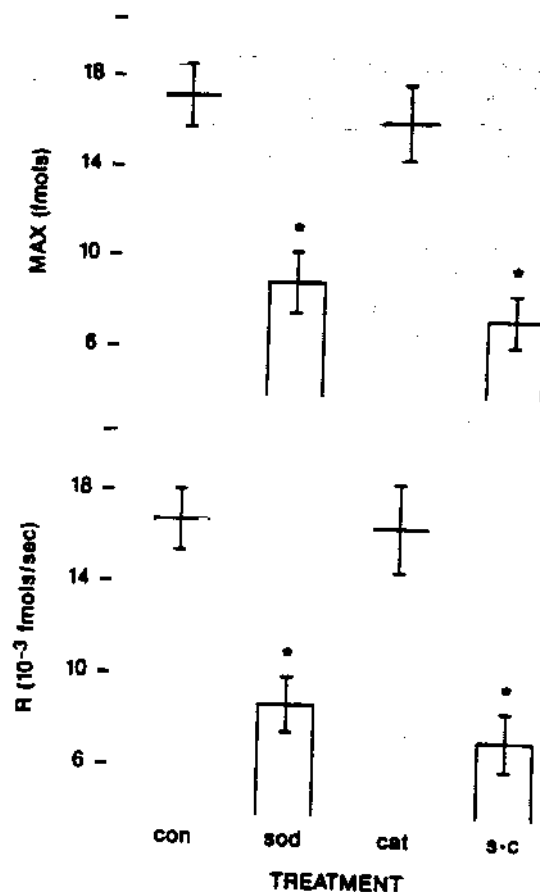


FIG. 5. Top: total diformazan produced (MAX); bottom: maximum rate (R) of diformazan production in presence of superoxide dismutase (SOD), catalase (CAT), and SOD with catalase (S-C). Values are means ± SE from 24 cells. * P < 0.01.

reaction product were unsuccessful.

Pick et al. (26) have used NBT in a similar densitometric microassay for superoxide release from whole populations of macrophages in culture. A variety of soluble compounds were used to stimulate adhered PAM. In the present study, once PAM were attached they could not be stimulated by either soluble compounds or particulates. However, cells produced superoxide during attachment to the bottom of the culture dishes and this stimulation was not enhanced further by the addition of stimulants to the medium. These results are supported by other studies that have shown that adherence stimulates the respiratory burst (9, 31) and that prolonged adherence alters the ability of cells to release superoxide (9, 16). A possible explanation for the inability to stimulate adhered PAM in this study is that serum was not used in the resuspension medium, whereas it was in the study by Pick et al. (26).

As NBT concentration was increased diformazan production increased and the time delay decreased. Also, the measurement area (window size) decreased with increasing NBT concentration. These changes indicated that at low NBT concentrations superoxide diffused further from the cell surface before reacting. The most conclusive evidence for this fact came from observations of the videorecorded images. In contrast, with the highest concentration of NBT (2.0 mg/ml) diformazan appeared concentrated on the cell, indicating that there was no

interference from reaction products produced by other cells. In addition, background variation was negligible. For these reasons, and the larger values for total cumulative diformazan production, the highest NBT concentration provided the most sensitive measurement of superoxide production.

The electrooptical system responded linearly using neutral density filters. The use of different window sizes on the IPM photoanalyzer did not affect this calibration curve because the filters provide a homogeneous light intensity in the window. If the reduction of NBT to a diformazan precipitate by a cell is not homogeneous, then the OD as calculated in this study underestimates the true OD (2, 11). Such distributional errors occur commonly in microspectrophotometry whenever the light-absorbing material does not distribute uniformly within the measurement area. More sophisticated image-analysis methods can eliminate this problem by calculating OD for a number of pixels (smaller homogeneous areas) comprising the total cell area and determining an average OD from these values. It was not possible to do this with the equipment available in this study. However, OD calculated for one window covering an entire cell was compared with the OD calculated by summing OD values for a number of smaller windows over the same cell. In all cases there were no significant differences indicating that distributional errors were probably minimal.

IOD, CHL, SOD, and BSA significantly inhibited, but not completely, the total diformazan produced and the maximum rate of diformazan production when compared with control cells. These results support the specificity of superoxide for NBT reduction. The small inhibition provided by IOD and CHL may have resulted from the low concentrations used, however, no dose-response studies were done.

SOD specifically catalyzes the dismutation of superoxide to hydrogen peroxide and oxygen and thus should be a specific inhibitor of NBT reduction by superoxide. Since SOD at 100 $\mu\text{g}/\text{ml}$ did not completely inhibit NBT reduction (49%) perhaps an optimum concentration was not used. However, other studies have also shown incomplete inhibition of NBT reduction using different concentrations of SOD (4, 26). Therefore, it is possible that other antimicrobial agents or membrane enzymes reduced 51% of the NBT.

It is not clear why there was nonspecific inhibition of NBT reduction by BSA, although other investigators (4, 26) have also shown nonspecific inhibition of NBT reduction by BSA and other proteins. However in this study, catalase, which is also a nonspecific protein for superoxide, did not cause inhibition of NBT reduction. Large ditetrazolium salts, such as NBT, readily bind to tissue components (3), therefore, BSA may have inhibited reduction by simply complexing with NBT. Alternatively, it has been suggested that BSA may be a scavenger of oxygen radicals (20).

The time course observed for diformazan production by single PAM in this study is very similar to that exhibited by groups of phagocytes, as measured by SOD-inhibitable cytochrome *c* reduction and chemiluminescence (10, 13, 23, 24, 28). The derivative of the exponen-

tial equation used to fit the data provided an unbiased estimate of the *R*. To assume 50% of the diformazan produced results from reaction of superoxide with NBT, and that the stoichiometry of the reaction requires two moles of superoxide per mole of diformazan (8), values of the rate of superoxide release reported in this study ranged between 9 and 31 $\text{fmol O}_2^{\cdot-} \cdot \text{s}^{-1} \cdot \text{cell}^{-1} \times 10^{-3}$. Values reported for whole cell cultures by Holian et al. (18, 19), for guinea pig PAM, and by Sherman and Lehrer (28), for adult rabbit PAM, using various stimulants ranged between 18–67 and 33–57 $\text{fmol O}_2^{\cdot-} \cdot \text{s}^{-1} \cdot \text{cell}^{-1} \times 10^{-3}$, respectively.

PAM have been shown to represent a heterogeneous population with respect to superoxide production, immunological function, enzyme release, morphological characteristics, phagocytosis, and respiratory burst activity (15, 19, 32). Most of these studies were performed by separating phagocytes into smaller fractions based on cell size or cell density. However, Gallin (15) has suggested that significant variability may exist even in cells separated by a common characteristic such as density. This study supports this suggestion and provides a means to quantify such heterogeneity in terms of superoxide release. Cells from the same animal and under the same experimental conditions showed large variability in diformazan production.

In conclusion, a technique has been developed to measure superoxide production by single pulmonary alveolar macrophages isolated in culture. Further development and refinement of the technique will provide a useful method to study cellular parameters associated with macrophage function.

We acknowledge the support of West Virginia University Center for Generic Respirable Dust Technology Grant G1135142 awarded to E. V. Ciento and R. C. Lantz and of CDC-National Institute for Occupational Safety and Health (1K01-OH00019-01) awarded to R. C. Lantz.

Received 11 August 1986; accepted in final form 20 January 1987.

REFERENCES

1. ALTMAN, F. P. The quantification of formazans in tissue sections by microdensitometry. II. The use of BPST, a new tetrazolium salt. *Histochem. J.* 8: 501–506, 1976.
2. ALTMAN, F. P. The quantification of formazans in tissue sections by microdensitometry. III. The effect of objective power and scanning spot size. *Histochem. J.* 8: 507–511, 1976.
3. ALTMAN, F. P. Tetrazolium salts and formazans. *Prog. Histochem. Cytochem.* 9: 1–56, 1976.
4. AMANO, D., U. KAGOSAKI, AND T. USUI. Inhibitory effects of superoxide dismutases and various other proteins on the nitroblue tetrazolium reduction by phagocytizing guinea pig polymorphonuclear leukocytes. *Biochem. Biophys. Res. Commun.* 66: 272–279, 1975.
5. AUCLAIR, C., AND E. VIOSIN. Nitroblue tetrazolium reduction. In: *CRC Handbook of Methods for Oxygen Radical Research*, edited by R. A. Greenwald. Stony Brook, NY: CRC Press, 1985.
6. BABIOR, B. M. The enzymatic basis for $\text{O}_2^{\cdot-}$ production by human neutrophils. *Can. J. Physiol. Pharmacol.* 60: 1353–1358, 1982.
7. BABIOR, B. M. The respiratory burst of phagocytes. *J. Clin. Invest.* 73: 599–601, 1984.
8. BAEHNER, R. L., L. A. BOXER, AND J. DAVIS. The biochemical basis of nitroblue tetrazolium reduction in normal human and chronic granulomatous disease polymorphonuclear leukocytes. *Blood* 48: 309–313, 1976.
9. BERTON, G., AND S. GORDON. Superoxide release by peritoneal and bone marrow-derived mouse macrophages. Modulation by

SUPEROXIDE RELEASE FROM SINGLE MACROPHAGES

- adherence and cell activation. *Immunology* 49: 693-704, 1983.
10. BHATNAGAR, R., R. SCHIRMER, M. ERNST, AND K. DECKER. Superoxide release by zymosan-stimulated rat kupffer cells in vitro. *J. Biochem.* 119: 171-175, 1981.
 11. BITENSKY, L. Microdensitometry. *Excerpta Med. Int. Congr. Ser.* 181-202, 1980.
 12. CASTRANOVA, V., L. BOWMAN, AND P. R. MILES. Transmembrane potential and ionic content of rat alveolar macrophages. *J. Cell. Physiol.* 101: 471-480, 1979.
 13. COHEN, H. J., M. E. CHOVANIEC, AND S. E. ELLIS. Chlorpromazine inhibition of granulocyte superoxide production. *Blood* 56: 23-29, 1980.
 14. GALLIN, E. K., AND D. R. LIVENGOOD. Nonlinear current-voltage relationships in cultured macrophages. *J. Cell Biol.* 85: 160-165, 1980.
 15. GALLIN, J. I. Human neutrophil heterogeneity exists, but is it meaningful? *Blood* 63: 977-983, 1984.
 16. GERBERICK, K., J. B. WILLOUGHBY, AND W. F. WILLOUGHBY. Serum factor requirement for reactive oxygen intermediate release by rabbit alveolar macrophages. *J. Exp. Med.* 161: 392-408, 1985.
 17. HALLIWELL, B. Oxygen is poisonous: the nature and medical importance of oxygen radicals. *Med. Lab. Sci.* 41: 157-171, 1984.
 18. HOLIAN, A., AND R. P. DANIELE. The role of calcium in the initiation of superoxide release from alveolar macrophages. *J. Cell. Physiol.* 113: 87-93, 1982.
 19. HOLIAN, A., J. H. DAUBER, M. S. DIAMOND, AND R. P. DANIELE. Separation of bronchoalveolar cells from the guinea pig on continuous gradients of percoll: functional properties of fractionated lung macrophages. *J. Reticuloendothel. Soc.* 33: 157-164, 1983.
 20. HOLT, M. E., M. E. T. RYALL, AND A. K. CAMPBELL. Albumin inhibits human polymorphonuclear leucocyte luminol-dependent chemiluminescence: evidence for oxygen radical scavenging. *Br. J. Exp. Pathol.* 65: 231-241, 1984.
 21. KIMURA, A., E. GOLDSTEIN, R. M. DONOVAN, N. P. VERWOERD, AND J. S. PLOEM. Comparison of lavaged and intrapulmonary macrophages in respect to lysozyme content and size in the rat. *Am. Rev. Respir. Dis.* 129: 149-154, 1984.
 22. KLEBANOFF, S. J. Oxygen metabolism and the toxic properties of phagocytes. *Ann. Intern. Med.* 93: 480-489, 1980.
 23. MILES, P. R., L. BOWMAN, AND V. CASTRANOVA. Transmembrane potential changes during phagocytosis in rat alveolar macrophages. *J. Cell Physiol.* 106: 109-117, 1981.
 24. MILES, P. R., V. CASTRANOVA, AND P. LEE. Reactive forms of oxygen and chemiluminescence in phagocytizing rabbit alveolar macrophages. *Am. J. Physiol.* 235 (Cell Physiol. 4): C103-C108, 1978.
 25. MYRVIK, Q. N., E. S. LEAKE, AND B. FARISS. Studies on pulmonary alveolar macrophages from the normal rabbit: a technique to produce them in a high state of purity. *J. Immunol.* 86: 128-132, 1961.
 26. PICK, E., J. CHARON, AND D. MIZEL. A rapid densitometric microassay for nitroblue tetrazolium reduction and application of the microassay to macrophages. *J. Reticuloendothel. Soc.* 30: 581-593, 1981.
 27. ROOS, D., C. E. ECKMANN, M. YAZDANBAKSH, M. N. HAMERS, AND M. DEBOER. Excretion of superoxide by phagocytes measured with cytochrome c entrapped in resealed erythrocyte ghosts. *J. Biol. Chem.* 259: 1770-1775, 1984.
 28. SHERMAN, M. P., AND R. I. LEHRER. Superoxide generation by neonatal and adult rabbit alveolar macrophages. *J. Leukocyte Biol.* 36: 39-50, 1984.
 29. SUOVANIEMI, O. The vertical measurement principle in photometry. *Am. Biotech. Lab.* 2: 40-43, 1984.
 30. WEISS, S. J., AND A. F. LOBUGLIO. Biology of disease: phagocyte-generated oxygen metabolites and cellular injury. *Lab. Invest.* 47: 5-18, 1982.
 31. WILLIAMS, A. J., AND P. J. COLE. In vitro stimulation of alveolar macrophage metabolic activity by polystyrene in the absence of phagocytosis. *Br. J. Exp. Path.* 62: 1-7, 1981.
 32. ZWILLING, B. S., L. B. CAMPOLITO, AND N. A. REICHES. Alveolar macrophage subpopulations identified by differential centrifugation on a discontinuous albumin density gradient. *Am. Rev. Respir. Dis.* 125: 448-452, 1982.

Mucins Secreted by Rat Tracheal Explants in Culture: Characterization and Influence of Coal Dust

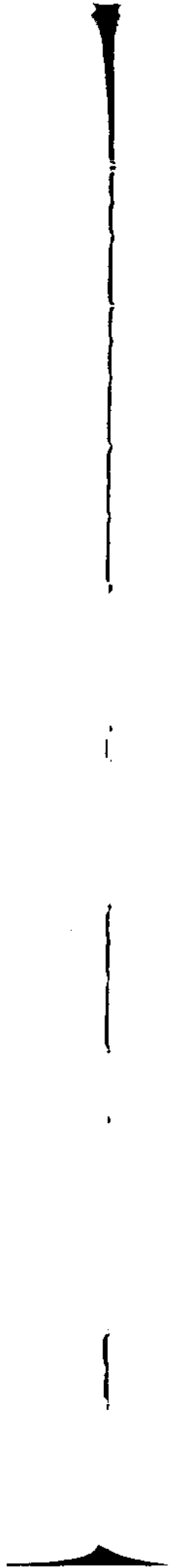
V.P. Bhavanandan and S.B. Dubbs

Department of Biological Chemistry, The Milton S.
Hershey Medical Center, The Pennsylvania State University,
Hershey, PA

The mucus secreted in the respiratory tract provides the first barrier against inhaled particulate and gaseous toxicants. The major component of mucus which is responsible for the physical properties and protective functions of the respiratory mucus is mucin. We have initiated investigations to determine the effects of coal mine dust on the synthesis of respiratory mucin by rat trachea under *in vitro* and *in vivo* conditions. In this study we have established optimum conditions for the aseptic growth and mucin secretion of rat tracheal explants in culture. The best outgrowth of ciliated epithelial cells and maximum mucin production was obtained in CMRL 1066 medium containing 10% fetal calf serum. The explants continued to secrete mucin even after three weeks in culture. For the estimation and characterization of mucins the tracheae were cultured in the presence of [³H]glucosamine and [³⁵S]sulfate or [¹⁴C]leucine. The mucins were isolated from the medium by gel filtration, treatment with hyaluronidase, ion exchange chromatography and CsBr density gradient centrifugation. Precipitation of polyanionic material in the culture media with cetyl pyridinium chloride and fractional extraction with NaCl also yielded mucin free of glycosaminoglycans, but in low yields. The tritium label in the purified mucin was distributed in sialic acid (50%) galactosamine (37%) and glucosamine (13%). The density of purified mucin as determined by CsBr gradient centrifugation was about 1.43g per ml in comparison to 1.46g per ml for human respiratory mucin with a carbohydrate content of about 80% by weight. Alkaline borohydride treatment released saccharides which contained about 80% of the radioactivity. The effect of adding varying amounts of coal dust to the culture medium is under investigation. (Supported by U.S. Bureau of Mines Grant G1135142, Project 4210).

V

**RELATIONSHIP OF MINE
ENVIRONMENT, GEOLOGY AND
SEAM CHARACTERISTICS TO DUST
GENERATION AND MOBILITY**



Application of the Size and Elemental Characteristics of Airborne Coal Mine Dust for Dust Source Identification

C. Lee¹ and J.M. Mutmansky²

¹Dong-A University, Pusan, Korea

²Department of Mineral Engineering, The Pennsylvania State University, University Park, PA

ABSTRACT: Measurement of the size and elemental characteristics was performed on airborne coal mine dust samples collected by multi-stage cascade impactors as well as channel samples of the geologic materials. Size distributions were obtained using precise weighing techniques on the impactor substrates. Elemental analysis on the samples was performed by the proton-induced x-ray emission (PIXE) method, a rapid and nondestructive method of multi-element analysis.

The various analyses were performed on 9 major and 21 trace elements. The results indicate the importance of intake air and shuttle car movements as sources of dust. The association of coal dust characteristics with channel samples was investigated using the coefficient of proportional similarity as a statistical measure. Results show a strong relationship between major elements and the geologic material being cut but a similar relationship between trace elements and geologic materials is not consistent.

1. INTRODUCTION

The most significant occupational disease in the coal industry is known as coal workers' pneumoconiosis (CWP). While CWP has existed for centuries, its mechanism of occurrence and association with coal dust has been well understood for only a few decades. In the 1930s, the significance of this disease led state and government officials in the USA to perform extensive epidemiological and environmental studies in the major coalfields. Study of these results plus later studies in the coal-producing countries of Europe eventually led to the dust regulations that appear in the Federal Coal Mine Health and Safety Act of 1969.

The impacts of the 1969 act were a productivity decline and increased production cost. Many analysts attributed this in large part to

difficulties in complying with the new dust standards (Brezovic 1981). However, compliance was met in most continuous miner sections rather quickly. The remaining problem area is that of longwall mining where the procedures and layout of the mining system make it difficult to meet the standards.

Medical efforts to control CWP have been directed at identifying causal variables and establishing threshold limit values (Hammad et al. 1981). Epidemiological studies in many countries indicate significant regional differences in the prevalence of CWP. Subsequent efforts to correlate the environmental characteristics with this discrepancy resulted in a number of hypotheses to explain the differences in incidence values (Mutmansky and Lee 1984). The primary variables thought to play a part in

this process include mass of dust, rank of coal, free-silica content, and the chemical and mineralogical composition of the airborne dust.

This paper is oriented toward determining the size and elemental characteristics of airborne coal mine dust. Characterization of the size of the particles is essential in determining the mass of dust that will reach the human respiratory tract while the elemental characteristics will establish the potential for toxicity of the dust that may be related to regional differences in CWP prevalence. In addition, a study of the elements will enable us to identify the sources of the dust from the geologic horizons.

2. COAL MINE DUST SAMPLING AND CHARACTERIZATION

2.1 Sampling methods

The primary source for airborne dust in underground coal mines is normally the face operation while the intake air and reentrainment by equipment are secondary sources. Samples used for this study were all collected in the intake and return airways in continuous miner sections from six mines in Pennsylvania and West Virginia. Both airborne and channel samples were taken in each section. Channel samples were taken near the face with individual samples taken from each geologic layer that could be visually distinguished in the coal seam.

A typical mining section layout for the continuous miner sections is shown in Figure 1. All sections were in seams that were essentially flat and each utilized a continuous miner, a bolter and two shuttlecars as the primary equipment. Four of the sections used a single-split ventilation system while the other two employed double-split systems.

The airborne dust samples were all collected using Sierra Model 298 eight-stage impactor-type samplers. This type of sampler is ideal to

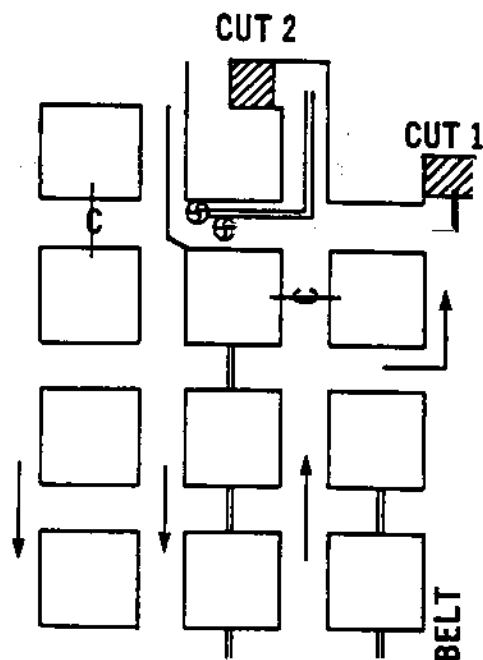


Figure 1. Typical continuous miner section.

associate dust characteristics with size and is widely used in the study of atmospheric aerosols (Ahlberg et al. 1978). The primary advantage of a multi-stage impactor is that the dust does not have to be dispersed in a fluid medium for size analysis, a procedure that may affect the agglomeration characteristics of the dust. In addition, the size determined is based on the aerodynamic diameter, an advantage in considering the effects upon the respiratory system.

The collection principle in an impactor is differential flow paths of small, low-inertia, versus large, high-inertia particles in an air flow where sharp changes in direction are utilized. The dust-laden air is drawn through the sampler by a 2.0 l/min pump and passes through a series of progressively smaller nozzles while the air flow changes directions on each stage. The stages have 50% cut sizes ranging from 21 μm down to 0.5 μm . A PVC filter collects most of the remainder.

The dust collected on each stage impacts on a mylar substrate coated with a sticky substance of some type.

SIZE AND ELEMENTAL CHARACTERISTICS

We tested paraffin, Apiezon L vacuum grease and petroleum jelly as collection media with petroleum jelly being most efficient (Lee 1986). This material may not be suitable in hot mines but it worked well for us. Its primary advantages were its organic nature, which prevents interference with the elemental analysis, and the ability to be sprayed onto the substrate. This was performed using an air brush to spray a mixture of petroleum jelly (20% by weight) and toluene in a controlled fashion. Weighing the substrates required careful control of moisture with the substrates being dried and weighed both before and after sampling.

2.2 Characterization methods

Selection of a method for elemental analysis of impactor substrate samples depends largely on the size of the samples and the objective of the research. Substrate loadings are generally in the vicinity of 50 to 1000 μg with the backup filter loading generally being less than 10 μg . In addition, the substrate dust mass is normally divided into six or twelve submasses due to design of the impactor stages. Therefore, the analytical method must be able to tolerate an extremely small mass of dust. In addition, other characteristics such as the mineralogy and physical characteristics of the dust were desired and thus a non-destructive method was necessary.

The problems associated with sample mass and the need for a non-destructive method are solved if the elemental analysis is performed by proton-induced X-ray emission spectroscopy (PIXE). The normal PIXE method involves bombarding a thin layer of the sample material by a beam of protons and measuring the characteristic X-rays emitted. The results are then statistically analyzed to determine an estimate of the elemental composition by mass in the sample. In samples from impactors, dust thickness has

invariably been below 5 mg/cm^2 . This results in negligible matrix absorption of the characteristic X-rays (Orlic et al. 1981).

One advantage of PIXE is that the variables related to the characteristic X-ray yield are known or can be experimentally determined (Johansson and Johansson 1976). As a result, it is an absolute method that does not require standard samples. In addition, degradation of the proton energy as a result of use on a thick sample has been studied (Chen et al. 1981). Thus, the method can be applied to the channel samples if they are blended, ground and formed into pellets of known thickness. Hence, PIXE applies to both aerosol and channel samples. Because PIXE has sensitivity for extremely small samples and can simultaneously analyze for numerous elements, it makes an effective and cost-efficient analysis method.

3. ANALYSIS OF SIZE AND ELEMENTAL DATA

The cascade impactors collect a sample of the total airborne mine dust. Differences in size and concentration between isokinetic and nonisokinetic inlets on the samplers have been insignificant in the samples collected. As a standard procedure, dust masses from the third (10-15 μm), fifth (3.5-6 μm) and seventh (0.9 to 2 μm) stages of the impactor were analyzed as well as the channel samples. Elements detected in the dust or channel samples include nine major elements (Mg, Al, Si, P, S, K, Ca, Ti and Fe) and 23 trace elements (Na, Cl, Sc, Ti, V, Cr, Mn, Co, Ni, Cu, Zn, Ga, Ge, As, Se, Br, Kr, Rb, Sr, Y, Zr, Mo, Cd and Pb).

The impactors classify according to the aerodynamic diameter. This is defined as the diameter of a hypothetical spherical particle of unit density with the same settling velocity as a given particle of arbitrary shape and density. Though airborne coal dust is a heterogeneous mixture of coal and other materials of

different chemical and physical characteristics, particles in the same aerodynamic size range will exhibit similar aerodynamic behavior. As a result, the influence of one sample on the others downstream can be studied by comparing the characteristics of particles in the same size range.

To compare any two dust or channel samples, the elemental compositions in the dust samples from the same size range must be statistically analyzed. This can be performed using the coefficient of proportional similarity (Imbrie and Purdy 1962), which analyzes the interrelationships between samples with multiple variables as follows:

$$\cos \theta_{m,n} = \frac{\sum_{j=1}^p X_{mj} X_{nj}}{\sqrt{\sum_{j=1}^p X_{mj}^2} \sqrt{\sum_{j=1}^p X_{nj}^2}} \quad (1)$$

where p is the number of elements and m and n denote the two different samples. This coefficient is the cosine of the angle between the two sample vectors in p-dimensional space. In the results reported here, the trace elements were studied separately from the major elements because the statistical significance of the trace elements with smaller weight fractions is likely to be underestimated.

Limited space prevents the authors from listing all the results. A complete set of results is provided for mining section A and partial results for the others. The sampling locations have been coded for brevity. The sample codes are defined in Table 1. Six continuous miner sections have been sampled. Details of the ventilation systems used in each section have been provided in Table 2. A summary of the study results in each of the mining sections is provided below.

3.1 Mining Section A

The entire matrix of coefficients of proportional similarity for the

Table 1. Definition of sampling location codes.

Code	Definition
IN	Intake airway
ININ	Intake airway inby the feeder-breaker
INOUT	Intake airway outby the feeder-breaker
CI	Immediate intake of the miner operation
CR	Immediate return of the miner operation
RI	Immediate intake of the bolter operation
RR	Immediate return of the bolter operation
CI/RI	Immediate intake of the miner as well as bolter operations
3	Third-stage (10-15 μm) sample
5	Fifth-stage (3.5-6 μm) sample
7	Seventh-stage (0.9-2 μm) sample

Table 2. Description of mining sections sampled.

Section	Ventilation System	Face Ventilation
A	Single-split	Brattice
B	Double-split	Brattice
C	Single-split	Tubing
D	Single-split	Tubing
E	Single-split	Brattice
F	Double-split	Tubing

samples from this mining section are provided in Table 3. The data shows that the two top noncoal benches are very similar as are the two bottom coal benches. In general, the major elements in the CR samples were similar to those in the coal seam while the trace elements were closer to those channel samples taken from coal benches alone.

In the size range of 3.5 to 15μm, the trace elements in the RR samples show high similarity to the two top benches which are mixtures of roof rock and coal. However, in the size range of 0.9 to 2.0 μm, the trace elements in the RR samples show low

SIZE AND ELEMENTAL CHARACTERISTICS

Table 3. The association matrix of the dust and channel samples for mining section A.

Samples	CI3	CI5	CI7	CR3	CR5	CR7	RI3	RI5	RI7
CI5	0.75 (0.97)								
CI7	0.59 (0.65)	0.97 (0.90)							
CR3	0.36 (0.61)	0.85 (0.70)	0.94 (0.90)						
CR5	0.37 (0.69)	0.87 (0.78)	0.96 (0.93)	0.99 (0.99)					
CR7	0.58 (0.66)	0.92 (0.74)	0.97 (0.93)	0.93 (0.99)	0.93 (0.99)				
RI3	0.49 (0.94)	0.94 (0.96)	0.98 (0.95)	0.95 (0.79)	0.97 (0.84)	0.94 (0.83)			
RI5	0.40 (0.88)	0.90 (0.88)	0.95 (0.69)	0.90 (0.47)	0.92 (0.55)	0.87 (0.52)	0.96 (0.86)		
RI7	0.39 (0.96)	0.89 (0.94)	0.94 (0.87)	0.95 (0.58)	0.97 (0.65)	0.90 (0.64)	0.97 (0.93)	0.98 (0.87)	
RR3	0.47 (0.88)	0.93 (0.87)	0.95 (0.72)	0.93 (0.50)	0.95 (0.57)	0.91 (0.55)	0.99 (0.87)	0.99 (0.99)	0.99 (0.88)
RR5	0.42 (0.92)	0.90 (0.90)	0.94 (0.80)	0.93 (0.57)	0.95 (0.63)	0.90 (0.62)	0.98 (0.92)	0.99 (0.96)	0.99 (0.94)
RR7	0.42 (0.92)	0.90 (0.87)	0.95 (0.76)	0.95 (0.41)	0.97 (0.49)	0.92 (0.48)	0.98 (0.84)	0.98 (0.82)	0.99 (0.87)
CH1	0.26 (0.47)	0.83 (0.47)	0.90 (0.37)	0.91 (0.33)	0.95 (0.35)	0.84 (0.35)	0.95 (0.52)	0.93 (0.75)	0.97 (0.44)
CH2	0.26 (0.39)	0.82 (0.38)	0.91 (0.32)	0.92 (0.36)	0.96 (0.37)	0.85 (0.36)	0.95 (0.43)	0.91 (0.61)	0.96 (0.31)
CH3	0.30 (0.36)	0.65 (0.46)	0.73 (0.73)	0.87 (0.95)	0.80 (0.91)	0.79 (0.93)	0.73 (0.58)	0.76 (0.24)	0.75 (0.32)
CH4	0.33 (0.36)	0.67 (0.46)	0.76 (0.73)	0.89 (0.95)	0.82 (0.91)	0.81 (0.93)	0.74 (0.58)	0.72 (0.24)	0.73 (0.32)
Samples	RR3	RR5	RR7	CH1	CH2	CH3			
RR5	0.99 (0.97)								
RR7	0.99 (0.83)	0.99 (0.89)							
CH1	0.95 (0.75)	0.97 (0.67)	0.95 (0.36)						
CH2	0.94 (0.61)	0.96 (0.53)	0.95 (0.20)	0.99 (0.94)					
CH3	0.75 (0.28)	0.74 (0.34)	0.78 (0.12)	0.62 (0.26)	0.63 (0.34)				
CH4	0.73 (0.27)	0.71 (0.34)	0.76 (0.12)	0.63 (0.25)	0.65 (0.33)	0.98 (0.99)			

- Notes: (1) CH1 denotes the first roof bench in the channel sample.
 (2) CH2 denotes the second roof bench in the channel sample.
 (3) CH3 denotes the coal bench in the channel sample.
 (4) CH4 denotes the bony coal and floor bench in the channel sample.
 (5) The values in parentheses are based only upon the trace elements.
 (7) The number affixed to the sample code denotes the impactor stage number.

similarity to the two top noncoal benches even though the major elements closely reflect the noncoal benches. In addition, the RR samples in this size range are similar to the CI and RI samples which are not associated with any of the benches in the coal seam. This implies that the intake air may be the primary source of the trace elements in the RR samples in the size range of 0.9 to 3.5 μm .

3.2 Mining Section B

Some of the pertinent coefficients for this section are shown in Table 4. Both major and trace elements in the two coal benches show high similarity. A relatively high concentration of dust was found in the intake airway, apparently due to the belt haulage. The major element compositions of the IN samples are similar to that of the coal seam. However, the similarity of the trace elements to the coal seam trace elements is low, particularly in the range of 0.9 to 2 μm . The influence of the intake air on the CI/RI samples is shown by high similarity coefficients in the range of 0.9 to 2 μm and low similarities between the CI/RI samples and the coal seam in the same size range. All other samples in this size range show high similarity with the coal seam.

3.3 Mining Section C

Some of the statistical data for this section are shown in Table 5. Two coal horizons with similar elemental properties were sampled. Two rock benches, significantly different in properties from the coal, also showed a high similarity. Two consecutive CR samples were taken, the first (CR1) during coal cutting and the second (CR2) during floor cleanup. The trace element composition in the fine size fraction (0.9 to 2 μm) of the CR1 sample shows a weak association with the coal horizons while both major and trace elements of the sample closely reflect the coal horizon properties

All three size fractions of the CR2 samples are dissimilar from the coal benches. However, only the two coarser size fractions show strong similarities with the noncoal channel samples. These results indicate that the fine size fractions of the CR1 and CR2 samples originate in the intake air stream rather than at the face.

3.4 Mining Section D

The layout for this typical development section is shown in Figure 1. Only one coal horizon was evident at this face and no rock was mined. The samples from the first (< 21 μm) and sixth (2 to 3.5 μm) stages were analyzed in addition to those from stage 3, 5 and 7. As shown in Table 6, the CR samples show major and trace element compositions in the range of 2 to 15 μm similar to that of the channel sample. However, the CR sample of 0.9 to 2 μm shows no major or minor element similarities to the channel sample and the sample of > 21 μm shows similarity to the channel sample only in the major element composition.

The discrepancy between the CR and channel samples in the 0.9 to 2 μm range can be explained by similarity in the CR and CI/RI samples, which suggests that the fine particles originated upwind of the face operation. In the < 21 μm range, the differences are probably due to the cutting of some of the roof materials. One point of interest is that the elemental composition of the CR1 and CR2 samples are remarkably similar even though they were taken during different cuts. Another interesting observation is that the CR and RR samples are quite similar. This is a result of the fact that the bolter was downstream of the miner about one-half of the time and thus the continuous miner is the source of the elemental properties in the RR samples.

SIZE AND ELEMENTAL CHARACTERISTICS

Table 4. The association matrix of the dust and channel samples for mining section B.

Samples	CI/RI3	CI/RI5	CI/RI5	CR3	CR5	CR7	CH1
CI/RI5	0.98 (0.98)						
CI/RI7	0.81 (0.78)	0.85 (0.87)					
CR3	0.99 (0.99)	0.99 (0.98)	0.85 (0.78)				
CR5	0.96 (0.97)	0.96 (0.99)	0.82 (0.90)	0.97 (0.97)			
CR7	0.73 (0.96)	0.78 (0.99)	0.98 (0.92)	0.79 (0.95)	0.72 (0.99)		
CH1	0.81 (0.94)	0.90 (0.89)	0.84 (0.56)	0.87 (0.94)	0.86 (0.85)	0.81 (0.84)	
CH2	0.81 (0.94)	0.90 (0.89)	0.87 (0.56)	0.88 (0.94)	0.88 (0.85)	0.85 (0.84)	0.99 (0.99)

Notes: (1) CH1 denotes the first coal bench in the channel sample.
 (2) CH2 denotes the second coal bench in the channel sample.

Table 5. The association matrix of the dust and channel samples for mining section C.

Samples	CR13	CR15	CR17	CR23	CR25	CR27	CH1	CH2	CH3
CR15	0.99 (0.91)								
CR17	0.92 (0.92)	0.94 (0.83)							
CR23	0.85 (0.32)	0.85 (0.37)	0.82 (0.34)						
CR25	0.80 (0.51)	0.81 (0.60)	0.79 (0.56)	0.99 (0.95)					
CR27	0.94 (0.56)	0.96 (0.85)	0.98 (0.99)	0.89 (0.34)	0.87 (0.58)				
CH1	0.99 (0.92)	0.99 (0.74)	0.93 (0.29)	0.85 (0.25)	0.79 (0.37)	0.94 (0.33)			
CH2	0.94 (0.10)	0.96 (0.08)	0.98 (0.04)	0.83 (0.95)	0.81 (0.81)	0.98 (0.04)	0.94 (0.09)		
CH3	0.99 (0.90)	0.99 (0.76)	0.96 (0.36)	0.84 (0.26)	0.79 (0.39)	0.96 (0.38)	0.99 (0.99)	0.98 (0.10)	
CH4	0.94 (0.04)	0.96 (0.03)	0.96 (0.01)	0.94 (0.94)	0.92 (0.79)	0.99 (0.01)	0.94 (0.04)	0.96 (0.99)	0.95 (0.04)

Notes: (1) CH1 denotes the first coal bench in the channel sample.
 (2) CH2 denotes the first slate bench in the channel sample.
 (3) CH3 denotes the second coal bench in the channel sample.
 (4) CH4 denotes the second slate bench in the channel sample.

THE RESPIRABLE DUST CENTER

Table 6. The association matrix of the dust and channel samples for mining Section D.

Samples	CR13	CR15	CR17	CR23	CR25	CR27	CI/RI3	CI/RI5	CI/RI7
CR13	0.99 (0.99)								
CR17	0.99 (0.73)	0.99 (0.73)							
CR23	0.95 (0.97)	0.99 (0.98)	0.98 (0.57)						
CR25	0.99 (0.99)	0.97 (0.99)	0.94 (0.72)	0.96 (0.98)					
CR27	0.96 (0.76)	0.98 (0.75)	0.96 (0.99)	0.97 (0.60)	0.99 (0.74)				
CI/RI3	0.92 (0.91)	0.91 (0.90)	0.88 (0.93)	0.94 (0.81)	0.93 (0.89)	0.93 (0.94)			
CI/RI5	0.99 (0.97)	0.99 (0.97)	0.98 (0.57)	0.99 (0.99)	0.94 (0.98)	0.95 (0.60)	0.92 (0.80)		
CI/RI7	0.87 (0.99)	0.86 (0.99)	0.85 (0.77)	0.89 (0.95)	0.88 (0.99)	0.90 (0.79)	0.96 (0.92)	0.88 (0.95)	
CH1	0.97 (0.96)	0.93 (0.96)	0.96 (0.50)	0.96 (0.99)	0.85 (0.96)	0.88 (0.54)	0.88 (0.75)	0.96 (0.99)	0.84 (0.94)

Notes: (1) CH1 denotes the whole seam channel sample.

Table 7. The association matrix of the dust and channel samples for mining Section E.

Samples	CI3	CI5	CI7	CR3	CR5	CR7	CH1	CH2	CH3
CI3	0.99 (0.99)								
CI7	0.74 (0.79)	0.76 (0.76)							
CR3	0.53 (0.31)	0.51 (0.22)	0.68 (0.52)						
CR5	0.51 (0.63)	0.49 (0.55)	0.70 (0.75)	0.98 (0.92)					
CR7	0.54 (0.82)	0.51 (0.77)	0.75 (0.81)	0.95 (0.70)	0.91 (0.87)				
CH1	0.46 (0.15)	0.43 (0.10)	0.65 (0.20)	0.97 (0.73)	0.99 (0.57)	0.98 (0.29)			
CH2	0.49 (0.91)	0.46 (0.91)	0.69 (0.64)	0.96 (0.27)	0.99 (0.51)	0.99 (0.63)	0.99 (0.37)		
CH3	0.52 (0.94)	0.51 (0.96)	0.81 (0.62)	0.84 (0.10)	0.91 (0.39)	0.95 (0.60)	0.89 (0.10)	0.94 (0.94)	
CH4	0.45 (0.09)	0.42 (0.05)	0.65 (0.09)	0.93 (0.54)	0.98 (0.36)	0.98 (0.11)	0.98 (0.78)	0.99 (0.38)	0.94 (0.18)

Notes: (1) CH1 denotes the roof and coal bench in the channel sample.
 (2) CH2 denotes the bony coal bench in the channel sample.
 (3) CH3 denotes the soft coal bench in the channel sample.
 (4) CH4 denotes the bottom rock and coal bench in the channel sample.

SIZE AND ELEMENTAL CHARACTERISTICS

3.5 Mining Section E

In this section, four benches were recognized in the coal seam. The top bench of roof rock and the bottom bench of rock were quite similar while the second bench of bony coal is similar to the main coal bench. As shown in Table 7, the CR samples in the 0.9 to 2 μm range are similar to the coal benches while the samples in the 10 to 15 μm range were similar to the noncoal benches. Again in this section, the bolter spent half of its time downstream of the miner. The CR samples are similar to the RI and RR samples. This is apparently due to low dust concentrations at the roof bolter.

3.6 Mining Section F

The two top benches in this coal section consist of roof rock, bony coal and draw slate. As indicated in Table 8, the trace elements in the two top benches are not similar to that of the coal benches but the major element composition is close to that of the coal benches. The trace elements in the CR samples are quite similar to those of the two top benches. Thus it is reasonable to assume that the trace elements in the fine size fraction of the CR samples originate from the noncoal benches.

The CR and RR samples show a high similarity in all size fractions. However, the trace element compositions of the RR samples show very poor association with the channel samples, particularly in the 0.9 to 2 μm range. The high similarity coefficient of this 0.9 to 2 μm RR sample with the ININ and INOUT samples indicates that the source of the trace elements in the fine-size RR sample is the intake air.

4. DISCUSSION AND CONCLUSIONS

Airborne coal mine dust sampled in the immediate return of the continuous miner operation showed that the major

elements in all the size fractions analyzed were closely associated with the coal seam. However, no consistent relationship was observed between the trace elements in the airborne dust and those in the coal seam. In some of the six sections sampled, the trace elements seemed to reflect the properties of the coal seam while in others they did not. As a result, we can conclude that in an airborne sample taken downstream of a continuous miner will take its major element composition from that of the coal seam but that a similar conclusion is not true on the trace elements. This is thought to be due to the differences in the modes of occurrence of the trace elements.

In the sections observed, dust control in the roof bolter operation was quite good and dust concentrations were very low by comparison. As a result, aerosol samples from the immediate return and intake of the bolter were quite similar. The section intake air appears to be a significant fine-size dust source in many sections as evidenced by the pattern of trace elements. It seems apparent that trace elements recurring in the mining section intake are also observed in the immediate intakes and returns of the face operations.

The overall importance of this study is that it may be possible to locate the sources of the various elements in airborne coal mine dust. As a result, it may be possible to pinpoint the areas of greatest concern in a continuous miner operation in a particular element or mineral is established as a primary cause or contributor of CWP.

5. ACKNOWLEDGEMENTS AND DISCLAIMER

This research has been supported by the Department of the Interior's Mineral Institutes program administered by the Bureau of Mines through the Generic Mineral Technology Center for Respirable Dust under allotment grant number G1135142.

THE RESPIRABLE DUST CENTER

Table 8. The association matrix of the dust and channel samples for mining Section F.

Samples	CI3	CI5	CI7	CR3	CR5	CR7	CH1	CH2
CI5	0.98 (0.90)							
CI7	0.94 (0.85)	0.94 (0.99)						
CR3	0.91 (0.26)	0.94 (0.65)	0.89 (0.72)					
CR5	0.93 (0.74)	0.95 (0.95)	0.89 (0.98)	0.99 (0.84)				
CR7	0.93 (0.88)	0.93 (0.99)	0.96 (0.99)	0.98 (0.69)	0.97 (0.95)			
CH1	0.79 (0.24)	0.84 (0.25)	0.76 (0.20)	0.96 (0.11)	0.96 (0.23)	0.90 (0.18)		
CH2	0.76 (0.24)	0.82 (0.26)	0.71 (0.21)	0.94 (0.11)	0.94 (0.23)	0.85 (0.19)	0.99 (0.99)	
CH3	0.85 (0.01)	0.88 (0.44)	0.89 (0.53)	0.97 (0.97)	0.96 (0.68)	0.97 (0.48)	0.94 (0.06)	0.90 (0.06)

Notes: (1) CH1 denotes the top rock and bony coal bench in the channel sample.
 (2) CH2 denotes the draw slate bench in the channel sample.
 (3) CH3 denotes the coal bench in the channel sample.

The opinions and conclusions expressed in this paper are those of the authors and do not represent the opinions of the sponsors. Citation of manufacturers' names in the paper were made for informational purposes and do not imply endorsement of the products by the authors.

6. REFERENCES

- Ahlberg, M.S., A.C.D. Leslie & J.W. Winchester 1980. Environmental and occupational health analysis using proton-induced X-ray emission. In P.A. Russell & A.E. Hutchings (eds.), *Electron microscopy and X-ray applications to environmental and occupational health analysis*. Ann Arbor, Michigan: Ann Arbor Science.
- Brezovec, D. 1980. Managers spur productivity gains. *Coal Age* 84(12):55-59.
- Chen, J.R. et al. 1981. Trace element analysis of bituminous coals using the Heidelberg proton microprobe. *Nuclear instruments and methods*. 181:151-157.
- Hammad, Y., M. Corn & V. Dharmarajan 1981. Environmental characteriza-
 tion. In H. Weill & M. Turner-Warwick (eds.), *Occupational lung diseases: research approaches and methods*. New York: Marcel Dekker.
- Imbrie, J. & E. Purdy 1962. Classification of Modern Bahamian carbonate sediments. *Classification of carbonate rocks*. 7:253-272.
- Johansson, S.A.E. & T.B. Johansson 1976. Analytical application of particle-induced X-ray emission. *Nuclear instruments and methods*. 137:473-516.
- Orlic, I. et al. 1981. Determination of trace elements in coal by X-ray emission spectroscopy. *International congress on analytical techniques in environmental chemistry*. Barcelona, Spain.
- Lee, C. 1986. Statistical analysis of the size and elemental composition of airborne coal mine dust. Ph.D. thesis. Pennsylvania State University, University Park, Pennsylvania.
- Mutmansky, J.M. & C. Lee 1984. An analysis of coal and geologic variables related to coal workers' pneumoconiosis. In S. Peng (ed.), *Coal mine dust conference proceedings*. West Virginia University, Morgantown, West Virginia.

Worldwide Coal Mine Dust Research - - - Where Are We Going?

J.M. Mutamansky

Department of Mineral Engineering, The
Pennsylvania State University

ABSTRACT: Coal mine dust research throughout the world has been stimulated by the recognition of its importance in the development of coal miners' diseases, particularly coal workers' pneumoconiosis (CWP). A historical look at the problem and the present state of knowledge in this area of importance to the worldwide coal industry is presented. A summary of progress made in this area is provided and some research ideas for the future are discussed.

1. INTRODUCTION

I thank Dr. Yong Won John, President of the Korean Institute of Mineral and Mining Engineers, for his invitation to address the International Symposium on Coal Mining and Safety. This presents me with an interesting opportunity to take a broad look at the research in coal mine dust and where we are going. From this broad perspective, we can all view the progress and problems that are apparent in the present state of knowledge of coal mine dust.

One important element in the review of coal mine dust research and its role in miners' diseases is that of its history. The existence of diseases attributed to the mine atmosphere is often traced back to Pliny the younger in the first century A.D. His work on natural history mentioned observed human effects attributed to mine fumes and vapors. However, the subject of the effects of dust in the mine was not mentioned in published literature until 1556 when Agricola discussed the ailments of miners in his day (Seaton 1975).

For many centuries, many medical ailments of the lungs were often categorized together and distinct diseases were often not recognized until more modern times. The ability to distinguish different lung diseases was limited until the discovery of X-rays in 1896. Nonetheless, Zenker in 1866 applied the term pneumoconiosis to any disease where dust gathers in the lymphatic depots of the lungs. This term was changed to pneumoconiosis in 1932. While pneumoconiosis was defined in the 1800s, scant attention was paid to control of miners' diseases until recent decades. The first attempt to control disease through control of the mine atmosphere has been attributed to the South Africans who instituted a silica control in 1910 (Drinker and Hatch 1954).

In several countries of the world, an awakening to the toxicity of mine dust came about in the 1930s. In the U.S., a tunnel driven through a sandstone mountain near Gawley Bridge, West Virginia, resulted in the deaths of 476 workers who were consumed by

silicosis after a few years of work in the tunnel (Seaton 1975). This historical event provided a turning point in the fight against miners' diseases and medical knowledge on silicosis and other industrial lung diseases has advanced rapidly ever since.

In the 1930s and 1940s, studies of an epidemiological nature began to pinpoint the existence of large numbers of coal workers who had lung diseases even though they were exposed only to coal dust. As a result, the belief that CWP was a disease distinct from silicosis became prevalent among medical personnel. During these decades, X-ray studies became important and, after several decades of progress, a CWP classification system based upon chest X-rays was established by the International Labor Organization (ILO) in 1950. This classification system for categorizing the degree of development of lesions in the lung has been updated several times since and is a very important tool in research. Nearly all of the CWP medical research during the last several decades has benefitted from this classification because it makes comparison between the various research studies possible.

Since 1950, a variety of research has been conducted around the world in an attempt to understand the causes of CWP and the methods for preventing the disease. Many studies have been performed that have improved the state of knowledge on how the disease occurs, how differing mine environments affect the disease, and how the mine environment can be altered to reduce the incidence of the disease. We will review these topics by beginning with some medical concepts.

2. LUNG DISEASE RELATED TO COAL MINING

For mineral engineers who work in the area of mine hygiene, a general knowledge of the primary miners' lung diseases is necessary. However, the jargon of the medical literature is often a problem to minerals personnel.

As a result, good general descriptions of the processes that are involved may be of help to those of you who are expert in some minerals field but who are not educated in the medical sciences. With some degree of trepidation, I will venture forth to provide these general descriptions. Readers of this paper may refer to the references cited for more complete technical information.

The two diseases of most concern in the coal mining industry are silicosis and coal workers' pneumoconiosis (CWP) with silicosis being the disease that was described first. Seaton (1975) defines silicosis as the fibrotic disease of the lungs caused by the inhalation of dust containing silicon dioxide, generally referred to as silica. The disease process begins when respirable dust particles (generally defined as those with a particle diameter of less than 5 microns) find their way into the lung in much greater than normal amounts. When impacted on the surfaces of the alveoli (the terminal openings of the lung), the dust triggers the movement of macrophages, wandering cells resident in the lung that attempt to rid the lung of the dust. The job of the macrophages is to phagocytose the dust, i.e., to engulf it in order to consume or remove it. In general, the macrophages move the dust to the mucociliary escalator (where the cilia can expel the dust from the area of the lungs by transporting it to the throat) or to the lymphatics where the lymphatic system can store or dispose of it (Wright 1978).

When large amounts of dust are introduced into the human lung, the capacity of the removal process may be exceeded, resulting in dust particles being lodged in the alveolar surfaces or collected in the lymphatics. If this persists, the fibroblasts (cells that produce fibrous tissue) begin to generate fibers of reticulin or collagen. The collagen fibers, which are often very prevalent when the invading dust is silica, are normally associated with scar tissue. Thus scarring of the lung tissue and an

accompanying reduction in the pulmonary function is the normal result of excessive silica in the lungs. Free crystalline silica exists as the minerals quartz, tridymite, cristobalite, coesite and stishovite. The first three of these minerals are all considered to be toxic. However, in most mining situations, quartz is the most common form of silica and is therefore the mineral of most concern. It should be noted that only 2 to 5 g of silica dust in the lungs is enough to cause the fibrosis peculiar to silicosis (Wright, 1978).

CWP is now considered by most medical personnel to be a separate entity and can be defined as the accumulation of coal dust in the lungs and the tissue's reaction to its presence (Morgan 1975). CWP is separated into two categories, depending on the degree of abnormality of the chest X-ray. The dust that gathers in the lungs causes opacities to develop and the size of the largest opacity determines whether simple pneumoconiosis or its most complicated form exists. For lungs with opacities below 1 cm, simple pneumoconiosis is diagnosed. If any of the opacities on the X-ray is greater than 1 cm, then complicated pneumoconiosis or progressive massive fibrosis (PMF) is indicated. Numerous subcategories are also recognized in the ILO classification in order to further classify the state of the disease.

It is thought by some medical personnel that the reaction of the lung to pure coal dust is decidedly different than the reaction to silica. The coal macules (focal deposits of coal dust) are generally believed to contain mostly reticulín rather than collagen fibers, thus resulting in less scarring of the lungs (Wright, 1978). In general, it takes about 20 to 50 g of coal dust in the lungs to cause PMF to develop. This would suggest that coal is not nearly as toxic to the lungs as silica. It should be mentioned, however, that a miner may suffer from both diseases if silica is present in the coal. However, the effects of silica and coal together in

the lungs are not well understood. This will be discussed in the next section.

The physical impairment caused by these diseases varies with the disease and the degree of abnormality. In simple CWP, impairment is minor and is not significant enough to shorten life-span. In some individuals that have PMF, there is a marked deterioration of pulmonary function, reduced ability to perform physical tasks and shortened life span (Wright, 1978). In cases where silicosis is diagnosed, the patient is likely to be much more severely disabled than patients with a matched radiographic category of CWP and death often results from the development of cardiorespiratory failure (Seaton 1975).

3. COAL MINE DUST DISEASE STUDIES

From the time that the first dust control effort was made in 1910 to the present, a great deal has been learned about dust-related diseases. However, much of the knowledge that applies to CWP has been obtained since the 1930s by practitioners in the field of epidemiology (the science of the incidence, distribution and control of disease). The important work in this field began in the 1930s in a number of different countries in response to the recognition that a large proportion of miners were suffering from lung disease. In 1934, a study was conducted by the U.S. Public Health Service in the anthracite coal fields of Pennsylvania (Anon. 1934). The results of this study showed that 22.7% of the anthracite miners had anthraco-silicosis (sic) as indicated by X-rays. At about the same time, the Medical Research Council in Great Britain started its studies in the South Wales coal fields. A few years later, CWP became a compensable disease based upon the findings in these fields (Hamilton, Ogden & Vincent 1983). Recognition of CWP as a disease distinct from silicosis

became more commonplace among medical personnel.

The nationalization of British coal mines in 1947 had a tremendous effect on the epidemiological study of CWP because it became easier to organize mines and miners in a systematic study of dust diseases. In 1953, the National Coal Board began the largest single study ever conducted on the prevalence of CWP by identifying 25 different mines from various regions of Great Britain. The research effort was a systematic attempt at defining the relationship between CWP incidence and the dust exposure measured in the selected mines. Full-chest X-rays, along with occupational histories, were obtained every five years on the entire underground workforce at these mines. Originally, dust concentrations were measured on a particle number basis and showed a weak correlation with CWP incidence; later measurements, made on a mass concentration basis, were much more highly correlated with the incidence.

The results of the statistical study performed over the next ten years was the basis of the dust concentration legislation in Great Britain. The results were significant because 30,000 miners were involved and 90% participation was achieved in each of the five-year surveys conducted (Jacobsen et al. 1970, Jacobsen 1972). The work resulted in the conclusion that no more than 8 mg/m³ of dust should be allowed in the return airways. This corresponds to approximately 4 mg/m³ in the workers' environment. As a result of this analysis, it was possible to estimate that no more than 3% of the workers in mines where the standard was enforced would develop Category 2 CWP or worse on the ILO scale after a 35-year working life. This research was extremely important because it did establish that dosage versus incidence curves were possible on a statistical basis and also established that mass concentration values were better than particle counts for disease studies.

Research conducted in the German Federal Republic indicated that similar

results in West German mines were observed. This study, initiated in 1960, involved more than 17,000 men at 13 mines over periods of up to 14 years. The results were based upon cumulative dust exposure and indicated that, on a mass concentration basis, an exposure of 4 to 5 mg/m³ would result in 5% of the miners contracting Category 2 CWP or worse in 35 years of underground work (Reisner 1972). These results tended to corroborate the results in Great Britain.

In the U.S., a number of epidemiological studies were conducted of a more limited scope. The results showed that CWP incidence was roughly comparable to mines in Great Britain and West Germany. However, some of the studies indicated that incidence of CWP varied considerably with the coal field, decreasing significantly with the rank (Morgan et al. 1973, Dessauer et al. 1972). Several hypotheses were made to explain the differences. However, it is still not yet certain whether free silica, specific harmfulness of the coal itself or some other factors are involved. This correlation with rank has been found in similar studies in other coal-producing countries and thus is generally accepted even though it may not be fully understood. However, recent studies conducted in the anthracite mines in Korea by Cho, Lee & Yun (1986) indicated a relatively low incidence of CWP. This is an interesting result and may be an indication that CWP incidence can be controlled in anthracite mines if all the other as yet unknown factors in the disease are favorable.

Other research that is of interest in the analysis of CWP has been carried out in France (Deguelire 1972) and Germany (Robock 1972) and involves the specific harmfulness of dust. Robock's work in attempting to analyze the CWP risk uses a statistical relationship as follows:

Risk = f(mass concentration,
quartz content, time of exposure,
individual factors)

This type of statistical relationship is valuable but it is difficult to achieve because of the problems in interpreting the response of the disease to silica in the coal and the many individual factors that are involved.

Response of miners to silica content in the coal is a topic that is most in need of clarification. Research of various types has yielded results that are difficult to reconcile. Martin et al. (1972) indicated that, for coal-quartz mixtures, the harmfulness of quartz when mixed with coal was less than that for the same quantity of pure quartz when administered to laboratory rats. On the other hand, British epidemiological studies (Hamilton, Ogden & Vincent 1983) have indicated that coals with less than 10% quartz do not appear to affect the probability of development of CWP. Work in France (Le Bouffant 1972) indicates that even in coal with less than 10% quartz, the quartz does cause pulmonary lesions in laboratory rats. However, Le Bouffant does conclude that certain minerals do appear to retard the damaging effects of the quartz. While studies with laboratory animals have been relatively common, Harrington (1972) points out the fact that very few studies have been performed using cells in vitro.

4. PROGRESS IN FIGHTING CWP

Throughout the world, considerable progress has been made in the last few decades in the fight against CWP. In most countries, the efforts have been made primarily in dust control within the working environment. In many ways, the U.S. has paralleled the rest of the world in this fight but it also has some peculiar problems. A review of the progress and problems in the U.S. may be of interest here.

Coal mine dust control in the U.S. was not implemented until the Federal Coal Mine Health and Safety Act of 1969 was enacted. This legislation required that the average dust concentration by

occupation be maintained below 3.0 mg/m³ after June 1970 and below 2.0 mg/m³ after December 1972. In addition, quartz content was to be held below 0.1 mg/m³ in the air regardless of the concentration of the total dust. It was not easy to meet these dust standards at first, particularly for certain mining occupations. As a result, a great effort was made by the U.S. Bureau of Mines (USBM) and other government agencies to develop and promote better dust control measures.

The attempts to provide good dust control in underground coal mines in the U.S. were conducted on a number of fronts. Particular areas of success were control of dust generation by better coal-cutting strategy, better design of water sprays for dust suppression and air movement, use of scrubbers and improved design of face ventilation systems. While meeting the new law was difficult for operators at first, a drastic improvement occurred over time so that dust control in continuous miner sections was soon meeting the requirements of the law. Dust concentrations for continuous miner operators dropped from an average of 6.5 mg/m³ in 1969 to only 1.3 mg/m³ in 1980 (Niewiadomski 1983).

While dust concentrations in mining sections have been dropping considerably, one problem area has been mining sections where quartz is a considerable portion of the airborne dust. In these sections, a reduced dust standard is applied to keep the quartz below 0.1 mg/m³ and many mines experience considerable difficulty in meeting the standards. This is one area where more definitive research information and better dust control measures are needed. The human response to coal dust/quartz mixtures is, as yet, uncertain and medical research is needed in this area.

The success of dust control on continuous miner sections has been a tremendous achievement. However, longwall dust levels have been much higher and the dust control problem is considerably more difficult because the workman must often travel downwind of the primary dust source. In

addition, longwall mining sections have rapidly increased in productivity and production capability over the last decade so that gains in the control of dust generated per unit of production have not necessarily reduced mass concentrations. As a result, many longwall mines still face great difficulty in meeting the dust laws. Much of the research progress in longwall has been concentrated in areas where success was achieved in continuous miner systems. However, dust avoidance systems have held a more important place in longwall mining operations (Jankowski, Kissell & Daniel 1986).

While great progress has been made in the area of dust control, many concerns have been expressed concerning dust technology issues because compensation payments to U.S. miners still total \$1.7 billion per year (Daniel 1984). In 1980, the National Academy of Sciences considered the needs for research in the respirable dust area and concluded that much in the way of research on respirable dust was needed. Their report (Anon. 1980) concludes, among other things, that:

- (1) variations in characteristics of respirable dust should be studied,
- (2) samples of respirable coal mine dust large enough to be characterized chemically, morphologically and physically should be collected,
- (3) research is needed on the fundamental mechanisms by which fragments are produced in coal mining, and
- (4) development of techniques for suppressing respirable coal mine dust near its source and for collecting it in high concentrations should be expanded vigorously.

Partially in response to this report, new research activities related to dust in coal mines have been initiated under the Generic Mineral Technology Center for Respirable Dust funded through the USBM. The Center is primarily manned by personnel from The Pennsylvania State University, West Virginia University, the University of Minnesota

and the Massachusetts Institute of Technology.

The center has initiated studies that deal primarily with the areas of analysis of varying dust characteristics and basic medical research dealing with in vitro and in vivo response of living tissue to respirable dust materials. While the Center is still in its infancy, several very interesting projects are currently ongoing. Some of the medical research topics of interest include:

- (1) an in vitro response study on proliferation of lung fibroblasts when in contact with coal dusts,
- (2) an in vitro study on the effects of coal dust on the metabolism of arachidonic acid by lung macrophages,
- (3) an investigation into the quality and/or quantity of respiratory secretions due to coal dust,
- (4) a study to compare macrophage responses in primates and rats,
- (5) an investigation into the role of free radicals in the development of disease, and
- (6) an in vitro research effort on the production of superoxides by alveolar macrophages.

In addition to these medical studies, characterization of coal mine dusts, development of characterization methods, research on dust generation during fracture and studies on wetting characteristics are also being conducted. Reports on some of the results of these efforts will be available soon (Frantz and Ramani 1987).

5. RESEARCH DIRECTIONS FOR THE FUTURE

Before bounding off into the future, it is important to analyze, as nearly as we can, what has been accomplished so far in the fight against CWP. Because most of our efforts at control of coal mine dusts have been instituted in the last twenty years, it is difficult to perform an assessment because it normally takes a full working life to assess the total impact of those controls. However, the general picture is one of

significant progress. Epidemiological data has shown that prevalence of CWP is dropping both in Great Britain (McLintock 1972) and in the U.S. (Althouse 1984). Much of the drop is due to the tighter control of dusts on the coal mine working faces. However, a number of important areas still need to be researched and it is not a time to simply relax our attention toward this problem.

One of the first areas that comes to mind for future research is the extension of in vitro and in vivo studies in the formation of dust diseases. Because of the many interesting research efforts being conducted in this area and the relative lack of intensive research in the past, this appears to be one of the most pressing needs. Another important reason for performing this type of research is the variety of phenomena that epidemiology has revealed without an apparent cause. One that comes to mind is the prevalent finding that CWP increases with the rank of the coal mined. It may not be possible for epidemiologists to find the causes of this phenomena but it may be feasible for a medical scientist working in a lab.

Research into coal/quartz mixtures and their effect on the human lung is another area where a real effort is necessary. It does not take a medical expert to realize that the studies done to date have conflicting results. The studies that show that other minerals may have a retarding effect on the harmfulness of quartz are interesting and may have some connection with the protection mechanisms that are operative in aluminum therapy. Only a more comprehensive research effort will answer that questions.

Other characteristics of dust and some measure of the individual response variation should also be investigated. Several interesting, though limited, studies on the effects of trace elements were previously published. However, the limited nature of the research prevents us from gaining much in the way of conclusions from those

studies. Much the same is true with regard to individual factors. In particular, individual susceptability, smoking habits, respirator use and other personal variables need to be investigated.

One final area of research that must be tackled by the medical people is the measurement of the effects of dust and diesel particulates in the mine atmosphere. For many years, diesel emissions were thought to be relatively innocuous. However, more recent studies have pointed out that such a conclusion may not be true. Study of diesel emissions and their effects both with and without dust will certainly be important due to the proliferation of diesels in the mining world.

Finally, it is important to note that while a great deal of progress has been made in the area of dust control throughout the world, new problems arise as the mining methods, equipment and productivity change. It is therefore very important for all mining and mineral engineers to continue their quest for improved dust control techniques.

The worldwide mining industry has changed considerably over the last few decades. This is certainly true in the efforts made to control coal mine dust diseases. Nearly all of the progress in this area has been accomplished in the last fifty years. However, it is reasonable to expect that progress in this field will accelerate. One reason for this is the tremendous increase in the worldwide level of social awareness and the belief that every worker can and should work in a safe and healthy environment.

A second reason to feel optimistic is the improved cooperation between scientists, engineers and medical personnel in the fight against industrial dust disease. In the last few decades, cooperation between scientists and engineers has enabled mankind to put men on the moon. Even more significant, cooperation between medical personnel, scientists and engineers has resulted in the development of human heart replacement

devices. Certainly, a means of eliminating CWP is achievable in an environment of cooperation between the world's most productive professionals.

While there is certainly some reason to feel pride in the improvement of the mine atmosphere for mine workers, there is much that remains to be done. The progress being made in engineering, science and medicine appears to be accelerating. This being the case, progress in the control of coal mine dust diseases during the next fifteen years may equal the progress made during the last fifty. One additional point was made by one of my colleagues in the medical profession that points out the importance of the minerals engineers in the fight against CWP. His comment emphasized that a cure for disease is always a second choice to prevention. The minerals engineer therefore holds a key position in the fight against CWP. I wish all of you success in your endeavors in this area, an area which is of extreme importance to the health of the world's coal miners.

6. ACKNOWLEDGEMENTS AND DISCLAIMER

This paper was compiled during research supported by the Department of the Interior's Mineral Institutes program administered by the Bureau of Mines through the Generic Mineral Technology Center for Respirable Dust under allotment grant number G1135142.

The author gratefully acknowledges Dr. Gerald L. Bartlett, Professor of Pathology, Hershey Medical Center, The Pennsylvania State University; Mr. Robert A. Jankowski, Supervisory Physical Scientist, U.S. Bureau of Mines, Pittsburgh; Mr. R.L. Frantz, Associate Dean for Continuing Education and Industry Programs, The Pennsylvania State University; and Dr. R.V. Ramani, Professor of Mining Engineering, The Pennsylvania State University, for their helpful comments and suggestions relating to this paper.

The opinions and conclusions expressed in this paper are those of the author alone and do not represent

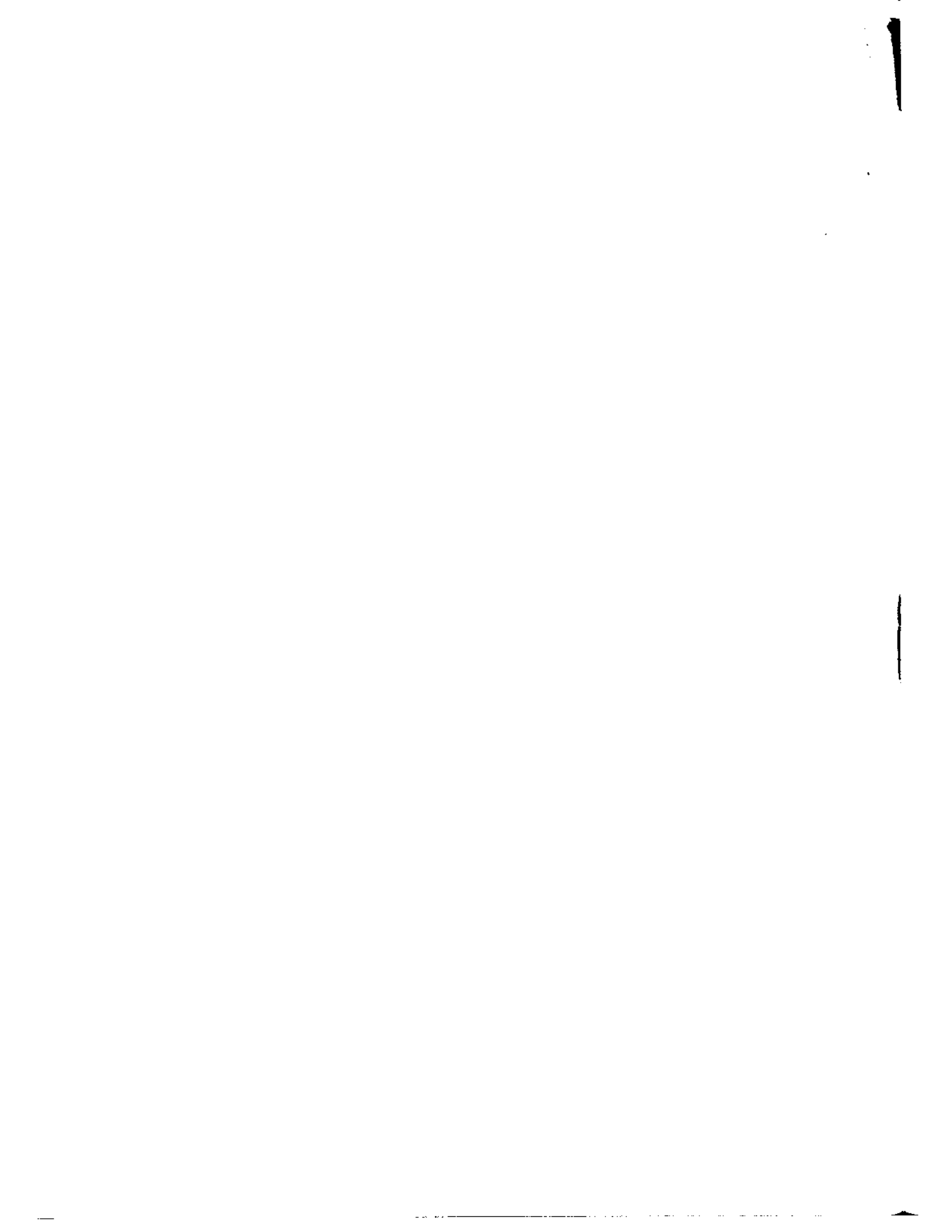
the opinions of the Generic Mineral Technology Center for Respirable Dust, the Pennsylvania Mining and Mineral Resources Research Institute or the USBM.

7. REFERENCES

- Althouse, R. 1984. The national coal workers' health surveillance program: 1970-1980. In S.S. Peng (ed.), Proceedings, coal mine dust conference, p. 151-155. Morgantown, West Virginia: W. Va. Univ.
- Daniel, J.H. 1984. Respirable dust control: the Bureau of Mines program. In S.S. Peng (ed.), Proceedings, coal mine dust conference, p. 1-7. Morgantown, West Virginia: W. Va. Univ.
- Anon. 1934. Anthraco-silicosis. Special Bulletin 41. Harrisburg, Pennsylvania: Dept. of Labor and Industry, Commonwealth of Pennsylvania.
- Anon. 1980. Measurement and control of respirable dust in mines. Washington, D.C.: Nat. Acad. of Sci.
- Cho, K.S., S.H. Lee & I.G. Yun 1986. Preliminary report on the progression of pneumoconiosis among Korean coal-face workers with special reference to anthracite exposure. Ann. Am. Conf. Gov. Ind. Hyg. 14:163-169.
- Deguelire, G. 1972. Towards a criterion for measuring the harmfulness of mining dust. In Proceedings, conference on health in mines. Luxembourg: Commission of the European Communities.
- Dessauer, P. 1972. Development of patterns of coal workers' pneumoconiosis in Pennsylvania and its association with respiratory impairment. In I.J. Selikoff, M.M. Key & D.H.K. Lee (eds.), Coal workers' pneumoconiosis, p. 220-251. New York: N.Y. Acad. of Sci.
- Drinker, P. & T. Hatch 1954. Industrial dust. New York: McGraw-Hill.

COAL MINE RESEARCH

- Frantz, R.L. & R.V. Ramani 1987. Proceedings, international symposium on respirable dust in the mineral industries. Cincinnati, Ohio: Am. Conf. Gov. Ind. Hyg.
- Hamilton, R.J., T.L. Ogden & J.H. Vincent 1983. Status of work-environment aerosols in Great Britain. In V.A. Marple & Y.H. Liu (eds.), *Aerosols in the mining and industrial work environment*, V. 1, p. 3-20. Ann Arbor, Michigan: Ann Arbor Science.
- Harrington, J.S. 1972. Investigative techniques in the laboratory study of coal workers' pneumoconiosis: recent advances at the cellular level. In I.J. Selikoff, M.M. Key & D.H.K. Lee (eds.), *Coal workers' pneumoconiosis*, p. 816-834. New York: N.Y. Acad. of Sci.
- Jacobsen, M. et al. 1970. New dust standards for British coal mines. *Nature*. 227:445-447.
- Jacobsen, M. 1972. Progression of coal workers' pneumoconiosis in Britain in relation to environmental conditions underground. In *Proceedings, conference on health in mines*. Luxembourg: Commission of the European Communities.
- Jankowski, R.A., F.N. Kissell & J.H. Daniel 1986. Longwall dust control: an overview of progress in recent years. *Mining Engineering*, 38:953-958.
- Le Bouffant, L. 1972. Harmfulness of dust in relation to its quartz content. In *Proceedings, conference on health in mines*. Luxembourg: Commission of the European Communities.
- McLintock, J.S. 1972. The changing prevalence of coal workers' pneumoconiosis in Great Britain. In I.J. Selikoff, M.M. Key & D.H.K. Lee (eds.), *Coal workers' pneumoconiosis*, p. 278-291. New York: N.Y. Acad. of Sci.
- Martin, J.C. et al. 1972. The role of quartz in the development of coal workers' pneumoconiosis. In I.J. Selikoff, M.M. Key & D.H.K. Lee (eds.), *Coal workers' pneumoconiosis*, p. 127-141. New York: N.Y. Acad. of Sci.
- Morgan, W.K.C. et al. 1972. A comparison of the prevalence of coal workers' pneumoconiosis and respiratory impairment in Pennsylvania bituminous and anthracite miners. In I.J. Selikoff, M.M. Key & D.H.K. Lee (eds.), *Coal workers' pneumoconiosis*, p. 252-259. New York: N.Y. Acad. of Sci.
- Morgan, W.K.C. 1978. Coal workers' pneumoconiosis. In W.K.C. Morgan & A. Seaton, *Occupational lung diseases*, p. 149-215. Philadelphia: W.C. Saunders Co.
- Niewiadomski, G. 1983. Improving dust control technology for U.S. mines. In J.A. Barrett et al. (eds.), *Proceedings of the symposium on control of respirable coal mine dust*, p. 41-70. Beckley, West Virginia: Mine Safety & Health Adm.
- Reisner, M. 1972. Pneumoconiosis and exposure to dust in coal mines in the German Federal Republic. In *Proceedings, conference on health in mines*. Luxembourg: Commission of the European Communities.
- Robock, K. 1972. Research on the specific harmfulness of respirable dust. In *Proceedings, conference on health in mines*. Luxembourg: Commission of the European Communities.
- Seaton, A. 1975. Silicosis. In W.K.C. Morgan and A. Seaton, *Occupational lung diseases*, p. 80-111. Philadelphia: W.C. Saunders Co.
- Wright, G.W. 1978. The pulmonary effects of inhaled inorganic dust. In G.D. Clayton & F.E. Clayton (eds.), *Patty's industrial hygiene and toxicology*, p. 165-202. New York: Wiley Interscience.



INDEX

THE CUMULATIVE AUTHOR INDEX

Authors are sorted alphabetically. Papers by the same author are sorted in decreasing chronological order which puts the more recent papers first.

Authors' names appear in standardized form, that is, last names and initials. This is not necessarily the way the name appears on the paper.

THE CUMULATIVE SUBJECT INDEX

Every entry in the CUMULATIVE SUBJECT INDEX contains the following information:

- 1) Last name of the first listed author with the number of authors in parenthesis if the article had multiple authors.
- 2) A short descriptive phrase, generally the title of the paper.
- 3) The year in which the paper was published or presented.
- 4) The location of the paper in The Respirable Dust Center publication volume.

1

1

1

1

GENERIC MINERAL TECHNOLOGY CENTER FOR RESPIRABLE DUST

CUMULATIVE AUTHORS INDEX
1984-1987

- Ananth, G. Vol. 5, 244-248
Andre, R. A. Vol. 5, 319-327
Aplan, F. F. Vol. 6, 94-105; Vol. 5, 123-128; Vol. 5, 129-138
- Bartlett, G. L. Vol. 5, 274-281
Bates, D. Vol. 5, 261-273
Begley, R. D. Vol. 4, 9-55
Bhaskar, R. Vol. 5, 55-60; Vol. 5, 61-71; Vol. 4, 109-118; Vol. 3, 25-31
Bhavanandan, V. P. Vol. 6, 170
Bicniawski, Z. T. Vol. 6, 3-17; Vol. 5, 3-10; Vol. 5, 11-17
Bise, C. J. Vol. 4, 155-157; Vol. 3, 85-90
- Caldow, R. Vol. 6, 152
Cantrell, B. Vol. 6, 152
Castranova, V. Vol. 6, 157-162; Vol. 5, 261-273; Vol. 4, 121-139; Vol. 3, 53-60
Chander, S. Vol. 6, 76-93; Vol. 6, 94-105; Vol. 6, 106-122; Vol. 5, 123-128
Cheng, L. Vol. 6, 123-133
Chiang, H. S. Vol. 5, 72-81; Vol. 5, 95-108; Vol. 5, 129-138; Vol. 5, 139-147;
Vol. 3, 32-34
Cliento, E. V. Vol. 6, 163-169; Vol. 5, 257-260; Vol. 3, 63-67
- Dalal, N. S. Vol. 6, 134-137; Vol. 6, 138-140; Vol. 5, 194-199; Vol. 5, 200-202
Demers, L. M. Vol. 5, 282-288
DeVilder, W. M. Vol. 4, 56-63
DiGregorio, K. A. Vol. 6, 163-169; Vol. 5, 257-260; Vol. 3, 63-67
Dower, J. M. Vol. 5, 352-358
Dubbs, S. B. Vol. 6, 170
Dumm, T. F. Vol. 6, 59-65; Vol. 6, 66-75; Vol. 5, 148-154; Vol. 5, 155-185;
Vol. 5, 186-193
- Edelson, R. E. Vol. 5, 282-288
- Fang, C. P. Vol. 6, 151; Vol. 6, 153
Fissan, H. J. Vol. 5, 244-248
Frantz, R. L. Vol. 5, 361-365
- Grayson, R. L. Vol. 5, 319-327; Vol. 5, 328-345; Vol. 3, 35-42; Vol. 3, 91-94
Greene, F. H. Y. Vol. 5, 200-202; Vol. 4, 121-139
- Hathaway, P. Vol. 4, 121-139
Hering, S. Vol. 5, 224-243
Hill, C. A. Vol. 6, 141-148; Vol. 5, 261-273
Hinton, D. Vol. 5, 289-293; Vol. 4, 157-163
Hogg, R. Vol. 6, 59-65; Vol. 6, 66-75; Vol. 6, 76-93; Vol. 5, 148-154; Vol. 5, 155-185;
Vol. 5, 186-193
- Irr, W. Vol. 6, 138-140

THE RESPIRABLE DUST CENTER

Jafari, B. Vol. 6, 134-137; Vol. 5, 194-199; Vol. 5, 200-202
Jones, W. G. Vol. 5, 346-351
Jung, S. Vol. 6, 18-31

Keane, M. J. Vol. 6, 141-148; Vol. 5, 261-273; Vol. 4, 121-139; Vol. 4, 140-149;
Vol. 3, 53-60
Khair, A. W. Vol. 6, 18-31; Vol. 5, 18-41; Vol. 5, 42-52; Vol. 4, 3-8; Vol. 4, 9-55;
Vol. 4, 56-63; Vol. 4, 64-91; Vol. 4, 92-106; Vol. 3, 3-10; Vol. 3, 11-22
Kim, H. Vol. 5, 346-351; Vol. 5, 352-358
Kittleson, D. B. Vol. 6, 153

Lantz, R. C. Vol. 6, 163-169; Vol. 5, 257-260; Vol. 4, 157-163; Vol. 3, 63-67
Lee, C. Vol. 6, 173-182; Vol. 5, 295-305; Vol. 5, 306-318; Vol. 3, 71-84
Lui, B. Y. H. Vol. 5, 113-120
Luo, Y. Vol. 5, 95-108

Marple, V. A. Vol. 6, 149; Vol. 6, 150; Vol. 6, 151; Vol. 6, 153; Vol. 5, 109-112;
Vol. 5, 204-223; Vol. 5, 224-243; Vol. 5, 244-248; Vol. 3, 45-52
McCawley, D. Vol. 4, 157-163
Meloy, T. P. Vol. 5, 249-250; Vol. 5, 251-254
Mohal, B. R. Vol. 6, 94-105; Vol. 6, 106-122; Vol. 5, 123-128; Vol. 5, 129-138;
Vol. 5, 139-147
Moore, M. P. Vol. 3, 85-90
Mutmansky, J. M. Vol. 6, 173-182; Vol. 6, 183-191; Vol. 5, 295-305; Vol. 5, 306-318;
Vol. 4, 155-157; Vol. 3, 71-84

Olson, K. Vol. 6, 152
Ong, T. M. Vol. 3, 53-60

Pederson, A. B. Vol. 5, 274-281
Peng, S. S. Vol. 5, 72-81; Vol. 5, 95-108; Vol. 5, 328-345; Vol. 3, 32-34; Vol. 3, 35-42;
Vol. 3, 91-94
Pisano, F. Vol. 4, 157-163
Plummer, R. W. Vol. 5, 346-351; Vol. 5, 352-358
Prasad, K. V. K. Vol. 6, 35-49
Pui, D. Y. H. Vol. 6, 152

Raghootama, P. S. Vol. 6, 123-133
Ramani, R. V. Vol. 6, 35-49; Vol. 6, 50-56; Vol. 5, 55-60; Vol. 5, 61-71; Vol. 5, 361-365;
Vol. 4, 109-118; Vol. 3, 25-31
Reddy, N. P. Vol. 5, 18-41; Vol. 5, 42-52; Vol. 4, 64-91
Regad, E. D. Vol. 4, 121-139
Robinson, V. Vol. 4, 140-149
Rose, M. Vol. 5, 282-288
Rubow, K. L. Vol. 6, 149; Vol. 6, 150; Vol. 6, 153; Vol. 5, 109-112; Vol. 5, 204-223;
Vol. 5, 244-248; Vol. 3, 45-52

Saus, F. Vol. 5, 261-273
Sechra, M. S. Vol. 6, 123-133
Shi, X. Vol. 6, 138-140; Vol. 5, 194-199
Simonyi, T. Vol. 5, 319-327
Stanley, C. Vol. 5, 289-293; Vol. 4, 157-163
Stobbe, T. J. Vol. 5, 346-351; Vol. 5, 352-358
Sun, G. C. Vol. 3, 32-34
Superdock, D. T. Vol. 5, 282-288
Suryan, B. Vol. 6, 134-137; Vol. 5, 194-199

INDEX

Thompson, S. D. Vol. 5, 82-94
Tsai, C. J. Vol. 6, 152

Ueng, T. H. Vol. 5, 82-94

Vallyathan, V. Vol. 6, 134-137; Vol. 6, 138-140; Vol. 5, 200-202; Vol. 5, 261-273;
Vol. 4, 121-139; Vol. 4, 140-149; Vol. 3, 53-60
VanDyke. Vol. 6, 157-162

Wallace, W. E. Vol. 6, 141-148; Vol. 5, 261-273; Vol. 4, 121-139; Vol. 4, 140-149;
Vol. 3, 53-60
Wang, Y. J. Vol. 5, 82-94

Zhiqun, Z. Vol. 5, 113-120
Zipf, Jr., R. K. Vol. 6, 3-17; Vol. 5, 3-10; Vol. 5, 11-17

GENERIC MINERAL TECHNOLOGY CENTER FOR RESPIRABLE DUST

CUMULATIVE SUBJECT INDEX 1984-1987

CONTROL OF DUST AND PARTICULATE MATTER GENERATION

- Begley, Richard D.** (2) Coal fracture analysis using two simultaneous wedge indentors and laser holographic interferometry, 1985, Vol. 4, 56-63.
- Khair, A. Wahab** (2) An analysis of respirable dust generation by continuous miner, 1986, Vol. 5, 18-41.
- Khair, A. Wahab** (2) Characterization of coal breakage as a function of operating parameters, 1986, Vol. 5, 42-52.
- Khair, A. Wahab** Characterizing fracture types in rock/coal subjected to quasi-static indentation using acoustic emission technique, 1985, Vol. 4, 3-8.
- Khair, A. Wahab** (2) Correlation of fragment size distribution and fracture surface in coal cutting under various conditions, 1985, Vol. 4, 9-57.
- Khair, A. Wahab** Design and fabrication of a rotary cutting simulator, 1984, Vol. 3, 3-10.
- Khair, A. Wahab** (2) Identification of fracture in coal by AE in dynamic test, 1987, Vol. 6, 18-31.
- Khair, A. Wahab** (2) Mechanisms of respirable dust generation by continuous miner, 1985, Vol. 4, 92-106.
- Khair, A. Wahab** Study of fracture mechanisms in coal subjected to various types of surface tractions using holographic interferometry, 1984, Vol. 3, 11-22.
- Zipf, Jr., R. Karl** (2) Development of a mixed mode testing system for geological materials, 1987, Vol. 6, 3-17.
- Zipf, Jr., R. Karl** (2) Fracture mode and loading rate influences on the formation of respirable size fragments on new fracture surfaces, 1986, Vol. 5, 11-17.
- Zipf, Jr., R. Karl** (2) Mixed mode testing for fracture toughness of coal based on critical - energy - density, 1986, Vol. 5, 3-10.

DILUTION, DISPERSION, AND COLLECTION OF DUST

- Bhaskar, R.** (2) Behavior of dust clouds in mine airways, 1985, Vol. 4, 109-118.
- Bhaskar, R.** (2) Comparison of the performance of impactors and gravimetric samplers, 1987, Vol. 6, 50-56.
- Bhaskar, R.** (2) Experimental studies of dust dispersion in mine airways, 1986, Vol. 5, 55-60.
- Chiang, H. S.** (3) Size distribution of the airborne dust in longwall coal faces, 1986, Vol. 5, 95-108.

INDEX

- Chiang, H. S.** (4) Some factors influencing the airborne dust distribution in longwall face area, 1984, Vol. 3, 32-34.
- Grayson, Robert L.** (2) Analysis of an airborne dust study made for a southwestern Pennsylvania underground bituminous coal mine, 1984, Vol. 3, 35-42.
- Marple, V. A.** (3) Numerical technique for calculating the equivalent aerodynamic diameter of particles, 1986, Vol. 5, 113-120.
- Peng, S. S.** (2) Air velocity distribution measurements on four mechanized longwall coal faces, 1986, Vol. 5, 72-81.
- Ramani, R. V.** (2) Application of knowledge based systems in mining engineering, 1987, Vol. 6, 35-49.
- Ramani, R. V.** (2) Dust transport in mine airways, 1984, Vol. 3, 25-31.
- Ramani, R. V.** (2) Theoretical and experimental studies on dust transport in mine airways, 1986, Vol. 5, 61-71.
- Rubow, K. L.** (2) Application of a particle dispersion system for obtaining the size distribution of particles collected on filter samples, 1986, Vol. 5, 109-112
- Ueng, T. H.** (3) Simulations on dust dispersion for a coal mine face using a scale model, 1986, Vol. 5, 82-94.

CHARACTERIZATION OF DUST PARTICLES

- Chander, S.** (3) Wetting behavior of coal in the presence of some nonionic surfactants, 1986, Vol. 5, 129-138.
- Chander, S.** (3) Wetting characteristics of particles and their significance in dust abatement, 1986, Vol. 5, 123-128.
- Dalal, N. S.** (4) Electron spin resonance detection of reactive free radicals in fresh coal dust and quartz dust and its implications to pneumoconiosis and silicosis, 1986, Vol. 5, 194-199.
- Dalal, N. S.** (4) Oxygen effects on free radicals and cytotoxicity of freshly crushed coals, 1987, Vol. 6, 134-137.
- Dumm, T. F.** (2) A procedure for extensive characterization of coal mine dust collected using a modified personal sampler, 1986, Vol. 5, 186-193.
- Dumm, T. F.** (2) Distribution of sulfur and ash in ultrafine coal, 1987, Vol. 6, 66-75.
- Dumm, T. F.** (2) Estimation of particle size distributions using pipet-withdrawal centrifuges, 1986, Vol. 5, 148-154.
- Dumm, T. F.** (2) Particle size distribution of airborne dust, 1987, Vol. 6, 59-65.
- Dumm, T. F.** (2) Standard respirable dusts, 1986, Vol. 5, 155-185.
- Fang, C. P.** (2) Crossflow influence on collection characteristics of multi-nozzle micro-orifice impactor, 1987, Vol. 6, 151.
- Hering, Susanne** (2) Low-pressure and micro-orifice impactors for cascade impactor sampling and data analysis, 1986, Vol. 5, 224-243.

- Hogg, R.** (2) Surface characterization for coal processing, 1987, Vol. 6, 76-93.
- Jafari, B.** (3) Detection of organic free radicals in coal-dust exposed lung tissue and correlations with their histopathological parameters, 1986, Vol. 5, 200-202.
- Marple, V. A.** (2) An impactor with respirable penetration characteristics and size distribution capabilities, 1987, Vol. 6, 150.
- Marple, Virgil A.** (2) Instrumentation for the measurement of respirable coal mine dust, 1984, Vol. 3, 45-52.
- Marple, Virgil A.** (2) Low pressure and micro-orifice impactors, 1986, Vol. 5, 224-243.
- Marple, Virgil A.** (4) Micro-orifice uniform deposit impactor, 1986, Vol. 5, 244-248.
- Marple, Virgil A.** (2) Theory and design guidelines for cascade impactor sampling and data analysis, 1986, Vol. 5, 204-223.
- Meloy, Thomas P.** A hypothesis on the possible contribution of coal cleats to CWP, 1986, Vol. 5, 249-250.
- Meloy, Thomas P.** A working hypothesis on how silica and silica surface may cause silicosis and CWP, 1986, Vol. 5, 251-254.
- Mohal, B. R.** (2) A new technique to determine wettability of powders--inhibition time measurements, 1986, Vol. 5, 139-147.
- Mohal, B. R.** (2) Surfactant adsorption and wetting behavior of freshly ground and aged coal, 1987, Vol. 6, 106-122.
- Rubow, K. L.** (2) A method for resuspending particles deposited on filters, 1987, Vol. 6, 149.
- Rubow, K. L.** (4) Measuring the size distribution of diesel exhaust and mine dust aerosol mixtures with the micro-orifice uniform deposit impactor, 1987, Vol. 6, 153.
- Seehra, M.** (3) Photoacoustic spectroscopy of quartz, 1987, Vol. 6, 123-133.
- Tsai, C. J.** (5) Fragment size distribution from simple fracture of coal and rock, 1987, Vol. 6, 152.
- Vallyathan, V.** (4) Role of reactive oxygen radicals in silica cytotoxicity, 1987, Vol. 6, 138-140.
- Wallace, Jr., W. E.** (4) In vitro biologic toxicity of native and surface-modified silica and kaolin, 1985, Vol. 4, 140-149.
- Wallace, W. E.** (3) Mutagenicity of diesel exhaust particles and oil shale particles dispersed in lecithin surfactant, 1987, Vol. 6, 141-148.
- Wallace, Jr., W. E.** (5) Pulmonary surfactant interaction with respirable dust, 1984, Vol. 3, 53-60.
- Wallace, Jr., W. E.** (7) Suppression of inhaled particle cytotoxicity by pulmonary surfactants and re-toxication by phospholipase--distinguishing properties of quartz and kaolin, 1985, Vol. 4, 121-139.

INDEX

INTERACTION OF DUST AND LUNGS

- Bartlett, G. L.** (2) Effects of coal dusts and alveolar macrophages and growth of lung fibroblasts, 1986, Vol. 5, 274-281.
- Bhavanandan, V. P.** (2) Mucins secreted by rat tracheal explants in culture, characterization and influence of dust, 1987, Vol. 6, 170.
- Cilento, E. V.** (3) Measurement of superoxide release from single pulmonary alveolar macrophages, 1987, Vol. 6, 163-169.
- Demers, Lawrence M.** (4) The effects of coal mine dust particles on the metabolism of arachidonic acid by pulmonary alveolar macrophages, 1986, Vol. 5, 282-288.
- DiGregorio, K. A.** (3) Superoxide release from single pulmonary alveolar macrophages, 1986, Vol. 5, 257-260.
- DiGregorio, K. A.** The development of an electro-optical technique to measure superoxide release from pulmonary alveolar macrophages exposed to coal dusts, 1984, Vol. 3, 63-67.
- Lantz, R. Clarke** (3) Development of alternations in the lung induced by inhaled silica: a morphometric study, 1986, Vol. 5, 289-292.
- Pisano, F.** (5) Evaluation of the size distribution of large aerosols in an animal exposure chamber, 1984, Vol. 4, 153-159.
- VanDyke, K.** (2) Detection of receptor and synthesis antagonists of platelet activating factor in human blood and neutrophils using luminol-dependent chemiluminescence, 1987, Vol. 6, 157-162.
- Wallace, W. E.** (7) The effect of lecithin surfactant and phospholipase enzyme treatment on some cytotoxic properties of respirable quartz and kaolin dusts, 1986, Vol. 5, 261-273.

RELATIONSHIP OF MINE ENVIRONMENT, GEOLOGY AND SEAM CHARACTERISTICS TO DUST GENERATION AND MOBILITY

- Andre, R. A.** (3) Variation in mineral and elemental composition of respirable coal mine dusts by worker locations and coal seams, 1986, Vol. 5, 319-327.
- Bise, Christopher** (2) Coal mine respirable dust, 1985, Vol. 4, 163-165.
- Grayson, R. L.** (2) Characterization of respirable dust on a longwall panel, 1986, Vol. 5, 328-345.
- Grayson, R. L.** (2) Correlation of respirable dust mass concentration with worker positions, 1984, Vol. 3, 91-94.
- Lee, Changwoo** (2) A strategy for coal mine respirable dust sampling using multi-stage impactors for characterization purposes, 1986, Vol. 5, 295-305.
- Lee, Changwoo** (2) Application of the size and elemental characteristics of airborne coal mine dust, 1987, Vol. 6, 173-182.
- Lee, Changwoo** (2) Statistical analysis of the elemental characteristics of airborne coal mine dust, 1986, Vol. 5, 306-318.
- Moore, Michael P.** (2) The relationship between the hardgrove grindability index and the potential for respirable dust generation, 1984, Vol. 3, 85-90.

THE RESPIRABLE DUST CENTER

Mutmansky, J. M. An analysis of coal and geological variables related to coal workers' pneumoconiosis, 1984, Vol. **3**, 71-84.

Mutmansky, J. M. World wide coal mine dust research, 1987, Vol. **6**, 183-191.

Stobbe, Terrence J. (4) A methodology for determining the mineral content and particle size distribution of airborne coal mine dust, 1986, Vol. **5**, 346-351.

Stobbe, Terrence J. (4) Characterization of coal mine dust, 1986, Vol. **5**, 352-358.

COORDINATION

Frantz, Robert L. (2) A review of the programs and activities of the Generic Mineral Technology Center for Respirable Dust, 1986, Vol. **5**, 361-365.